UNIVERSIDADE D
COIMBRA

João Filipe Alves de Amorim

Understanding the Underlying Mechanisms Regulating Aging and Longevity

Tese no âmbito do Programa Doutoral em Biologia Experimental e Biomedicina, ramo Biologia Molecular, Celular e do Desenvolvimento, orientada pelo Professor Doutor Carlos Manuel Marques Palmeira, pelo Professor Doutor David Andrew Sinclair e pela Professora Doutora Anabela Pinto Rolo, apresentada ao Instituto de Investigação Interdisciplinar da Universidade de Coimbra.

Agosto de 2019

INSTITUTE FOR INTERDISCIPLINARY RESEARCH (IIIUC)

• U C •

UNDERSTANDING THE UNDERLYING MECHANISMS REGULATING AGING AND LONGEVITY

Doctoral thesis in Experimental Biology and Biomedicine, branch of Molecular, Cellular and Developmental Biology

João Filipe Alves de Amorim

August 2019

PhD thesis presented to the Institute for Interdisciplinary Research from the University of Coimbra (IIIUC) for the fulfilment of the requirements for a Doctoral degree in Experimental Biology and Biomedicine, branch of Molecular, Cellular and Developmental Biology, under the supervision of Professor Carlos Manuel Marques Palmeira (Department of Life Sciences, Faculty of Science and Technology, University of Coimbra) and co-supervision of Professor David Andrew Sinclair (Genetics Department, Harvard Medical School).

INSTITUTO DE INVESTIGAÇÃO INTERDISCIPLINAR (IIIUC)

COMPREENSÃO DOS MECANISMOS SUBJACENTES QUE REGULAM O ENVELHECIMENTO E A LONGEVIDADE

Tese de Doutoramento em Biologia Experimental e Biomedicina, ramo de Biologia Molecular, Celular e do Desenvolvimento

João Filipe Alves de Amorim

Agosto 2019

Tese de Doutoramento apresentada ao Instituto de Investigação Interdisciplinar da Universidade de Coimbra (IIIUC) para prestação de provas necessárias à obtenção do grau de Doutor em Biologia Experimental e Biomedicina (ramo Biologia Molecular, Celular e do Desenvolvimento), realizada sob orientação científica do Professor Doutor Carlos Manuel Marques Palmeira (Departamento de Ciências da Vida, Faculdade de Ciências e Tecnologia, Universidade de Coimbra) e co-orientação do Professor Doutor David Andrew Sinclair (Departamento de Genética, Harvard Medical School).

This work was performed at CNC — Centre for Neuroscience and Cell Biology, University of Coimbra (Coimbra, Portugal) and Harvard Medical School (Boston, USA) having been financed by Portuguese national funds via the European Regional Development Fund (ERDF), through the Centro 2020 Regional Operational Programme: project CENTRO-01-0145-FEDER-000012-HealthyAging2020, the Portugal 2020 - Operational Programme for Competitiveness and Internationalization, the Portuguese national funds via FCT – Fundação para a Ciência e a Tecnologia, I.P.: project POCI-01-0145-FEDER-016770, as well as by UID/NEU/04539/2013 (CNC.IBILI Consortium strategic project) and under a PhD scholarship **SFRH**/PD/BD/114173/2016, assigned by the doctoral programme in Experimental Biology and Biomedicine (PDBEB) of CNC.

Part of this work was performed in collaboration with Professor David Andrew Sinclair (Genetics Department, Harvard Medical School).

Este trabalho foi realizado no CNC — Centro de Neurociências e Biologia Celular, Universidade de Coimbra (Coimbra, Portugal) e Harvard Medical School (Boston, EUA), tendo sido financiado pelos fundos nacionais portugueses através do Programa Operacional Regional Centro 2020, Fundo Europeu de Desenvolvimento Regional (FEDER): projeto CENTRO-01-0145-FEDER-000012-HealthyAging2020, o Portugal 2020 - Programa Operacional de Competitividade e Internacionalização, o fundo nacional português através da FCT - Fundação para a Ciência e Tecnologia, projeto POCI-01-0145-FEDER- 016770, bem como pelo UID/NEU/04539/2013 (projeto estratégico do CNC.IBILI Consortium) e com a bolsa de doutoramento SFRH/PD/BD/114173/2016, atribuído pelo programa de doutoramento em Biologia Experimental e Biomedicina (PDBEB) do CNC.

Parte deste trabalho foi realizado em colaboração com o professor David Andrew Sinclair (Departamento de Genética da Harvard Medical School).

“The idea is to die young as late as possible”

- Ashley Montagu

Acknowledgements

Não poderia deixar de agradecer a todos aqueles que ao longo deste percurso estiveram sempre presentes, assim como aqueles que, embora distantes, estiveram sempre próximos de mim, dando-me força e ânimo para nunca desistir. Todos eles também contribuíram para que esta tese de doutoramento fosse possível.

Ao Professor **Carlos Palmeira**, o meu orientador, agradeço não só a confiança depositada e a oportunidade que me deu de abrir os meus horizontes, mas também toda a dedicação, compreensão e amizade, que em muito contribuiu para que este trabalho fosse possível. Obrigado pela força e motivação dada nos momentos menos fáceis, que sem dúvida ajudaram com que me torna-se melhor investigador!

To Professor **David Sinclair**, my co-supervisor, for welcoming me into his lab and teaching me how to think big and how to be a better scientist. All the challenges, difficult projects, and hard days were always better to deal with thanks to your encouragement and advices. Without them would not be possible to push past all these difficulties. I'm grateful to be part of the amazing team and community, and pleasure and privileged to learn from and work with you!

À Professora **Anabela Rolo**, o meu muito obrigado por toda a disponibilidade e apoio demonstrados, assim como todos os conselhos sábios transmitidos ao longo desta jornada.

Ao grupo *"MitoLab"*, incluindo todos aqueles que já seguiram por outros caminhos – **João**, **Filipe**, **Ana**, **José** e **Rui** – o meu muito obrigado por todos os momentos partilhados e por todos o apoio demonstrado! Foi um prazer trabalhar convosco!

Thank you to my colleagues in the *"Sinclair Lab"*. From the senior to my fellow graduate students, **Michael Schultz**, **Michael Cooney**, **Yuancheng Lu** and **Patrick Griffin**, it was a pleasure working and learning from and with you in the many moments we shared together.

Ao meu grupo e meus amigos BEB – **Marcos**, **Luís** e **Maria Inês** – pelos pequenos e tão bons momentos partilhados ao longo desta jornada. Obrigado por todo o carinho e amizade demonstrado.

Ao **Francisco**, ao **Ludgero** e à **Sofia Morais**, obrigado por todos os momentos que passámos e passamos juntos. Coimbra não teria sido a mesma sem vocês. Nunca esquecerei todas as histórias e experiências que partilhamos juntos. Obrigado!

Aos meus amigos de sempre – **Ana Francisca**, **Diogo**, **Tiago**, **António**, **Paulo**, **Raul**, **Tadeu**, **João Paulo** – amigos que tendo a sua vida fora do mundo da ciência, estiveram sempre presentes, nunca deixando de fazer parte dele. Agradeço por esta amizade que é para a vida!

À **Renata** e à **Silvia**, o meu muito obrigado por todo o apoio, amizade e carinho transmitidos, dando-me força nos momentos mais difíceis.

To my senior colleagues and friends – **Giuseppe, Jae, Alice** and **Israel** – thank you for the tireless availability, for the friendship as well as for the all rigorous knowledge transmitted that has greatly contributed to enrich this still short scientific career.

To **Michael Bonkowski**, thank you for the countless skills that you've taught me. Thank you for the discussions and science lessons that helped me to be a better scientist today! You always pushed me, even when I was a shy guy, just to make me speak. I'll never forget those days in the back of the lab.

To **Jaime Ross**, thank you for being a huge mentor to me, both in lab and in life. Thank you for the tireless availability, for the friendship as well as for all the rigorous knowledge transmitted. You were very important for this thesis become true. I'll never forget all the help and I'll be eternally thankful.

Os meus "amigos do costume" – **Ana**, **António**, **Mariana**, **Pedro**, **Teresa**, **André**, **Zé**, **Catarina** e **Xana** – agradeço toda a disponibilidade, amizade e companhia. Foi um prazer fazer parte desta família e partilhar tantos e tão bons momentos convosco. Nunca irei esquecer todos os jantares, caminhadas, passeios, jogo de futebol anual e as nossas longas conversas. Obrigado por tudo!

À **Sofia**, por todos os momentos, conselhos e gargalhadas que partilhamos desde os tempos de Vila Real. Embora longe, sempre estiveste presente e disponível durante esta etapa, um ombro amigo sempre que precisei. Podes contar com o teu Afilhado sempre que precisares!

To **Sofia** and **Randy** thank you for everything that you have made for me since the day I arrived. You received me as a family and I'll never forget that. All the advices and the shared moments were really important in my journey and this moment would not be possible without you.

Os meus **pais**, meu muito obrigado por todo o apoio, motivação, carinho e coragem demonstrados, que sempre tudo fizeram para que pudesse ultrapassar mais uma etapa na minha vida. A eles, minha irmã **Joana,** ao **Zé** e a toda a minha família devo o apoio incondicional na concretização deste objetivo. Estarei eternamente grato! Esta conquista também é vossa!

À **Ana**, porque quaisquer palavras seriam poucas, obrigado por teres entrado na minha vida! Obrigado pela presença, apoio e carinho constantes. Por toda a compreensão e sobretudo paciência. Obrigado pelo amor e alegria com que preenches todos os meus dias. Acima de tudo, obrigado por partilhares a tua vida comigo. És para mim um exemplo de força, exigência e superação. Esta é apenas mais uma conquista nossa! Obrigado por tudo!

Table of Contents

Abbreviations List

4-OHT – 4-Hydroxytamoxifen

AADPR – *O*-acetyl-ADP-ribose

AAV – Adeno-associated Viruses

AD – Alzheimer's Disease

ADP – Adenosine Diphosphate

ALT – Alanine Aminotransferase

AMC - Aminomethylcoumarin

AMP - Adenosine Monophosphate

AMP – Adenosine Monophosphate

AMPK – Adenosine Monophosphate-activated Protein Kinase

AROS – Active Regulator of SIRT1

AST – Aspartate Aminotransferase

ATP – Adenosine Triphosphate

AUC – Area Under Curve

CD – Catalytic Domain

CLAMS – Comprehensive Lab Animal Monitoring System

CNS – Central Nervous System

CO_2 – Carbon Dioxide

CR – Caloric Restriction

CTR – Terminal Regulatory Segment

DBC1 – Deleted in Brest Cancer 1

DMEM – Dulbecco's Modified Eagle Medium

DNA – Deoxyribonucleic Acid

DSB – Double Strain Breaks

dSIR2 – *SIR2 O*rtholog

DTA – Diphtheria Toxin A

E230 – Glutamine 230

EPM – Elevated Plus Maze

ERC – Extrachromosomal rDNA circle

ER^{T2} – Estrogen Receptor Nuclear Translocation Domain

ES – Embryonic Stem cells

EtOH – Ethanol

FBS – Fetal Bovine Serum

FI – Frailty Index

FOXO – Forkhead Box O

FOXO3a – Forkhead Box O3

GFP – Green Fluorescent Protein

GH – Growth Hormone

GLUT4 – Glutamate Transporter Type 4

GTT – Glucose Tolerance Test

H3 - Histone H3

H3-K9 – Methylation of Histone H3 at Lysine 9

H4 - Histone H4

H4-K16 – Methylation of Histone H4 at Lysine 16

HCl – Hydrochloric Acid

HDAC – Histone Deacetylase

HDL – High-density Lipoprotein

HFD – High Fat Diet

HOMA-IR – Homeostatic Model Assessment – Insulin Resistance Calculator

ICE – Inducible Changes in Epigenome

IGF1 – Insulin/insulin-like Growth Factor

IIS – Insulin-IGF1 signaling

ITT – Insulin Tolerance Test

KDAC – Protein Lysine Deacetylase

K_m – Michaelis-Menten constant

LDL – Low-density Lipoprotein

LDT – Light-Dark Transition

LKB1 – Liver Kinase B1

MEF – Mouse Embryonic Fibroblast

MRI – Magnetic Resonance Imaging

mRNA – Messenger Ribonucleic Acid

mtDNA – Mitochondrial DNA

mTOR – Mammalian Target of Rapamycin

NA – Nicotinic Acid

NAD^+ – Nicotinamide Adenine Dinucleotide (oxidized form)

NADH – Nicotinamide Adenine Dinucleotide (reduced form)

$NADP^+$ – Nicotinamide Adenine Dinucleotide phosphate (oxidized form)

NADPH – Nicotinamide Adenine Dinucleotide phosphate (reduced form)

NAM – Nicotinamide

NaMN – Nicotinic Acid Mononucleotide

NAMPT – Nicotinamide Phosphoribosyltransferase

ncRNA – Noncoding RNA

nDNA – Nuclear DNA

NEO – Neomycin

NF-kB – Nuclear Factor Kappa-light-chain-enhancer of Activated B Cells

NIA – National Institute of Aging

NMN – Nicotinamide Mononucleotide

NMNAT – Nicotinamide Mononucleotide Adenylyltransferase

NPT – Nicotinic Acid Phosphoribosyltransferase

NR – Nicotinamide Riboside

NRF-1 – Nuclear Respiratory Factor 1

NRK – Nicotinamide Riboside Kinase

NTD – N-terminal Domain

O_2 – Oxygen

ORF – Open Reading Frame

p53 – Protein Tumor p53

PARP – Poly (ADP-ribose) polymerase

PBS – Phosphate-Buffered Saline

PCR – Polymerase Chain Reaction

PGC-1α – Peroxisome proliferator-activated receptor-y co-activator 1 α

PI – Propidium Iodine

PKA – Protein Kinase A

PTP1B – Protein Tyrosine Phosphatase 1B

QA – Quinolinic acid

RCM – Redistribution of Chromatin Modifiers

rDNA - Ribosomal DNA

RER – Respiratory Exchange Ratio

RNA – Ribonucleic Acid

RSV – Resveratrol

RT – Room Temperature

SAMR1 – Sterile Alpha and Toll/interleukin-1 Receptor Motif-containing 1

SARM1 – Toll/interleukin-1 Receptor Motif-containing 1

SBD – STAC Binding Domain

SD – Standard Diet

SDH – Succinate Dehydrogenase

SDS – Sodium Dodecyl Sulphate

SEM – Standard Error of Mean

SIR2 – *Silent Information Regulator 2*

siRNA – Small Interference RNA

SIRT – Sirtuin

STACs – Sirtuin Activating Compounds

SWARM^{O} – Simplified Whole-panel Amplification Reaction Method

TAMRA - Tetramethylrhodamine

TBS – Tris Buffered Saline

TBS-T – Tris Buffered Saline Solution 0.1% Tween-20

TC – Total Cholesterol

TE – Tris-EDTA

TFAm – Mitochondrial Transcription Factor A

TOR – Target of Rapamycin

WAT – White Adipose Tissue

WHO – World Health Organization

WT – Wild-type

XAMB – Ambulatory Activity Count

ZTOT – Total Vertical Motor Activity

RESUMO

O envelhecimento é caracterizado por uma perda progressiva da função dos vários órgãos, resultando num maior risco de morte devido a várias doenças. Doenças crónicas relacionadas com a idade, como diabetes mellitus tipo II, doenças neurodegenerativas, cancro e doenças cardiovasculares, estão entre as principais causas de morbidade e morte no mundo. Nas últimas décadas foram alcançados importantes avanços na área, em particular com a descoberta de que o ritmo de envelhecimento é coordenado, pelo menos em parte, por vias genéticas e processos bioquímicos conservados.

Estudos em leveduras levaram à descoberta de uma dessas vias, uma família de enzimas conservadas, conhecidas como as sirtuínas. As sirtuínas (SIRT1-7) são uma família de deacetilases dependentes do dinucleótido de nicotinamida e adenina (NAD^+) com capacidades extraordinárias para prevenir doenças e até mesmo reverter alguns aspectos do envelhecimento. Em particular a SIRT1, a sirtuína mais estudada da família, demonstrou ter um papel fundamental na regulação do metabolismo, reparação do DNA, inflamação, estrutura da cromatina assim como o envelhecimento em mamíferos.

A descoberta de que o resveratrol e outras moléculas derivadas de plantas, conhecidas como STACs (compostos de ativação de SIRT1), tinham a capacidade de ativar a SIRT1 *in vitro* e *in vivo*, proporcionaram uma procura de ativadores desta enzima, com o objetivo de estudar os seus benefícios para a saúde. No entanto, continua por desvendar se as STACs como o resveratrol e o SRT1720 medeiam os seus benefícios através da ativação direta da SIRT1. Com o objetivo de abordar esta questão, produzimos um modelo animal, um mutante homozigoto para E222K (SIRT1-E222K), com uma ativação defectiva na SIRT1, que não responde à ativação de STACs *in vitro*. Deste modo, este modelo animal permitiu-nos determinar quais dos efeitos benéficos do resveratrol são devidos à direta ativação da SIRT1. Neste trabalho demonstramos que o resveratrol, adicionado à dieta dos animais, aumentou significativamente a sobrevivência de WT, mas não dos animais portadores da mutação E222K, quando estes foram alimentados com uma dieta rica em gordura. A adição de resveratrol à dieta do animal resultou numa melhoria geral da sua saúde levando a uma maior longevidade. Igualmente verificámos uma redução da patologia hepática, um aumento da sensibilidade à insulina, uma maior resistência e atividade locomotora, assim como uma normalização dos indicadores de inflamação.

Para além das STACs tradicionais, uma nova classe de compostos começou a ser recentemente explorada. Estudos em leveduras mostraram que estes compostos aumentam a via de reciclagem de NAD, que recicla NAD^+ a nicotinamida (NAM), prolongando a longevidade e mimetizando os benefícios de restrição calórica. Esta descoberta levou os investigadores a testar moléculas capazes de restabelecer os níveis de NAD^+. Este trabalho teve como objetivo explorar a possibilidade de testar várias intervenções genéticas através de estratégias sinérgicas para assim estudar doenças relacionadas com a idade e o

envelhecimento. Depois de aumentar a expressão génica e a atividade das sirtuínas, observámos que o tratamento com mononucleotídeo de nicotinamida (NMN) evitou a perda de peso dos animais relacionada com a idade, com um aumento não significativo na longevidade (p=0,15).

O trabalho realizado com as sirtuínas, através do aumento da sua atividade ou da sua expressão génica, demonstrou ser fundamental para se perceber como tratar de uma só vez todas as doenças associadas com a idade, e assim ajudar a aumentar o tempo de vida e a saúde dos idosos. A complexidade das doenças, a necessidade de compreender como retardar o processo de envelhecimento e de descubrir novas terapias, faz com que seja fundamental o desenvolvimento de modelos animais que melhor mimetizem doenças relacionadas com a idade. Estudos anteriores demonstraram que "RCM" (relocalização de modificadores de cromatina), é uma causa importante para o envelhecimento em mamíferos. Neste trabalho desenvolvemos um novo modelo animal, "ICE" (para mudanças indizíveis no epigenoma), que nos permitiu induzir cortes no DNA, em regiões não-codificadoras do genoma dos animais. De acordo com a hipótese RCM, o rato ICE exibiu fenótipos relacionados com uma idade avançada, assim como doenças relacionadas com a mesma. Estes resultados demonstraram que mudanças epigenéticas, associadas ao processo de reparação do DNA, são a causa do envelhecimento em mamíferos.

Estes resultados criam uma melhor compreensão sobre os mecanismos fundamentais de ativação alostérica de enzimas complexas, assim como os meios para testar múltiplas intervenções genéticas para promover a saúde e a longevidade. Desta forma, estamos mais perto de determinar quais as doenças que as STACs poderão tratar em humanos e como poderemos melhorar a sua potência. Finalmente, acreditamos que o modelo ICE será uma ferramenta importante para estudar doenças humanas e avaliar se o processo de envelhecimento pode ser retardado ou revertido usando novos ou conhecidos compostos.

Palavras chave: Envelhecimento; Sirtuínas; Compostos ativadores de sirtuínas (STACs); Resveratrol; Ativador alostérico; Deacetilase; Longevidade; Metabolismo; Mitocôndria; Musculo; NAD^+; NMN; Epigenética; DSBs; Reparação de DNA; Metilação de DNA.

ABSTRACT

Aging is accompanied by a progressive loss of healthy function in multiple organ systems, leading to impaired function and increased vulnerability to death from multiple diseases. Chronic, age-related diseases, such as type II diabetes mellitus, neurodegenerative diseases, cancers, and cardiovascular diseases are already among the leading causes of morbidity and death in the world. Unprecedented advances have been achieved in the aging field in the last decades, particularly with the discovery that the rate of aging is coordinated, at least in part, by genetic pathways and conserved biochemical processes. Historically, however, researchers have focused their attention on investigating individual pathways in isolated organs as a strategy to unravel the root cause of aging, with the ultimate goal of designing better drugs. Studies in yeast led the discovery of one of these pathways, a family of conserved enzymes, known as the sirtuins. The sirtuins (SIRT1-7) are a family nicotinamide adenine mononucleotide (NAD^+)-dependent deacetylases with extraordinary abilities to prevent diseases and even revert some aspects of aging. Importantly, SIRT1, which is the most studied sirtuin of the family, has been shown to play a key role in the regulation of metabolism, DNA repair, inflammation, chromatin structure, and aging in mammals.

The discovery that resveratrol and other plant-derived molecules, known as STACs (for SIRT1 activating compounds), could activate SIRT1 *in vitro* and *in vivo* led the field to seek for SIRT1 activators and study their potential health benefits. However, whether STACs such as resveratrol and SRT1720 mediate their health benefits via direct SIRT1 activation remains an unsolved question in the field. In order to address this major question, we have generated a knock-in mouse model that is a homozygous mutant for E222K (SIRT1-E222K), an activating-defective mutant, shown not to respond to STACs activation *in vitro*, and we used it to precisely determine which of the biological effects of resveratrol are due to SIRT1 activation. Here, we show that resveratrol significantly increased survival of wild-type (WT) mice, but not of mice carrying the E222K mutation when fed a high-fat diet. Resveratrol produced changes associated with longer lifespan, reduced liver pathology, increased insulin sensitivity, enhanced endurance and locomotor activity, as well as normalized markers of inflammation (Baur *et al.*, 2006).

In addition to traditional STACs, a newer class of compounds is gaining attention in the field. Up-regulation of the NAD salvage pathway, which recycles NAD^+ from nicotinamide (NAM), was shown to extend lifespan and mimic caloric restriction (CR) in yeast. This discovery drove the field to test molecules that restore NAD^+ levels in elderly individuals. Herein, we tested if synergistic strategies accelerate the ability to test multiple genetic interventions, to study aging and age-related diseases. We tested the effects of boosting gene expression and activity of the entire sirtuin gene family and observed that (nicotinamide mononucleotide) NMN supplementation protected against age-related decreases in body weight, with a non-significant increase in longevity ($p=0.15$).

Prior research in the sirtuin field was critical to understanding how treating all age-associated diseases at once, whether by boosting sirtuin activity or their expression, could help increase lifespan and healthspan of the elderly. However, in order to fully understand the best approaches to slow down the aging process and develop therapies for age-related diseases, there has been need to develop mouse models that better recapitulate human-like age-related diseases (Justice and Dhillon, 2016). Accumulating evidence shows that an epigenetically-driven process, called “RCM” (relocalization of chromatin factors), is an important cause of aging in mammals (Vijg and Hasty, 2006). Here, we have developed a novel animal model called the “ICE mouse” (for inducible changes in epigenome) that has allowed us to induce a few DNA cuts in non-coding regions of the mouse genome across all tissues and monitor the effects on key tissues and age-related physiology. In agreement with the RCM hypothesis, the ICE mouse exhibited early onset of age-related phenotypes, as well as of age-related diseases. These results are consistent with the epigenetic shift driven by the DNA repair process as being an upstream cause of aging in mammals.

Together, the results presented herein provide insights into the fundamental mechanisms of allosteric activation of complex enzymes and the means to test multiple genetic interventions to promote healthspan and longevity. In this way, we are closer to determine which diseases STACs could treat in humans and how they can be improved to increase their potency. Finally, we envision that the ICE model will be a novel tool used to model human diseases and assess whether the aging process can be slowed down or reverted using known and novel agents.

Keywords: Aging; Sirtuins; SIRT1; Sirtuin-activating compound (STAC); Resveratrol; Allosteric activator; Deacetylase; Longevity; Metabolism; Mitochondria; Muscle; NAD^+; NMN; Epigenetics; DSBs; DNA repair; DNA methylation.

CHAPTER 1

Introduction

Aging is a multifaceted biological process common for all living organisms and is characterized by a gradual loss of normal physiological functions after reaching sexual maturity, culminating in loss of function, and ultimately ending in disease and death. In most organisms, advanced age is also the largest risk factor for several diseases, such as certain forms of cancer, as well as neurodegenerative and cardiovascular diseases, with the rate of aging inversely proportional to an organism's mean lifespan (Sen *et al.*, 2016). Importantly, whenever we study aging and talk about lifespan, it is important to have another key consideration, known as "healthspan", which represents the duration of time when an organism remains free of chronic diseases. Therefore, finding ways to increase both lifespan and healthspan represent the leading research efforts in the gerontology field.

In recent decades, several factors such as the increase of both the average and, to a lesser extent, the maximal human lifespan, the increase in the aged population, as well as the increase in health expenditures, have motivated the rapid expansion in aging research (Wachter and Finch, 1997).

The average human life expectancy has increased in most of the developed countries over the past 200 years (Oeppen and Vaupel, 2002). Better quality of water, food, hygiene, housing, and lifestyle, as well as advances fighting infectious diseases, antibiotics, and improved medical care (Fogel and Costa, 1997; Waite, 2004), are among the major contributions to the observed reduction in mortality. After 1950, people of 70 years of age or older also stared to benefit from improved quality of life (Vaupel *et al.*, 1998; Oeppen and Vaupel, 2002), and survival rates and mean life expectancy are expected to increase in the elderly (Kontis *et al.*, 2017). Additionally, several aspects of age-related health have also been shown to improve, with an increase in both motor and cognitive functioning during aging (Christensen *et al.*, 2013; Zeng *et al.*, 2017).

Data from biological, epidemiological, and demographical studies have been used to identify a cause or process to explain the cause of aging as well as its inevitable consequence, death (Buhroo *et al.*, 2018). The pursuit to explain the increase in life expectancy has ruled out any possible genetic contributions due to the rapid rate in life expectancy change (Burger *et al*., 2012). Thus, people in the field quickly concluded that aging should be seen as an extremely complex, multifaceted process (Kowald and Kirkwood, 1996), and that a single gene or the decline of a key body system by themselves are unlikely to be the cause of aging.

Moreover, individuals who survive to greater ages are predominantly common in the so-called "blue zones" of the world, such as Ikaria in Greece, Loma Linda in the United States, Nicoya in Costa Rica, Okinawa in Japan, and part of Sardinia in Italy (Partridge *et al*., 2018). Remarkably, these populations have not been found to be genetically different from their neighbors, but their environment and lifestyles, including social networks, have been claimed to have an important role in the healthy aging of these people (Poulain *et al*., 2013; Partridge

et al., 2018). Furthermore, additional factors such as diet, education, and consistent physical activity (Cooper *et al.*, 2014), as well as conditions during early life and parental health (Fogel *et al*., 1997) have important effects on mortality.

A great achievement in our civilization was reached with the improvement in health conditions for all ages, leading to the extension of life expectancy. Nevertheless, healthspan has not followed as great of an increase as lifespan (Crimmins, 2015). Reports of life expectancy between 2000 and 2015 have shown a global increase in lifespan of 5 years but only a 4.6-year increase in "healthy" life expectancy (http://apps.who.int/gho/data/view.main.SDG2016LEXREGv?lang=en). Currently, an average of 16-20% of life is spent in late-life morbidity (Jagger *et al.*, 2008), predominantly in females and in individuals with a lower socio-economic status or those with obesity (Jagger *et al.*, 2008; WHO, 2015; Stenholm *et al.*, 2017). The flip-side of longer life expectancy is that older age is the major risk factor for several chronic deadly diseases, including cancers and cardiovascular diseases, as well as neurodegenerative diseases (Niccoli and Partridge, 2012), which are now falling mainly on older people, due to impairments in sensory, motor, and cognitive functions, all of them decreasing quality of life. Thus, although people from most nations are living longer, their healthspan is not increasing. Facing and finding ways to combat the length and severity of such late-life morbidities should, in this way, be a major aim in our times.

1.1. The fight for slowing aging

Recent advances in longevity research have exposed the possibility of interventions that may treat diseases affecting multiple organs, increasing healthspan, and compressing the morbid later-stage lives.

Caloric restriction (CR) without malnutrition was one of the most important discovers in the gerontology field, being considered the gold standard as the most vigorous way to slow down aging and age-related diseases. The discovery was first presented in the 1930s by McCay and colleagues and later reported with the lifespan extension of rats (McCay *et al*., 1989), however, the explanation as to why a reduction in caloric intake can result in health benefits was a mystery in that time, with some inconsistent experimental hypothesis being presented are rapidly ruled out (Anderson and Weindruch, 2012).

Caloric restriction has been shown to extend lifespan of virtually all species tested through the activation of a physiological low-energy program (Mair and Dillin, 2008). In addition to improved longevity, CR has been proven to protect against diverse and unrelated age-associated disease, such as metabolic diseases, cardiovascular diseases, neurodegenerative diseases, and cancers (Masoro, 2002). Despite the fact that CR presents an exceptional therapeutic capacity, adherence to a strict regimen is a serious challenge. Thus, unraveling

the molecular mechanisms underlying CR in order to develop pharmacological targets and therapeutics has now been the aim of several research groups. Although this goal has not yet been achieved, research in several model organisms, such as yeast, worm, and fly, have started to uncover a highly conserved network of pathways functioning as the core of the CR low-energy switch (Figure 1).

Over the years, several studies in different animal models have suggested that the beneficial effects of caloric restriction on lifespan were governed by a set of evolutionary conserved longevity pathways (Sinclair, 2005). Work using several animal models, from yeast to rodents, have uncovered dozens of genes and pathways that may be important targets to compress the period of morbidity and extend lifespan in humans. From these targets, target of rapamycin (TOR), adenosine monophosphate-activated protein kinase (AMPK), the nicotinamide adenine mononucleotide (NAD^+)-dependent sirtuin deacetylases, and insulin/insulin-like growth factor 1 (IGF1) signaling (IIS) (Kenyon, 2010; López-Otín *et al.*, 2013) were reported and are currently the major signaling targets in lifespan studies. Remarkably, research has also discovered that several natural occurring molecules can also activate these same survival pathways and extend lifespan in mammals (Martin-Montalvo *et al.*, 2013; Miller *et al.*, 2014).

Suppression of the insulin/insulin-like growth factor 1 (IGF1) signaling (IIS) pathway has been shown to dramatically extend lifespan in multiple systems (Fontana *et al*., 2010; Kenyon, 2011). The IGF1 signaling pathway responds to nutrients levels in the body, mediating feeding, development, and growth, together with macromolecular biosynthesis and storage. In this highly conserved pathway, the family of Forkhead box O (FOXO) transcription factors have been shown to act downstream of the IGF1 signaling pathway, becoming nuclear and activated only when the pathway is inhibited (Matsuzaki *et al.*, 2003). Research in *C. elegans* mutants to the insulin receptor, DAF-2, showed complete dependence on the FOXO ortholog in worms, DAF-16, in lifespan extension (Kenyon *et al.*, 1993). Moreover, even though mutants of the IGF1 signaling pathway can extend lifespan in flies, rodents, and possibly also in humans (Suh *et al.*, 2008; Pawlikowska *et al.*, 2009; Fontana *et al*., 2010), the precise mechanisms behind lifespan extension remain unclear. Dependence on AMPK has been suggested due to their multiple, interesting interactions with FOXO transcription factors (Greer *et al.*, 2007; Greer *et al.*, 2007a; Tullet *et al.*, 2014); however, FOXO has been shown to interact with sirtuins as well, thus suggesting that this mechanism may be evolutionary conserved.

On many levels, TOR and AMPK co-exist almost like perfect counterparts, having mutual antagonists in order to maintain cellular balance. While the TOR kinase complex is activated by nutrient abundance to stimulate anabolic functions, helping cell growth and proliferation, AMPK responds to energy depletion by enhancing cellular catabolic responses. In this way,

and perhaps unsurprisingly, components of the TOR signaling pathways are all practically anti-longevity factors (Johnson *et al*., 2013). TOR inhibition was shown to extend lifespan in organisms ranging from yeast to mammals, and AMPK has an important role in this pathways (Fabrizio *et al.*, 2001; Vellai *et al.*, 2003; Kapahi *et al.*, 2004; Harrison *et al.*, 2009). Lying on their opposing roles, TOR and AMPK share a number of regulatory targets, and reciprocally regulate several process including lipid metabolism, autophagy, and protein synthesis (Burkewitz *et al*., 2016). The reciprocal regulation between TOR and AMPK complexes makes it difficult to tease out which kinase plays a major or upstream role in lifespan regulation, which suggests that additional mechanisms through which the TOR pathway may regulate AMPK and vice-versa probably still have to be discovered.

Besides the increase in the AMP/ADP:ATP ratio that is responsible for AMPK activation, another indicator of nutrient depletion is a rise in the NAD^+:NADH ratio, favoring the oxidized form. Sirtuins, a conserved family of protein deacetylases and deacylases, require NAD^+ for their function, and similarly to AMPK, their activity also correlates with conditions of nutrient depletion. The first evidence that sirtuins function was sufficient to promote healthy aging and longevity as a CR mediator came from work in yeast (Kaeberlein *et al*., 1999; Lin *et al*., 2000). These findings led the field to extend research to include additional species, and even though there are concerns due to genetic backgrounds and technical issues have arisen, the field has clearly demonstrated that sirtuins can modulate lifespan and regulate age-related pathology in different models, including rodents by overexpressing SIRT1 and SIRT6 family members (Burnett *et al.*, 2011; Kanfi *et al.*, 2012a; Guarente, 2013; Satoh *et al.*, 2013). Like several interactions observed in these longevity pathways, data from several studies have denoted that sirtuins and AMPK can interact and promote each another's activation. AMPK was shown to indirectly activate the mammalian sirtuin homolog SIRT1 in cells through its effects on NAD^+:NADH ratio (Fulco *et al.*, 2008; Cantó *et al.*, 2010). On the other hand, the upstream AMPK kinase, liver kinase B1 (LKB1), was shown to be a direct target of SIRT1 deacetylation, showing that SIRT1 can promote AMPK activation (Lan *et al.*, 2008; Price *et al.*, 2012). The age dependent decline in NAD^+ in rodents was shown to result in decreased SIRT1 activity, ultimately through a failure in maintaining mitochondrial homeostasis (Gomes *et al.*, 2013). In this work, the researchers found that supplementation with NAD^+ in old mice reserved the age-related decline in skeletal muscle strength, as well as evidence of altered AMPK activity; however, it remains unclear if this altered AMPK activity plays a major role in these rejuvenating effects (Gomes *et al.*, 2013).

The field is driven by the final goal of finding better medicine that can target multiple age-related diseases and prevent countless others. Rapamycin, discovered from bacterium on Easter Island and an inhibitor of mechanistic TOR (mTOR) (Spindler, 2010; Mercken *et al.*, 2012), as well as metformin, an AMPK-activating molecule from the Hellebore buttercup plant

(Check-Hayden, 2015), are both candidate molecules for possible intervention and clinical trials are underway to test their possible abilities to slow down aspects of aging (Check-Hayden, 2015). Particularly, the search for activators of these pathways has led the field to concentrate its attention on sirtuins as well. Potent sirtuin activators have been designed and seem to show that pharmacological activation of sirtuins can mimic some of the physiological effects of caloric restriction, both in animals and in humans.

Although sirtuins have generated a significant amount of excitement and scrutiny over the years, many questions remain to be answered. From the activator's specificity, direct beneficial benefits, physiological roles of the newly described activities of sirtuins (Feldman *et al.*, 2015) to the pharmacokinetics and pharmacodynamics of NAD precursors, as well as how they are affected by route of delivery are missing some clarifications. In the work described herein, some of the questions and challenges will be addressed in order to provide a better understanding of sirtuin biology to the scientific community, which will perhaps illuminate us about their full potential in medicine.

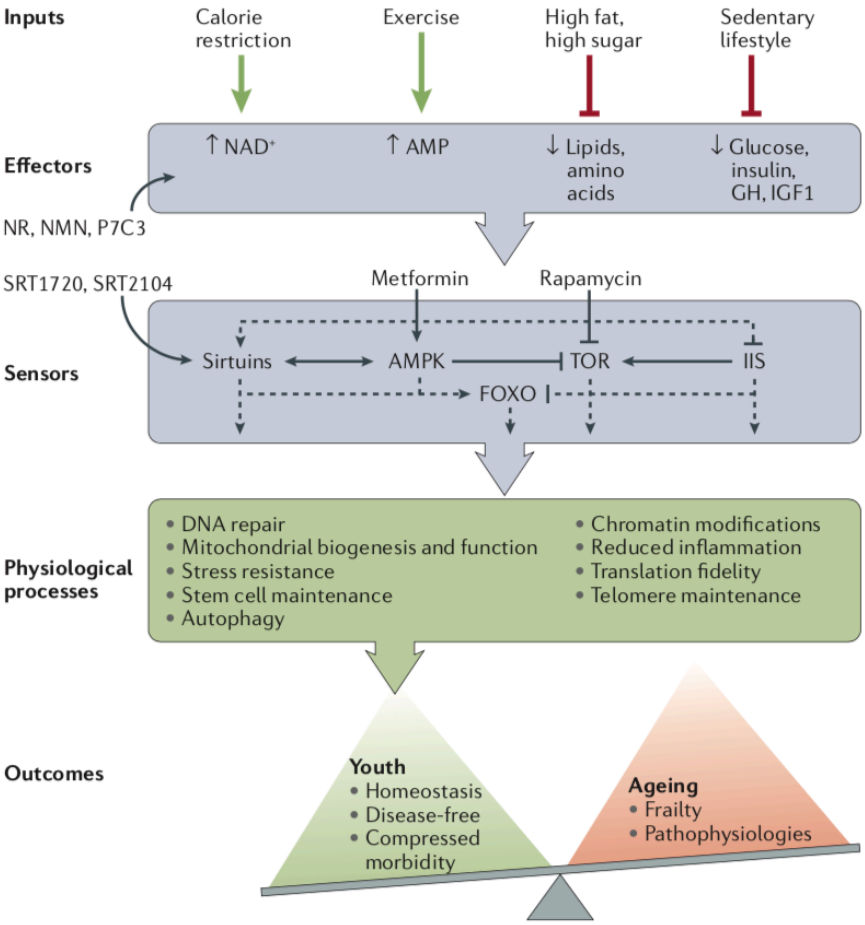

Figure 1. Nutrient-responsive signaling pathways involved in supporting health and extending lifespan. Caloric restriction, while reducing the concentration of glucose, amino acids and lipids, rises the concentration of metabolic effectors, such as, nicotinamide adenine dinucleotide (NAD+) and adenosine monophosphate (AMP). Exogenous administration nicotinamide riboside (NR), nicotinamide mononucleotide (NMN) or the nicotinamide phosphoribosyltransferase (NAMPT) activator P7C3 can increase NAD^+ levels while exercise increase AMP levels. High caloric diet increases lipid and amino acid levels and sedentary lifestyle increases glucose, insulin, growth hormone (GH) and insulin/insulin-like growth factor 1 (IGF1). Caloric restriction is responsible for reduction in the levels of hormonal effectors, GH and IGF1. Metabolic sensors such as sirtuins (SIRTs), AMP kinase (AMPK), target of rapamycin (TOR), insulin–IGF1 signaling (IIS) and forkhead box O (FOXO) transcription factors are stimulated or inhibited by these effectors. Sirtuin-activating compounds (STACs) such as SRT1720 and SRT2104 directly activate SIRT1, while rapamycin is a direct inhibitor of TOR. Metformin activates AMPK. Downstream activities, such as, DNA repair, mitochondrial function and biogenesis, stress resistance, stem cell and telomere maintenance, autophagy, chromatin modifications, translational fidelity and reduced inflammation are positively regulated by these metabolic sensors. The overall ultimate effect favors the homeostasis, compressed morbidity and disease-free state, contraposing a frail, disease-associated state. Copied from (Bonkowski and Sinclair, 2016).

CHAPTER 2

Objectives

Aims

1. **Test which of the biological effects of STACs are abolished in mice with activation defective SIRT1-E222K.** One of the biggest questions in the sirtuin field is whether STACs such as resveratrol, mediate their health benefits via direct SIRT1 activation. Sinclair Lab has previously shown that deleting SIRT1 in myocytes and adult mice blocks the ability of resveratrol to alter muscle metabolism and mitochondrial function. Additionally, the discovery of an activation-defective mutant of SIRT1 (human E230K and mouse E222K) allows us for the first time to test which effects of the STACs are mediated by direct SIRT1 activation in cells and mice. Thus, the main objective of this aim was to test which of the physiological effects of STACs is due to direct activation of SIRT1.

2. **Test the ability to accelerate the test of age-related diseases with synergistic strategies.** Different approaches to studying aging have been used, however, synergistic strategies between them have been cost and time prohibitive. In this aim, we pursued a strategy to accelerate the ability to test multiple genetic interventions by boosting the expression and activity of the entire sirtuin gene family as well as boost NAD^+ levels by given the NAD^+ precursor NMN (nicotinamide mononucleotide).

3. **Determine if epigenetic decay underlies aging *in vivo*.** Accumulating evidence showing that an epigenetically-driven aging process called “RCM” (relocalization of chromatin factors) is a cause of aging in mammals (Vijg and Hasty, 2006). In this aim, we tested the RCM hypothesis *in vivo* using our “ICE mouse” (for inducible changes in epigenome). We tested if the ICE mouse exhibited early-onset age-related phenotype as well as age-related diseases.

CHAPTER 3

A novel mouse model to unravel the mechanism of SIRT1 activation

Part of this chapter was published in a conference paper:

Amorim, J. Tackur, S. Bonkowski, M. Rolo, A. Palmeira, C. Sinclair, D. A NEW MOUSE MODEL TO UNRAVEL THE MECHANISM OF SIRT1 ACTIVATION. (2018) *Innovation in Aging*, **Volume 2**, Issue suppl 1, Page 878, https://doi.org/10.1093/geroni/igy031.3277

3.1. Abstract

SIRT1 is a NAD^+-dependent deacetylase and one of the seven-member family of sirtuins that play a key role in the regulation of metabolism, DNA repair, inflammation, chromatin structure, and aging in mammals. Activation of SIRT1 improves mitochondrial function, treats hyperglycemia and fatty liver in mice and provides cardioprotection. The SIRT1 deacetylase reaction is one of the most complicated in the biological world, carrying out a two-step reversible reaction involving a covalently attached peptidyl intermediate. Well-known targets of SIRT1 include H3-K9 and H4-K16, p53, NF-κB, FOXO3a, and PGC-1α. While numerous chemical inhibitors of enzymes have been developed, comparatively little is known about allosteric enzyme activation.

In 2003, resveratrol and other plant-derived molecules, known as STACs (for SIRT1 activating compounds), were reported, and bind to the N terminus of SIRT1 to activate SIRT1 *in vitro* and *in vivo* and lower the Michaelis-Menten constant (K_m) for the substrate (Howitz *et al.*, 2003). Additionally, it was also shown that activation of human SIRT1 by small molecules requires a single amino acid, glutamine 230 (E230), located in a structured N-terminal activation domain adjacent to the STAC binding domain (SBD) (Hubbard *et al.*, 2013). Moreover, STACs have been shown to increase the mean and maximal lifespan of mice (Mercken *et al.*, 2014; Mitchell *et al.*, 2014). In humans, SRT2104, was able to alleviate psoriasis (Krueger *et al.*, 2015). Whether STACs, such as resveratrol and SRT1720, mediate their health benefits via direct SIRT1 activation remains an unsolved question in the field, but one that will help guide future drug development.

We have generated a knock-in mouse model that is a homozygous mutant for E222K (SIRT1-E222K) and used it to precisely determine if the biological effects of STACs are due to SIRT1 activation. Here, we showed that the STAC resveratrol significantly increased survival of WT mice but not in the mice carrying the E222K mutation. Resveratrol produced changes associated with longer lifespan, reduced liver pathology, increased insulin sensitivity, enhanced endurance and locomotor activity, and normalized markers of inflammation.

These experiments have provided valuable insights into the fundamental mechanisms of allosteric activation of complex enzymes and allowed us to test if the health benefits of STACs are mediated via direct SIRT1 activation *in vivo*, an unanswered question that has dogged the field for over a decade. These studies will determine which diseases STACs might be able to treat in humans and may determine how to better increase their potency.

3.2. Introduction

More than twenty years ago, an evolutionarily conserved, critical regulator for aging and longevity in diverse organism models, was described for the first time. The *Silent Information Regulator 2* (SIR2) gene, originally identified by Klar and colleagues (Klar, Fogel and Macleod, 1979), provided a novel paradigm to the aging field research. Responsible for the Sir2 family proteins, known as sirtuins, the *SIR2* gene was shown to repress genome instability of budding yeast *Saccharomyces cerevisiae* (Sinclair and Guarente, 1997; Kaeberlein, Mcvey and Guarente, 1999), making sirtuins one of the first families of longevity genes to be revealed (Friedman and Johnson, 1988b, 1988a; Kenyon *et al.*, 1993; Kennedy *et al.*, 1995). Additional studies have also shown that *SIR2* is a pivotal gene for silencing yeast telomerase as well as ribosomal DNA (rDNA) (Smith and Boeke, 1997; Bryk *et al.*, 2007).

The first evidence for the enzymatic activity of Sir2 came from a study in Sir2-like protein, CobB (Tsang and Escalante-Semerenat, 1999), derived from *Salmonella typhimurium*. CobB is able to substitute the function of CobT, a protein that transfers phosphoribose from nicotinic acid mononucleotide to dimethylbenzimidazole in the cobalamin synthesis pathway (Trzebiatowski and Escalante-semerena, 1997), suggesting that Sir2 might be able to catalyze a related pyridine nucleotide transfer reaction. Two years later, Frye (Frye, 1999) showed that both human and *Escherichia coli* derived Sir2 proteins were indeed able to transfer ^{32}P from [^{32}P]NAD to bovine serum albumin. The moiety transferred was ADP-ribose, using histones as subtracts, which lead Tanny and colleagues (Tanny *et al.*, 1999) to propose that ADP-ribosyltransferase activity of Sir2 was essential for silencing *in vivo*. In the meantime, Imai and Guarente observed that only acetylated peptides of the amino-terminal tails of H3 or H4 could accept ^{32}P from [^{32}P]NAD (Imai *et al.*, 2000a). However, it was the Sir2 mass spectrometry experiments that surprised the field, which found that the relative molecular weight of the reaction product was smaller than that of the acetylated subtract by 42 daltons, and undoubtedly indicated the major enzymatic activity of Sir2 was as a deacetylase, not a ADP-ribosyltransferase (Imai *et al.*, 2000b). Sir2 could specifically deacetylate lysine 16 of H4 in a NAD-dependent manner, suggesting the vital role of the NAD-dependent deacetylase activity in silencing *in vivo*. On the other hand, NADH, NADP, and NADPH were not able to substitute for NAD in this reaction.

Later on, sirtuins in other species were rapidly identified due to their homology to yeast Sir2, mainly to the conserved central catalytic core (Figure 3.1). Also, the NAD-dependent deacetylase activity was also highly conserved between yeast and mouse Sir2. Therefore, Sir2 and closely related homologs were suggested to function as a sensor of the cellular energy status, due to the absolute requirement of NAD^+ for the deacetylase activity. Sir2 and Hst2, a yeast Sir2 homolog, were shown to catalyze both the NAD-nicotinamide exchange

reaction and the NAD-dependent deacetylation (Landry *et al.*, 2000). Additionally, Smith and colleagues (Smith *et al.*, 2000) also confirmed that Sir2 proteins from yeast, bacteria, and humans exhibit NAD-dependent histone deacetylase activity. Hence, the evolutionary conserved NAD-dependent deacetylase activity of Sir2 proteins provided a novel framework to link NAD, metabolism, and aging through different organisms.

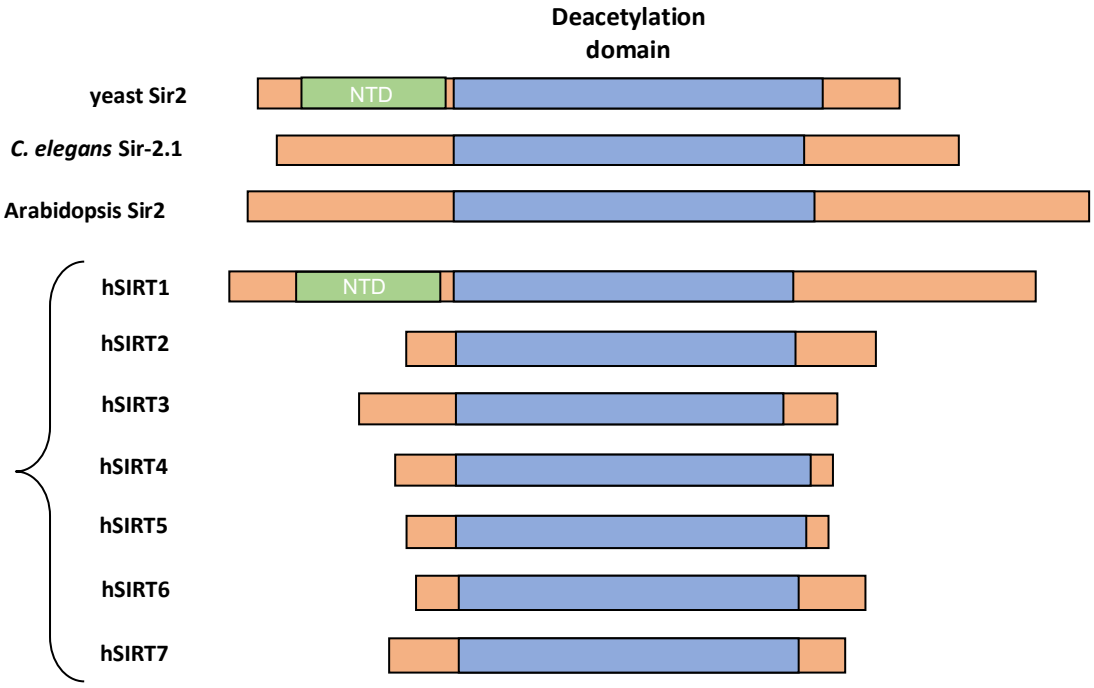

Figure 3.1. Homology between yeast Sir2 and seven mammalian sirtuins (SIRT1-7). Blue: the conserved catalytic domain, present in all sirtuins. NTD: The N-terminal domain (NTD) unique to yeast Sir2 and mammalian SIRT1 (green).

3.2.1. Physiological role of sirtuins in aging and longevity

Since their discovery, Sir2 and its closest orthologs have emerged as critical regulators for aging and longevity in several experimental model organisms, such as yeast, worms, and flies (Blander and Guarente, 2004; Longo and Kennedy, 2006).

Initially, the role of sirtuins in aging was discovered in yeast via a model of replicative lifespan, as measured by the number of times a yeast mother cell produces a daughter cell before becoming senescent. In 1997, Sinclair and Guarente (Sinclair and Guarente, 1997) identified the cause of yeast aging as stemming from recombination at rDNA loci. The development of an extrachromosomal rDNA circle (ERC) by homologous recombination was shown to be the initial event that leads to the amplification of ERCs in aging mother yeast cells due to their replication and preferential segregation within mother cells (Sinclair and Guarente, 1997). By adding an extra copy of the *SIR2* gene, Kaeberlein and colleagues shown an

extended replicative lifespan by ~30% due to suppression of rDNA recombination and decreased ERC formation. Deletion of the *SIR2* gene was found to increase ERCs and shorten lifespan (Kaeberlein, Mcvey and Guarente, 1999).

Over the years, additional evidence has clarified that the yeast *SIR2* gene is but one member among a large family of conserved genes found in many organisms ranging from bacteria to mammals (North and Verdin, 2004). Studies in more complex model organisms, such as *Caenorhabditis elegans* and *Drosophila melanogaster*, have revealed the conserved functional role of sirtuins in aging. In *C. elegans*, the *sir-2.1* mediated lifespan extension requires the worm forkhead protein DAF-16, but apparently without requiring of intact insulin signalling pathway (Tissenbaum and Guarente, 2001; Wang and Tissenbaum, 2006). *Sir-2.1* was also shown to bind and directly activate DAF-16 during stress, such as heat shock and oxidative stress, without responding to changes in insulin signalling (Wang and Tissenbaum, 2006). In the fruitfly *Drosophila melanogaster*, increasing the copy number of the *SIR2* ortholog (*dSIR2*) also extends lifespan (Rogina and Helfand, 2004).

3.2.2. Mammalian Sirtuins

Due to the exciting discovery that *SIR2* gene manipulation (*e.g.* increasing their amount) in yeast, worms, and flies can prolong lifespan, studies of mammalian sirtuins were spurred. Many central questions were driving the field at the time: Do sirtuins extend mammalian lifespan? Do mammalian sirtuins improve health and protect against aging-associated diseases? Are sirtuins critical for mediating the beneficial effects of caloric restriction? All these questions were scrutinized, and a lot of progress was made over the years.

In mammals, there are seven sirtuin enzymes (SIRT1-7) categorized by their highly conserved central NAD^+-binding and catalytic domains, the sirtuin core domain (Frye, 2000). Despite the conserved nature of sirtuins, their N and C termini differ, which in turn makes them highly different regarding their biological function, their partners and subtracts, as well as their distinct subcellular localization and expression patterns (reviewed in Haigis and Guatente, 2006). Mechanistically, sirtuins use NAD^+ as a cosubstrate to remove acetyl moieties from lysines on histones and proteins (Figure 3.2) (Houtkooper *et al.*, 2010). During sirtuin-mediated deacetylation of target lysine residues, an amide group is cleaved from NAD^+ generating nicotinamide (NAM) and a covalent ADP-ribose peptide-imidate intermediate. The intermediate O-acetyl-ADP-ribose is then formed and the deacetylated subtract is released (Sauve *et al.*, 2001; Borra *et al.*, 2004; Schmidt *et al.*, 2004). NAM can then act as a sirtuin inhibitor by binding to the C-pocket of sirtuins, which lies head-to-head to the NAD^+-binding pocket (Landry *et al*., 2000; Bitterman *et al.*, 2002).

The NAD^+ consumption during deacetylation is in this way what determines sirtuins as type III lysine deacetylases (KDACs), and divides them from type I, II, and IV KDACs. Regarding

their activity, SIRT1, SIRT2, and SIRT3 have been identified as having strong deacetylase activity (Imai *et al.*, 2000; Vaziri *et al.*, 2001; Schwer *et al.*, 2002; North *et al.*, 2003), as compared to the weak activity of SIRT4, SIRT5, and SIRT6. Additionally, deacetylation activity is not the singular function of all sirtuins. SIRT4 has been described as a NAD^+-dependent mono-ADP-ribosyl transferase along with SIRT6 (Liszt *et al.*, 2005; Haigis *et al.*, 2006), and has lipoamidase activity (Mathias *et al.*, 2014). Furthermore, SIRT6 also has the ability to remove long-chain fatty acyl groups from lysine residues (Jiang *et al.*, 2013), whereas SIRT5 has been described to act as a demalonylase, desuccinylase, and deglutarylase (Du *et al.*, 2011; Tan *et al.*, 2014). Lastly, SIRT7 is proposed to be a NAD^+-dependent deacetylase with few known *in vivo* and *in vitro* substrates (Vakhrusheva *et al.*, 2008; Chen *et al.*, 2013; Ryu *et al.*, 2014).

The subcellular localization of these proteins has been described in numerous cellular compartments in mammals depending on cell type, stress status, and molecular interactions. SIRT1, SIRT6 and SIRT7 are predominantly located in the nucleus (Michan and Sinclair, 2007), but reports, through finding its targets, have shown that SIRT1 can shuttle in and out of the nucleus (Michishita *et al.*, 2005; Tanno *et al.*, 2007). This particularity of SIRT1 is due to the presence of two primary amino acid nuclear export signals (Tanno *et al.*, 2007) in addition to the nuclear localization signals that SIRT6 and SIRT7 also possess. Three sirtuins, SIRT3-5, contain N-terminal mitochondrial targeting sequences and are believed to localize within the mitochondrial matrix (Onyango *et al.*, 2002; Schwer *et al.*, 2002; Michishita *et al.*, 2005); however, two different studies have suggested that SIRT3 may also translocate into the nucleus during cellular stress (Scher, Vaquero and Reinberg, 2007; Nakamura *et al.*, 2008). SIRT2 is primarily cytosolic and regulates gene expression of transcription factors that shuttle from cytosol to nucleus (Jing, Gesta and Kahn, 2007), but SIRT2 has also been found to localize into the nucleus and interact with nuclear proteins (North and Verdin, 2007). Hence, evidence show that mammalian sirtuins are highly distributed throughout the cell and that their localization may be dynamic, varying by tissue/cell-type and dependent on physiological conditions.

3.2.2.1. Mammalian sirtuins and caloric restriction

The discovery that Sir2 is a preserved regulator of lifespan in lower organisms coupled with the fact that sirtuin activity relies upon NAD^+ has led increased interest in elucidating the role of Sir2 in caloric restriction (CR). Several studies have shown that reduction in calorie intake, also known as CR, promotes lifespan extension in a wide range of lower organisms (Sinclair, 2005); however, whether-or-not Sir2 activity mediates CR benefits was unclear. Several studies of yeast replicative lifespan, have shown that *SIR2* is required for lifespan extension by CR. Additionally, a moderate CR diet (0.5% glucose) supresses rDNA

recombination, upregulates Sir2 activity, and increases mitochondrial respiration (Lin *et al.*, 2002; Anderson, Bitterman and Wood, 2003). Moreover, replicative lifespan was also shown to be regulated by Hst1 and Hst2, the yeast homologous of Sir2.

All this research consequently generated a significant interest in understanding the role of mammalian sirtuins in CR (Haigis and Sinclair, 2010). Caloric restriction was shown to upregulate SIRT1 expression in a variety of tissues, such skeletal muscle, liver, adipose tissue, kidney, and brain (Cohen *et al.*, 2004). Additionally, several mouse models showed the important link between SIRT1 and CR (Chen *et al.*, 2005; Bordone *et al.*, 2007; Banks *et al.*, 2008; Pfluger *et al.*, 2008). Studies using SIRT1 null mice have also been important to understand the role of SIRT1 in mediating aspects of CR. For example, whole-body SIRT1 null mice have been shown to prevent the increase in activity normally mediated by CR as seen in wild-type mice (Chen *et al.*, 2005), suggesting the requirement of SIRT1 for this phenotype of CR (Chen *et al.*, 2005; Boily *et al.*, 2008). Moreover, SIRT1 null mice have also been shown to have a shorter lifespan as compared to wild-type littermates, and that lifespan was not improved with CR (Li *et al.*, 2008), providing additional evidence that SIRT1 may be required for lifespan extension due to CR in mammals.

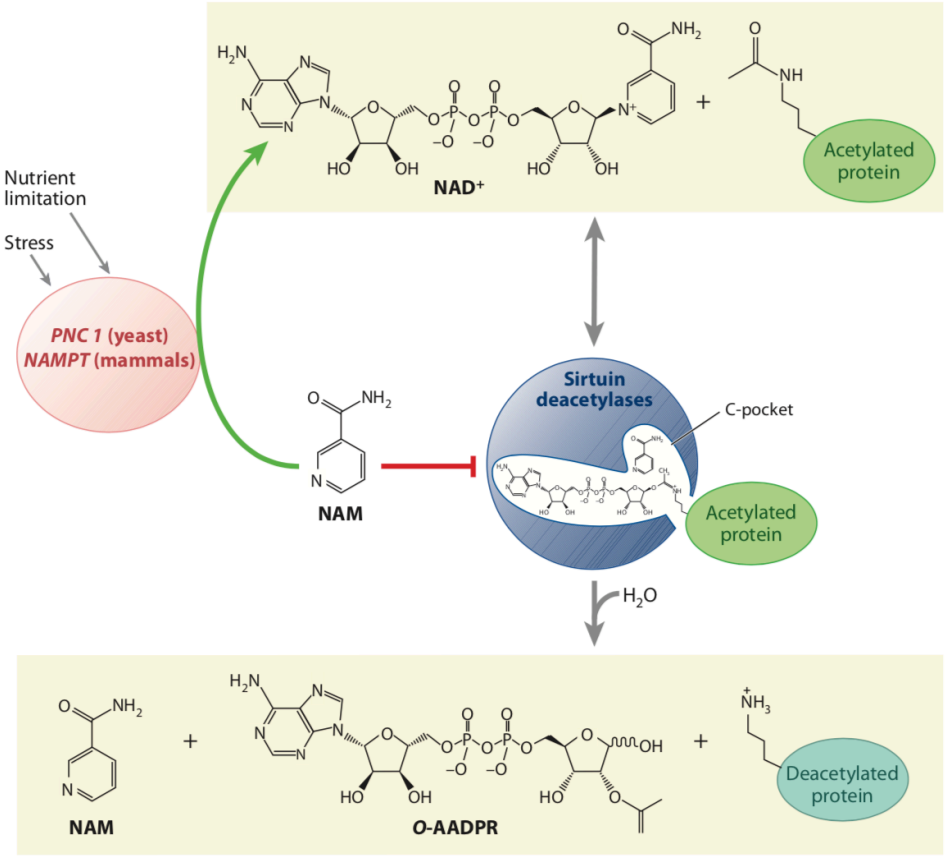

Figure 3.2. The sirtuin deacetylation reaction and its regulation by stress and nutrition. Sirtuin deacetylases, unlike type I and type II deacetylases, catalyze a two-step biological reaction, consuming NAD^+, and releasing NAM, *O*-acetyl-ADP-ribose (AADPR), and the deacetylated substrate. Overall sirtuin reaction is favored by hydrolysis of NAD^+. ADP-ribose peptide-imidate complex is then formed due to an electrophilic capture of acetyl oxygen in an ADP-ribosyltransfer reaction. After that, NAM enter the C-pocket and catalyze a reverse reaction. Removal of NAM and its conversion to NAD^+ by two genes upregulated by stress and nutrient limitation, *PNC1* (yeast) or *NAMPT* (mammals), facilitates activation of sirtuins. Copied from (Haigis and Sinclair, 2010).

3.2.2.2. Physiological role of mammalian sirtuins in aging and longevity

Over the years, sirtuins have attracted significant attention as research efforts try to understand how they work at the molecular level, as well as how they induce changes that promote survival, especially during times of adversity in response to signals like the amount of energy, the timing of daylight, and the stress from the environment. Since NAD^+ has emerged as a vital cofactor in the regulation of NAD^+-consuming enzymes such as sirtuins (Imai et al. 2000), several reports have arisen to try to understand the metabolic control of sirtuins and to try to modulate their activity by small molecules to combat multiple age-associated diseases.

Sirtuins interact with all major preserved longevity pathways, such as AMPK (Wang *et al*.,

2011), and insulin-IGF1 signaling, with targets including protein kinase A (PKA) (Gerhart-Hines *et al.*, 2011), mTOR (Armour *et al.*, 2009; Liu *et al.*, 2010), forkhead box O (FOXO) (Mouchiroud *et al.*, 2013), PGC-1α (Rodgers *et al.*, 2005), NF-kβ (Yeung *et al.*, 2004), p53 (Vaziri *et al.*, 2001), and IGF1 (Longo, 2009). During times of energy deficiency and reduced carbohydrate energy sources, sirtuins prompt cellular adaptations to improve metabolic efficiency. Regarding SIRT1, the most known and studied sirtuin, fasting (Rodgers *et al.*, 2005; Cantó *et al.*, 2010), caloric restriction (Chen *et al.*, 2008), exercise (Canto *et al.*, 2009), or low glucose availability (Fulco *et al.*, 2008) can increase enzymatic activity. Additionally, mitochondrial metabolism also increases in several tissues due to SIRT1-dependent deacetylation of transcription factors, cofactors, and histones (Rodgers *et al.*, 2005; Boily *et al.*, 2008; Feige *et al.*, 2008; Canto *et al.*, 2009; Cantó *et al.*, 2010; Price *et al.*, 2012; Menzies *et al.*, 2013). Fat and cholesterol catabolism in liver, skeletal muscle, and adipose tissue are also stimulated by SIRT1 (reviewed in Silva and Wahlestedt, 2010). Animal models of SIRT1 overexpression have also been used to show the impact of SIRT1 in preventing metabolic age-related complications, such as obesity, insulin resistance, and hepatic steatosis (Banks *et al.*, 2008; Pfluger *et al.*, 2008; Herranz *et al.*, 2010). High fat diet (HFD)-related lifespan reduction was also protected after pharmacological activation of SIRT1 (Baur *et al.*, 2006; Minor *et al.*, 2011). Remarkably, another transgenic mouse model of SIRT1 overexpression replicates several benefits of CR, including higher metabolic activity, reduced blood lipid levels, and improved glucose metabolism, without increasing lifespan (Bordone *et al.*, 2007). Like SIRT1, overexpression of SIRT6 has also been shown to increase lifespan in mice (Kanfi *et al.*, 2012b). Furthermore, research on loss-of-function models have also been performed over the years, with SIRT1, SIRT3, and SIRT7 models shown to be associated with higher susceptibility for metabolic and age-related diseases as well as reduced lifespan (Vakhrusheva *et al.*, 2008; Hirschey *et al.*, 2011; Boutant and Cantó, 2014; Ryu *et al.*, 2014). Experiments with SIRT6 models have revealed higher postnatal death susceptibility due to severe hypoglycemia within the first month of life (Mostoslavsky *et al.*, 2006; Zhong *et al.*, 2010). In contrast, *Sirt2*- and *Sirt5*-deficient mice do not present with any evident metabolic phenotypes in the basal state (Beirowski *et al.*, 2011; Bobrowska *et al.*, 2012; Yu *et al.*, 2013), while, contrarily to the most sirtuins, SIRT4 deficiency enhances oxidative metabolism (Laurent *et al.*, 2013).

3.2.2.3. Physiological role of mammalian SIRT1 in metabolism

Association between sirtuins and obesity and obesity-related issues has been highly implicated due extensive research in the field over the past few years. Numerous independent studies have elucidated the regulatory role of sirtuins in the metabolic pathways regarding the expression of adipocyte cytokines (adipokines), insulin secretion, variation of plasma glucose levels, cholesterol and lipid homeostasis, as well as mitochondrial energy capacity (Liang, Kume and Koya, 2009).

While recent studies have revealed novel roles for several of the six sirtuin members, the majority of the mammalian sirtuin research is focused on the function of SIRT1. SIRT1 has the greatest degree of sequence identity in the highly conserved core domain compared to yeast Sir2 (Frye, 1999) (Figure 3.1) and the physiological roles of SIRT1 in the regulation of metabolism and stress resistance are better understood.

SIRT1 seems to stimulate fatty acid oxidation by promoting adiponectin synthesis (Iwabu *et al.*, 2010), has been implicated in the hypothalamic control of energy balance (Çakir *et al.*, 2009), plays a role in adipogenesis (Picard *et al.*, 2004), and responds to fasting by regulating lipolysis and fatty acid mobilization (Picard *et al.*, 2004). Moreover, mice deficient in SIRT1 present with hyperglycemia, oxidative damage, and insulin resistance, which, consequently, become obese when faced with HFD (Purushotham et al. 2012; Wang et al. 2011).

Besides SIRT1 being a master regulator of key metabolic adaptations to nutrient deprivation in peripheral tissues, it is highly expressed in hypothalamus and has been implicated as critical player in normal body weight, energy homeostasis, and regulation of food intake (Ramadori *et al.*, 2008; Çakir *et al.*, 2009). Hence, fasting-induced SIRT1 upregulation was also found to be altered in obese mice (Ramadori *et al.*, 2008). Additionally, models of pharmacological SIRT1 inhibition in hypothalamus have shown to decrease food intake and body weight gain (Çakir *et al.*, 2009), which may suggest that hypothalamic inhibition of SIRT1 might be a strategy to suppress appetite.

Over the years, several studies using different transgenic mice with SIRT1 over- and underexpression in different tissues have linked SIRT1 with obesity. In adipose tissue from both *db*/*db* leptin-resistant obese mice and HFD-induced obese mice, expression of SIRT1 was significantly low (Qiao and Shao, 2006; Chalkiadaki and Guarente, 2012). Furthermore, experiments using mice where SIRT1 was specifically knocked out in white adipose tissue (WAT) showed enhanced adipogenesis and compromised fatty acid mobilization from WAT; however, WAT SIRT1 overexpression attenuated adipogenesis and boosted lipolysis (Picard *et al.*, 2004). In two different studies it was observed that mice overexpressing SIRT1 presented the characteristic phenotype of being leaner compared to littermate controls, and shown decreased levels of plasma cholesterol, insulin, and fasting glucose, as well as, reduced adiposity (Bordone *et al.*, 2007; Banks *et al.*, 2008). In another study, Paul Pfluger

and colleagues (Pfluger *et al.*, 2008), observed that overexpression of SIRT1 in transgenic mice subject to HFD caused beneficial effects such as decreased inflammation, improved glucose tolerance, and greater protection against hepatic steatosis; however, an anti-obesity effect was not observed. As in rodents, SIRT1 expression in obese pigs was shown to be less than in lean pigs (Pang *et al.*, 2013).

Since accumulation of lipids in adipose tissue in obesity triggers inflammatory events and obesity-related inflammation is documented as a major risk factor for the pathogenesis of diseases correlated with metabolic syndrome (Hotamisligil, 2006), this field has been widely studied to find potential new targets and strategies against obesity and its related complications. Two different studies have shown that SIRT1 deficient mice subject to HFD present with systemic inflammation, whereas modest overexpression of SIRT1 instigates suppression of inflammatory responses, (Xu *et al.*, 2010; Purushotham, Xu and Li, 2012). Hence, the beneficial effects of SIRT1 on metabolic syndromes have been argued to be due to its ability to repress activation of NF-kβ, which is the key transcriptional factor of inflammatory responses (Kauppinen *et al.*, 2013). Overexpression of SIRT1 in transgenic mice reduced serum levels of IL-6 and TNF-α in mice fed with HFD as well as the response of TNF-α-induced NF-kβ activation in embryonic fibroblasts (Pfluger *et al.*, 2008).

SIRT1 has been shown to deacetylate and consequently repress NF-kβ, causing a reduction in the production of pro-inflammatory cytokines (Yeung *et al.*, 2004). Contrarily, inhibition of SIRT1 appears to be pro-inflammatory. Using small interference RNA (siRNA) to knockdown SIRT1, Yoshizaki and colleagues (Yoshizaki *et al.*, 2009) described an increase in TNF-α-induced MCP-1 together with other inflammatory-related genes in 3T3-L1 adipocytes. Moreover, adipose tissue from SIRT1-specific knockdown mice subjected to HFD showed increased macrophage recruitment, but overexpression of SIRT1 inhibited macrophage accumulation (Gillum *et al.*, 2011). It is interesting to note, however, that antagonistic crosstalk may be present between SIRT1 and NF-kβ signaling in the regulation of obesity-related inflammatory responses. In addition to the regulatory inhibition of SIRT1 on NF-kβ, NF-kβ has been shown to down-regulate SIRT1 activity through expression of pro-inflammatory cytokines, such as IFNγ (Li *et al.*, 2012). Furthermore, inflammation of adipose tissue has been recognized has a hallmark of insulin resistance (Boe *et al.*, 2006), and SIRT1 expression in different tissues has been linked to insulin sensitivity. In adipocytes, SIRT1 has been shown to regulate insulin-stimulated glucose uptake as well as GLTU4 translocation, and increasing SIRT1 activity attenuates insulin resistance (Yoshizaki *et al.*, 2009). SIRT1 has also been reported to have reduced activity in highly insulin resistance cells, while the insulin insensitivity can be attenuated by increasing SIRT1 expression (Banks *et al.*, 2008). In skeletal muscle, SIRT1 contributes to the improvement of insulin sensitivity by repressing the protein

tyrosine phosphatase 1B (PTP1B) gene, which is critical in insulin signaling (Sun *et al.*, 2007). Complementary experiments using transgenic mice as well as *in vitro* studies have clarified the role of SIRT1 in the regulation of insulin secretion. Increasing SIRT1 expression was found to improve insulin secretion (Bordone *et al.*, 2006), and using a transgenic mouse overexpressing SIRT1 specifically in pancreatic β-cells was found to enhance glucose-stimulated insulin secretion and improve in the glucose tolerance. These observations were shown to persist during aging and also when animals were subjected to HFD (Moynihan *et al.*, 2005; Ramsey *et al.*, 2008). Additionally, using disease models, SIRT1 transgenic mice exhibited improved glucose tolerance and insulin sensitivity, presenting with decreased hepatic glucose production as well as increased hepatic insulin sensitivity (Banks *et al.*, 2008).

Contrary to animal studies, the number of human studies implicating sirtuins in obesity is limited. The available data are derived from studies where weight loss and caloric restriction analyses were made. SIRT1 transcriptional levels were shown to be significantly lower in obese individuals when compared to normal-weight controls. In these studies, the researchers have shown that the decreased transcriptional levels could be restored by weight loss obtained by CR (Crujeiras *et al.*, 2008; Pedersen *et al.*, 2008; Dong *et al.*, 2011; Clark *et al.*, 2012; Moschen *et al.*, 2013; Song *et al.*, 2013). As discussed above, decreased SIRT1 expression levels might be associated with obesity-related inflammation and excessive fat accumulation in adipose tissue. SIRT1 mRNA expression levels were also found to be lower in adipose tissue from obese patients as compared to controls (Costa *et al.*, 2010; Song *et al.*, 2013). Moreover, in another study performed in nondiabetic offspring of type 2 diabetes patients, SIRT1 mRNA expression in adipose tissue correlated with energy expenditure and insulin sensitivity (Rutanen, Yaluri and Modi, 2010). Similarly, de Kreutzenberg and colleagues also observed an association between insulin resistance and metabolic syndrome with decreased SIRT1 expression levels (Kreutzenberg *et al.*, 2010). Nevertheless, these findings must be further studied to better understand if the inverse relationship between SIRT1 expression and obesity relies on protection, resistance, or is in response to dietary, lifestyle, and environmental factors. Taken together, these studies increase our knowledge of the various possible actions that sirtuins may have in obesity and related issues. However, limitations of genetic manipulation have been noted and due to this there is a growing interest in the field over the years in order to try to identify possible potent and selective sirtuin activators for the treatment of these diseases.

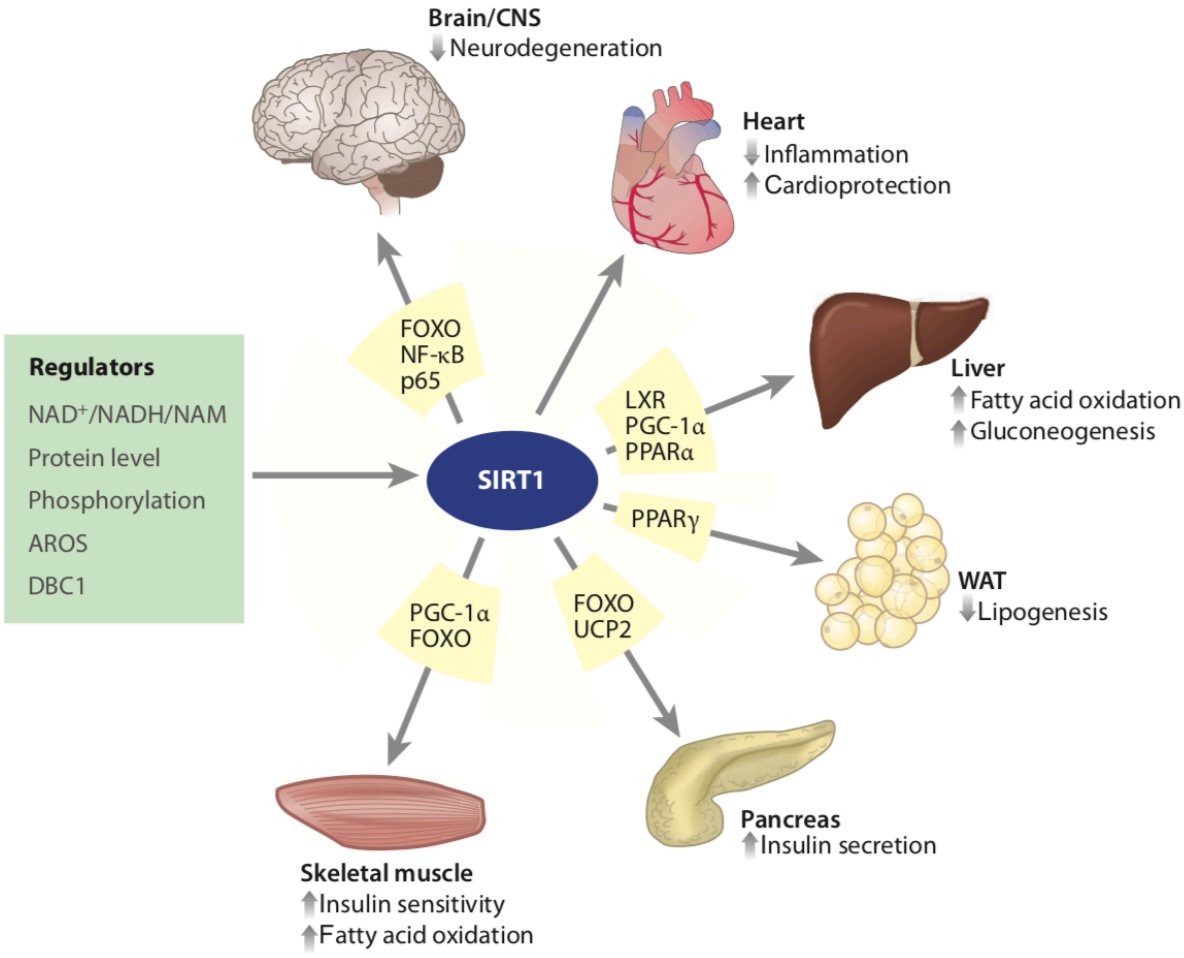

Figure 3.3. Sirtuin activation and its disease relevance. SIRT1 activity can be regulated through various mechanisms: by increasing NAD^+ and NAM concentrations, by SIRT1 protein level, and by phosphorylation, and through activation by active regulators of SIRT1 (AROS) and inhibition by DBC1 (deleted breast cancer 1). By direct or indirect action, SIRT1 target more than 100 signaling pathways relevant for human disease in a variety of tissues (reviewed in (Friedman and Johnson, 1988a)). SIRT1 protects cardiomyocytes from death and survival in neurons. In the liver, SIRT1 stimulates fatty acid oxidation and gluconeogenesis during nutrient deprivation through LXR, PGC-1α, and PPARα. WAT decreases fat storage through repression of by PPARγ SIRT1. Insulin secretion and pancreatic ß-cell survival are stimulated by SIRT1 by suppression of UCP2 and interaction with FOXO, respectively. In skeletal muscle, SIRT1 stimulates mitochondrial biogenesis through activation of PGC-1α. Copied from (Haigis and Sinclair, 2010).

3.2.3. Sirtuins activation for therapy

Following the role of sirtuins in the regulation of lipid and glucose metabolism as well as adipogenesis and appetite control, sirtuins have attracted significant interest as potential drug targets. Over the years some activators and inhibitors have been described for potential clinical application to treat disease like diabetes, cardiovascular diseases, cancers, and neurodegenerative diseases, yet many challenges face the development of STACs as possible medicines, including technical issues, bioavailability, and determination of the target disease to prioritize.

The discovery that yeast cells could live longer with an extra copy of the sirtuin-encoding gene SIR2 lead the research community to pursue a molecule that could activate sirtuins. Although activators are rare and much harder to study, distinct advantages make them more attractive: they are less prone to be rendered ineffective by residual enzymatic activity, they often have greater target specificity, and they cause fewer side effects (Zorn and Wells, 2010).

The seek for activators of sirtuins started in 2003 when Howitz and colleagues (Howitz *et al.*, 2003) proved that allosteric activation of sirtuins was possible through a high-throughput screen that identified the first potent activators using recombinant human SIRT1. Over ~18000 compounds were screened and more than 20 sirtuin activators were described (Howitz *et al.*, 2003). Several plant-derived metabolites including flavones (for example, quercetin), stilbenes (for example, resveratrol), chalcones (for example, butein), and anthocyanidins were shown to directly activate SIRT1 *in vitro* by increasing their affinity to peptide substrates through an allosteric mechanism that lowers the K_m (Howitz *et al.*, 2003). Thus, these molecules lower the binding affinity of SIRT1 to the substrate by increasing enzymatic activity by ten-fold (Howitz *et al.*, 2003).

Of all the natural SIRT1 activators described to date, resveratrol (3,5,4'-trihydroxystilbene) is still the most powerful (Figure 3.4). The phytoalexin derived from the dried root of white hellebore, *Veratrum grandiflorum* was described for the first time in 1940 (Baur and Sinclair, 2006), and was later was also shown to be present in Japanese knotweed *Polygonum sachalinense* (Baur and Sinclair, 2006). However, in the 1990s, the interest in resveratrol increased when it was discovered to be an active component of red wine. This discovery lead many to propose it as an explanation for the unusual low rates of mortality from chronic heart diseases in French people, the so-called "French paradox", in regions with high red wine (Richard, 1987; Renaud and de Lorgeril, 1992; Frankel, Waterhouse and Kinsella, 1993).

Resveratrol rapidly became the molecule of choice to test SIRT1 activation because it was shown to be potent, nontoxic, naturally available, and inexpensive. Several studies since then have shown that resveratrol can extend maximal lifespan in yeast (Jarolim et al. 2004; Yang et al. 2007; Morselli et al. 2009), worms (Viswanathan *et al.*, 2005; Zarse *et al.*, 2010), flies (Bauer *et al.*, 2004, 2009; Wood *et al.*, 2004) and even honeybees (Rascón *et al.*, 2012).

In mice fed a HFD, resveratrol was shown to have the capacity to improve metabolism and protect against obesity and insulin resistance (Baur and Sinclair, 2006; Baur *et al.*, 2006; Lagouge *et al.*, 2006), which was correlated with longer lifespan. In the same study, it was also observed that resveratrol was able to prevent the formation of fatty liver and could increase PGC-1α activity, a well-known regulator of mitochondrial biogenesis (Baur and Sinclair, 2006; Baur *et al.*, 2006). Likewise, the beneficial effects of resveratrol were also observed in rat models (Aubin *et al.*, 2008; Shang *et al.*, 2008; Rocha *et al.*, 2009). Moreover, Rivera and colleagues (Rivera *et al.*, 2009), observed improved lipid parameters such as plasma triglycerides and free fatty acids in obese Zucker rats after prolonged resveratrol administration (8 weeks) as compared to animals without resveratrol treatment. Regarding the central nervous system, administration of resveratrol was shown to limit consequences of high-caloric diet in mice (Ramadori *et al.*, 2009). Similarly, *in vitro* studies also support the beneficial effects of resveratrol in the obesity paradigm. Reduction in both fatty acid synthesis and triglyceride accumulation in hepatocytes (Shang *et al.*, 2008; Gnoni and Paglialonga, 2009) as well as inhibition of adipogenesis in isolated cells have been described (Fischer-Posovszky *et al.*, 2010).

The capacity of resveratrol to alleviate secondary phenotypes associated with diabetes, like diabetic nephropathy and tissue inflammation, was also described (Jiang *et al.*, 2013). In non-human primates, resveratrol has been shown to enhance metabolism (Fiori *et al.*, 2013), and in rhesus monkeys fed with a high-fat, high-sugar diet, resveratrol improved adipose insulin signaling (Jimenez-Gomez *et al.*, 2013). In this latter study, researchers also reported the anti-inflammatory effect that resveratrol exerts in visceral WAT from the monkeys (Jimenez-Gomez *et al.*, 2013). Additionally, chronic administration of moderate resveratrol doses was suggested to improve insulin sensitivity in both obese Zucker rats and mice subjected to HFD (Baur *et al.*, 2006; Lagouge *et al.*, 2006; Rivera *et al.*, 2009); however, *in vitro* studies have shown that resveratrol is capable of inhibiting insulin pathways, such as Akt, MAPK, PI3K, and PKB (Zhang, 2006; Fröjdö *et al.*, 2007).

Unfortunately, resveratrol has been shown to not be a successful drug due to its insolubility and poor bioavailability. Its half-life was also shown to be low, between 12-15 min (Asensi *et al.*, 2002; Marier *et al.*, 2002), and systemic concentrations were shown to only be in the low micromolar range after gram amounts were administered orally (Subramanian *et al.*, 2010). Surprisingly, Walle and colleagues (Walle *et al.*, 2004) observed that the half-life of resveratrol conjugates was much high (~9h) when compared to its native form, which has opened the possibility to use such conjugates *in vivo* to obtain a greater pharmacokinetic effect.

Clinical trials have been conducted to explore the health impact of resveratrol in individuals with obesity, diabetes, and cardiovascular diseases (Baur and Sinclair, 2006; Timmers *et al.*, 2011). In some cases, improvements were shown upon resveratrol treatment, including

improved insulin sensitivity, neuro-cognition, and cardiovascular diseases (Baur and Sinclair, 2006; Pearson *et al.*, 2008). Additionally, the toxicity of resveratrol was examined for possible signs of severe adverse effects in animals, and have showed no serious effects after controlled administration of resveratrol (Juan *et al.*, 2002; Crowell *et al.*, 2004). However, different side effects have been reported in the gastrointestinal tract (Brown *et al.*, 2010; Yoshino *et al.*, 2012).

The discovery of natural SIRT1 activators, such as resveratrol, lead to a search for new possible synthetic activators that could be more potent and efficacious, surpassing the bioavailability problems that resveratrol presented at the time. Some of these synthetic compounds have been shown to be more powerful than resveratrol and appear to be more effective in extending lifespan, as is the case for the compound tri-acetyl-stilbene (Yang *et al.*, 2007). However, in 2007 a new method was developed to identify novel sirtuin activators structurally unrelated to resveratrol (Milne *et al.*, 2007), and the first synthetic sirtuin activators were chemically distinct from resveratrol and based on an imidazothiazole scaffold (e.g., SRT1460, SRT1720, SRT2183) (Milne *et al.*, 2007). Similar to resveratrol, these molecules activate SIRT1 by a similar mechanism and lower the K_m for its substrates (Milne *et al.*, 2007). Later, synthetic compounds based on thiazolopyridines (for example, STAC-2), benzimidazole (for example, STAC-5), and bridged ureas (for example, STAC-9) were also described (Dai *et al.*, 2010; Hubbard and Sinclair, 2014) (Figure 3.4).

STACs were shown to mimic caloric restriction in mice by increasing mitochondrial function and protecting from fatty liver and muscle wasting, and have strong antidiabetic, cardioprotective, and anti-inflammatory effects in disease models (Milne *et al.*, 2007). Additionally, STACs can also extend a mouse's lifespan by up to 15%, even when intervention is started at 1 year of age (average mouse lifespan is 2 years) (Minor *et al.*, 2011; Mercken *et al.*, 2014; Mitchell *et al.*, 2014). The beneficial effects of STACs were shown to be partially or completely SIRT1-dependent. Using *Sirt1* germline knockouts, the ability of resveratrol in preventing skin tumors was blunted (Boily *et al.*, 2009), and using a *Sirt1*-knockout strain, the mitochondrial function was not increased by resveratrol in skeletal muscle (Price *et al.*, 2012). Moreover, synthetic STACs that are much more specific, such as SRT1720 and SRT2104, have been shown to trigger deacetylation of peroxisome proliferator-activated receptor-γ co-activator 1α (PGC1α) and thus increase mitochondrial biogenesis in a SIRT1-dependent manner (Feige *et al.*, 2008), as well as increase mitochondrial mass in mouse muscle and liver (Mercken *et al.*, 2014; Mitchell *et al.*, 2014).

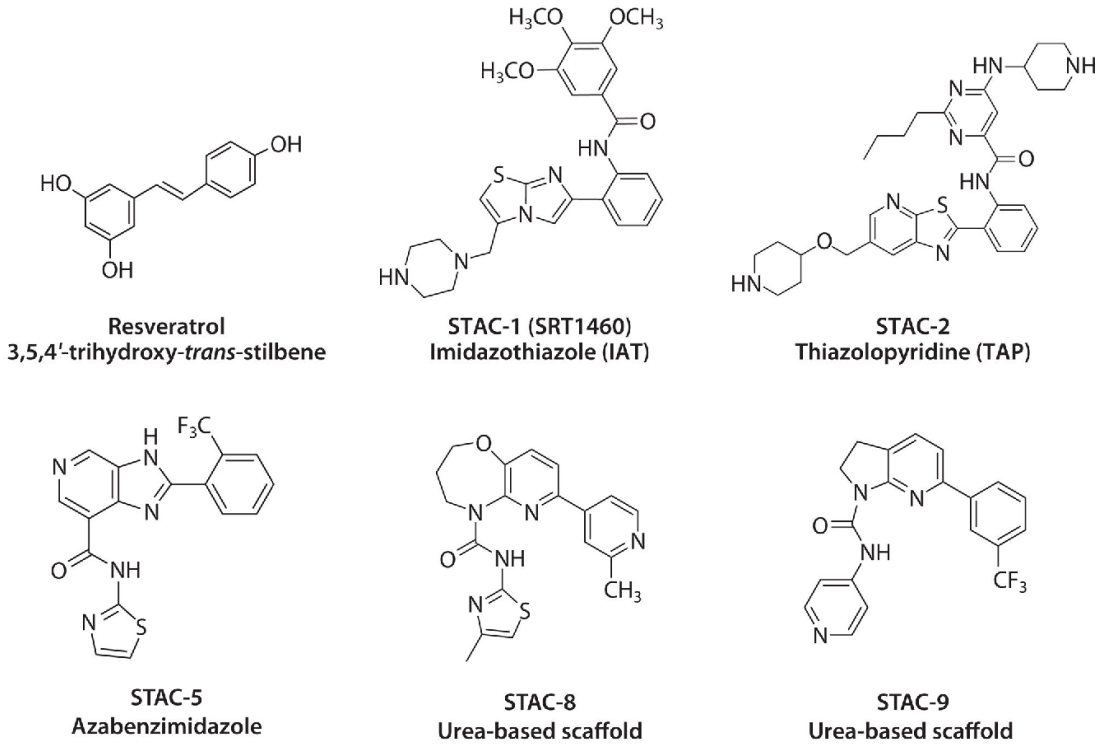

Figure 3.4. Sirtuin activating compounds (STACs) that extend lifespan and/or healthspan. Copied from (Sinclair and Guarente, 2014).

3.2.4. The allosteric activation of SIRT1

Despite the central role of sirtuins in biology, the mechanism by which STACs activate SIRT1 is poorly understood. The original fluorescent-based screens used to discover STACs prompted speculation that SIRT1 was only activated when a bulky and hydrophobic fluorescent moiety was attached to the peptide substrate and therefore acts via an indirect mechanism *in vivo* (Huber *et al.*, 2010; Pacholec *et al.*, 2010; Stünkel and Campbell, 2011; Park *et al.*, 2012). This controversy led to the discovery that SIRT1 has several structural and positional requirements of amino acids adjacent to the acetylated Lys residue for facilitating subtract recognition (Chen *et al.*, 2012) and SIRT1 activation (Borra *et al.*, 2004; Kaeberlein *et al.*, 2005; Dai *et al.*, 2010). The major finding came from the discovery that SIRT1 activation is favored when a large hydrophobic residue is present on the carboxy-terminal side of the acetylated Lys (Lakshminarasimhan *et al.*, 2013). Following these findings, Hubbard and colleagues (Hubbard *et al.*, 2013) used natural peptides as substrates to reveal that bulky hydrophobic amino acids (Trp, Tyr or Phe) at the position +1 and +6 relative to the acetyl-Lys could substitute for the fluorescent groups in the original assays. These results indicated that in order for SIRT1 to recognize its target substrate, specific hydrophobic amino acids should be present adjacent to the target Lys. In the same study, Hubbard and colleagues identified a mutation in SIRT1 (substitution of Glu230 with Lys) that prevented its activation by resveratrol,

as well as more than 100 synthetic STACs indicating that both natural and synthetic STACs activate SIRT1 by a common mechanism.

Contrary to what Zorn and Wells (Zorn and Wells, 2010) have stated, “one of the simplest ways to activate an enzyme with small molecules is to bind to an allosteric site within the catalytic domain of that enzyme and induce a conformational change which changes the affinity of that enzyme for its native substrate”, evidence from crystal structures and enzymological and biophysical studies has indicated that STACs function not by binding within the catalytic domain but by binding to a relatively rigid helix-turn-helix N terminus called the STAC-binding domain (SBD) (Dai *et al.*, 2015). Resveratrol and synthetic STACs physically bind to the N terminus, which itself can activate SIRT1 in *trans* (Ghisays *et al.*, 2015). These data have shown that the N-terminal domain may function to activate SIRT1 in *trans* when SIRT1 is a dimer, or in *cis* enhancing the binding to the SIRT1 catalytic core (Ghisays *et al.*, 2015).

Moreover, crystallographic and amino acid substitution studies in human SIRT1 have identified the residues in which STACs come in contact, suggesting an activation mechanism that is consistent with a “bend-at-the-elbow” model (Dai *et al.*, 2015). STACs bind to the α-helical SBD in the N terminus, leading to the flip over of the domain to the site of interaction between the substrate and catalytic domain (Figure 3.5 A) (Ghisays *et al.*, 2015). The hinge residues Arg234 and Glu230, located within a polybasic linker (KRKKRK), allow the STAC-bound SBD to interact with the catalytic domain through a salt bridge formed between the guanidinium group of the SBD and the carboxylate group of Asp475 and hydrogen bonds to His473 and Val459 (Figure 3.5 B). Briefly, the negatively charged Glu230 makes contact with the positively charged Arg466, explaining why the substitution of Glu230 to Lys (a negative to a positive charge) blocks SIRT1 activation and why subsequent replacement of Arg446 with Glu (a positive to negative charge) restores SIRT1 activation through STACs. Additional work using yeast Sir2, which is the catalytic component of a Sir2-Sir3-Sir4 complex, has provided clues to the mechanism of allosteric activation of sirtuins. Molecular dynamic simulations have suggested that the substrate-binding channel alternate between an open and closed conformation, where Sir4 maintains the N-terminal helix in an active conformation (Hubbard et al. 2013). Remarkably, mammalian the SIRT1 Glu320 residue structurally aligns with a similar negatively charged residue in yeast Sir2 (Asp223), which was shown to be required for gene silencing (Cuperus *et al*., 2002).

(A) Human SIRT1-STAC complex **(B) Suggested model for STAC binding**

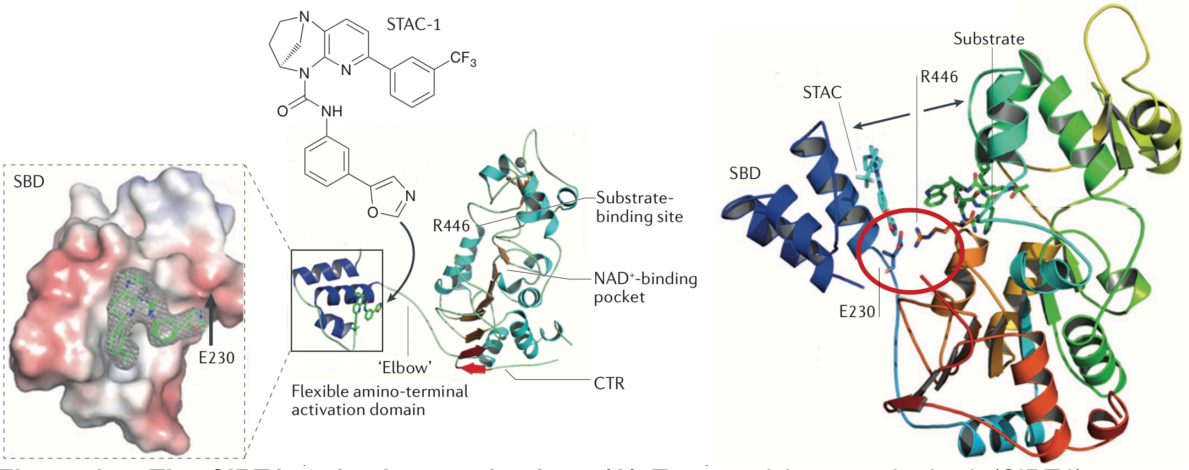

Figure 3.5. The SIRT1 activation mechanism. (A) Truncated human sirtuin 1 (SIRT1) structure coupled with a synthetic sirtuin-activating compound (STAC). The complex shows the binding of STAC-1 at the amino-terminal STAC-biding domain (SBD). The binding of STAC promotes the interaction between the SBD and the central catalytic domain, lowering the K_m for both the substrate and NAD^+, increasing SIRT1 activity. The deacetylase activity is therefore stabilized by the carboxyl-terminal regulatory segment (CTR). Substitution of Glu230 (E230) with a Lys residue impairs the enzymatic activation of SIRT1 by reducing the electrostatic interaction between G230 at the SBD and the Arg446 at the substrate-binding domain. **(B)** Design on the mechanism of SIRT1 activation by STACs. Structural analysis as well as mutagenesis have shown that amino acids Glu230 and Arg446 form a salt bridge (red circle) facilitating the binding of the amino terminal of SIRT1 with the catalytic core (movement illustrated by arrows). Sirtuin-activating compound 1 and an acetylated p53 peptide substrate are represented in cyan and green, respectively. Adapted from (Dai *et al.*, 2015; Bonkowski and Sinclair, 2016).

3.2.5. Unravelling the specificity of SIRT1 activators *in vivo*

Numerous studies have shown the beneficial effects of STACs in a rodent's overall health in a SIRT1-dependent manner; however, how STACs impart these benefits has been hotly debated, with some researchers proposing that direct activation is an artefact of the assays used *in vitro*. Additionally, resveratrol is a nonspecific compound, meaning that it interacts with numerous proteins within the cell (Howitz and Sinclair, 2008). In addition to SIRT1, resveratrol has been shown to target AMPK (Fulco *et al.*, 2008; Canto *et al.*, 2009), phosphodiesterases (Park *et al.*, 2012), F1-ATPase (Gledhill *et al.*, 2007), mitochondrial complex III of the electron transport chain (Zini *et al.*, 1999), PARP1, and Tyr-tRNA synthetase (Sajish and Schimmel, 2015). Clarifying which beneficial effects are mediated by SIRT1 and which are mediated by other players has been a considerable task. For example, whether resveratrol acts on SIRT1 or AMPK. Resveratrol have been shown to activate AMPK through SIRT1-mediated

deacetylation as well as activate AMPK kinase LKB1 (Hou *et al.*, 2008; Ivanov *et al.*, 2008; Lan, Jose M Cacicedo, *et al.*, 2008; Price *et al.*, 2012). Therefore, SIRT1 can activate AMPK and AMPK can activate SIRT1. Interestingly, resveratrol was shown to activate both AMPK and SIRT1 *in vivo*, but the leading target is highly dose-dependent (Price *et al.*, 2012).

The breakthrough in the field came with the identification of a SIRT1 point mutation that blocked STAC activation *in vitro*, providing the perfect means to investigate if beneficial effects mediated by SIRT1 are due STACs activation. Work using human HeLa cells and mouse primary myocytes, both engineered to express the SIRT1-E230K mutation, showed that resveratrol and synthetic STACs (SRT1720 and SRT2014) failed to improve predictable changes in mitochondrial physiology (mitochondrial mass, gene expression, and cellular ATP concentration). With this work, Hubbard and colleagues provided strong evidence to suggest that STACs work by direct activation of SIRT1 (Hubbard et al. 2013).

After it been demonstrated how STACs function *in vitro*, the next step is to address how STACs function *in vivo*, repeating these experiments in a mouse model carrying SIRT1-E230K knock-in mutation.

3.3. Materials and Methods

3.3.1. Generation of SIRT1-E222K mouse model

Based on *Sirt1* cDNA sequence (NM_019812), gene organization, and the predicted functional protein structure, we have disrupted the murine *Sirt1* gene function by inserting a E222K point mutation into exon 3 of the *Sirt1* gene encoding for the HIST1H1E interaction region (figure 3.6). The mutated *Sirt1* gene is expressed under the control of the endogenous murine *Sirt1* promoter (ATG) located in exon 1. The knock-in model was generated by homologous recombination in embryonic stem (ES) cells. For this propose, a targeting vector containing regions homologous to the genomic *Sirt1* sequences was constructed. This vector was generated with a neomycin (NEO) positive selection gene flanked by FRT sites, which was remove *in vivo* using a deleter mice expressing F1p recombinase (figure 3.6). Additionally, the vector was engineered with the presence of the negative selection marker, Diphtheria Toxin A (DTA), to reduce the isolation of non-homologous recombined ES cell clones. Detection of homologous recombination events was performed in two successive steps. First, an initial PCR screening for homologous recombination at the 5' end of the targeting vector was performed. Second, the clones positive for this PCR based screening were further confirmed by 5' and 3' Southern blot analysis.

Linearization of the targeting vector was acheived by restriction enzyme digestion. The resulting fragment was isolated and purified by phenol/chloroform extraction following ethanol precipitation and transfected into ES cells according to genOway's standard electroporation protocol (*i.e.* 5x10^6 ES cells in presence of 40 μg of linearized plasmid, 260 Volt, 500 μF). Positive selection was started 48 hours after electroporation, by adding 200 μg/mL of G418. G418 resistant colonies were selected and screened for homologous recombination.

Based on the ES cell screening results, the recombined ES cell clones were injected into blastocysts isolated from pregnant C57BL/6J females. Blastocysts were then re-implanted into OF1 females and allowed to develop. Approximately 3 weeks later, offspring were born and the contribution of the recombined ES cells to each of them was assessed using coat color markers. Embryonic stem (ES) cells were derived from the inner cell mass from the 3.5-day-old embryos (blastocyst stage). When implanted into blastocyst-stage embryos, these pluripotent cells, are able to colonize the host embryo and contribute to every cell linages of the future animal, including the germ layer.

Embryonic stem (ES) cells used in this work were originally derived from a C57BL/6J mouse strain that have a black coat color. These cells were injected into blastocysts derived from an albino C57BL/6J strain (C57BL/6J-Tyrc-2J/J) that have a white coat color. The resulting offspring were thus chimeras of two different cell types (ES cell-derived cells and

host blastocysts-derived cells) and the degree of chimerism was monitored by the percentage of light and dark patches on these animals.

The generation of F1 animals was performed by breeding chimera males derived from ES cell clones with C57BL/6 F1p deleter females in order to excise the neomycin selection cassette (Neo) and to generate heterozygous mice carrying the Neo-excised knock-in allele. The genotype of the pups derived from the F1 breeding with the F1p deleter mice were tested by PCR to analyze the excision status of the Sirt1 allele after DNA preparation from a tail biopsy as previously described (Montero-Pau and Africa Gómez, 2008). The primer pair used: Forward 5'-3' (TTA CCA GAA ACA ATT CCT CCA CCT GAG C) and Reverse 5'-3' (GAG GCT CTC TTC AGT TTT TAT GAA CAA AGG C), were designed by hybridizing close to the Neo-cassette within the homologous arm to detect the F1p-mediated excision of the neomycin selection cassette. The heterozygous mice were then bred another generation with C57BL/6J wild-type mice in order to generate a pure line of Neo-excised point-mutant mice. The resulting pups were genotyped using the same genotyping strategy as described above.

After reaching sexual maturity, identified male and female heterozygous knock-in mice were interbred to generate the *Sirt1* homozygous point mutant line. PCR genotyping of the F2 generation was performed after DNA isolation from tail biopsies taken from the offspring pups and were genotyped using the same F1p-excision PCR strategy used for genotyping the heterozygous animals. This PCR enabled us to detect both the wild-type and knock-in alleles and thus allows us to discriminate between wild-type, heterozygous, and homozygous knock-in animals. By using the primers previously described in this section, the knock-in allele should yield an amplification product of 394 bp, whereas the wild-type allele should yield an amplification product of 285 bp.

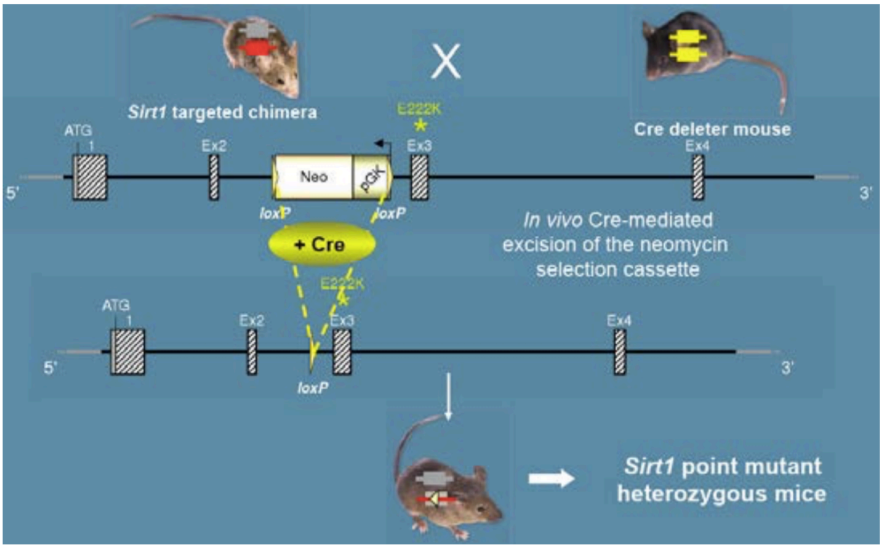

Figure 3.6. The SIRT1-E222K knock-in mouse (C57Bl/6J). Crossing a Cre-deleter mouse removed the neomycin (Neo) targeting cassette leaving behind a single loxP site and altering one amino acid in exon 3 of SIRT1.

3.3.2. Animals, diets and treatments.

Male C57BL/6J wild-type and homozygous knock-in mice bred within the lab's colony were maintained on standard purified mouse diet LabDiet® 5053 for 4 months prior to the start of the experiment. Mice around 4-5 months of age were randomly separated into 6 different groups with an average body weight of 29.3 ± 0.4 grams for each group. The groups presented in this study are WT and SIRT1-E222K (E222K) mice fed a standard diet (SD), WT and E222K fed a high-fat AIN-93G diet (HFD) (modified by the addition of hydrogenated coconut oil to provide 60% of calories from fat, HC), and WT and E222K groups receiving HFD plus 0.04% resveratrol. In this work, coconut oil was chosen over animal fats such as lard to avoid high levels of dietary cholesterol and because using coconut oil allows the possible to add large quantities to the food pellets without changing the consistency since its solid at room temperature. Additionally, using coconut oil helps prevent overgrowth of the teeth, which can be observed with high-fat paste-like diets given over an extended period of time.

Resveratrol (>98%) was purchased from Orchid Pharmaceuticals (Aurangabad, India) and homogeneity mixed during manufacturing of the diets (Dyets Inc., Bethlehem, PA). Chow was kept away from light in order to ensure the stability of resveratrol. Stock resveratrol and all diets were stored in the dark at -80°C and/or 4°C respectively, and the food was provided in cages for no more than 1 week at a time to prevent spoilage. The stability of resveratrol in the stored food was tested several times during the experiment using the Fluor-de-Lys SIRT1 assay (Biomol, Plymouth Meeting, PA). The mice were maintained on a 12-hour light/dark

cycle and maintained between 20-22°C according to animal protocols and NIH guidelines. Food intake and body weight were measured every week during all study.

Metabolic experiments, such as glucose tolerance test (GTT), insulin tolerance test (ITT), homeostatic model assessment – insulin resistance calculator (HOMA-IR) as well as treadmill tolerance test, behavioral tests, comprehensive lab animal monitoring system (CLAMs), and frailty index (FI) were performed at different timepoints of the experiment before harvesting of the tissues. Mice used for survival curves were kept on special diet until they died. Statistical analyses were performed by doing a two-way Cox Multivariate Analysis for main effects of genotype (E222K) and diet (HFD ± Resveratrol) using appropriate software (SPSS, IBM Developer, Armonk, NY, USA), with an alpha level of 0.05. All data are presented as means with standard error of the mean (SEM).

3.3.3. Frailty Index Score

Frailty index was scored as described (Whitehead et al., 2014). Briefly, mice were weighed, and measured their body surface temperature twice at the abdomen using an infrared temperature probe (La Crosse Technology, La Crosse, WI, USA). A hearing test was measured by making sound with a dog training clicker, and a ruler was used to calculate vision capacity. A frailty index score for each mouse was calculated addressing more than 30 clinical signs of frailty using a checklist as previously described (Whitehead et al., 2014). Clinical assessment included evaluation of the integument, digestive/urogenital, ocular/nasal, physical/musculoskeletal, as well as respiratory and discomfort systems. Scores of 0, 0.5, and 1 were used. 0 indicated no sign of a deficit, 0.5 indicated a mild deficit, and 1 indicated a severe deficit. A complete list of the clinical signs evaluated can be found in Appendix 1.

3.3.4. Glucose and Insulin Tolerance Test

For glucose tolerance tests (GTTs), mice that had been fasted overnight received an intraperitoneal dose of 2 g/kg glucose. Immediately before and 15, 30, and 60 min after glucose administration, glucose was measured in retro-orbital blood using a glucose meter (Ascensia Elite, Bayer, Mishawaka, IN, USA). For insulin tolerance test (ITT), mice that had been fasting for 6 hours received an intraperitoneal dose of 0.75 U/Kg body weight of insulin (Novolin® R). Immediately before and 15, 30, and 60 min after insulin administration, glucose was measured in retro-orbital blood using a glucose meter (Ascensia Elite, Bayer). Areas under the curves (AUC) for both glucose and insulin were determined using the “Area Below Curves” function in Sigma Plot 8.0 (Systat, Point Richmond, CA, USA).

3.3.5. Homeostasis Model Assessment (HOMA)

Insulin resistance was estimated using the HOMA2 Calculator software available from the Oxford Centre for Diabetes, Endocrinology, and Metabolism Diabetes Trials Unit website as described (Levy, Matthews and Hermans, 1998).

Blood samples were taken by eye bleeding between 7 AM and 11:00 AM in mice that had been fasting overnight. For insulin measurements, whole blood was spun at 2000 x *g* using a benchtop centrifuge for 20 min at 4ºC to pellet blood cells. The serum was transferred to a fresh tube and placed on dry ice, after which it was stored at -80ºC. Insulin levels were measured from plasma using an ELISA kit (Crystal Chem Inc., Downers Grove, IL, USA).

3.3.6. Endurance Tolerance Test

Endurance tolerance test was conducted between 9:00 AM and 5:00 PM (light phase) in a sound attenuated room, where the mice were acclimatized for 1 h prior to testing. The apparatus was cleaned with 70% ethanol solution after each session.

An electrical stimulation grid was adjusted to 1 mA and the slope was set to 15 degree. During first day in the training, mice walked on the treadmill at 10 m/min speed for 10 min, followed by a 10 min break and then walking again at 10 m/min speed for 10 min. On the second and third days, the initial two steps were same as the first day: walking at 10 m/min speed for 10 min, then a 10 min break. Then, walking was started at 10 m/min and the speed was increased by 1 m/min every minute until a maximum speed of 20 m/min was reached. On Day 4 of the experiment, the animal's maximum exercise endurance was measured. Mice were placed on the treadmill and the belt speed was started at 5 m/min for 5 min to allow the mice warm up. The speed was then increased by 1 m/min until the speed reached 20 m/min. After running for 5 min at 20 m/min, the speed was increased to 21 m/min for 10 min. Then, mice ran at 22 m/min until the mice could no longer perform and thus stayed on the electrical stimulation grid for 10 seconds. Blood collected from tails was taken at pre-exercise and post-exercise and serum lactate levels were measured with a lactate meter (LACTATE PLUS, Nova Biomedical, Waltham, MA, USA).

3.3.7. Metabolic and Physical Activity

The metabolic rate of the animals was monitored by indirect calorimetry in open-circuit oxymax chambers using the Comprehensive Lab Animal Monitoring System (CLAMS; Columbus Instruments, Columbus, OH, USA). Mice were singly housed with water and food available *ad libitum* under a 12-12-hour light-dark cycle at approximately 24°C. The mice were kept in the monitoring cages for 2 days, allowing them to acclimatize before the last 24h when the parameters were analyzed.

Sample air was pumped through the test chambers, equipped with an oxygen (O_2) sensor for determination of O_2 content. Oxygen concentration in the air entering the chamber compared with air leaving the chamber allowed for the determination of O_2 consumption. The percentage of O_2 and CO_2 gas levels in each chamber environment was measured periodically and the changes observed in these levels were used to determine O_2 consumption (VO_2), CO_2 production (VCO_2), respiratory exchange ratio (RER), and heat.

Spontaneous activity measured by both horizontal (XAMB) and vertical (ZTOT) movements was also monitored. The system is equipped with infrared beams able to monitor all of the chamber's axes. The beams were horizontally 130 mm apart in order to provide a greater resolution grid covering the XY-planes. The data were recorded and presented in terms of the number of "beam breaks".

3.3.8. Magnetic Resonance Imaging

Measurements of the lean body mass and fat mass were acquired in live mice by magnetic resonance imaging using the EchoMRI™-100H (Echo Medical Systems). Mice were scanned using a primary accumulation level of 1 and the water stage was excluded.

3.3.9. Grip Strength Test

To measure muscular strength, a grip strength test was used (BIO-G53, Bioseb, USA). A mouse was held by the tail and allowed to hold onto a mesh grip with its front paws. Grip strength was assessed by pulling the mouse backwards by the tail until its grip was liberated. The experiment was repeat 3 times after 10 min breaks.

3.3.10. Behaviour experiments

All behavioral tests were conducted between 9:00 AM and 5:00 PM (light phase) in a sound attenuated room, where the mice were acclimated for 1 h prior to the experiments. The apparatus and objects were cleaned with 70% ethanol solution after each session. The behavior testing was video-monitored and recorded using the video tracking system and analyzed using appropriate software (TopScanLite, CleverSys Inc, Reston, VA, USA).

3.3.10.1. Open Field Test

The open field test consists in a simple sensorimotor test, commonly used to determine spontaneous and locomotor activity, as well as, exploration habits in mice. After habituation in the test room, nice were placed in the center of a chamber (48.5 cm x 48.5 cm) and allowed to freely move for 1 h to assess their exploration in the novel environment. Exploratory activity in the peripheral area and total activity in the chamber were recorded using a video tracking system and analyzed using appropriate software (TopScanLite).

3.3.10.2. Y-maze Spontaneous Alternation Test

Y-maze spontaneous alternation test is a behavioural assay used for measuring the willingness of the mouse to explore new environments. Mice characteristically favour to explore the novel arm rather than return to the one formerly visited. The test occurs in a Y-shape maze with three plastic arms at 120º angle from each other. Mice were placed in the Y-maze apparatus in the testing room with visual cues on the walls and allowed to explore the Y-maze apparatus for 5 min during which time one arm was blocked. After a 15-minute rest period, the mice re-explored for 5 min the Y-maze apparatus, but now with all the arms opened. We measured the number of entries and the time spent in the novel arm as a measure of short spatial and working memory using the video tracking system and analyzed using appropriate software (TopScanLite).

3.3.10.3. Light-Dark Transition Test

The light-dark transition test (LDT) was used to evaluate anxiety-related behavior of mice. This test is based on the natural repulsion of mice to brightened areas as well as on their empirical behavior in response to minor stressors such as a change in the environment and light. The LDT apparatus comprises a box divided into a small (one third) dark chamber and a big (two thirds) brightened chamber. Mice were placed into the brightly-lit compartment and allowed to explore for 10 min. We measured latency to enter to the dark compartment and the total time spent in the brightly-lit compartment as a measure of anxiety-like behavior. Transition between both compartments were measured as index of activity-exploration of the mouse. Their behavior was recorded using the video tracking system and analyzed using appropriate software (TopScanLite).

3.3.11. mtDNA copy number

Snap frozen tissues were placed in a 1.5 mL eppendorf containing 0.6 mL lysis buffer [10 mM Tris-HCl (pH 8.0), 1 mM EDTA, and 0.1% SDS] and 0.06 mL of a 15 mM proteinase K solution (P2308, Sigma-Aldrich, St Louis, MO, USA), and incubated at 55 ºC overnight. Lysate solutions were vortex vigorously and the non-soluble fraction was pelleted by centrifugation (8000g, 15 min). The consequent supernatant was transferred to a new tube and an equal amount of phenol/chloroform/isoamyl alcohol (24:4:1) (PCIAA) was added. After mixing, samples were centrifuged (8000g, 15 min), and 0.45-0.5 mL of the supernatant was transferred to a new tube. An equal volume of chloroform was added to the supernatant, the solution was vigorously vortexed and centrifuged (8000g, 15 min). The 0.4 mL resultant supernatant was transferred to a new tube and mixed with 0.04 mL NaAc (3 M) and 0.44 mL isopropanol. The tube was incubated at -20 ºC for 1m min to facilitate DNA precipitation and then centrifuged (8000g, 15 min) to pellet the DNA. Pelleted DNA was finally washed with 1

mL of 70% ethanol, air dried and dissolved in Tris-EDTA (TE) buffer. The primers were designed targeting 18S ribosomal and COX2 genes and were used to calculate the ratio of mtDNA to genomic DNA. Primers used were as follow: mouse 18S, 5`-TGTGTTAGGGGACTGGTGGACA-3` (Forward) and 5`-CATCACCCACTTACCCCCAAAA-3` (Reverse), mouse COX2, 5`- ATAACCGAGTCGTTCTGCCAAT-3` and 5`-TTTCAGAGCATTGGCCATAGAA -3` (reverse).

3.3.12. Gene Expression

Total RNA was extracted from tissue using TriPure reagent according to the product manual. Total RNA was transcribed to cDNA using QuantiTect Reverse Transcription Kit (Qiagen). Expression of selected genes was analyzed using the LightCycler480 system (Roche) and LightCycler® 480 SYBR Green I Master reagent (Roche). The acidic ribosomal protein 36b4 gene (ribosomal protein, large, P0, Rplp0) was used as a housekeeping reference. Primer sets for quantitative real-time PCR analyses are shown in Table 1.

3.3.13. Metabolite Measurements

Serum concentration of ALT, AST and Cholesterol were analyzed using a Vitros 350 blood analyzer.

3.3.14. Cytokines Measurements

Serum TNF-α was analyzed using a BD™ CBA Mouse Th1/Th2/Th17 Cytokine (BD Biosciences, San Jose, CA, USA).

3.3.15. Statistical analysis

Data were analyzed by a two-way ANOVA with multiple comparisons. Statistical tests were performed with GraphPad Prism (San Diego, CA, USA). Survival curve was analyzed by a two-way Cox Multivariate Analysis for main effects of genotype and diet using appropriate software (SPSS, IBM Developer, Armonk, NY, USA). Data are presented as means ± SEM.

3.4. Results

One of the most consistent effects of resveratrol and synthetic STACs in mice is the protection from the deleterious effects of a high fat diet (HFD). Previous studies have clearly shown that resveratrol protects mice from the undesirable effects of HFD (Baur *et al.*, 2006; Lagouge *et al.*, 2006).

The discovery that an activation-defect mutant of SIRT1 (human E230K and mouse E222K) has allowed us for the first time to test which beneficial effects of STACs are mediated by direct SIRT1 activation. Previous work has shown that SIRT1-E222K is resistant to activation by resveratrol *in vitro*, blocking the effects of resveratrol in primary cells (Hubbard *et al.*, 2013). Next, we wanted to test whether these effects translate into *in vivo* models.

3.4.1. Resveratrol increased survival in WT but not in SIRT1-E222K mice

Our initial goal was to test the natural compound resveratrol in SIRT1-E222K mouse, since the compound has been extensively characterized (Lagouge *et al.*, 2006; Hubbard *et al.*, 2013).

To test the chronic effect of resveratrol treatment, 4-5-month-old male mice (WT and SIRT1-E222K) were fed with 60% HFD with and without resveratrol (400 mg/kg food) for 34 weeks and/or during all of their lifespan. As expected, mice on HFD gained much more weight as compared to mice on SD during the study. Surprisingly, there was no significant difference in weight gained as well as in food intake between the HFD groups (Figure 3.7).

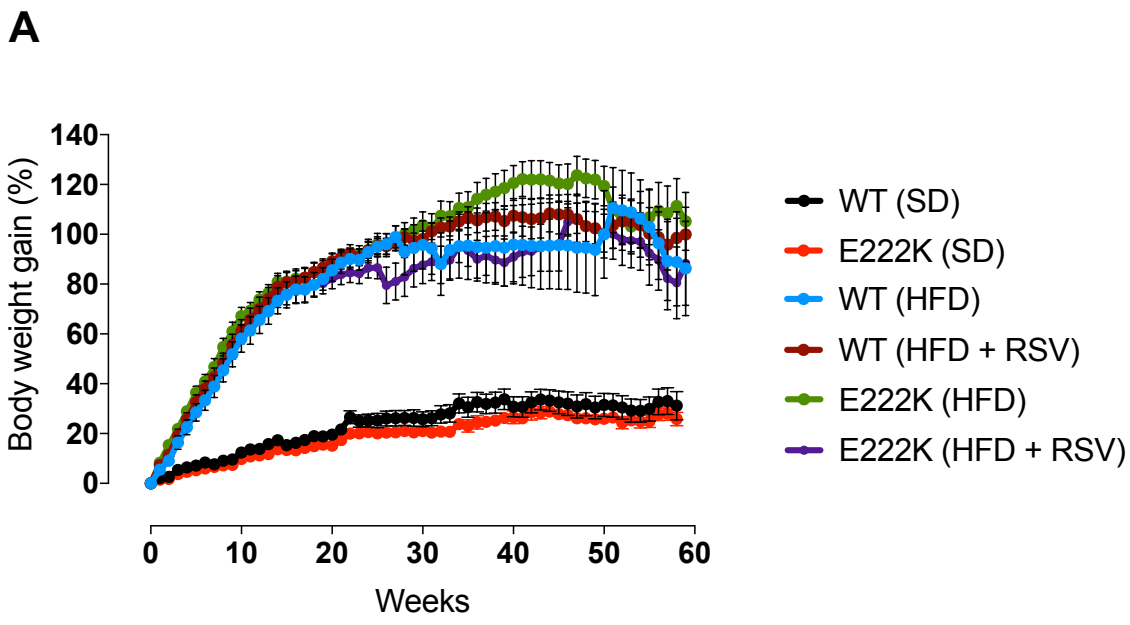

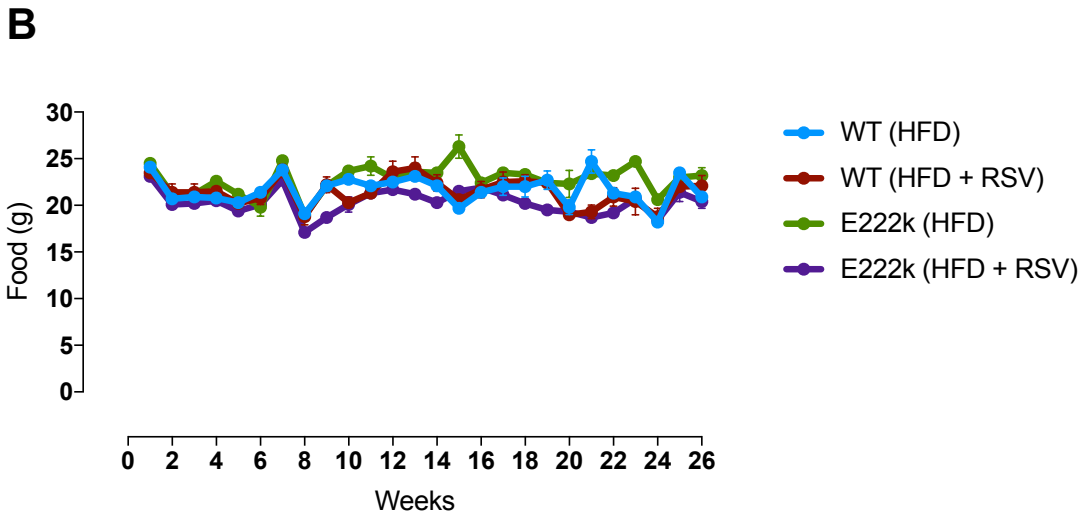

Figure 3.7: **HFD-fed mice gained weight without changes in food intake**. (A) Percentage of body weight gain. (B) Food intake. N= 15-20 mice/group.

At 300 days of age the survival curves of WT fed HFD without resveratrol, SIRT1-E222K fed HFD with and without resveratrol started to diverge from the WT fed HFD with resveratrol and remained separated by a 11-12-month interval (Figure 3.8 A). Importantly, in agreement with resveratrol increased survival, it is important to note that health status, measured by frailty index, was improved in WT mice feed with resveratrol, but not in any other group (Figure 3.8 B).

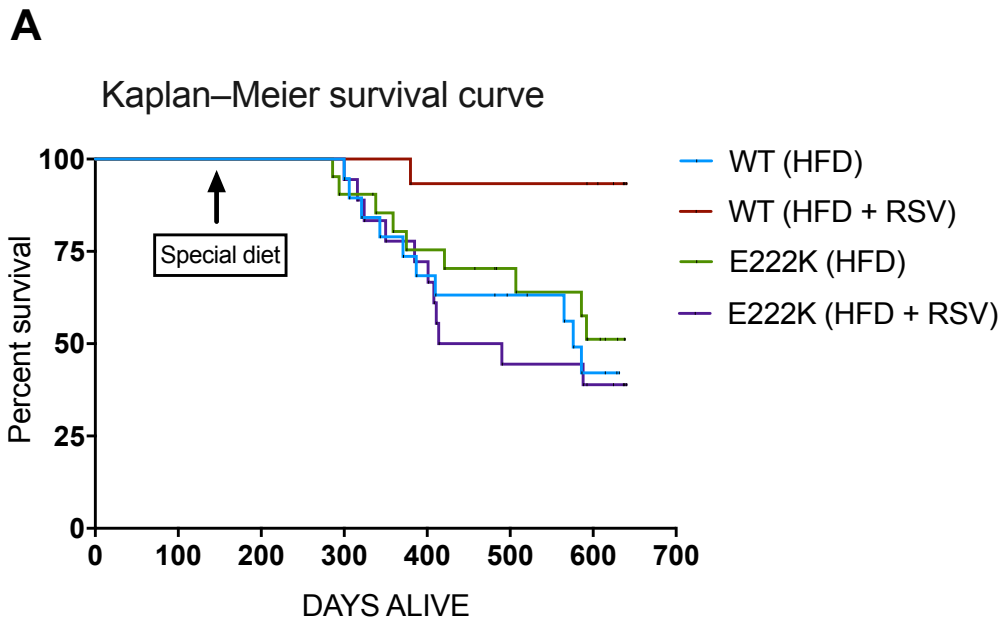

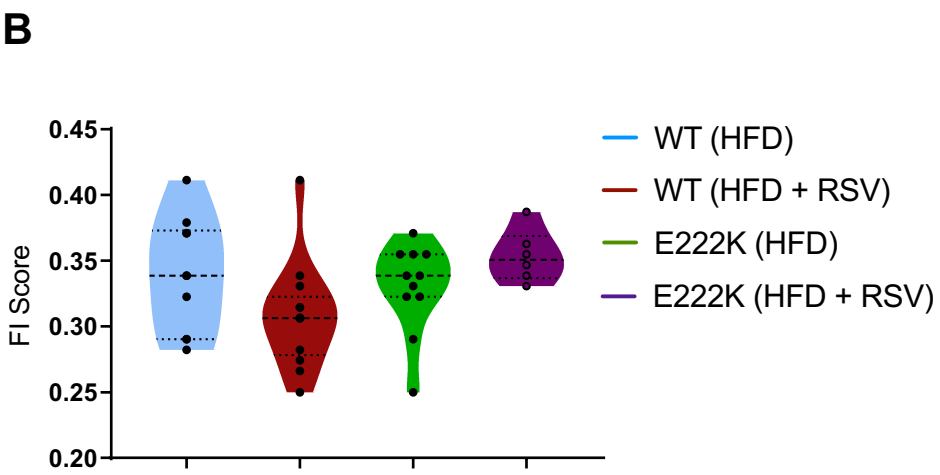

Figure 3.8: Resveratrol increased survival and health in WT but not SIRT1-E222K mice. (A) Kaplan-Meier curve with survival for all groups. Two-way Cox Multivariate Analysis for main effects of genotype (E222K) and diet (HFD ± Resveratrol). Interaction: *p = 0.037. n= 15-20 mice/group. (B) Frailty index score. Two-way ANOVA Tukey's multiple comparisons test. Interaction: *p = 0.0321. n = 6-11 mice/group, 40 weeks on HFD. Values are mean ± SEM.

3.4.2. Resveratrol improves insulin sensitivity, conferring hepatic protection and decreasing inflammation

Human lifestyle is associated with high-calorie diets and is related with numerous pathological conditions, such as increased glucose and insulin levels that can lead to diabetes, cardiovascular diseases, and non-alcoholic fatty liver diseases, a condition without any effective treatment (Siebler and Galle, 2016).

Exposure of HFD or diet-induced obesity leads to a chronic inflammation response, which is believed to be critical for the development of glucose intolerance and insulin resistance (Hotamisligil, 2006), and resveratrol has been shown to reduce levels of inflammatory cytokines in different models of HFD-induced obesity (Jeon *et al.*, 2012; Andrade *et al.*, 2014; Ding *et al.*, 2018).

Accordingly, levels of TNF-α, one of the major pro-inflammatory cytokines, was significantly elevated in serum from mice on a chronic HFD; however, resveratrol was able to reduce those levels both in WT and SIRT1-E222K mice (Figure 3.9), revealing that the beneficial effect of resveratrol lowering inflammatory markers in HFD-induced obesity is not E222K-dependent.

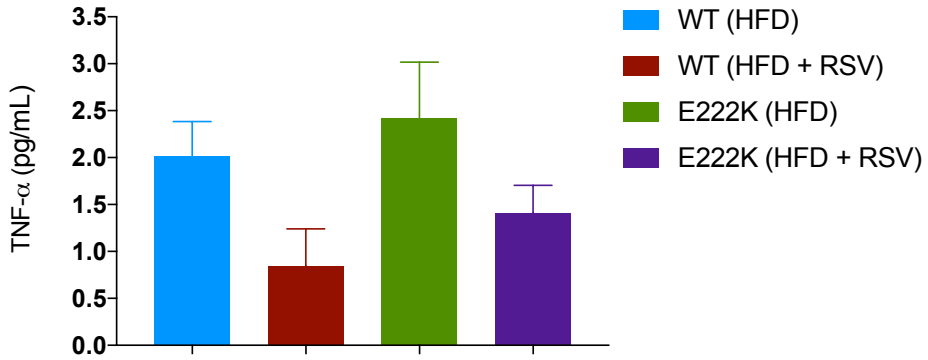

Figure 3.9: Resveratrol decreased inflammation independent of the E222K residue. Serum TNF-α levels in HFD-fed mice. Two-way ANOVA Tukey's multiple comparisons test. Diet: *p = 0.0230. n = 4 mice/group, 34 weeks on HFD. Values are mean ± SEM.

Assessments of liver function, via alteration in plasma levels of markers that predict the onset of diabetes and shortened lifespan were also measured. Transaminases alanine aminotransferase (ALT) and aspartate aminotransferase (AST), which are released into circulation following hepatocellular damage, both indicate compromised liver function in HFD fed mice. Treatment with resveratrol reduced ALT in WT but not in SIRT1-E222K animals (Figure 3.10 A) whereas resveratrol reduced levels of AST both in WT and SIRT1-E222K (figure 3.10 B), leading us to conclude that hepatic protection of resveratrol in liver is, at some extent, E222K-dependent. Additionally, total cholesterol levels (TC) in HFD-fed mice were lower in resveratrol groups independent on the genotype (Figure 3.10 C). These data suggest that resveratrol prevented HFD-induced lipid disturbance inflammation.

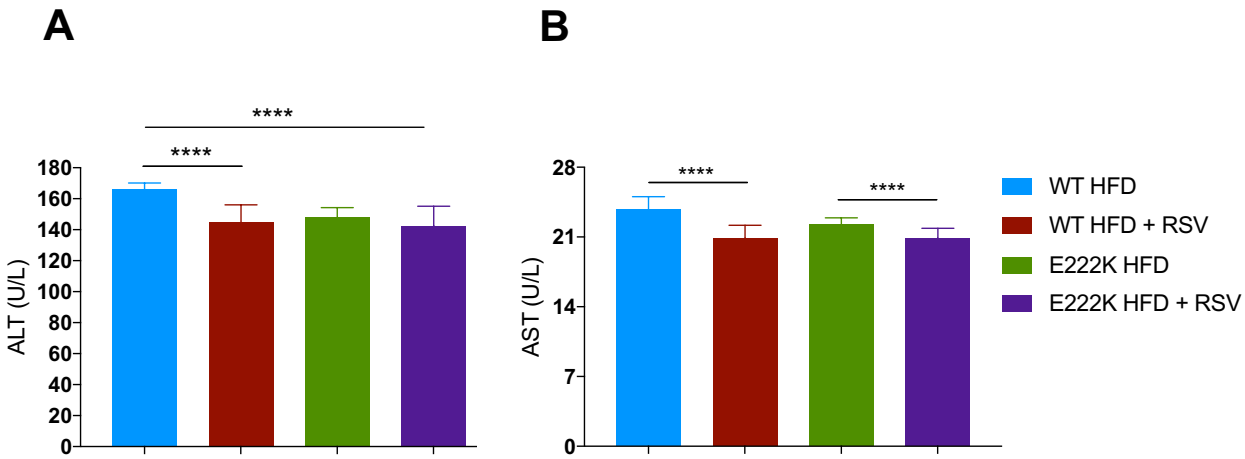

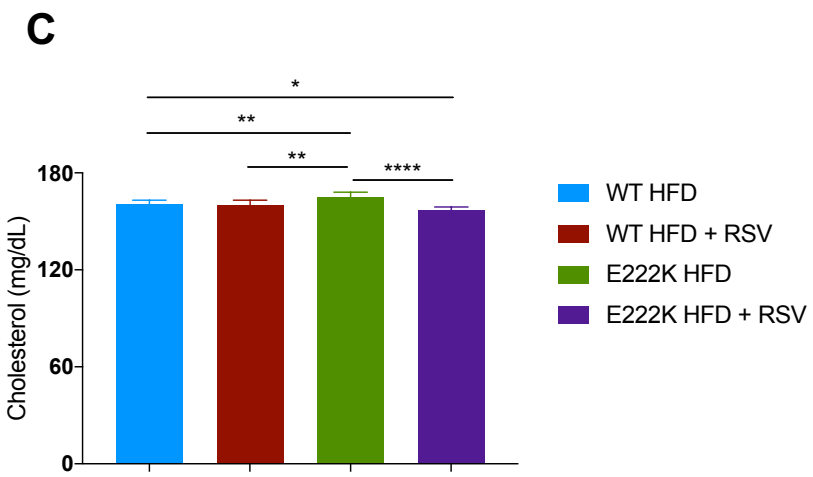

Figure 3.10: Resveratrol protected mice from hepatic inflammation. (A) Alanine Aminotransferase. Two-way ANOVA Tukey's multiple comparisons test. Interaction: **p = 0.0093, Diet: ****p < 0.0001, Genotype: **p = 0.0013. (B) Aspartate Aminotransferase. Two-way ANOVA Tukey's multiple comparisons test. Diet: ****p < 0.0001. (C) Cholesterol. Two-way ANOVA Tukey's multiple comparisons test. Interaction: ***p = 0.0004, Diet: ****p < 0.0001. n = 8-10 mice/group, 34 weeks on HFD. Values are mean ± SEM.

Moreover, one of the most reproducible effects of resveratrol in mice treated with HFD is increased insulin sensitivity (Baur *et al.*, 2006; Lagouge *et al.*, 2006; Knight *et al.*, 2011), and additional findings have shown that the same may be true for humans (Peeters *et al.*, 2008; Weyrich *et al.*, 2008; Zillikens *et al.*, 2009; Timmers *et al.*, 2011).

To access the protective effects of resveratrol against chronic HFD exposure on glucose homeostasis in more detail, we questioned if insulin sensitivity was improved by resveratrol treatment after 10 weeks on HFD. To assess the insulin sensitivity in these mice, we performed both GTT and ITT tests. As shown in figure 3.11, after intraperitoneal administration of glucose the WT mice fed HFD and resveratrol had better glucose and insulin tolerance as compared to WT controls fed HFD, which is in agreement with previous findings. However, SIRT1-E222K animals showed no response to resveratrol treatment: E222K mice fed with HFD with or without resveratrol had similarly high glucose and insulin levels in blood (Figure 3.11 A-B). Fasting insulin measurements showed that WT mice fed HFD on resveratrol had significantly lower fasting insulin levels, while resveratrol had no effect in SIRT1-E222K mice fed HFD, indicating the expected protection of resveratrol in an HFD-induced systemic glucose intolerance, a mechanism dependent on E222K residue. We also calculated HOMA (homeostatic model assessment) index, in order to evaluate beta cell function and insulin sensitivity, calculated from stimulatory models of GTT and ITT. Resveratrol lowered HOMA-

IR index significantly in WT mice fed HFD (Figure 3.11 C) but had no effect on SIRT1-E222K mice. Overall, SIRT1-E222K mice fed HFD showed a trend in higher fasting insulin levels and HOMA index as compared to WT mice fed HFD.

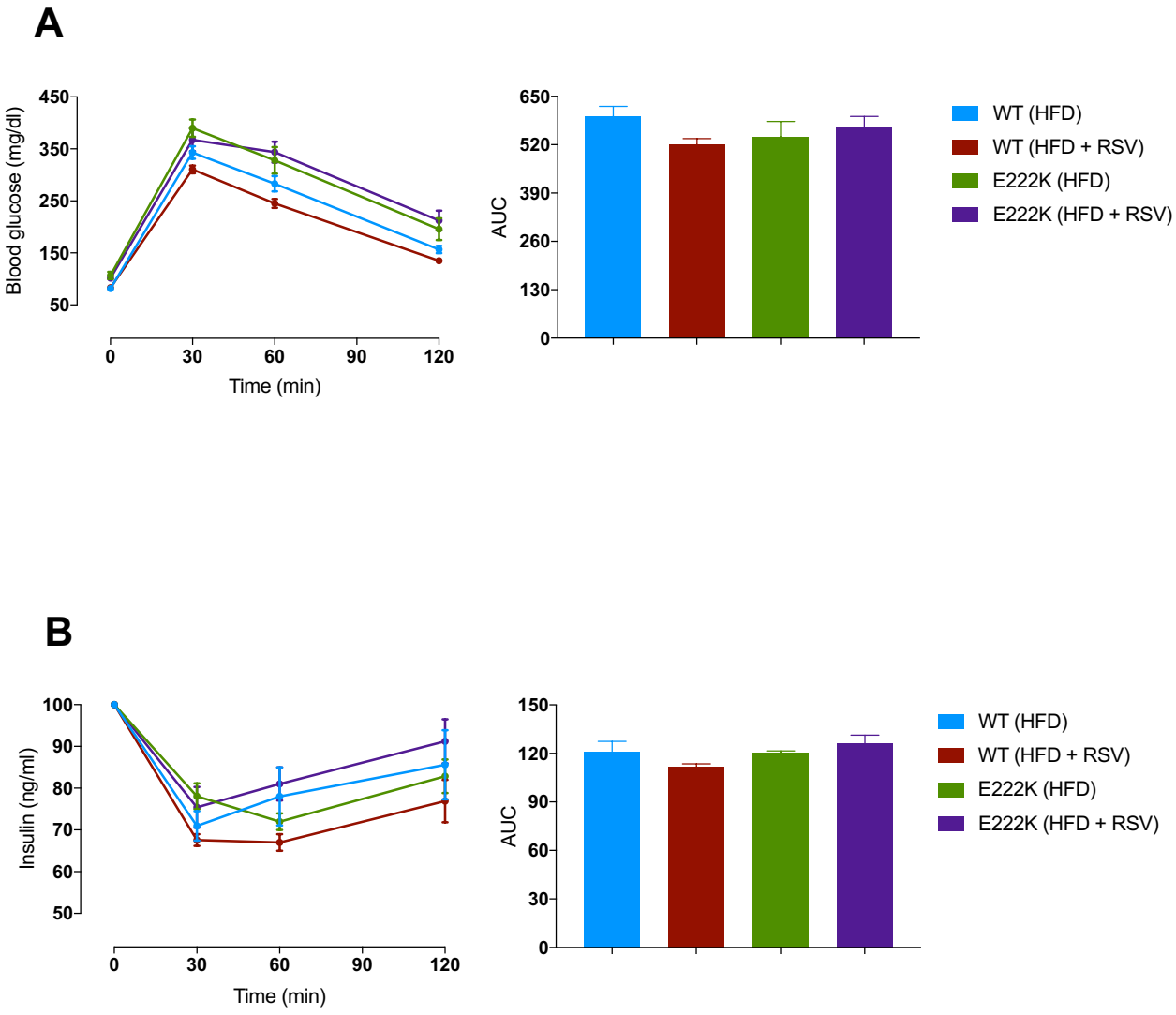

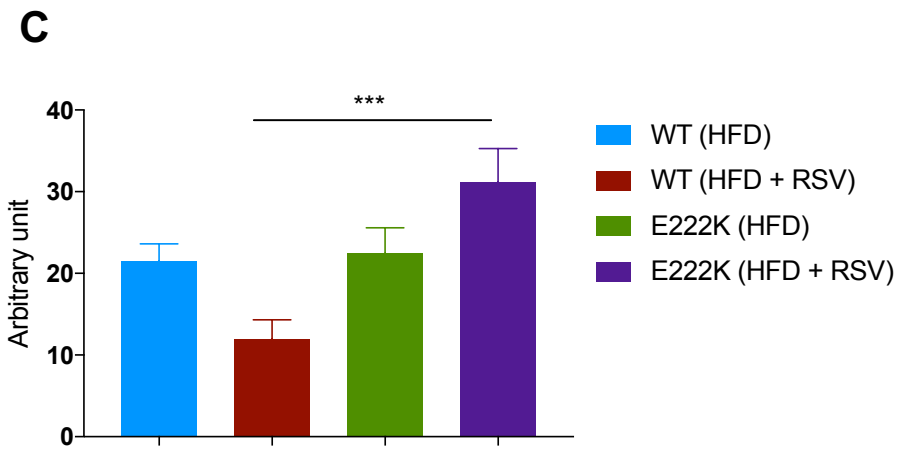

Figure 3.11: Resveratrol protected WT but not SIRT1-E222k mice from HFD-induced hepatic glucose intolerance. (A) Glucose tolerance test with blood glucose levels (left) and area under curve (right). Two-way ANOVA Tukey's multiple comparisons test. Interaction: p = 0.0890. n = 5-6 mice/group, 9 weeks on HFD. (B) Insulin tolerance test with blood insulin levels (left) and area under curve (right). Two-way ANOVA Tukey's multiple comparisons test. Interaction: p = 0.1092. n = 5-6 mice/group, 10 weeks on HFD. (C) HOMA-IR. Two-way ANOVA Tukey's multiple comparisons test. Interaction: **p = 0.0043, Genotype: **p < 0.0019. n = 7-10 mice/group, 17 weeks on HFD. Values are mean ± SEM.

3.4.3. Resveratrol improved endurance in WT mice but not in SIRT1-E222K mice

In muscle and liver the STACs increase mitochondrial function, fatty acid oxidation, produce a shift in muscle type towards oxidative fibers, reduce inflammation, and increase endurance on a treadmill (Lagouge *et al.*, 2006; Milne *et al.*, 2007; Feige *et al.*, 2008; Yamazaki *et al.*, 2009; Price *et al.*, 2012).

Consistent with the literature, the distance run to exhaustion in WT mice on high-fat and resveratrol diets was higher, as compared with every other group (Figure 3.12 A). It is important to note that SIRT1-E222K mice fed HFD remained at the level of WT controls fed HFD even after treatment with resveratrol. Analysis of lactate content in the blood post-exercise, which correlates with oxidative capacity of the muscles, showed that resveratrol reduced lactate levels in WT mice but not SIRT1-E222K mice (Figure 3.12 B), consistent with the hypothesis that resveratrol improves endurance via direct allosteric activation of SIRT1. However, grip strength analysis did not show improved muscle strength WT mice on HFD treated with resveratrol (Figure 3.12 C).

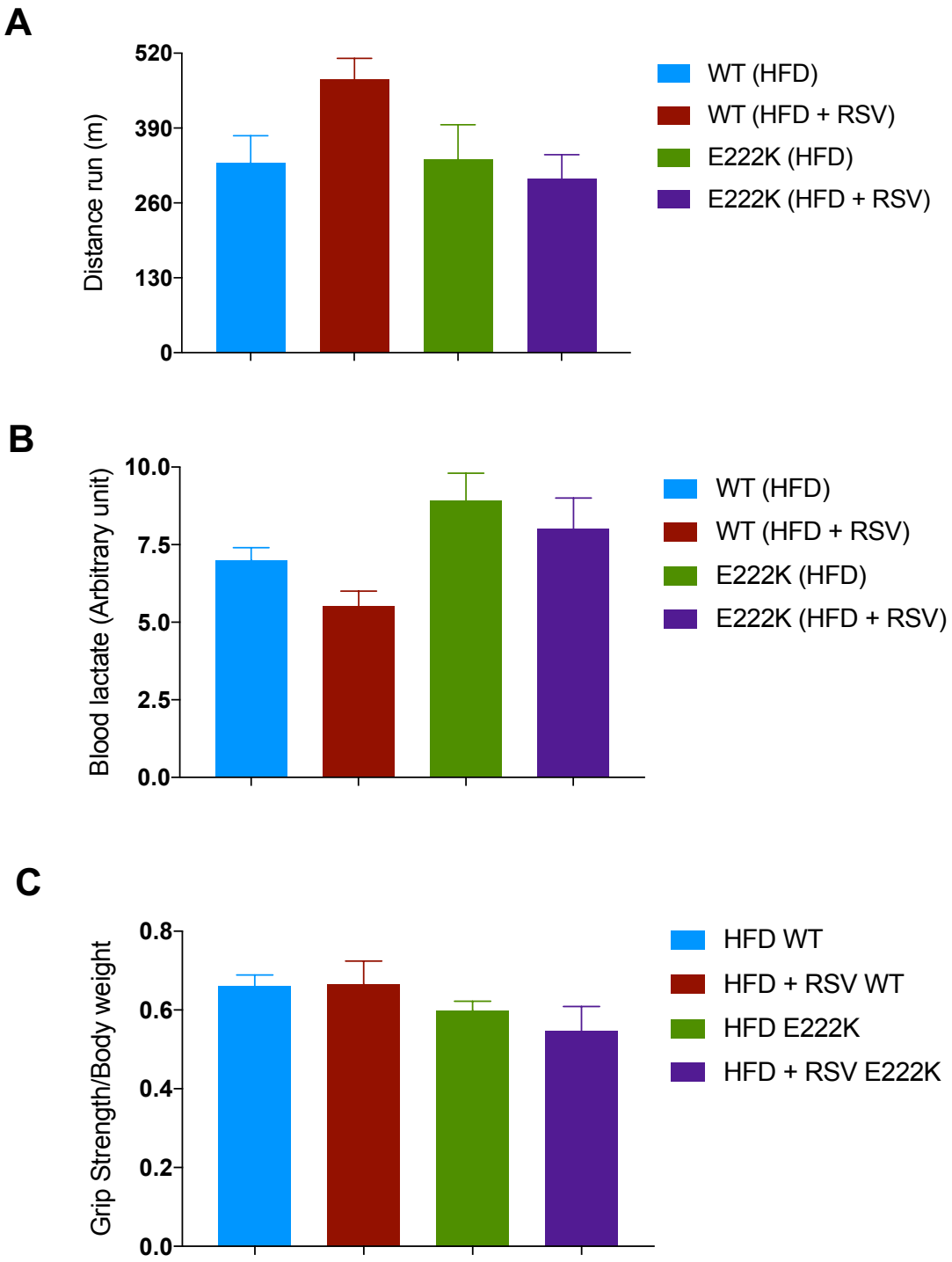

Figure 3.12: Resveratrol enhanced endurance and oxidative capacity in WT but not SIRT1-E222K mice. (A) Distance run until exhaustion. Two-way ANOVA Tukey's multiple comparisons test. Interaction: $p = 0.0825$. n = 5-6 mice/group, 11 weeks on HFD. (B) Lactate levels after run. Two-way ANOVA Tukey's multiple comparisons test. Genotype: $^{**}p < 0.0088$. n = 5-6 mice/group, 11 weeks on HFD. (C) Grip strength. Two-way ANOVA Tukey's multiple comparisons test. Genotype: $p = 0.0667$. n= 8 mice/group, 32 weeks on HFD. Values are mean ± SEM.

Because SIRT1 has been reported to be required to increase physical activity in response to CR (Chen *et al.*, 2005), we further investigated whether resveratrol-mediated increase in resistance to muscle fatigue was a result of a behavioral response or a metabolic consequence.

In agreement with no observed differences in body weight, we also did not find any changes in respiratory exchange ratio related among the groups (Figure 3.13 A). We did, however, observe that the energy source that the mice were using was mostly fat (RER around 0.7), which normal in HFD-fed mice. Moreover, the epididymal fat pad mass measurements showed no difference among either genotype or treatment (Figure 3.13 B).

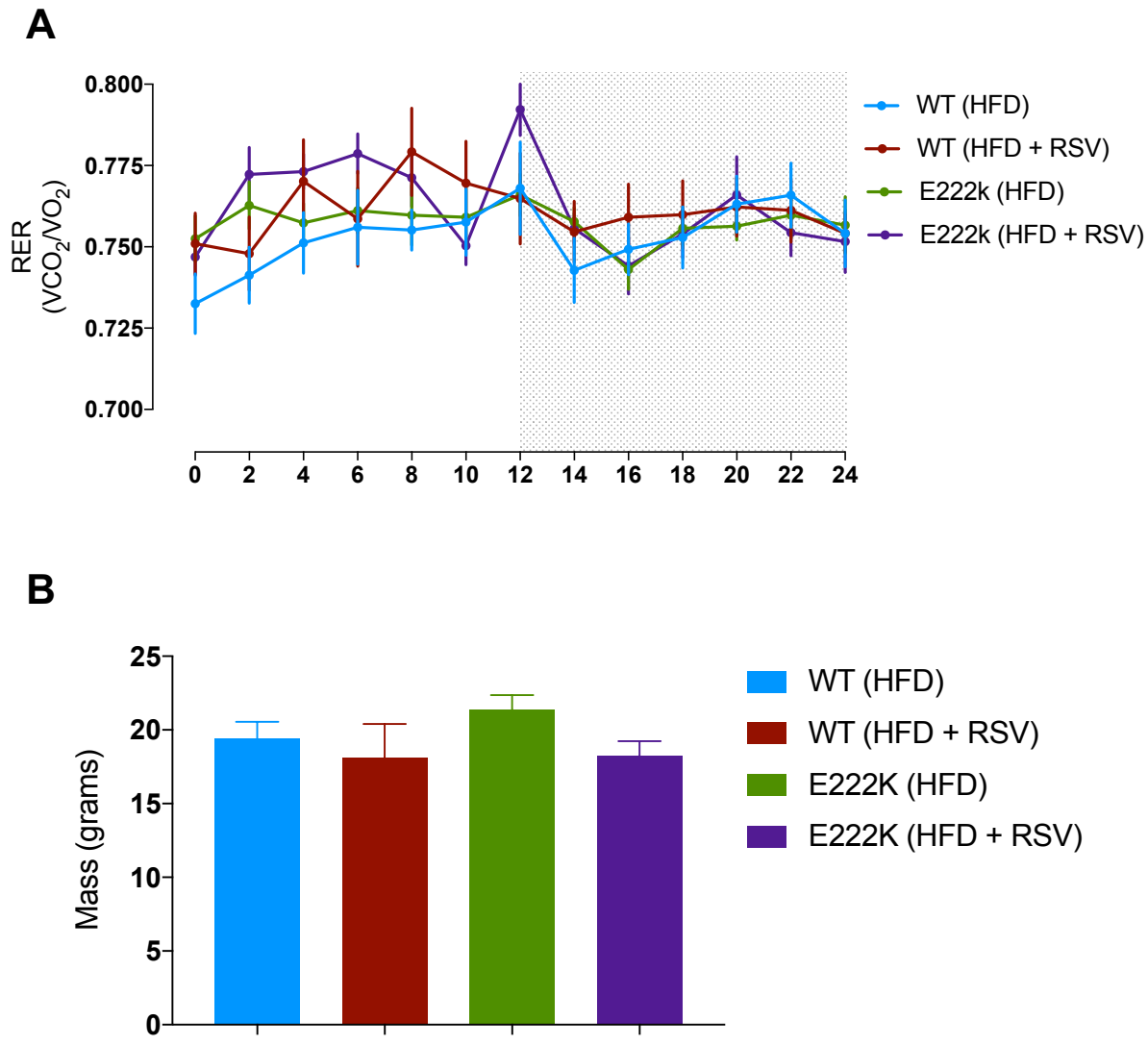

Figure 3.13: Resveratrol does not alter RER nor fat mass in HFD-fed mice. (A) Respiratory exchange ratio (RER). n= 8 mice/group, 28 weeks on HFD. (B) Fat mass. Two-way ANOVA Tukey's multiple comparisons test. n= 8 mice/group, 30 weeks on HFD. Values are mean ± SEM.

Next, we examined the effect of resveratrol on spontaneous activity in mice, by measuring their circadian locomotor activity. In X-axis analysis (XAMB, which includes grooming and feeding movements performed in a horizontal position) during the dark period, we could observe that resveratrol increased ambulatory activity in WT but not in E222K mice fed HFD. Regarding Y-axis analysis (ZTOT, which includes grooming movements performed in a vertical position), we also observed that resveratrol increased ambulatory activity in WT but not in E222K mice on HFD during the dark period (Figure 3.14 A-B).

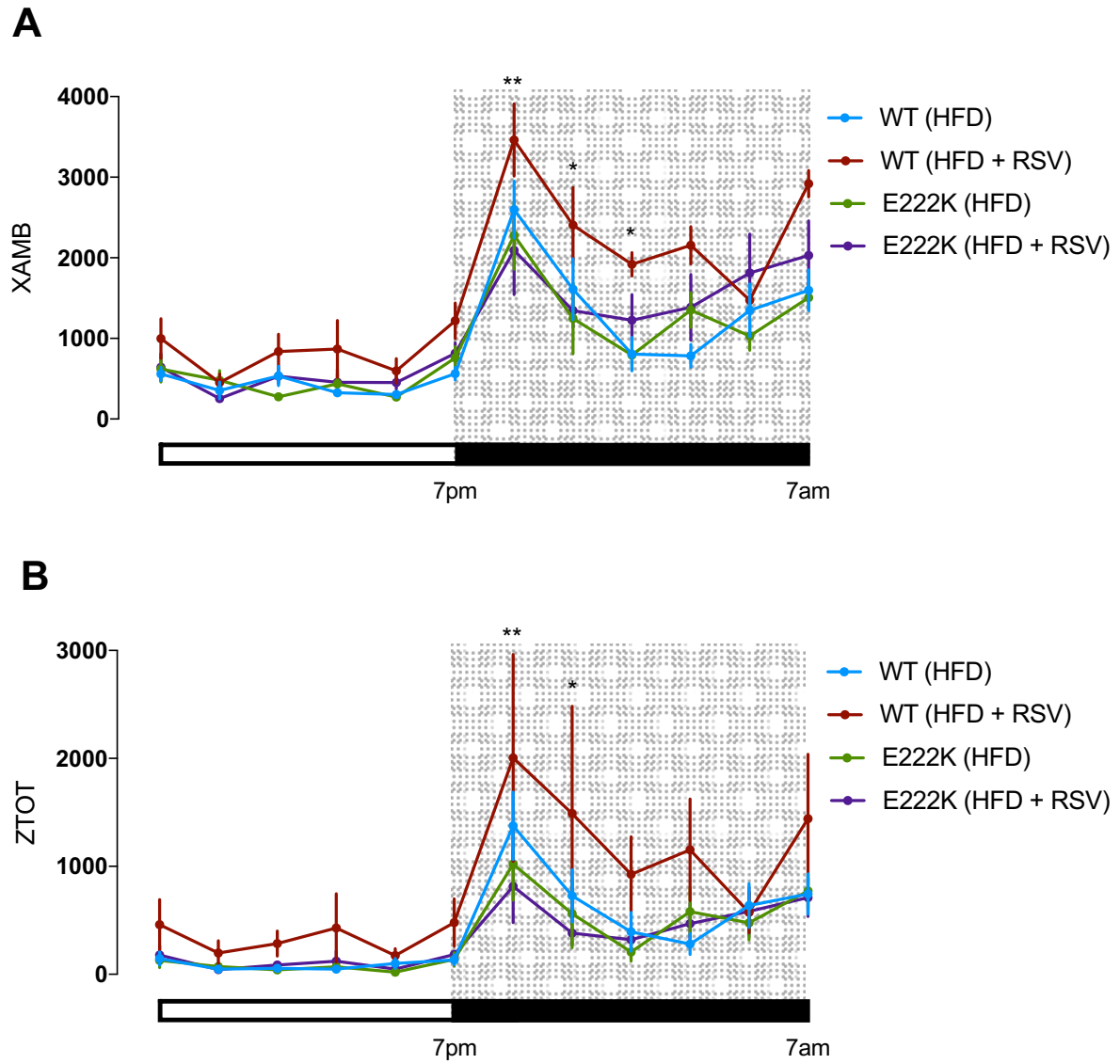

Figure 3.14: Resveratrol increased physical activity in WT but not SIRT1-E222K mice. (A) Representative histogram from the ambulatory activity count (last 24h). (B) Representative histogram from the vertical motor activity (last 24h). Significances were determined using an un-paired two-way ANOVA with Tukey's multiple comparisons test. *p < 0.05. n= 8 mice/group, 28 weeks on HFD. Values are mean ± SEM.

To discount the potential role of central nervous system (CNS)-mediated behavioral changes and to determine the effects of resveratrol treatment on other motor abilities, we next assessed anxiety and sensorimotor function. The observed behavior on spontaneous activity could be due increased cognition or to increased anxiety, the latter seemed unlikely to us because the results shown are only from the last 24h and the mice were in the metabolic cages for 4 days.

No significant differences were observed between genotype or treatment on anxiety or cognition, as evaluated by open-field (Figure 3.15 A), light/dark box (Figure 3.15 B), and Y-maze (Figure 3.15 C).

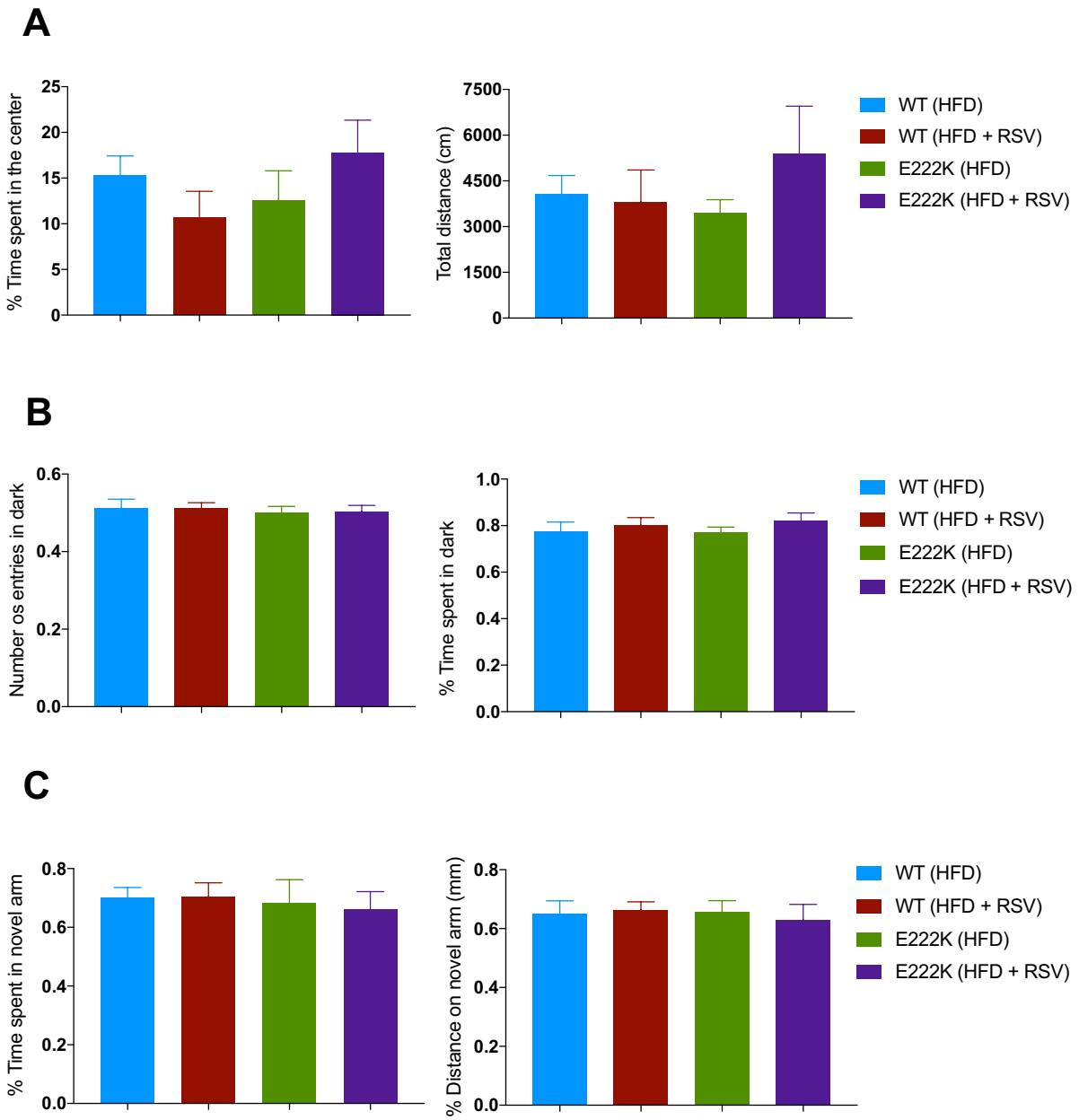

(Legend next page)

Figure 3.15: **Resveratrol-mediated increased in physical activity is not explained altered cognition.** (A) Open field test with time spent in the center (left) and total distance traveled (right). (B) Light-dark transition test with number the entries in dark (left) and total time spent in the dark (right). (C) Y-maze spontaneous test with time spent in novel arm (left) and total distance traveled in the novel arm (right). Significances were determined using an un-paired two-way ANOVA with Tukey's multiple comparisons test. n= 8 mice/group, 32 weeks on HFD. Values are mean ± SEM.

3.4.4. Exercise combined with resveratrol supplementation improved skeletal muscle mitochondrial biogenesis in WT but not in SIRT1-E222K mice

To investigate the relationship between muscle metabolic adaptation and mitochondrial quantity, we quantified mtDNA via RT-PCR analysis. The mtDNA content (normalized by genomic DNA) was upregulated in soleus from WT mice with resveratrol comparing to WT control, both on HFD (Figure 3.16 A). SIRT1-E222K mtDNA levels remained at the level of WT controls even after treatment with resveratrol.

Considering that PGC-1α is the master regulator of mitochondrial biogenesis (Benton, Wright and Bonen, 2008), we further investigated the hypothesis that mitochondrial activity was affected by resveratrol supplementation by measuring the expression of PGC-1α and its downstream transcription factors in soleus muscle. As shown in figure 3.16 B, the mRNA expression levels of PGC-1α did not changed upon resveratrol treatment in the both WT and SIRT1-E222K groups (Figure 3.16 B). Also, the expression levels of the downstream transcription factor of PGC-1α, nuclear respiratory factor 1 (NRF-1) (Patti *et al.*, 2003; Mootha *et al.*, 2004), was not altered by resveratrol in none on the groups (Figure 3.16 B). Finally, mitochondrial transcription factor A (TFAm), a nuclear encoded mitochondrial transcription factor that is essential for the expression of mitochondrial genes (Larsson *et al.*, 1998), and a target of NRF-1, was not altered by resveratrol (Figure 3.16 B).These results showed that the combined treatment might promote mitochondrial biogenesis mediated by the E222K residue, however, further analysis need to be performed in order to understand the underlying mechanism.

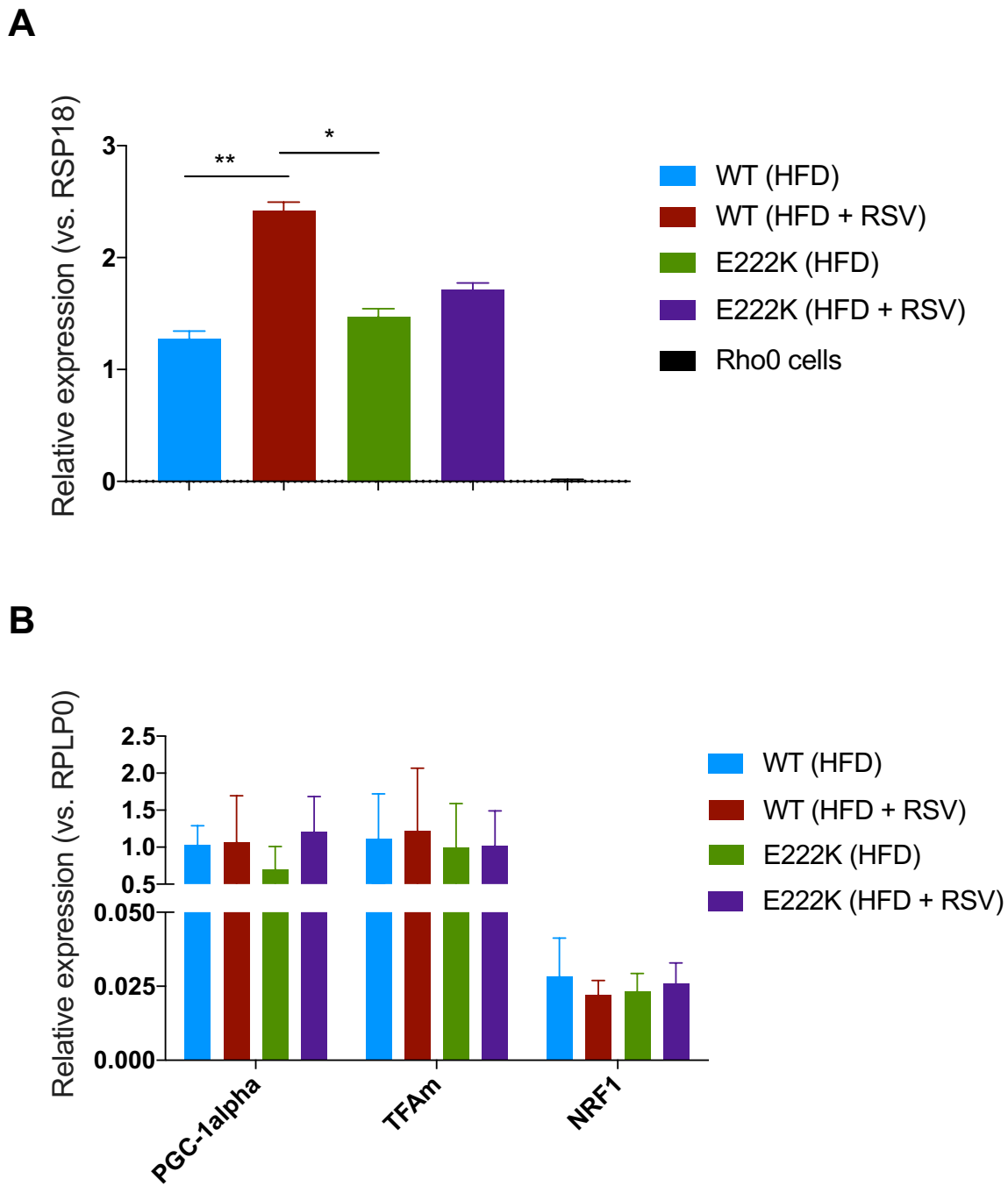

Figure 3.16: **Gene-expression profile of skeletal muscle from resveratrol treated mice is related with mitochondrial biogenesis and function.** (A) mtDNA copy number. Two-way ANOVA Tukey's multiple comparisons test. Interaction: *p = 0.0463, Diet: **p = 0.0033. n = 9/10 mice/group, 34 weeks on HFD. (B) Gene expression. Two-way ANOVA Tukey's multiple comparisons test. n= 3-4mice/group, 34 weeks on HFD. Values are mean ± SEM.

3.5. Discussion

The idea that a drug could treat one disease and prevent a dozen others, leaving behind the idea to treat one disease at the time, has been debatable among many scientists and regulatory entities. Yet, abundant data collected in the past few decades shows that multiple diseases of aging can be prevented (and at some point, reversed) by small molecules in rodents (Baur *et al.*, 2006) and primates (Venkatasubramanian *et al.*, 2013), which seems to open the possibility for such interventions.

SIRT1 diverges from other mammalian sirtuins due to their extended NTD, which was shown to be the target for allosteric activation of SIRT1 activators. Despite the debate with regard to SIRT1 activation, it is known that sirtuins arbors an NTD responsible for an allosteric activation mechanism towards native subtracts. Previously shown, binding of Sir4, mainly throughout the NTD of Sir2, incites deacetylation of H4K16 by Sir2 (Tanny *et al.*, 2004; Hsu *et al.*, 2013), and attachment by AROS and Lamin A, proposed via the NTD of SIRT1, favors the activity of SIRT1 on p53 (Kim *et al.*, 2007; Liu *et al.*, 2012).

The ability of sirtuin activators, such as resveratrol, to prevent or reverse the detrimental consequences of excess caloric intake, as well as, the modulation of suggested longevity pathways indicates that resveratrol and similar molecules might be important instruments to find key regulators of metabolism, health, and longevity.

SIRT1 and AMPK have long been shown to play many similar roles, including their ability to respond to stress and nutrient status, stimulate mitochondrial biogenesis, regulate glucose homeostasis, as well as control the activity of important transcription factors such as PGC-1α, FOXO, and p300 (Fulco and Sartorelli, 2008). Additionally, the beneficial effects of both CR and resveratrol have been suggested to entangle activation of SIRT1 and AMPK (Boily *et al.*, 2008; Um *et al.*, 2010).

The debate as to whether resveratrol mediates its beneficial effects through SIRT1 and/or AMPK was clarified with a study using adult-inducible SIRT1 knockout mice. In this study, the researchers have clarified for the first time the risk of using high doses of resveratrol. The ability of resveratrol treatment to increase AMPK phosphorylation both *in vivo* and *in vitro* was dependent upon SIRT1, but only at moderate doses. When used high doses of resveratrol (>50 μM), SIRT1-independet activation of AMPK was accompanied by toxic effects including reduction in mitochondrial membrane potential and cellular ATP levels (Price *et al.*, 2012).

The breakthrough in the field came with the discovery that a single mutation that converts a glutamic acid to a lysine at the position 230 (E230K) can significantly attenuate SIRT1 activation by resveratrol. This substitution did not impair the basal catalytic activity of hSIRT1: the V_{max}, K_m NAD^+, the K_m of several substrates, circular dichroism (CD) patterns, and thermal denaturation profiles were indistinguishable from wild-type SIRT1 (Hubbard *et al.*, 2013). The

fact that a single amino acid in SIRT1 mediates activation suggests the existence of a common mechanism for activation that is not specific to one chemical class or substrate, and has provided us with the means to investigate how SIRT1 activation might occur *in vivo* and if a therapeutic intervention strategy for different aged-associated diseases would be possible.

Still, and despite the progress, several key questions remained unanswered. For example, which, if any, of the effects of STACs are due to direct SIRT1 activation versus indirect or off-target effects? Does SIRT1 target different downstream factors in response to changes in diet or in response to STACs? If we mutate SIRT1 in mice (e.g. E222K residue) so that it cannot be activated, do STACs still work? Is there an endogenous activator that the STACs mimic? In the present study, we could answer some of these questions helping the field to fill the void in our understanding about how protein-modifying enzymes can be precisely controlled by endogenous and synthetic molecules to maintain metabolic homeostasis. In this study, we took advantage of a mouse model carrying the SIRT1-E230K knock-in mutation, which enabled us to test whether the beneficial effects of chronic resveratrol treatment were dependent of SIRT1 *in vivo*.

The beneficial effects of resveratrol and synthetic sirtuin activators are associated with improvements in glucose homeostasis and insulin sensitivity in different models of obesity. Resveratrol was shown to improve metabolism and protect against obesity and insulin resistance in mice fed with HFD (Baur and Sinclair, 2006; Baur *et al.*, 2006; Lagouge *et al.*, 2006), which correlated with longer lifespan. The ability of resveratrol to prevent the formation of fatty liver and to increase PGC-1α activity, the well-known regulator of mitochondrial biogenesis, were also observed. Likewise, the beneficial effects of resveratrol were also observed in rat models (Aubin *et al.*, 2008; Shang *et al.*, 2008; Rocha *et al.*, 2009). In non-human primates, resveratrol enhanced metabolism (Fiori *et al.*, 2013), and improved adipose insulin signaling in rhesus monkeys fed with a high-fat, high-sugar diet (Jimenez-Gomez *et al.*, 2013). Additionally, chronic administration of moderate doses of resveratrol was suggested to improve insulin sensitivity in obese Zucker rats subjected to HFD (Rivera *et al.*, 2009); however *in vitro* studies have shown that resveratrol is capable of inhibiting insulin pathways such as Akt, MAPK, PI3K, and PKB (Zhang, 2006; Fröjdö *et al.*, 2007). In this work, we have shown that the capacity of resveratrol to improve metabolism and protect against obesity and insulin resistance in mice fed with HFD was due to direct activation of SIRT1, being dependent on the E222K residue.

The capacity of resveratrol to alleviate secondary phenotypes associated with diabetes, like diabetic nephropathy and tissue inflammation, has also been described (Jiang *et al.*, 2013). Anti-inflammatory effects of resveratrol were also reported in visceral WAT from monkeys (Jimenez-Gomez *et al.*, 2013). Moreover, Leonor Rivera and colleagues (Rivera *et al.*, 2009) observed improved lipid parameters such as plasma triglycerides and free fatty

acids after prolonged administration (8 weeks) of resveratrol in obese Zucker rats, when compared with animals without resveratrol treatment. Here, we found that reduction of the inflammatory cytokine TNF-α by resveratrol was independent of the E222K residue since the levels were reduced both in WT and in SIRT1-E222K mice fed HFD. Moreover, the beneficial effects of resveratrol in reduction of cholesterol levels seemed to be independent of E222K residue. Similar to findings *in vivo*, *in vitro* studies also support the beneficial effects of resveratrol in an obesity paradigm. Reduction in both fatty acid synthesis and triglyceride accumulation in hepatocytes (Shang *et al.*, 2008; Gnoni and Paglialonga, 2009), as well as inhibition of adipogenesis in isolated cells have been described (Fischer-Posovszky *et al.*, 2010).

Besides the improvements in glucose homeostasis and insulin sensitivity, resveratrol has also been shown to be beneficial for mouse perform on treadmill tests (Lagouge *et al.*, 2006), serving as a exercise mimetic (Timmers *et al.*, 2011). In our experiments, we could observe that the beneficial effects of resveratrol in an endurance performance were due to direct activation of SIRT1. Moreover, since it was reported that SIRT1 was required to increase physical activity in response to CR (Chen *et al.*, 2005), our data further have clarified that the resveratrol-mediated increase in physical activity is due to direct activation of SIRT1.

The beneficial effects of resveratrol have encouraged the biotechnology world to develop dietary supplements or food that contain small amounts of resveratrol. Supporting this, a few clinical studies have been conducted with resveratrol in order to evaluate the possible beneficial effects on human metabolism. Foremost, a double-blind crossover study on obese but healthy man was performed. In this study the researchers treated the subjects with placebo or 150 mg/day resveratrol (dose comparable to what was used in previous animal study (Baur *et al.*, 2006)), and it was discovered that 30 days of resveratrol supplementation induced increased insulin sensitivity, glucose tolerance, increased SIRT1 and PGC-1α levels, decreased circulating levels of triglycerides and lipid content, all mimicking CR (Timmers *et al.*, 2011). Additionally, type 2 diabetes patients treated for 4 weeks with resveratrol showed progress in insulin sensitivity as well as decreased oxidative stress as compared with non-treated patients (Brasnyó *et al.*, 2011). However, a negative study with non-obese woman with normal glucose tolerance found that treatment with 75 mg/day of resveratrol for 12 weeks did not improve any metabolic functions (Yoshino *et al.*, 2012).

Despite natural compounds, synthetic activators for sirtuins have also been studied, especially for obesity-related issues. First, SRT1720 has been shown to have similar effects as RSV on obese mice, improving metabolic parameters related to glucose homeostasis and insulin sensitivity, as well as decreasing oxidative stress markers (Yamazaki *et al.*, 2009; Mitchell *et al.*, 2014). Additionally, SRT1720 has been described to extend lifespan of mice

both subjected to HFD and on a standard chow diet (Minor *et al.*, 2011; Mitchell *et al.*, 2014). Moreover, SRT2379 was also tested in Zucker fa/fa rats and improved in glucose tolerance, reduced hyperinsulinemia, as well as enhanced glucose uptake during a hyperinsulinemic-euglycemic clamp study were observed (Yoshizaki *et al.*, 2010). In the same study, the researchers also observed reduced levels of inflammatory markers in adipose tissue as well as a reduction in the inflammatory state of macrophages in adipose tissue. Another sirtuin activator, SRT2104, has been shown to mimic aspects of CR and extend lifespan in male mice (Mercken *et al.*, 2014). Sirtris Pharmaceuticals (Cambridge, MA, USA) also developed a resveratrol formulation, SRT501 (Sirtris Pharma, 2007), and showed that this compound could mimic CR by enhancing mitochondrial biogenesis, improving metabolic signaling pathways, and by blunting pro-inflammatory pathways in mice subjected to HFD. Additionally, SRT501 was also shown to improve glucose and insulin homeostasis, again mimicking CR (Smith *et al.*, 2009).

Like natural compounds, synthetic activators of sirtuins were also tested in humans and human models of diseases. Type 2 diabetes patients between 30 and 70 years old were supplemented for 28 day with SRT2104 and showed improvements in lipid profiles, with lower levels of LDL as well as higher HDL levels. However, improvements in glucose and insulin homeostasis were not seen in these patients (Baksi *et al.*, 2014). Two additional clinical trials testing SRT2104 in elderly volunteers and healthy smokers described a slight reduction in body weight, an improvement in cholesterol ratio, as well as a decrease in triglyceride levels (Libri *et al.*, 2012; Venkatasubramanian *et al.*, 2013). Furthermore, SRT501 was shown to improve glucose tolerance in absence of any adverse side effect in type 2 diabetes patients (Smoliga *et al*., 2011).

Pharmaceutical companies are continuing to develop sirtuin activators to improve their therapeutic proprieties; however, the beneficial metabolic effects stimulated by these activators must be investigated with careful attention since side effects due to exaggerated activation of sirtuins may cause serious damage in human patients. In this work, we provide insights into fundamental mechanisms of allosteric activation of SIRT1 and clarified some of the health benefits that STACs might mediate by direct SIRT1 activation *in vivo*, a question that has dogged the field for over a decade. Using these results, we can now determine which diseases STACs can treats in humans and how they can be improved to increase their potency.

Besides the beneficial effects of direct activation of SIRTs through STACs, it has been known for several years that upregulation of the NAD salvage pathway, which recycles NAD^+ from NAM, is able to extend lifespan and mimic CR in yeast (Anderson *et al.*, 2002; Anderson *et al.,* 2003). The gene responsible for the rate-limiting step in this pathway in yeast, *PNC1*

(encoding for nicotinamidase), was shown to be activated by several stress and CR, resulting in a greater flux through the pathway and increased Sir2 activity.

NAD^+-boosting molecules represent a newer class of STACs which are increasing attention in the field, as a way to restore NAD^+ levels in elderly individuals, and potentially, activate all seven sirtuins with only one compound. Some examples include NMN, NR (Ramsey *et al.*, 2008; Gomes *et al.*, 2013; Gong *et al.*, 2013; Mouchiroud *et al.*, 2013; Zhang *et al.*, 2016) and inhibitors of CD38 such as apigenin (Escande *et al.*, 2013), quercin (Escande *et al.*, 2013) and GSK 897-78c (Haffner *et al.*, 2015) have been tested in rodents using several routes of administration (Ramsey *et al.*, 2008; Gomes *et al.*, 2013; Gong *et al.*, 2013; Mouchiroud *et al.*, 2013; Zhang *et al.*, 2016), showing a surprisingly broad effects on physiology without any apparent side effects (Gong *et al.*, 2013).

Although many questions regarding this new class of STACs remain to be answered. Important knowledge on pharmacokinetics, pharmacodynamics as well as how NAD boosters are affected by the route of delivery need clarification. In the next chapter we will try to understand some of these questions as well as understand if synergistic strategies to accelerate the ability to test multiple genetic interventions are suitable approaches to study aging and age-related diseases.

CHAPTER 4

Multiplexing health and longevity

4.1. Abstract

The mammalian sirtuin gene family (SIRT1-7), well known as NAD^+-dependent enzymes, have been shown to promote health, with two sirtuins associated with increased longevity. By regulating NAD^+-sensing enzymes, NAD^+ is able to control fundamental processes from energy metabolism to cell survival. NAD^+ levels have been shown to decline during aging, a hallmark that has been implicated in the decline of sirtuin activity, which can contribute to decreased genomic and epigenetic stability, as well as increased inflammation, mitochondrial dysfunction, and increased susceptibility to age-related diseases. Different approaches to study aging have been used; however, synergistic strategies between them has been cost and time prohibitive. We thus pursued a strategy to accelerate the ability to test multiple genetic interventions by boosting the expression and activity of the entire sirtuin gene family and infecting 20-month old C57B/6J mice with adeno-associated viruses carrying all seven sirtuins each. Half of the transgenic mice and half of the GFP control mice were given the NAD^+ precursor NMN (nicotinamide mononucleotide) orally (300 mg/kg/day) post-viral delivery to test possible synergies. We observed that NAD^+ supplementation was able to protect at some extent the age-related decrease in body weight, with a non-significant increase in longevity ($p=0.15$). The use of gene therapy-based methods to test synergistic strategies in wild-type mice may serve as a model to rapidly screen for and identify interactions between multiple genetic interventions to promote healthspan and longevity.

4.2. Introduction

Nicotinamide adenine mononucleotide (NAD) is one of the most critical and interesting molecules in the body, and is required for more than 500 enzymatic reactions, playing key roles in the regulation of all major biological processes (Ansari and Raghava, 2010).

Described for the first time in 1906 by Harden and Young (Harden and Young, 1906), NAD was shown to be a cell component that enhanced alcohol fermentation. Later, Warburg discovered that NAD is required for redox reactions (Warburg and Christian, 1936), leading to the notion that NAD is a chemical respective to charge, where "NAD^+" and "NADH" refer to the oxidized and reduced forms, respectively.

The 1963 discovery that NAD^+ as a co-substrate for the addition of poly-ADP-ribose to proteins (Chambon *et al.*, 1963) completely changed the way these molecules were seen. Additionally, due to the discovery that NAD has a role in regulating sirtuins activity, there is continued interest in the aging research field (Frye, 1999; Landry *et al.*, 2000; Imai *et al.*, 2000). The critical role of NAD^+ in different biological processes as well as their crucial role as substrates of NAD^+-consuming enzymes such as poly-ADP-ribose polymerases (PARPs), sirtuins, CD38/157 ectoenzymes (Chambon *et al.*, 1963; Imai *et al.*, 2000; De Flora *et al.*,

2005), and the newly discovered class of NAD^+ hydrolases, sterile alpha and Toll/interleukin-1 receptor motif-containing 1 (SARM1) (Essuman *et al.*, 2017), has lead the field to investigate the potential use of "NAD^+-boosting molecules" for treatment of multiple diseases and potentially even aging.

4.2.1. NAD^+ biosynthesis pathway

Although it was considered to be relatively stable, NAD^+ is now known to be in a constant transient state of synthesis, degradation, and recycling, not only in the cytoplasm but also within major organelles such as the nucleus, Golgi, and peroxisomes (Anderson *et* al., 2003). Additionally, NAD^+ concentration and distribution, as well as its metabolites have been shown to differ in response to physiological stimuli and cellular stresses (Dölle *et al.*, 2010; Cambronne XA *et al.*, 2016; Cameron *et al.*, 2016). Two main pools of NAD^+ have been categorized, the "free" pool and the protein-associated or the "bound" pool, in which their ratio was shown to vary across different organelles, cell types, tissues, and even the ages of individuals (Zhang *et al.*, 2012).

In mammals, with the exception of neurons, cells cannot up take NAD^+, leading them to rely on *de novo* synthesis either from the kynurenine pathway by converting the amino acid tryptophan or by forms of vitamin B3 such as nicotinamide (NAM) or nicotinic acid (NA) (figure 4.1). Nevertheless, the majority of NAD^+ levels are maintained by NAD^+ recycling via salvage pathways rather than by *de novo* generation. NAM is the product of the enzymes CD38 and PARPs (Magni *et al.*, 1999), and represents the major substrate for NAD^+ salvage; however, various forms of niacin are taken up from the diet including NAM, NA, nicotinamide riboside (NR), and NMN, which can be also used for NAD^+ recycling (Bogan and Brenner, 2008; Mills *et al.*, 2016; S. A. Trammell *et al.*, 2016; Ummarino *et al.*, 2017). Nicotinamide is converted to NMN, the key NAD^+ intermediate, by NAM phosphoribosyltransferase (NAMPT), the rate-limiting enzyme in this pathway (Revollo *et al*., 2004), in which, along with NAD^+, has been shown to be reduced in various tissues in obesity and high caloric diet circumstances. NMN adenylyltransferase (NMNAT) then converts NMN into NAD^+ (Wang *et al.*, 2006; Bogan and Brenner, 2008), and nicotinic acid phosphoribosyltransferase (NPT) convert NA to NaMN (Revollo *et al*., 2004; Wang *et al.*, 2006; Bogan and Brenner, 2008). On the other hand, the precursor NR needs to be converted to NMN by NR kinases (NRK1/2) (Ratajczak *et al.*, 2016) (figure 4.1).

Cell survival and function relies on adequate NAD^+ biosynthesis, and environmental changes during normal NAD^+ homeostasis can largely affect not only the NAD^+/NADH pool required for redox reactions, but also the activity of several NAD^+-dependent enzymes that are crucial for cellular functions.

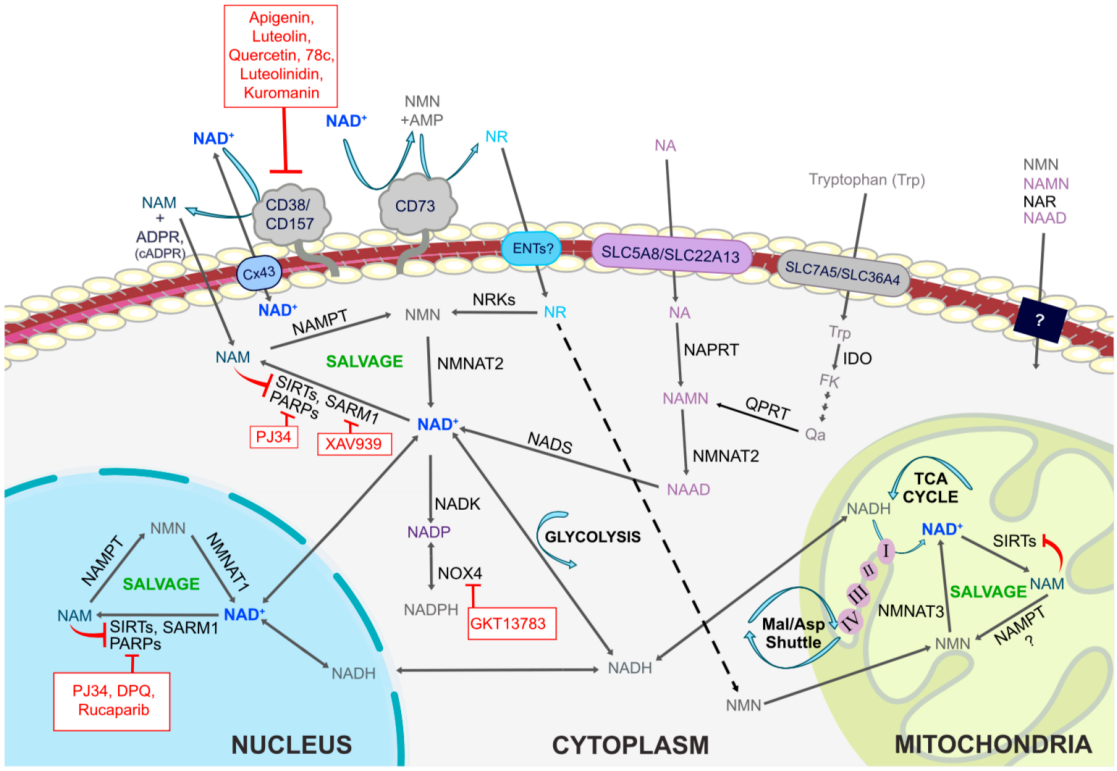

Figure 4.1. NAD metabolism pathways. The *de novo* synthesis and salvage pathway are the two major pathways responsible for NAD synthesis. In the *de novo* pathway NAD is synthetized by converting tryptophan to quinolinic acid (QA) through the kynurenine pathway. The salvage pathways, which can occur in several cellular compartments from nucleus to mitochondria, are responsible for the recycling of nicotinamide mononucleotide (NMN), nicotinamide riboside (NR), nicotinamide (NAM), as well as nicotinic acid (NA). Nucleotide phosphatases (CD73) and glycohydrolases (CD38 and CD157) act through the cleavage of extracellular NAD. CD72 cleave NAD yielding NMN which is then re-cleave to yield NR. CD38 or CD157 cleave NAD yielding NAM. Within the cells NAM is also produced by action of NAD^+-consuming enzymes such as sirtuins, PARPs, and SARM1. NAMPT and NRKs are responsible for the conversion of NAM and NR, respectively, to NMN. Then, NMN and NaMN are renovated to NAD and NAAD correspondingly, and NADS amidated NAAD to produce NAD. Levels of cellular NAD^+ can be both modulated by activators of the salvage pathway or inhibited by enzymes that consume NAD^+ such as CD38, PARPs, and SARM1. Copied from (Rajman *et al*., 2018).

4.2.2. NAD^+ decline during aging

Despite all the new discoveries that have been reached over the recent years regarding the impact of sirtuins on several age-related diseases, there has been much interest about sirtuin regulating mechanisms, such as the availability of NAD^+ within the cell. Thus, the general decline in NAD^+ with age has arisen as a likely explanation for the effects of sirtuin during aging.

The first evidence of declining NAD^+ levels during aging was originally documented in mice overexpressing SIRT1 in pancreatic ß cells (BESTO mice) (Ramsey *et al.*, 2008). Contrary to what was observed in young BESTO mice, where a significant improvement in glucose-stimulated insulin secretion was witnessed, as they aged, this phenotype was completely lost. The confirmation that NAD^+ levels declined with age as the cause for the loss of the BESTO phenotype stemmed from an experiment where NMN supplementation restored the phenotype in aged BESTO mice, and interestingly even improved the glucose-stimulated insulin secretion in aged wild-type mice (Mouchiroud *et al.*, 2013). These discoveries suggested that glucose-stimulated insulin secretion may be controlled by a NAD^+ pool, and declining NAD^+ levels with age may be the cause for the observed age-associated impairment. Consequently, several reports rapidly came out demonstrating declining NAD^+ with age in different organisms (Haigis and Sinclair, 2010; Imai and Guarente, 2014, 2016; Yoshino *et al*., 2017), and specifically in mice the decreased levels of NAD^+ with age were observed in several tissues and organs and responsible for metabolic dysfunctions, cardiovascular diseases, cancers, and neurodegenerative diseases (Ramsey *et al.*, 2008; Yoshino *et al.*, 2011; Mouchiroud *et al.*, 2013; Yoshino *et al*., 2017).

The cause of the NAD^+ decline during aging has been strongly associated with decreased NAMPT-mediated NAD^+ biosynthesis. Expression of *Nampt* at both the mRNA and protein levels was shown to decrease with age in several tissues (Yoshino, Kathryn F. Mills, *et al.*, 2011; Stein and Imai, 2014), which leads to a reduction in NAD^+ in those same tissues, thereby affecting the activity of NAD^+-dependent enzymes and redox reactions within the cell and causing functional decline. Interventions with NAD^+ intermediates, such as NMN or NR, can therefore restore the NAD^+ pool and cellular function in aged animals.

In addition to a decline in NAMPT-mediated NAD^+ biosynthesis, lower levels of NAD^+ during age has also been linked to an increase in NAD^+ consumption, mainly due activation of PARPs (Bai *et al.*, 2011). PARP1, for instance, is well known to be hyperactivated in response to DNA damage, depleting NAD^+ in the cell, most critically in mitochondria, and consequently inducing apoptosis. Inhibition of PARP1 raises NAD^+ levels in mice, improves mitochondrial function, and protects against the effects of an HFD (Bai *et al.*, 2011; Pirinen *et al.*, 2014). Moreover, ectopic PARP1 expression has been associated with multiple age-associated phenotypes (Mangerich *et al.*, 2010). Studies where PARP1 was knocked-out have also confirmed the role of PARP1 in NAD^+ decline (Bai *et al.*, 2011). Moreover, co-regulation of both sirtuins and PARPs, which share a role in response to stress and injury, have been shown to be regulated by NAD^+ in aging. It has also been shown that deleted in breast cancer 1 (DBC1) can bind to NAD^+, which then prevents it from binding to PARP1 (Li *et al.*, 2017). As NAD^+ declines with age, DBC1 binds to PARP1 and reduces its DNA damage repair capacity

and consequently contributes to the accumulation of DNA damage during aging (Li *et al.*, 2017).

Finally, CD38, a major consumer of NAD^+ in mammals (Rajman *et al.*, 2018), has also been reported to contribute to age-associated NAD^+ decline. Supporting this notion, mice lacking CD38 or treated with the CD38 inhibitor apigenin have about 50% more NAD^+ levels (Escande *et al.*, 2013), and expression and activity of CD38 increases in various tissues during aging with a simultaneous drop in NAD^+ levels (Aksoy *et al.*, 2006; Camacho-Pereira *et al.*, 2016). At 32 months of age, wild-type mice showed half of the NAD^+ levels observed in young mice, while CD38 knockout mice were able to maintain their NAD^+ levels and were also resistant to the deleterious effects of an HFD, such as liver steatosis and glucose intolerance (Barbosa *et al.*, 2007; Escande *et al.*, 2013).

Decreased NAD^+ biosynthesis in combination with increased NAD^+ consumption intensifies the depletion of NAD^+ and can cause a variety of age-associated pathophysiologies (Ramsey *et al.*, 2008; Yoshino *et al.*, 2011; Mouchiroud *et al.*, 2013). No matter the cause for this decline, depletion of NAD^+ may be cell-type and tissue specific, and NAD^+ supplementation intermediates may have therapeutic potential since they have been shown to be proof of concept molecules for the development of drugs to treat age-related diseases.

4.2.3. Pharmacological interventions: NAD^+-boosting

The certainty that systematic NAD^+ decline is one of the fundamental molecular events regulating aging and possibly limiting organismal lifespan has contributed to the notion that NAD^+-boosting therapies can be seen as a new class of molecules to restore NAD^+ levels and potentially activate or restore NAD^+-dependent enzymatic activities in different age-related diseases. Three main approaches are currently being pursued in order to boost NAD^+ levels: supplementation with NAD^+ precursors, activation of NAD^+ biosynthetic enzymes, and inhibition of NAD^+ degradation.

The first indication that NAD^+ boosting could increase lifespan came from work in yeast cells. The yeast gene *PNC1* encodes the enzyme that catalyzes the first step in the NAD^+ salvage pathway from NAM and is one of the yeast genes more highly upregulated in response to environmental stresses, such as heat, osmotic stress, and the restriction of amino acids and glucose. Overexpression of *PNC1* was sufficient to increase lifespan in yeast cells and resistance to stress, whereas deletion of this gene blunted the ability of yeast cells to respond positively to caloric restriction (Anderson *et al*., 2003). Evidence from other organisms have also been reported, for example the overexpression of the Pnc1 homolog D-NAAM was shown to increase mean lifespan in *Drosophila* by 30% (Balan *et al.*, 2008), demonstrating that the mechanism to upregulate NAD^+ synthesis might be a conserved longevity mechanism.

Despite the fact that NAD^+-boosting molecules have been shown in some studies to have a broad range of beneficial effects, ranging from improvements in glucose metabolism and mitochondrial function to recovery from tissue injury, such as heart, eyes, and ears (Yoshino *et al.*, 2012; Mouchiroud *et al*., 2013; Mouchiroud *et al.*, 2013), the reason why it has been a challenge to constitutively increase NAD^+ levels in mammals remain unclear (Frederick *et al.*, 2015). The most common strategy used by the field to raise NAD^+ levels has been a pharmacological approach. Examples include NR and NMN molecules, which are soluble, orally bioavailable (Conze *et al*., 2016; Trammell *et al.*, 2016), and are reported to not cause flushing or inhibition of PARPs and sirtuins as observed with NAM (Bitterman *et al.*, 2002).

Regarding NMN supplementation, administration of NMN in 12 month-old mice showed age-associated body weight gain enhancement, improved energy metabolism and physical activity, as well as reversion in many gene expression changes associated with aging (Mills *et al.*, 2016); findings which helped to establish NMN as an effective anti-aging agent. Moreover, NMN administration has also been shown to be beneficial in different age-associated disease models. Regarding the central nervous system, NMN was reported to improve mitochondrial respiration in an Alzheimer's Disease (AD) model, which is considered a hallmark of progression of AD and other neurodegenerative diseases (Long *et al.*, 2015). Administration of NMN has also been shown to improve mouse cognitive behavior in the context of AD as well as recover electrophysiological deficits *ex vivo* (Wang *et al.*, 2016; Yao *et al.*, 2017), suggesting that NMN could be a promising therapeutic agent for the treatment of AD and other neurodegenerative diseases. Furthermore, NMN as well as NR have been shown to increase mitochondrial function and improve glucose homeostasis, in a SIRT1-dependent manner, in obese mice (Yoshino *et al.*, 2011; Cantó *et al.*, 2012; Gomes *et al.*, 2013). Gomes and colleagues (Gomes *et al.*, 2013), have shown that NMN could restore several key aspects in aging in mice, such as muscle-type switching, insulin sensitivity, oxidative phosphorylation, and gene expression. Yoshino and colleagues (Yoshino *et al.*, 2011) showed that NMN was capable of restoring NAD^+ levels and prevented diet- and age-induced type 2 diabetes in wild-type mice.

Besides the positive effects mediated by NMN, NR has been shown to be more efficient in boosting NAD^+ than NA and NAM *in vivo* in rodents and has also been shown to be beneficial in treating age-associated disorders. For example, NR administration in pre-diabetic and diabetic mice under HFD, both models of age-associated metabolic diseases, improved liver steatosis, glucose tolerance, and weight gain (Trammell *et al.*, 2016; Trammell *et al.*, 2016). Additionally, moderate extension of lifespan was found when mice were supplemented with NR for two years (Zhang *et al.*, 2016). Similar to NMN, NR was also reporter to have beneficial effects in age-associated neurodegenerative disease models. For instance, NR supplementation significantly increased NAD^+ levels in cerebral cortex and also improved

cognitive deterioration in a mouse model of AD (Gong *et al.*, 2013). Specifically, electrophysiological deficits on long-term potentiation in the hippocampal CA1 region were ameliorated by NR. Moreover, it was found that NR increased PGC-1α and better regulated ß-secretase as well as decreased amyloid-beta peptide levels. These findings suggest that NAD^+ depletion could be a main event in neurodegenerative diseases, and thus treatment with NAD^+-consuming enzymes could play a central role in the beneficial effects reported. Furthermore, since nuclear DNA damage has been linked to neurodegenerative diseases (Chow and Herrup, 2015), treatment with NR or NMN could be used as an effective agent to prevent and/or ameliorate neurodegenerative diseases, a fact that was not addressed in the study.

Although we are only in the beginning of using NAD^+ as a new therapeutic approach for diseases where sirtuin activity appears to be compromised, these so-called NAD^+-boosting molecules have been shown to have promising effects in treating age-associated diseases in animal models. Thus, NAD^+ supplementation as well as modulation of NAD^+-dependent enzymes may appear to be a window for new studies in the field. However, a better understanding of how these different NAD^+ precursors are metabolized as well as an assessment of the bioavailability and effectiveness of these precursors are needed before approaching human therapy.

The initial discovery that genetic interventions aiming to up-regulate NAD^+ biosynthesis could increase both stress resistance and lifespan in yeast cells and *Drosophila* (Anderson *et al.*, 2002; Anderson *et al*., 2003; Balan *et al.*, 2008) has led the field to seek for NAD^+ boosters in rodents, using both wild-type and disease models. Several strategies have been used over the years, however, synergistic strategies have been cost and time prohibitive. In this work, we pursued a strategy to accelerate the ability to test multiple genetic interventions and tested the effects of boosting both the expression and activity of the entire sirtuin gene family.

4.3. Materials and Methods

4.3.1. AAV production

AAVs were produced in 293T cells using methods previously described (Grieger *et al*., 2006). Briefly, confluent 293T cells in 15 cm plates were split 1:3 into 15 cm plates. Three to four hours before transfection, the medium was removed from cells and replaced with fresh medium. Transfection mix using polyethylenimine (PEI) was prepared into 15 mL polystyrene tubes using the following order: 12 µg pXX680, 10 µg pHelper, 6 µg pITR, 500 µL serum-free medium and 110 µL PEI (1mg/mL). The mix was vortex, let sit down at room temperature for 5 min and added to a single 15 cm plate of 293T cells, distributed throughout. Forty-eight to seventy-two hours post-transfection, the virus was harvested and purified using a discontinuous iodixanol gradient.

4.3.2. Animals and Treatments

All experiments were conducted according to protocols approved by the Institutional Animal Care and Use Committee at Harvard Medical School. Aged male C57BL/6 wild-type mice were purchased from the National Institute of Aging aging mouse cohort (NIA, Bethesda, MD, USA) and were maintained on a standard purified mouse LabDiet® 5053 during the entire experiment. After acclimating for two weeks, mice were anesthetized with isoflurane and viruses were delivered by retroorbital injection. NMN (GeneHarbor, Shatin, N.T., Hong Kong) was delivered in the drinking water, given at 2.4 g/L. Mice were monitored daily and weighted twice a month. All animals were monitored for survival and only euthanized if determined likely to not survive the next 48 hours by an experimental researcher or veterinarian. This euthanasia time point was based on exhibition of at least two of the following: inability to eat or drink, severe lethargy or persistent recumbence, severe imbalance or gait disturbance, rapid weight loss (<20%), an ulcerated or bleeding tumor, and dyspnea or cyanosis. Survival curves were plotted using the Kaplan-Meier method, including all alive animals at each time point.

4.3.3. Western Blots Analysis

Protein extracts were obtained by adding sodium dodecyl sulphate-polyacrylamide gel electrophoresis (SDS-PAGE) sample buffer [(0.5 M Tris 0.4% SDS, pH 6.8), 30% glycerol, 10% SDS, 0.6 M dithiothreitol and 0.012% of bromophenol blue] to tissue homogenates and boiled at 95°C for 5 min. Pre-stained molecular weight markers (Bio-Rad Labs, Hercules, CA, USA) and 20-40 µg of protein samples were separated by 4-20 % gradient SDS-PAGE electrophoresis under reducing conditions at 100-120 mV and electro-transferred onto 0.45 µm nitrocellulose membranes (GE Healthcare, Chicago, IL, USA). After blocking for 1 h at RT

with 5% milk diluted in Tris-buffered saline solution with 0.1% Tween-20 (TBS-T) (50 mM Tris, 150 mM NaCl, and 0.1% Tween-20, pH 7.6), the membranes were incubated overnight at 4°C with primary antibodies (1:1000) (Table 2) diluted in TBST-T with 5% milk. After three washing periods of 10 min each with TBS-T, the membranes were incubated with the appropriate secondary antibody (dilutions of 1:10 000 - 20 000) diluted in TBS-T with 5% milk for 2 h at RT. After three 10 min washes with TBS-T, membranes were incubated with ECL reagent (GE Healthcare) for 5 min at RT. The immunoreactivity was visualized using a chemiluminescence apparatus (ChemiDoc Imaging System, BioRad) and analyzed using appropriate software (Fiji software).

4.3.4. Behavioural experiments

All behavioral tests were conducted as previously described in Chapter 3, between 9:00 AM and 5:00 PM (light phase) in a sound attenuated room, where all mice were acclimatized for 1 h prior to testing. All apparatuses and objects were cleaned with 70% ethanol solution after each session. Behavioral experiments were video-monitored and recorded using the video tracking system and analyzed using appropriate software (TopScanLite).

4.3.4.1. Open Field Test

The open field test consists in a simple sensorimotor test, commonly used to determine spontaneous and locomotor activity, as well as, exploration habits in mice. After habituation in the test room, nice were placed in the center of a chamber (48.5 cm x 48.5 cm) and allowed to freely move for 1 h to assess their exploration in the novel environment. Exploratory activity in the peripheral area and total activity in the chamber were recorded using a video tracking system and analyzed using appropriate software (TopScanLite).

4.3.4.2. Y-maze Spontaneous Alternation Test

Y-maze spontaneous alternation test is a behavioural assay used for measuring the willingness of the mouse to explore new environments. Mice characteristically favour to explore the novel arm rather than return to the one formerly visited. The test occurs in a Y-shape maze with three plastic arms at 120º angle from each other. Mice were placed in the Y-maze apparatus in the testing room with visual cues on the walls and allowed to explore the Y-maze apparatus for 5 min during which time one arm was blocked. After a 15-minute rest period, the mice re-explored for 5 min the Y-maze apparatus, but now with all the arms opened. We measured the number of entries and the time spent in the novel arm as a measure of short spatial and working memory using the video tracking system and analyzed using appropriate software (TopScanLite).

4.3.4.3. Elevated Plus Maze Test

The elevated plus maze (EPM) test was used to assess anxiety-related behavior in mice. The EPM apparatus is an elevated "+"-shape maze composed by two oppositely placed closed arms, two oppositely placed open arms, and a center area. After habituation in the test room, mice were placed in the EPM apparatus with visual cues on the walls and allowed to explore for 10 min. We measured the mouse preference for being in the open arms as compared to the closed arms as an indicator of anxiety-like behavior. Their behavior was recorded using a video tracking system and analyzed using appropriate software (TopScanLite).

4.3.4.4. Gait Analysis

Gait analysis was measured using the TreadScan System (Clever Sys, Inc., Reston, VA, USA). Forced walking was performed on a treadmill (Columbus Instruments; Columbus, OH). A high-speed digital video camera recorded images of the ventral side of the mouse through a transparent treadmill belt reflected off a mirror. Mice walked on a treadmill for approximately 24-sec at speeds of 13, 19, and 25cm/s. We identified each individual paw of the mouse in each frame as it walked on the treadmill and measures of stance and swing duration, among other measures, were analyzed.

4.3.5. Metabolic and Physical Activity

The metabolic rate of the animals was monitored by indirect calorimetry in open-circuit oxymax chambers using the Comprehensive Lab Animal Monitoring System (CLAMS; Columbus Instruments, Columbus, OH, USA). Mice were singly housed with water and food available *ad libitum* under a 12-12-hour light-dark cycle at approximately 24°C. The mice were kept in the monitoring cages for 2 days, allowing them to acclimatize before the last 24h when the parameters were analyzed.

Sample air was pumped through the test chambers, equipped with an oxygen (O_2) sensor for determination of O_2 content. Oxygen concentration in the air entering the chamber compared with air leaving the chamber allowed for the determination of O_2 consumption. The percentage of O_2 and CO_2 gas levels in each chamber environment was measured periodically and the changes observed in these levels were used to determine O_2 consumption (VO_2), CO_2 production (VCO_2), respiratory exchange ratio (RER), and heat.

Spontaneous activity measured by both horizontal (XAMB) and vertical (ZTOT) movements was also monitored. The system is equipped with infrared beams able to monitor all of the chamber's axes. The beams were horizontally 130 mm apart in order to provide a greater resolution grid covering the XY-planes. The data were recorded and presented in terms of the number of "beam breaks".

4.3.6. Statistical Analysis

Data were analyzed by a two-way ANOVA with multiple comparisons. Statistical tests were performed with GraphPad Prism (San Diego, CA, USA). Survival curve was analyzed by a two-way Cox Multivariate Analysis for main effects of genotype (E222K) and diet (HFD ± Resveratrol) using appropriate software (SPSS, IBM Developer, Armonk, NY, USA). Data are presented as means ± SEM.

4.4. Results

In order to test whether our synergistic strategy of overexpressing all members of the sirtuin gene family together with NAD^+ boosting molecules could have any positive effects on healthspan and lifespan in an already aged mouse, we injected AAV9 viruses containing each of the seven sirtuins, or GFP as a control, in 20 month-old old C57B/6J mice. Half of the injected mice from each group were then treated with NMN (300 mg/kg) as a way to boost NAD^+ levels. This schematic allowed us to take a novel approach in which we could study our hypothesis in three different levels: redundancy, addition, or synergetic effects (figure 4.2).

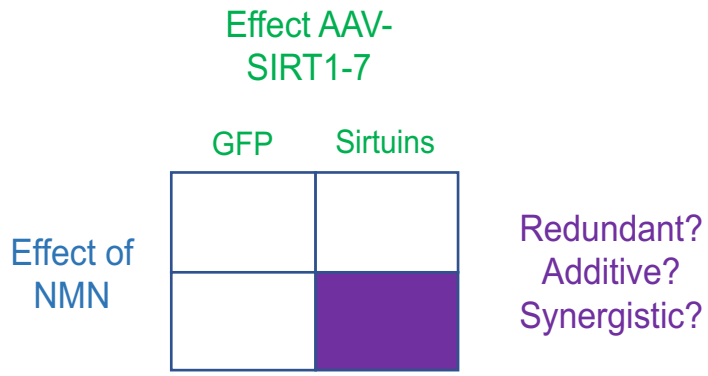

Figure 4.2. Experimental design. Experiment design set up for testing three variables: effect of sirtuin overexpression, effect of NMN supplementation, and the interaction between these two interventions.

4.4.1. Genetic approach to overexpressing SIRT1-7 (SIRTs)

Before applying sirtuin gene therapy in aged mice, we first tested the effectiveness of overexpressing SIRT1-7 (SIRTs) as well as acute toxicity using young mice. We produced eight types of AAV9 viruses expressed under the UBC1 promoter, seven of which contained all 7 sirtuin isoforms with one containing only GFP. Sirt4 and Sirt7 were first produced and tested at both a low dose (1×10^{10} particles) and a high dose (1×10^{11} particles). We observed good expression of both constructs in liver, two weeks post-injection (Figure 4.3 A-B). Due to better expression of the higher dose of AAV9 in liver, we chose to proceed with this dosage. The remaining five sirtuins were overexpressed using the higher dose of AAV9 in young mice, and after 2 weeks post-injection we found that all constructs were able to increase expression of SIRTs in liver (Figure 4.3 C-G).

In order to determine if our pan-sirtuin gene therapy may cause some acute toxicity in young mice, all seven sirtuins viruses were injected in eight young mice (for a total of 7×10^{11} particles), and half of these mice were treated with NMN in the drinking water (2.4 g/L, corresponding to approximately 300 mg/kg/day). We monitored the animals for 8 weeks post-

injection and did not observe any loss in body weight or in any other sign of distress. We thus concluded that sirtuin gene therapy in combination with NMN supplementation was acutely safe, at least in young mice.

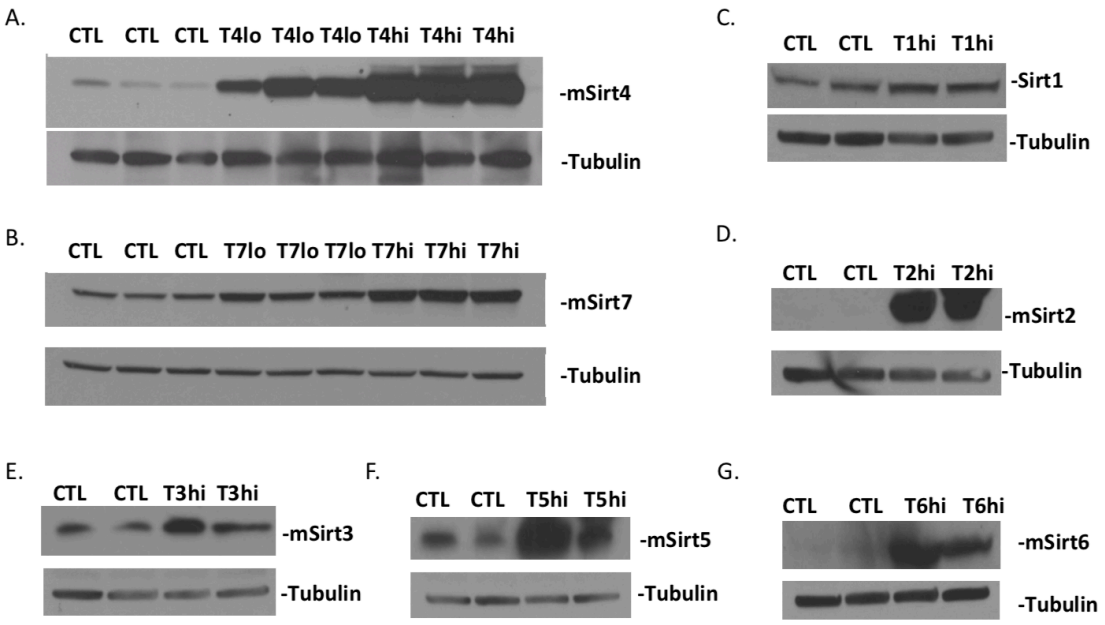

Figure 4.3: Liver homogenates from mice treated with AAV9 viral constructs to overexpress SIRTs. Western blot for Sirt4 (A), Sirt7 expression two weeks post-injection with low dose (1 x 1010 particles) and high dose (1 x 1011 particles) AAV9 delivery. (C) Expression of Sirt1 (D) Sirt2 (E) Sirt3 (F) Sirt5 and (G) Sirt6 two weeks post high dose injection.

4.4.2. NAD^+ supplementation protected against age-related decrease in body weight and slightly increased lifespan

One of the major goals of our study was to test if NMN alone or in combination with overexpression of SIRTs is able to extend lifespan. In order answer this question, we delivered either all seven sirtuins or a GFP-containing virus using a viral approach to 20-month-old wild-type C57B16/J mice. Two weeks after viral injection, drinking water containing NMN was provided to half of the mice in each group (n=37 animals per group). NMN was maintained in the drinking water for the duration of the study and no differences were observed in water consumption between the groups (Figure 4.4 A).

Similar to what is observed during normal aging, during the first few months of the study there was a moderate loss of body weight among all the groups. Importantly, the groups that received NMN, independent of gene therapy, showed delayed loss in body weight by several months (Figure 4.4 B), with these groups starting to lose weight around 28 months of age.

Throughout the experiments, we followed the four groups of mice with minimal interventions until their natural death. Between 25-26 months of age, we observed that the SIRTs/NMN group had a “squaring of the curve” with enhanced survival during the earliest quartile to die, however, none of the groups showed significant increase in lifespan, as compared with the control group (GFP/water) (Figure 4.4 C). Notably, when we compared the NMN effect alone among the groups, they appeared to be a positive, but non-significant (p=0.15) benefit on longevity (Figure 4.4 D) with a slight increase in medial but not maximal lifespan.

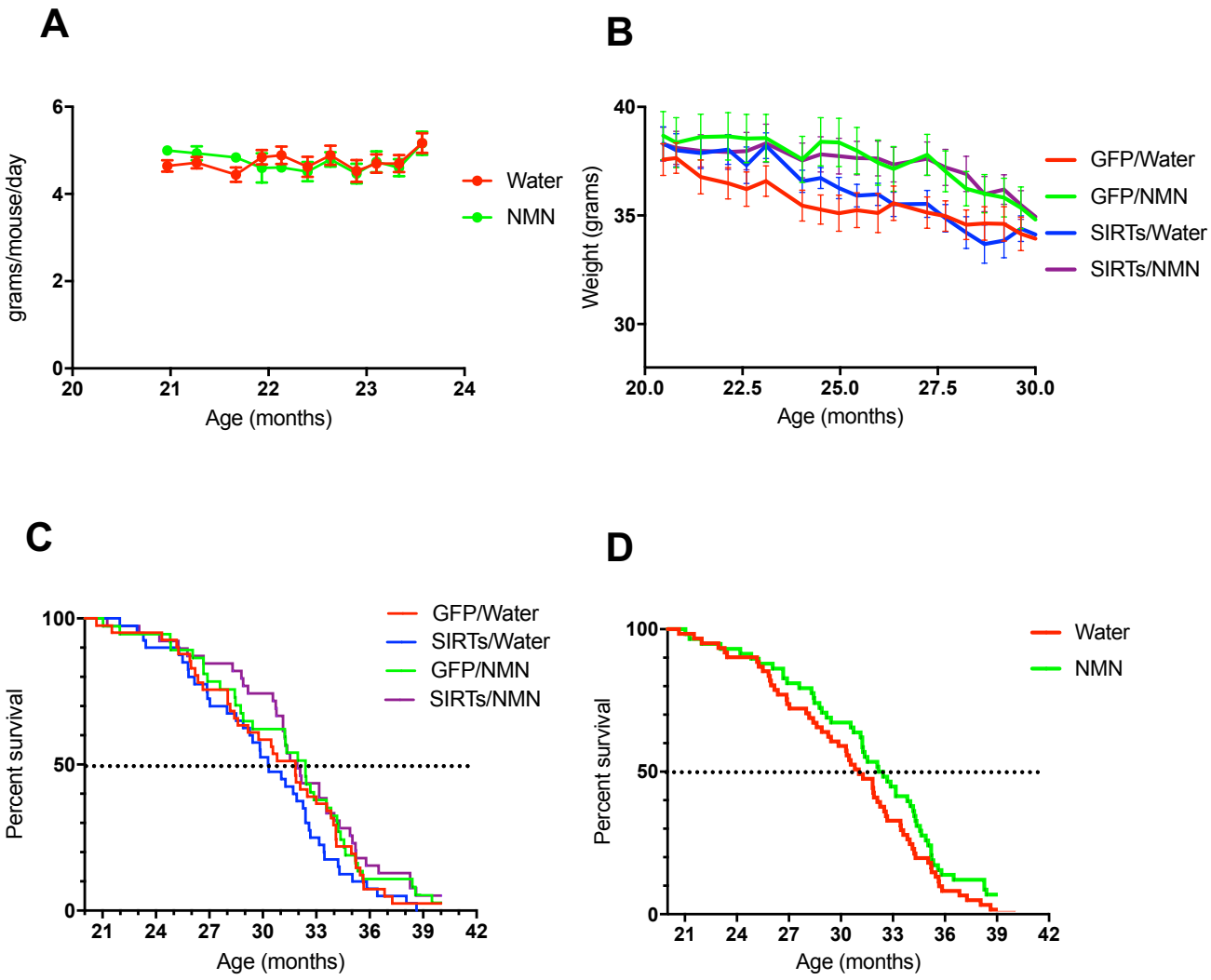

Figure 4.4: Effect of SIRTs gene therapy and NMN on body weight and lifespan. (A) Water consumption. (B) Average body weight per group. (C) Kaplan-Meier curve with survival for all groups. (D) Kaplan-Meier curve with survival for combined water and NMN groups. Two-way Cox Multivariate Analysis for main effects of genotype and diet.

4.4.3. SIRTs overexpression and NAD$^+$ supplementation does not improve cognitive function in old mice

In addition to trying to understand how NMN supplementation alone or in combination with overexpression of the entire sirtuin gene family might impact lifespan, we prepared a second cohort of mice using the same parameters to study if our treatments may have any added health benefits.

To determine if locomotor behavior as well as cognition were impacted, we performed a batch of behavioral experiments. As shown in figure 4.5 open field testing showed that neither NMN supplementation alone nor in combination with SIRTs overexpression changed locomotor behavior of the mice, as indicated by undifferentiated percentage of time spent in center and velocity among all groups (Figure 4.5 A). Moreover, total distance remained the same between the groups (Figure 4.5 A).

We next evaluated the impact of our treatment in anxiety-related behavior of the mice using the elevated plus maze test (Figure 4.5 B) and found no difference among groups as indicated by the percentage of time spent in the open arms. Interestingly, mice treated with SIRTs independent of NMN showed slight decrease in time spent in open arms (p=0.07). Using the Y-maze we tested if there were any changes in short-term spatial/working memory and found no difference in the time spent in the novel arm among all groups (Figure 4.5 C). Notably, we found decreased latency to the novel arm (Figure 4.5 C) among the mice treated with SIRTs gene therapy independent of NMN (p=0.03).

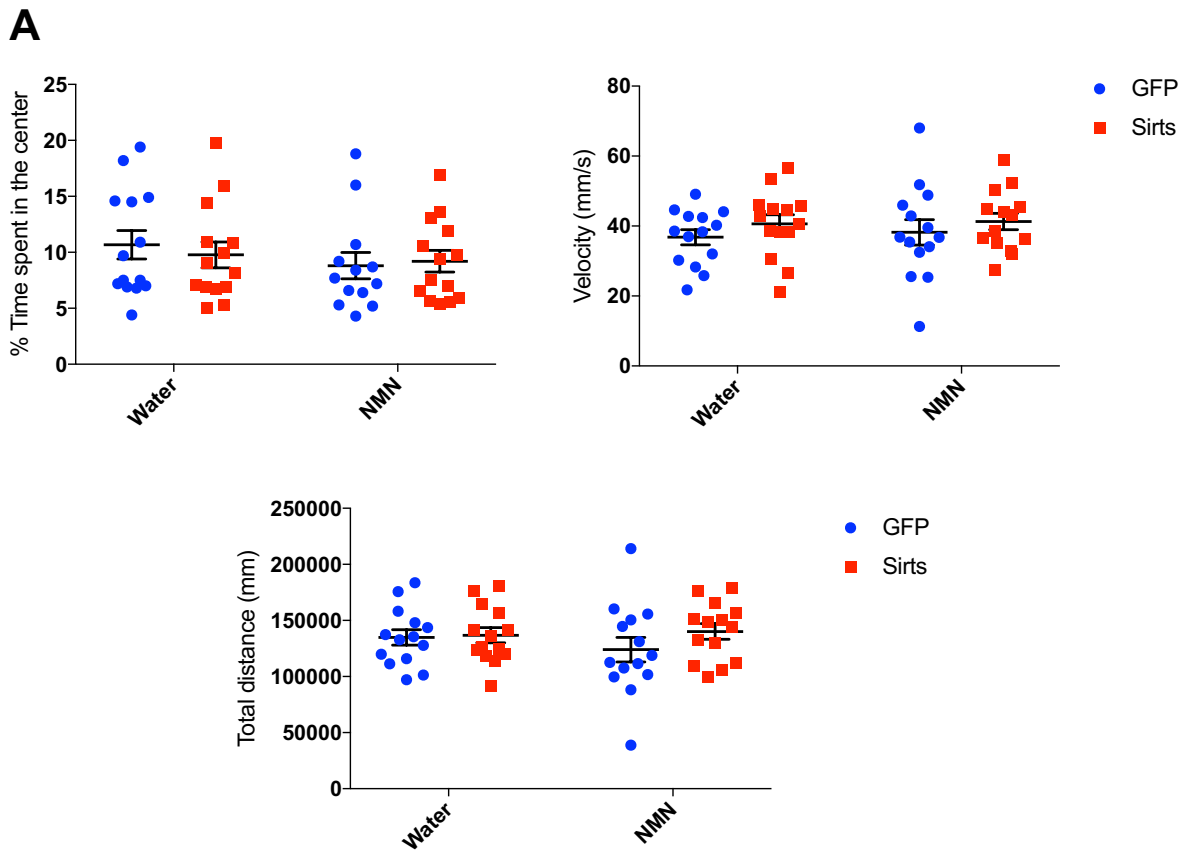

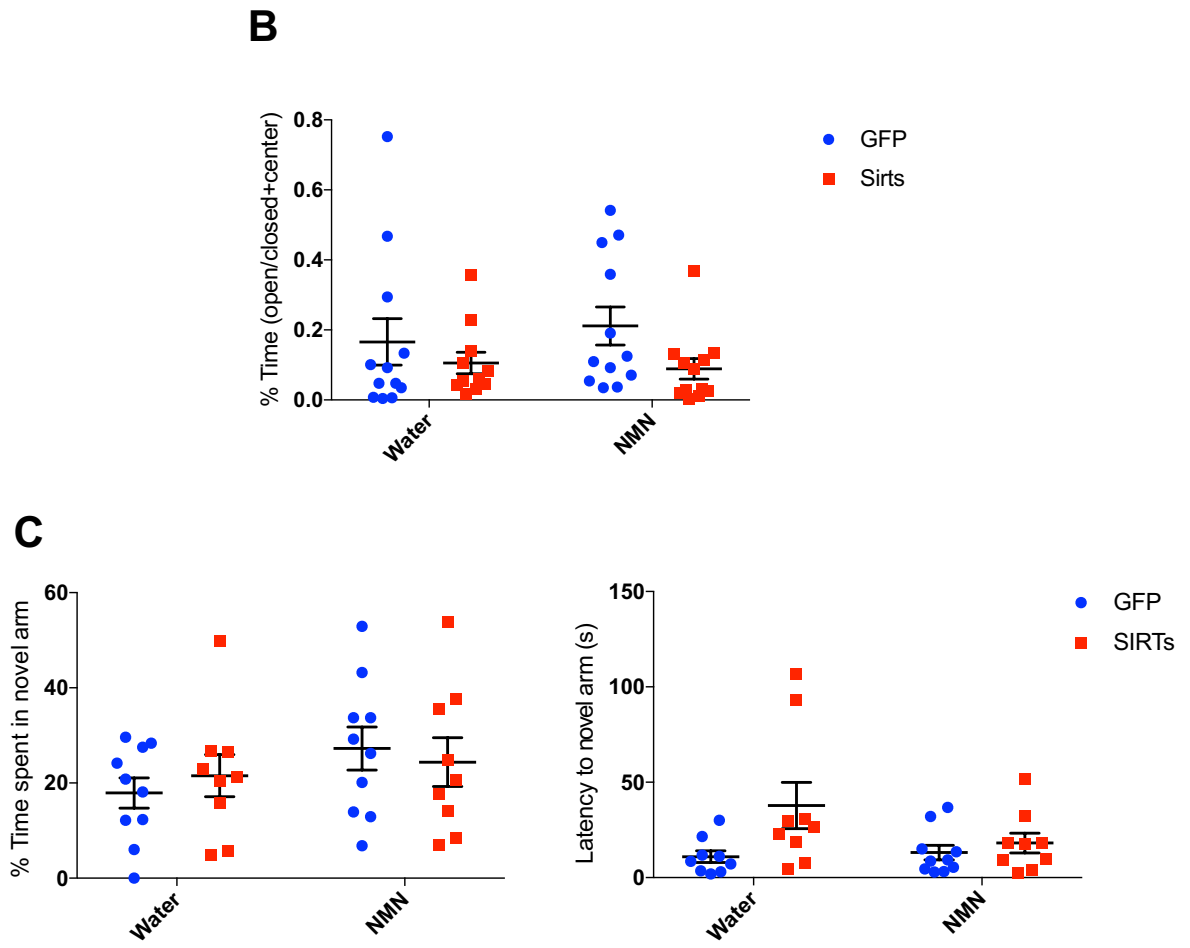

Figure 4.5: NMN and SIRTs gene therapy effects on locomotor activity, anxiety, and cognition. (A) Open field test with percentage of time spent in the center (top left), velocity (top right), and total distance (bottom). Two-way ANOVA Tukey's multiple comparisons test. n = 14 mice/group. (B) Elevated plus maze test with percentage of time spent in the open arms. Two-way ANOVA Tukey's multiple comparisons test. Gene therapy p = 0.07. n = 14 mice/group. (C) Y-maze test with percentage of time spent in closed arm (left) and the latency to the close arm (right). Two-way ANOVA Tukey's multiple comparisons test. Gene therapy *p = 0.03. n = 9-10 mice/group. Values are mean ± SEM.

4.4.4. SIRTs and NAD$^+$ supplementation improved muscle function in old mice

To further evaluate the impact of our treatment on locomotor behavior, we evaluated the impact of our treatment on spontaneous activity in mice measuring their circadian locomotor activity. We observed that the NMN treated groups, both in the presence and absence of SIRTs, showed decreased ambulatory activity in both the X-axis (XAMB, which includes grooming and feeding movements performed in a horizontal position) and Y-axis (ZTOT, which includes grooming movements performed in a vertical position) during the dark period (Figure 4.6 A,B). Interestingly, no differences in respiratory exchange ratio were observed between the groups (Figure 4.6 C).

A

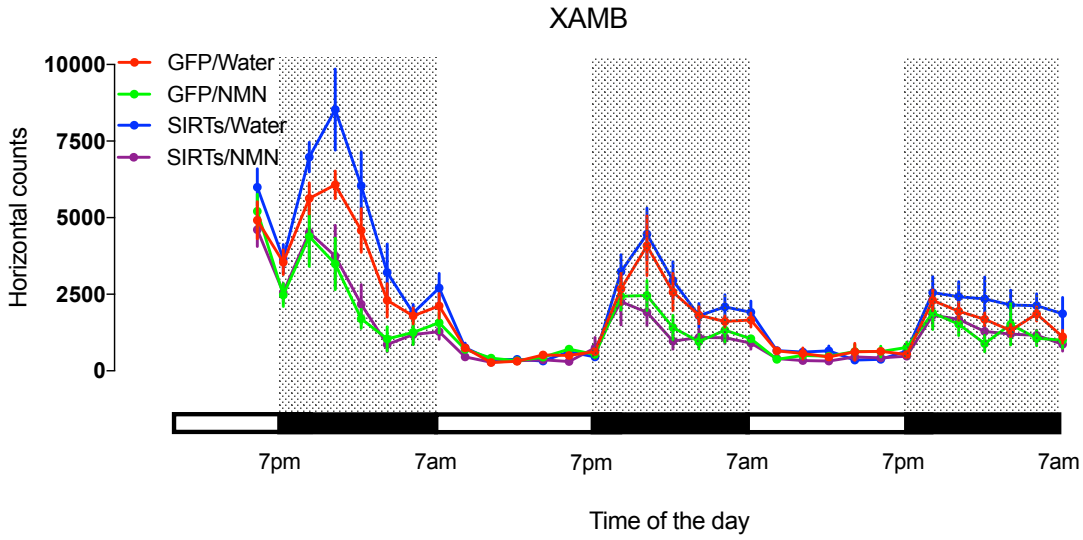

B

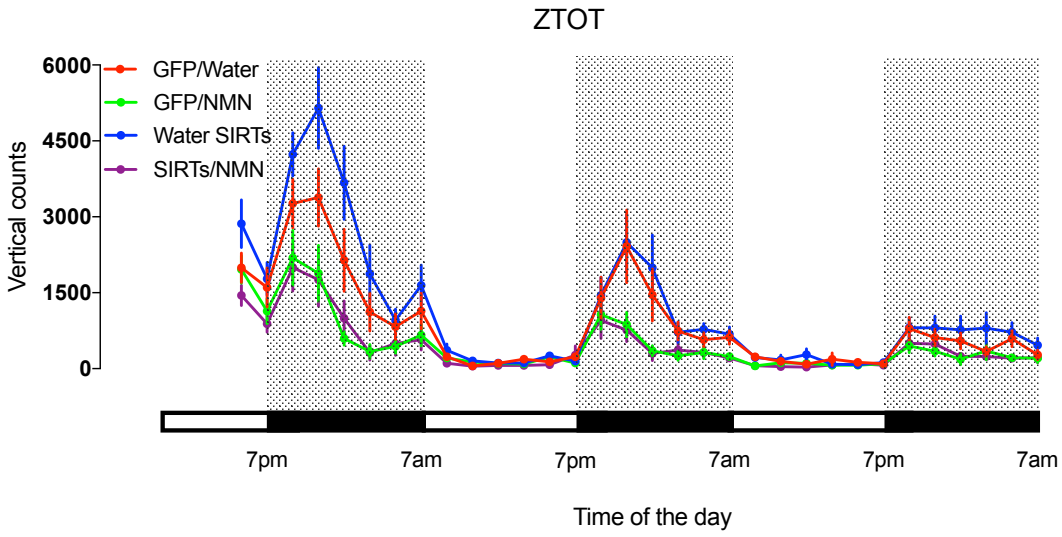

C

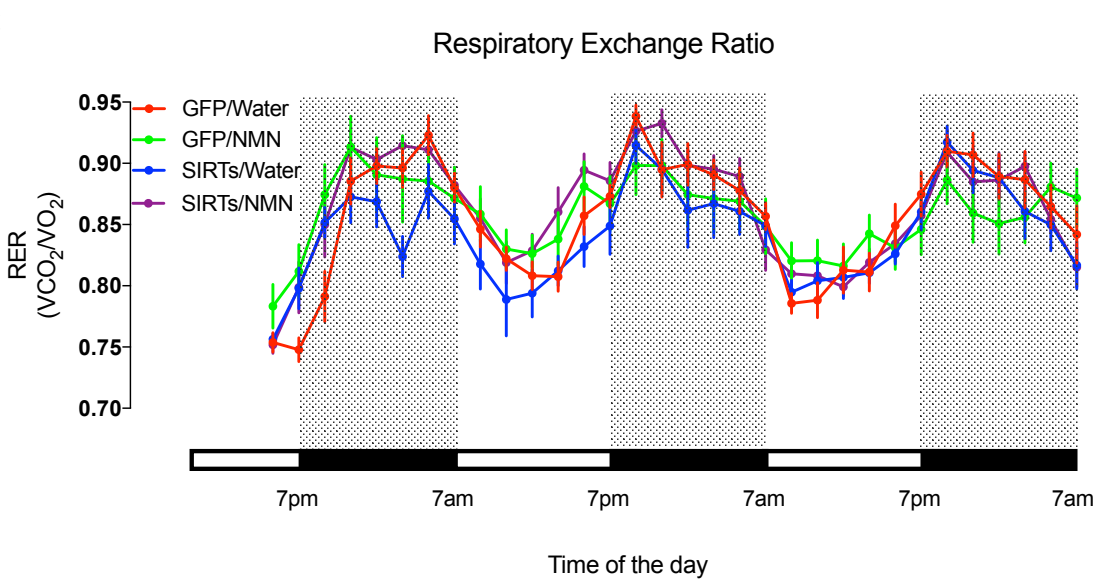

(Legend next page)

Figure 4.6: NMN and SIRTs gene therapy effects on circadian locomotor activity without changing metabolism. Daily locomotor activity (last 24h) represented as total movement along (A) horizontal (ZTOT) and (B) vertical (XAMB) axes. (C) Daily respiratory exchange ratio (RER, calculated from the rate of CO_2 production (VCO_2) and the oxygen consumed (VO_2)). Two-way ANOVA Tukey's multiple comparisons test. Values are mean ± SEM.

In order to better understand the circadian activity results, we performed gait analyses. As shown in Figure 4.7, mice treated with SIRTs presented with improvements in gait parameters. In particular, we observed a greater percentage of time spent in the swing portion of the gait in the forelimbs and a decrease in the proportion of time spent in the stance position independent of NMN treatment (Figure 4.7 A-B). Moreover, mice that received SIRTs gene therapy showed greater maximum longitudinal deviation in both fore and hindlimbs, indicating a more dynamic gait (Figure 4.7 C-D). Altogether, we conclude that overexpression of sirtuins may have a beneficial effect and may prevent the decline of gait in old mice (Figure 4.7 E). Further analysis of muscle mass, normalized by body weight, showed that in very old age (29 months-old) SIRTs gene therapy was able to increase muscle mass (Figure 4.7 F-G), which could explain, at least in part, the observed improvements in gait.

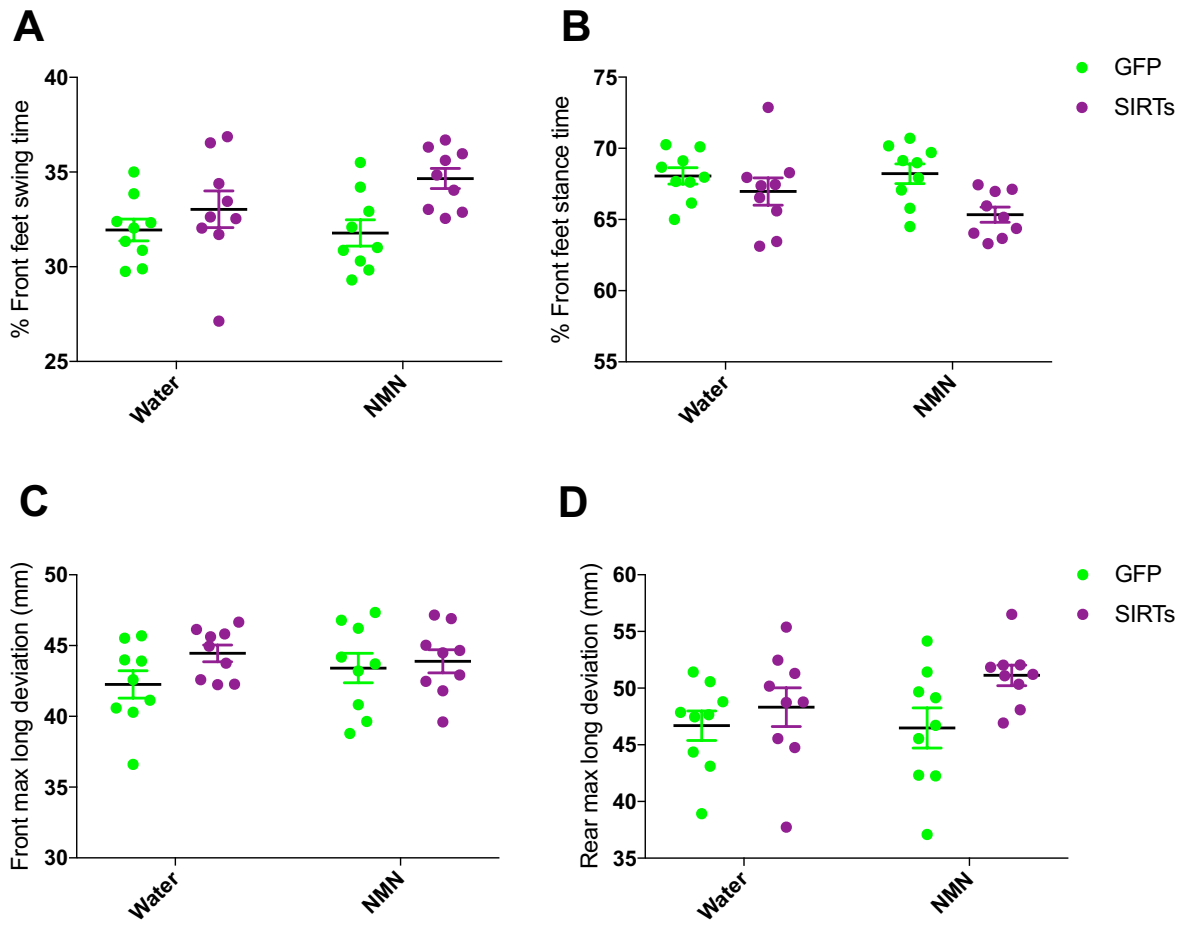

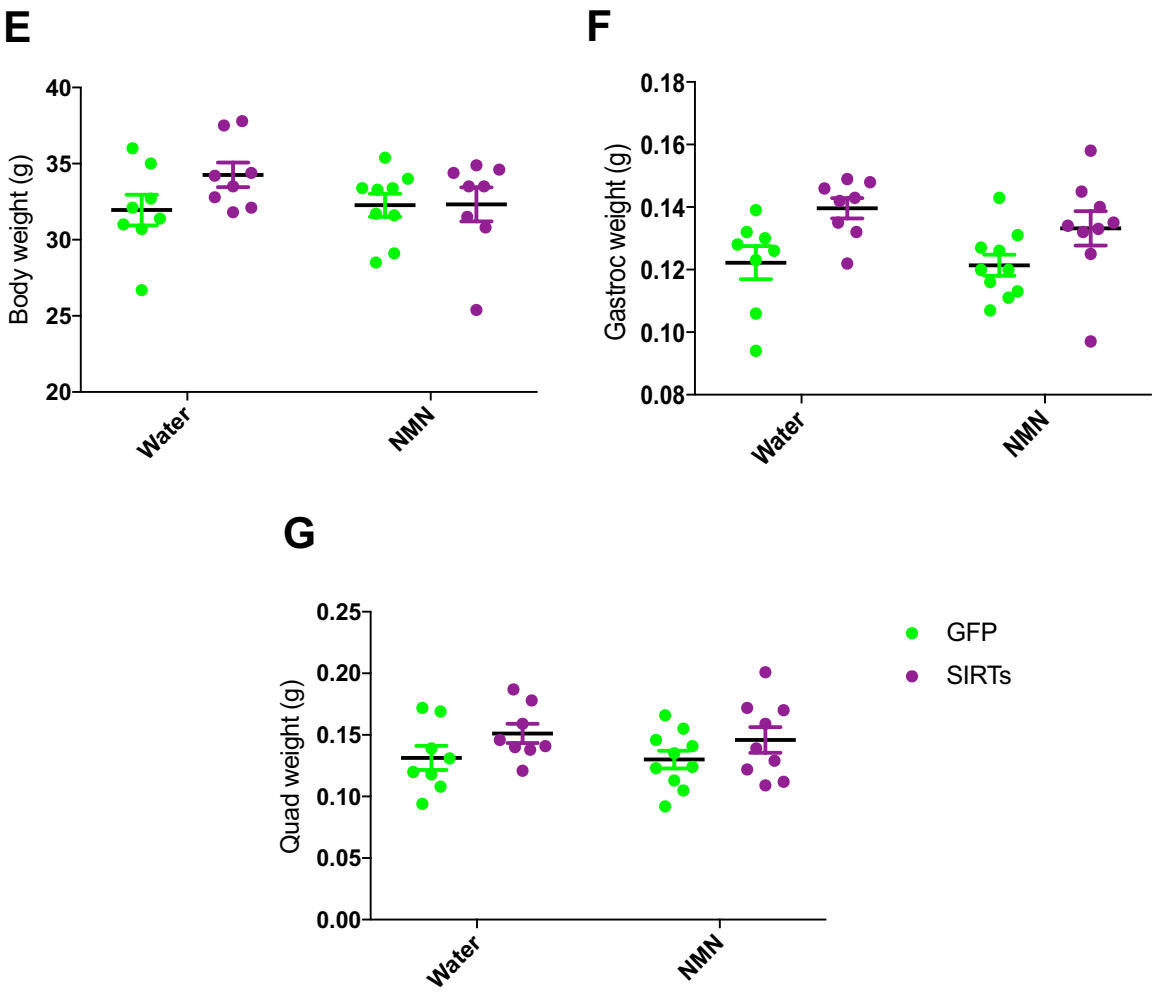

Figure 4.7: NMN and SIRTs gene therapy effects on gait and muscle mass. (A) Percentage of walking gait parameters front feet swing time. Two-way ANOVA Tukey's multiple comparisons test. Gene therapy **p = 0.001. n = 9 mice/group. (B) Percentage of front feet stance time. Two-way ANOVA Tukey's multiple comparisons test. Gene therapy *p = 0.01. n = 9 mice/group. (C) Front feet maximum longitudinal deviation. Two-way ANOVA Tukey's multiple comparisons test. Gene therapy p = 0.1. n = 9 mice/group. (D) Rear feet maximum longitudinal deviation. Two-way ANOVA Tukey's multiple comparisons test. Gene therapy *p = 0.04. n = 9 mice/group. (E) Body weights. Two-way ANOVA Tukey's multiple comparisons test. 8/9 mice/group. (F) Gastrocnemius weights. Two-way ANOVA Tukey's multiple comparisons test. Gene therapy *p = 0.05. n = 8/9 mice/group. (G) Quadriceps weights. Two-way ANOVA Tukey's multiple comparisons test. Gene therapy *p = 0.05. n = 8-9 mice/group. Values are mean ± SEM.

4.5. Discussion

The initial discovery that genetic interventions could be used to up-regulate NAD^+ biosynthesis in order to increase both stress resistance and lifespan of yeast cells and *Drosophila* (Anderson *et al.*, 2002; Anderson *et al.,* 2003; Balan *et al.*, 2008), has attracted much attention. Using both wild-type and disease rodent models to test NAD^+ boosting has thus become a strategy in hopes of accelerating testing time using multiple genetic interventions. However, investigating synergistic strategies has been cost and time prohibitive. In this study we presented a synergistic strategy to study how boosting the expression of and activity of the entire sirtuin gene family might affect both health and lifespan in old mice. Based on our results, we observed a modest but relevant benefit. NMN showed to be protective in age-related body weight loss and could, at some extent, extend longevity. Based on these findings, we now plan to administer a higher dose of NMN as well as start treatment at a younger age (12 months), which should increase our ability to detect any significant differences that were masked by using old mice and a lower dosage.

Aging is associated with muscle mass loss, described as sarcopenia, as well as decreased muscle function, which is mainly caused by loss of muscle homeostasis and decreased metabolism through mitochondria. One of most interesting results from our study was the beneficial effect of SIRTs overexpression in gait parameters and muscle mass. Indeed, increased stance time has been shown to be present in disease models that affect gait (Poulet *et al.*, 2014), and the stance time in our SIRTs overexpression model mimics that effect. Moreover, we were surprised by the increase in skeletal muscle mass by SIRTs gene therapy since our AAV9 showed relatively low expression in muscle. Thus, we hypothesize that this may be an indirect effect through, at least to some extent, promotion of endothelial cell proliferation and improved vascularization (Das *et al.*, 2018).

Gomes and colleagues (Gomes *et al.*, 2013) have shown that NMN was able to restore several key aspects in aging in mice, such as muscle-type switching, insulin sensitivity, oxidative phosphorylation, and gene expression. Currently, clinical treatments for sarcopenia are scarce, so the promotion of sirtuin activity may be one avenue to explore in further detail. Taken together, finding interventions to improve longevity has been a long path and our study suggests that boosting NAD^+ levels using NMN might be an approach that can promote longevity benefits.

One of the biggest needs in other to understand what the best approach and model is to treat aging and age-related diseases is a considerable need for a mouse model that can somehow recapitulate human diseases (Justice and Dhillon, 2016). Evidence that mammalian gene expression changes with age in the late ’80s were important findings that helped the field to start to uncover the fundamental cause of aging in eukaryotes. However, the

technologies to understand how those changes occur did not exist by that time. One decade later studies of aging in the budding yeast *S. cerevisiae* provided the first evidence that gene expression changes may not simply be a characteristic of aging but may be an underlying cause (Kennedy *et al.*, 1995, 1997; Imai and Kitano, 1998). In *S. cerevisiae*, Sir2 was shown to have a dual role: it maintains silent heterochromatin and aids with double-strand DNA break (DSB) repair (Martin *et al.*, 1999; McAinsh *et al.*, 1999; Mills, Sinclair and Guarente, 1999; Tamburini and Tyler, 2005). During yeast replicative aging, Sir2 constitutively relocalizes away from silent loci to the nucleolus, ostensibly to counteract DSBs at the rDNA locus (Kennedy *et al.*, 1997; Sinclair and Guarente, 1997). The resulting expression of mating-type genes causes sterility, a hallmark of aged yeast cells. Evidence is accumulating that a similar epigenetically-driven aging process called “RCM” (relocalization of chromatin factors) is a cause of aging in mammals (Vijg and Hasty, 2006). In the next chapter, we will test this model using unique research tools developed in our lab, describing what we think is the first model to comprehensively and accurately mimic human aging.

CHAPTER 5

DNA damage-induced epigenomic drift accelerates aging in mice

5.1. Abstract

Aging is a multifaceted biological process common for all living organisms and is characterized by a gradual loss of normal physiological functions culminating in loss of function and ultimately in disease and death. If there is a highly conserved cause of aging across species, perhaps it is due to a breakdown in the maintenance of biological systems such as the challenging task of maintaining a youthful gene expression pattern over an organism's lifetime. Changes in gene expression during aging have been studied for decades but precisely why they occur and if they contribute to senescence and aging are poorly understood.

The RCM hypothesis states that aging may be due in part to DNA repair-driven changes to the nuclear architecture and epigenome, leading to cellular dysfunction and eventually senescence. Evidence from our lab has shown that the act of repairing DNA leads to epigenetic changes that have relevance to Hutchison-Guilford progeria, including decreased nuclear Lamin B1 and histone loss. In our study, we used transgenic cells and mice that are designed to accelerate changes in the epigenome in order to determine if progression of senescence and aging can be delayed or even reversed via epigenetic control using state-of-the art genetic approaches and pharmacological agents. There is a considerable need for improved animal models of human frailty and resilience as well as those that recapitulate human disease for successful pre-clinical studies. Currently, largely due to cost, most age-related diseases are modeled in young mice. However, young mice do not accurately mimic old mice, let alone aged humans who have experienced 80 years of epigenetic changes.

We have developed a novel animal model called the "ICE mouse" (for inducible changes in epigenome) that allow us to induce a few DNA cuts in non-coding regions of the mouse genome across all tissues and monitor the effects on tissues and age-related physiology. In agreement with the RCM hypothesis, ICE mice exhibit early onset age-related phenotypes as well as age-related diseases. These experiments are consistent with the epigenetic shift driven by the DNA repair process as an upstream cause of aging in mammals.

We believe that the ICE mouse is the first model to comprehensively and accurately mimic human aging. We envision that the ICE model will be a novel tool to directly model several age-related human diseases and assess whether this form of aging process can be slowed down or reserved using know and novel agents.

5.2. Introduction

Over the years, research leading to discoveries in humans and model organisms has prompted a repetitive cycle, starting with observations in humans that lead to experimentation in mice, which then ultimately is validated in humans. This cycle has been proven to accelerate progress regarding the diagnosis, treatment, as well as the reversal and prevention of development disorders. In a few cases, true experimentation in humans is possible, however, the majority time, experiments are most practical in model organisms such as mice, where the research can be properly controlled along with adequate statistical power. Examples of disease genes like *Cftr* (Riordan *et al.*, 1989), *Htt* (MacDonald *et al.*, 1993), and *Mecp2* (Amir *et al.*, 1999) were first discovered in humans and then characterized in mice, whereas genes like *Lep*^{ob} (Zhang *et al.*, 1994), *Fto* (Peters *et al*., 1999), *Kitl* (Flanagan *et al*., 1991), and *Ubp1* (Koutnikova *et al.*, 2009), are examples of genes that were studied in mice and later shown to be relevant in human diseases.

Experiments in human genetics have been shown to be a challenge, with limitation in availability of biological materials, particularly from unaffected individuals, with low accessibility to cells and tissues, as well as lack of time-points before the onset of pathology. Another difficulty came with the fact that large samples sizes are needed for statistical power, as human samples introduce genetic and environmental heterogeneity. Additionally, studies *in vitro* also present some challenges, since in many conditions the critical cell-types are unknown, as well as the use of tissue culture is often times proven irrelevant since the combination of cells or communication between tissues or organs are difficult to mimic *in vitro*. Without animal models, where several of these challenges can be addressed and understood, it would be likely impossible to conduct the necessary experiments to validate human discoveries. On this note, in the aging field it is commonly accepted that there is a need for mouse models to better recapitulate human diseases (Justice and Dhillon, 2016). These mouse models would allow a level of experimental control and under conditions that are not possible in human studies. Extensively characterized, the mouse genome can be easily genetically engineered, making the mouse by far the most popular animal model in biomedical research, enabling unparalleled resources for researchers around the world. Experiments at the scale that enable statistically meaningful conclusions about developmental and physiological mechanisms are possible due to the feasibility to rapidly expand a mouse colony with inbred strains serving as rigorously controlled experiments, where relations between genotype and phenotype are being tested without the confounding effects of heterogeneous genetic backgrounds.

Nevertheless, even if a mouse model does not perfectly mimic human biology, when used properly they provide valuable insights about the human condition, facilitating the discovery of

fundamental biological principles, essential to prioritizing and testing hypotheses in human studies.

5.2.1. Animal models of aging

All over the years, several animal models have been critical to unraveling key pathways associated in the aging process. Research in lower organisms such as yeast have been important to study both replicative lifespan, measured by the number of times a yeast mother cell produces a daughter cell before becoming senescent, and chronological lifespan, measured by the length of time a cell can survive in a post-mitotic state (Kaeberlein *et* al., 2007). Moreover, studies in worms and flies have also been important to study key pathways associated in aging, especially due to their short lifespan (Tissenbaum, 2012; Brandt and Vilcinskas, 2015). Hence, even though studies in these models have been important to the aging field, they cannot fully recapitulate the multifaceted nature of human aging, particularly due to the lack of capability to carry age-associated diseases and decline in healthspan. Consequently, by taking advantage of the genetic proximity to humans and the possibility to genetically engineer their genome, vertebrate models such as mice have been used as models of premature aging (Quarrie and Riabowol, 2004). However, due to their relatively long lifespan, and in order to have more efficient laboratory studies of normal aging, mouse models are being replaced in some studies by alternative vertebrate models, such as the African turquoise killifish, *Nothobranchius furzeri* (Harel *et al.*, 2015), which has a lifespan of 4-6 months and are able to mimic some of the age-related pathological changes observed in humans.

Although there's no consensual animal model in the aging field, studies over the years have used different models that have been important to unraveling key aspects and pathways associated with aging. In addition to studies showing that genetic differences and somatic mutations play a role in aging and longevity, additional studies have also shown that non-genetic influences may also play an important role (Cournil and Kirkwood, 2001), creating a marked contrast in physical appearance, reproductive behavior, and lifespan. Studies on caloric restriction (Bordone and Guarente, 2005), interventions on basal metabolic rate (Ruggiero *et al.*, 2008), up-regulation of stress response (Migliaccio *et al.*, 1999), repair of mitonuclear communication (Houtkooper *et al.*, 2013), as well as reducing fertility (Westendorp and Kirkwood, 1998) have been shown to be associated with lifespan extension. All of these observations have led the field to start to investigate the role of "epi"-genetic mechanisms that modulate longevity pathways.

5.2.2. Epigenetics and aging

Traditionally, the word “epigenetics” started to be used to describe events that could not be explained by genetics. The credit for this term is given to Conrad Waddington (1905-1975), who defined epigenetics as “the branch of biology which studies the casual interactions between genes and their products, which bring the phenotype into being” (Waddington, 1942). This statement led many researchers to link several biological phenomena, some considered bizarre and inexplicable, to epigenetics. Paramutation in maize (described as an interaction between two alleles in which one allele triggers heritable changes to the other) as well as position effects variegation in *Drosophila* (where local chromatin environment of one gene governs its expression) are two examples of seemingly unrelated process lumped into the category of epigenetics.

Generally, epigenetics is a bridge between the genotype and the phenotype, where changes in the final outcome of a locus or chromosome are observed without altering the underlying DNA sequence. For instance, although the vast majority of cells in a multicellular organism share an identical genotype, during development the organism generates a variety of cell-types with diverse, yet stable, profiles of gene expression and distinct cellular functions. Therefore, cellular differentiation may be considered an epigenetic event, most likely governed by changes in the “epigenetic landscape”, rather than alterations in genetic inheritance (Figure 5.1) (Waddington, 1957). Moreover, epigenetics may be described as the study of any potentially stable and heritable change in gene expression or even cellular phenotype that happens without changes in base-pairing of DNA as described by Watson and Crick.

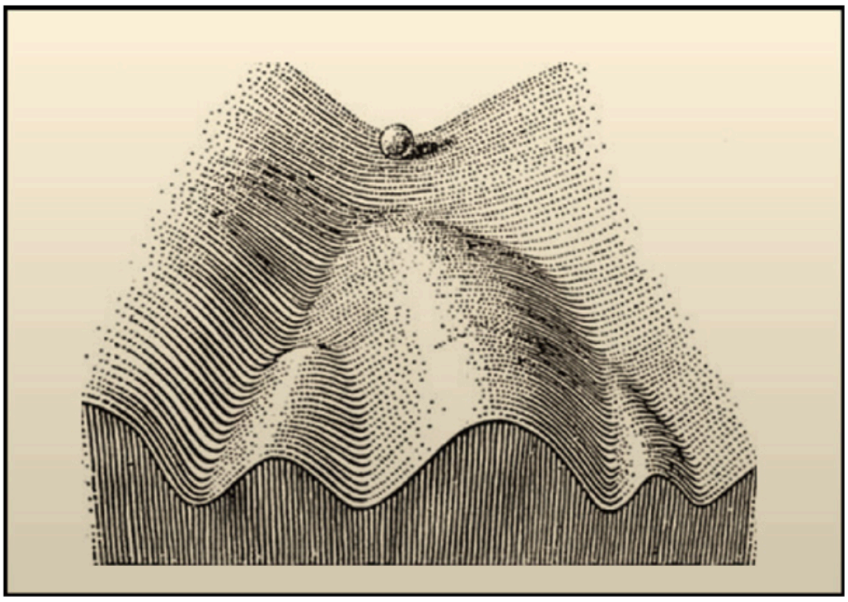

Figure 5.1: Waddington’s Classical Epigenetic Landscape (adapted from (Waddington, 1957)).

The epigenome is responsible for the functional use and stability of genetic information that is carried by the chromosomes within the genome, connecting the genotype with the phenotype (Goldberg *et al*., 2007; Muñoz-Najar and Sedivy, 2010; O'Sullivan and Karlseder, 2012; Zane *et al*., 2014). Within the epigenome, different types of epigenetic information, such as the presence or absence of histones on any particular DNA sequence, post-translational modifications of histone proteins, chromatin remodeling, DNA methylation, structural and functional variants of histones as well as transcription of noncoding RNAs (ncRNAs) have been reported (Feser and Tyler, 2011; O'Sullivan and Karlseder, 2012; Brunet and Berger, 2014; Pal and Tyler, 2016). All of these different types of epigenetic information have been shown to contribute to the function, cell and tissues fate, both at unicellular and multicellular levels (Pal and Tyler, 2016). Accordingly, it is believed that, during the aging process, each of these different types of epigenetic information have important functionalities. Moreover, chromatin structure, which has the important role of carrying much of the epigenetic information, has implicated been implicated as a main player in the aging process.

Chromatin is a polymer of nucleosomes and is composed of DNA enveloping the histone proteins, and may exist in two forms, the euchromatin, which is less condensed and can be translated, and the heterochromatin, which is highly condensed and typically not transcribed. By regulating access of transcriptional machinery to DNA, chromatin along with epigenetic factors have an important role in regulating gene expression, both dynamically and over long-time scales. Although the cause of aging is poorly understood and currently under extensive debate, several epigenetic studies have begun to link epigenetic alterations to the aging process. Supporting this idea, it is commonly recognized that a general loss of histones coupled with local and overall chromatin remodeling, the imbalance in activating or repressing histone modifications, as well as, global transcriptional changes are observed in aging models. However, it is unclear if changes in the activity of epigenetic enzymes influence the expression of critical longevity genes or even if alterations in longevity genes lead to epigenetic changes in the genome.

5.2.2.1. Epigenetic mechanism of aging

Epigenetic alterations, described as one of the cellular and molecular hallmarks of aging (López-Otín *et al.*, 2013), is characterized by a reversible, heritable mechanism that occurs without any changes in the underlying DNA sequence. Notably, the cause of these alterations can have been argued to be either spontaneous or driven by internal or external stimuli. Interestingly, epigenetic alterations have been associated as the factor that explains why the two genetically identical individuals, such as identical twins, or even, in the animal kingdom, between animals with equal genetic background, such as queen and worker bees, have remarkable different patterns of aging (Fraga *et al.*, 2005; Sargent, 2010; Brunet and Berger,

2014). Even though longevity studies in the human population have reported that genetic factors could explain at some extent differences observed in the lifespan of monozygotic twins, the major part of the remaining variation is believed to have arisen from the epigenetic drift throughout their lifetime (Herskind *et al.*, 1996; Fraga *et al.*, 2005; Poulsen *et al.*, 2007; Muñoz-Najar and Sedivy, 2011; O'Sullivan and Karlseder, 2012). Therefore, targeting the epigenome has been strongly proposed for therapeutic interventions since these alterations are due to enzymes and are consequently reversible, unlike genetic changes, which are presently irreversible in humans. Understanding the epigenetic events that occur during aging may potentially lead to the elaboration of novel beneficial interventions to delay aging and aging-related diseases.

5.2.2.1.1. Heterochromatin changes during aging

Heterochromatin domains are established early during embryonic development and are thought to be maintained throughout lifespan. Nevertheless, it is well known that loss of constitutive heterochromatin (mainly at telomeres, centromeres, pericentromeres) occurs during senescence and aging, triggered by telomere shortening, transcription changes at boundaries and breakdown of the nuclear periphery.

The "heterochromatin loss model of aging" was described for the first time by Bryant Villeponteau in 1997. This early proposed model suggests that the observed loss of heterochromatin during aging triggers changes in global nuclear architecture as well as in the expression of genes in those regions, leading directly or indirectly to cellular senescence and aging. Loss of transcriptional silencing due to loss of heterochromatin was shown to occur in all eukaryotes, from yeast to humans, during aging (Smeal *et al.*, 1996; Villeponteau, 1997; Haithcock *et al.*, 2005; Larson *et al.*, 2012; Tsurumi and Li, 2012), and supporting evidence has revealed that accelerating or reversing this process could either decrease or increase lifespan. Moreover, it was reported that manipulation of histone deacetylase (HDAC) activities, wither by inhibitors or even deleting genes encoding HDACs, can decrease lifespan, while interventions with novel chemicals, by both activating or overexpressing *SIR2* or sirtuins can increase lifespan (Haigis and Sinclair, 2010; Guarente, 2011).

Even though yeast Sir2 was initially discovered to be an H4K16Ac deacetylase, while mammalian SIRT1 was recognized as an H3K9Ac or H4K16Ac deacetylase (Haigis and Sinclair, 2010), it is now well valued that sirtuins not only deacetylase histones but also other transcriptional regulators, with their roles in aging being reported to involve genome maintenance as well (Oberdoerffer *et al.*, 2008). In budding yeast, previous reports have shown that during aging the redistribution of Sir proteins from the silent mating-type loci to sites of increased genomic instability lead to loss of silencing from heterochromatin mating-type loci and cause infertility and promote aging (Kennedy *et al.*, 1997). One of the first studies

from the age-related deregulation of heterochromatin came from findings in young, healthy yeast cells, where the Sir2 protein was shown to repress gene expression at the silent mating type loci HML and HMR and suppress recombination at the ribosomal DNA (rDNA) locus, which gave rise to toxic rDNA circles (ERCs) (Sinclair and Guarente, 1997). As yeast cells age, the Sir2/3/4 complex dissociates from the HM loci and moves to the nucleolus in response to ERC accumulation, causing sterility, a hallmark of yeast aging. Moreover, it was also reported that Sir proteins may also move to other sites of genome instability such as hyper LOH-events in old cells (McMurray and Gottschling, 2003). Thus, a redistribution of chromatin modifying factors and the resulting changes in transcription promote genomic instability and replicative aging in budding yeast (Villeponteau, 1997). Likewise, the mammalian homolog SIRT1, has been shown to suppress several regions throughout the mouse genome. In response to DNA damage, SIRT1 redistributes to these DNA breaks loci, altering gene expression, as is observed in the aging mouse brain (Oberdoerffer *et al.*, 2008). Thus, it is becoming clear that repression of heterochromatin repeat elements is evolutionary conserved and is particularly important in lifespan maintenance (Oberdoerffer and Sinclair, 2007; Oberdoerffer *et al.*, 2008).

Moreover, research in human diseases has supported the notion of heterochromatin loss as a model of aging. For several years, researchers in the field thought that mutations were the cause of aging but analysis of chromatin structures from Hutchinson-Gilford progeria syndrome (HGPS) and Werner syndrome stem cell models of premature aging has supported the heterochromatin loss theory (Goldman *et al.*, 2004; Scaffidi and Misteli, 2006; Shumaker *et al.*, 2006; O'Sullivan and Karlseder, 2012; Zhang *et al.*, 2015). These diseases, where it is observed either a mutation in genes encoding for the DNA repair system or the A-type lamin, lead to chaotic chromatin architecture indicating that genomic instability and chromatin deterioration may be causes of human aging. Hence, recapitulating some molecular and cellular changes characteristic of the natural aging process will provide a better understanding of the mechanisms underlying these human premature aging diseases and may provide us with critical information for understanding the complexity of aging.

5.2.2.1.2. DNA methylation changes during aging

Heterochromatin establishment and maintenance pathways have been strongly linked to aging in mammalian cells, where global and gene-specific changes lead to reduced cellular fitness. In addition to histone modifications, direct chemical modification in DNA are also linked to epigenetic changes.

DNA methylation is a well-studied and one of the best characterized epigenetic modifications that occurs during aging (Jung and Pfeifer, 2015), happening mostly on the 5-carbon of cytosine residues in CpG dinucleotides. Regarding aging models, DNA methylation

is more prominent in mammalian systems, comparing models that have no (e.g. yeast) or limited (e.g. worms and flies) DNA methylation, and is achieved by three DNA methyltransferases: DNMT1, having a maintenance role, and DNMT3a and b, which are *de novo* methylases.

At the promoters, CpG methylation leads to transcriptional suppression, due to the formation of condensed chromatin structures such as heterochromatin, a pattern coupled with focal increase in repressive modifications that fits the global heterochromatin deregulation aging model. In young cells, the majority of CpG sites within the genome have cytosine methylation, and with age the mammalian cells were shown to undergo global DNA hypomethylation and local DNA hypermethylation (Cruickshanks *et al.*, 2013). This phenomenon may be, at least in part, due to the loss of heterochromatin during aging. Loss of CpG methylation at repetitive sequences will increase the risk of retrotransposition incidents and consequently instability of the genome during aging, since retrotransposons comprise much of the repetitive DNA.

In humans, studies in identical twins have revealed that as they age their patterns of DNA methylation diverge due to epigenetic drift caused by environmental causes or even natural stochastic errors (Fraga *et al.*, 2005). This epigenetic drift leads to arbitrary alterations in the methylome of the aging individuals. Nevertheless, some of the methylation changes that occur during aging seems to occur in a no stochastic way, they appear to be directional and involve specific regions in the genome, indicating that at least some of the DNA methylation changes that occur with age may be relevant to biological means relevant in the aging process.

These observations in DNA methylation have led to a large-scale study from the University of California, Los Angeles (UCLA), where it was shown that DNA methylation status can serve as a notable predictor of age in normal tissues. In this study, approximately 8000 samples from 51 healthy human tissue and cell -ypes and approximately 6000 cancer samples were analyzed. DNA methylation at 353 CpGs (termed clock CpGs) but no other epigenetic modifications were identified to accurately predict age (Horvath, 2013, 2015). Additionally, a parallel study built a predictive model of aging methylome using blood from individuals aged between 19-101 years to explore the rate of DNA methylation changes during aging (Hannum *et al.*, 2013). In this study, the researchers identified a smaller set of 71 CpG sites that have a high correlation of age prediction occurring near genes relevant to aging. So far, human cells and tissues have been used to identify their clock and similar clocks in model organisms like mice are being developed. However, there is a considerable need for mouse models that recapitulate human diseases (Justice and Dhillon, 2016). Currently, most age-related diseases are modeled in young mice, a decision largely due to cost. However, young mice do not accurately mimic old mice, let alone aged humans who have experienced 80 years of

epigenetic changes. Here, we have developed the ICE mouse, which we believe is the first model that comprehensively and accurately mimics human aging.

5.3. Materials and Methods

5.3.1. Generation of ICE mouse model

I-PpoI^{STOP} cassette knock-in mouse ES cells were generated the following way. Briefly, an estrogen receptor nuclear translocation domain (ER^{T2}) tagged with HA at the N-terminus and I-*PpoI* were inserted into the STOP-eGFP-ROSA26TV plasmid (addgene, plasmid #11739), followed by an IRES and EGFP sequence. The HA-ER^{T2}-I-*PpoI*^{STOP} cassette was integrated at Rosa26 loci and the targeted C57BL/6 ES cells were injected into C57BL/6 albino (cBRD/cBRD) blastocysts. After back-crossing I-*PpoI* $^{STOP/+}$ chimeric mice with C57BL/6 mice, ICE mice were generated by crossing I-*PpoI*$^{STOP/+}$ mice to Cre$^{ERT2/+}$ mice harboring a single ER^{T2} fused to Cre recombinase which is expressed in the whole body (Ruzankina *et al.*, 2007). Four to six-month-old ICE mice were fed an AIN-93G Purified Rodent Diet with 360 mg/kg tamoxifen citrate for 3 weeks to carry out I-*PpoI* induction. The ER^{T2} contains three mutations and selectively binds to 4-hydroxytamoxifen (4-OHT), but not estradiol. The Cre-ER^{T2} protein is translocated into the nucleus by tamoxifen treatment followed by removal of the STOP cassette located upstream of I-*PpoI*. In the presence of tamoxifen, not only Cre- ER^{T2} but also HA-ER^{T2}-I-*PpoI* localize to the nucleus and DNA double strand breaks are induced. Wild-type aged mice were provided from the NIA Aged Rodent Colonies and the mice were housed at least for a month prior to testing. Mice were fed LabDiet® 5053 diet and received water *ad libitum,* and all animal care followed the guidelines of the Animal Care and Use Committees (IACUCs) at Harvard Medical School.

5.3.2. Frailty Index Score

Frailty index was scored as described (Whitehead et al., 2014). Briefly, mice were weighed, and measured their body surface temperature twice at the abdomen using an infrared temperature probe (La Crosse Technology, La Crosse, WI, USA). A hearing test was measured by making sound with a dog training clicker, and a ruler was used to calculate vision capacity. A frailty index score for each mouse was calculated addressing more than 30 clinical signs of frailty using a checklist as previously described (Whitehead et al., 2014). Clinical assessment included evaluation of the integument, digestive/urogenital, ocular/nasal, physical/musculoskeletal, as well as respiratory and discomfort systems. Scores of 0, 0.5, and 1 were used. 0 indicated no sign of a deficit, 0.5 indicated a mild deficit, and 1 indicated a severe deficit. A complete list of the clinical signs evaluated can be found in Appendix 1.

5.3.3. Behavioural experiments

All behavioral tests were conducted as previously described in Chapter 3, between 9:00 AM and 5:00 PM (light phase) in a sound attenuated room, where all mice were acclimatized for 1 h prior to testing. All apparatuses and objects were cleaned with 70% ethanol solution after each session. Behavioral experiments were video-monitored and recorded using the video tracking system and analyzed using appropriate software (TopScanLite).

5.3.3.1. Y-maze Spontaneous Alternation Test

Y-maze spontaneous alternation test is a behavioural assay used for measuring the willingness of the mouse to explore new environments. Mice characteristically favour to explore the novel arm rather than return to the one formerly visited. The test occurs in a Y-shape maze with three plastic arms at 120º angle from each other. Mice were placed in the Y-maze apparatus in the testing room with visual cues on the walls and allowed to explore the Y-maze apparatus for 5 min during which time one arm was blocked. After a 15-minute rest period, the mice re-explored for 5 min the Y-maze apparatus, but now with all the arms opened. We measured the number of entries and the time spent in the novel arm as a measure of short spatial and working memory using the video tracking system and analyzed using appropriate software (TopScanLite).

5.3.3.2. Elevated Plus Maze Test

The elevated plus maze (EPM) test was used to assess anxiety-related behavior in mice. The EPM apparatus is an elevated “+”-shape maze composed by two oppositely placed closed arms, two oppositely placed open arms, and a center area. After habituation in the test room, mice were placed in the EPM apparatus with visual cues on the walls and allowed to explore for 10 min. We measured the mouse preference for being in the open arms as compared to the closed arms as an indicator of anxiety-like behavior. Their behavior was recorded using a video tracking system and analyzed using appropriate software (TopScanLite).

5.3.3.3. Modified Barnes Maze Test

The modified Barnes maze test was performed under the delayed Match-to-Place testing usually performed in a typical water maze tank and was used to assess cognitive impairments in mice. This test was performed to measure learning abilities without forcing the mice to perform a task under unnatural conditions, such as swimming in water. Mice were put on a white spherical platform with numerous escape holes placed around the center of the elevated platform. Aversive stimulus were created by using bright overhead lighting, pushing the animal to seek out the target escape hole, which was attached to an escape box and protected from light. Visual cues with naïve shapes were placed around the maze to act as spatial cues. Mice

were placed in the center of the platform at the beginning of each training test and given some time to find the target hole. If the animal entered the target hole before the time ran out, the experiment ended. Animals that either did not find or enter the target hole were directed to it by the researcher and allowed to stay in the box for a few seconds before being returned to their home cage. The training trials were performed for 4 days. On the 5^{th} and 12^{th} days, the mice were tested for spatial memory. During the test day, the target hole box was removed and closed. Behavior of the mice was then recorded to measure for escape box position latency. Their behavior was recorded using a video tracking system and analyzed using appropriate software (TopScanLite).

5.3.4. Endurance Tolerance Test

Endurance tolerance test was conducted between 9:00 AM and 5:00 PM (light phase) in a sound attenuated room, where the mice were acclimatized for 1 h prior to testing. The apparatus was cleaned with 70% ethanol solution after each session.

An electrical stimulation grid was adjusted to 1 mA and the slope was set to 15 degree. During first day in the training, mice walked on the treadmill at 10 m/min speed for 10 min, followed by a 10 min break and then walking again at 10 m/min speed for 10 min. On the second and third days, the initial two steps were same as the first day: walking at 10 m/min speed for 10 min, then a 10 min break. Then, walking was started at 10 m/min and the speed was increased by 1 m/min every minute until a maximum speed of 20 m/min was reached. On Day 4 of the experiment, the animal's maximum exercise endurance was measured. Mice were placed on the treadmill and the belt speed was started at 5 m/min for 5 min to allow the mice warm up. The speed was then increased by 1 m/min until the speed reached 20 m/min. After running for 5 min at 20 m/min, the speed was increased to 21 m/min for 10 min. Then, mice ran at 22 m/min until the mice could no longer perform and thus stayed on the electrical stimulation grid for 10 seconds. Blood collected from tails was taken at pre-exercise and post-exercise and serum lactate levels were measured with a lactate meter (LACTATE PLUS, Nova Biomedical, Waltham, MA, USA).

5.3.5. Metabolic and Physical Activity

The metabolic rate of the animals was monitored by indirect calorimetry in open-circuit oxymax chambers using the Comprehensive Lab Animal Monitoring System (CLAMS; Columbus Instruments, Columbus, OH, USA). Mice were singly housed with water and food available *ad libitum* under a 12-12-hour light-dark cycle at approximately 24°C. The mice were kept in the monitoring cages for 2 days, allowing them to acclimatize before the last 24h when the parameters were analyzed.

Sample air was pumped through the test chambers, equipped with an oxygen (O_2) sensor for determination of O_2 content. Oxygen concentration in the air entering the chamber compared with air leaving the chamber allowed for the determination of O_2 consumption. The percentage of O_2 and CO_2 gas levels in each chamber environment was measured periodically and the changes observed in these levels were used to determine O_2 consumption (VO_2), CO_2 production (VCO_2), respiratory exchange ratio (RER), and heat.

Spontaneous activity measured by both horizontal (XAMB) and vertical (ZTOT) movements was also monitored. The system is equipped with infrared beams able to monitor all of the chamber's axes. The beams were horizontally 130 mm apart in order to provide a greater resolution grid covering the XY-planes. The data were recorded and presented in terms of the number of "beam breaks".

5.3.6. Grip Strength Test

To measure muscular strength, a grip strength test was used (BIO-G53, Bioseb, USA). A mouse was held by the tail and allowed to hold onto a mesh grip with its front paws. Grip strength was assessed by pulling the mouse backwards by the tail until its grip was liberated. The experiment was repeat 3 times after 10 min breaks.

5.3.7. PET-CT

Mice were anesthetized with 2% isoflurane gas in oxygen and injected with ~200 μCi F-18 labeled flourodeoxyglucose (FDG) via tail vein injection. After 45 minutes, mice were imaged on a Siemens Inveon small animal imaging scanner for positron emission tomography (PET) and computed tomography (CT) imaging under isolflurane. CT imaging was performed over 360 projections with a 80 kVp 500 uA x-ray tube and reconstructed using a modified feldkamp cone beam reconstruction algorithm (COBRA Exxim Inc., Pleasanton, CA) with 425 ms exposure time/projection during which Isovue-360 (Bracco Diagnostic Inc, Monroe Township, NJ) was pumped into the mouse via tail vein at a rate of 20 μl per minute. PET scans were reconstructed with ordered subset expectation maximization with maximum a posterior reconstruction algorithm with 2 OSEM iterations and 18 MAP iterations.

5.3.8. Micro CT scanning

Femurs were isolated and placed in 70% ethanol. Micro-CT was performed by using SCANCO Medical μ-CT35 at a core facility in Harvard School of Dental Medicine.

5.3.9. Dual Energy X-ray Absorptiometry (DEXA)

Dual Energy X-ray Absorptiometry was performed suing a PIXI-mus Small Animal Densitometer (LUNAR, Madison, WI). During the X-ray acquisition mice were anaesthetized

with 2% isoflurane in 700 mL O2/minute (in a chamber at 5% isoflurane and maintained by face mask).

5.3.10. Magnetic Resonance Imaging

MRI experiments were performed using a Bruker Biospec MRI with a horizontal bore 7 Tesla, 30 cm magnet with actively shielded gradients (200 mT/m maximum strength on each axis) and a 72 mm internal diameter proton birdcage resonator (Bruker Biospin MRI GmbH, Ettlingen, Germany). For each experiment, 3 mice (1 for each group) were placed in the resonator tail first in the prone position. A water phantom and a fat phantom were placed on either side of the mice to serve as intensity standards. T_2-weighted axial images from the neck to the abdomen were obtained using a spin echo sequence with TE = 11 ms, TR = 5 s, slice thickness = 1 mm, slice gap = 0 mm, number of signal averages = 2 or 6, matrix dimension = 256 $\times$ 256, field of view = 5 or 6 cm (read; anterior-posterior) $\times$ 7 cm (phase; left-right). Analysis subtraction was performed between corresponding water + fat measurement and water-only to obtain a fat-only measurement.

5.3.11. Western Blot Analysis

Protein extracts were obtained by adding sodium dodecyl sulphate-polyacrylamide gel electrophoresis (SDS-PAGE) sample buffer [(0.5 M Tris 0.4% SDS, pH 6.8), 30% glycerol, 10% SDS, 0.6 M dithiothreitol and 0.012% of bromophenol blue] to tissue homogenates and boiled at 95°C for 5 min. Pre-stained molecular weight markers (Bio-Rad Labs, Hercules, CA, USA) and 20-40 µg of protein samples were separated by 4-20 % gradient SDS-PAGE electrophoresis under reducing conditions at 100-120 mV and electro-transferred onto 0.45 µm nitrocellulose membranes (GE Healthcare, Chicago, IL, USA). After blocking for 1 h at RT with 5% milk diluted in Tris-buffered saline solution with 0.1% Tween-20 (TBS-T) (50 mM Tris, 150 mM NaCl, and 0.1% Tween-20, pH 7.6), the membranes were incubated overnight at 4°C with primary antibodies (1:1000) (Table 2) diluted in TBST-T with 5% milk. After three washing periods of 10 min each with TBS-T, the membranes were incubated with the appropriate secondary antibody (dilutions of 1:10 000 - 20 000) diluted in TBS-T with 5% milk for 2 h at RT. After three 10 min washes with TBS-T, membranes were incubated with ECL reagent (GE Healthcare) for 5 min at RT. The immunoreactivity was visualized using a chemiluminescence apparatus (ChemiDoc Imaging System, BioRad) and analyzed using appropriate software (Fiji software).

5.3.12. mtDNA copy number

Snap frozen tissues were placed in a 1.5 mL eppendorf containing 0.6 mL lysis buffer [10 mM Tris-HCl (pH 8.0), 1 mM EDTA, and 0.1% SDS] and 0.06 mL of a 15 mM proteinase K

solution (P2308, Sigma-Aldrich, St Louis, MO, USA), and incubated at 55 ºC overnight. Lysate solutions were vortex vigorously and the non-soluble fraction was pelleted by centrifugation (8000g, 15 min). The consequent supernatant was transferred to a new tube and an equal amount of phenol/chloroform/isoamyl alcohol (24:4:1) (PCIAA) was added. After mixing, samples were centrifuged (8000g, 15 min), and 0.45-0.5 mL of the supernatant was transferred to a new tube. An equal volume of chloroform was added to the supernatant, the solution was vigorously vortexed and centrifuged (8000g, 15 min). The 0.4 mL resultant supernatant was transferred to a new tube and mixed with 0.04 mL NaAc (3 M) and 0.44 mL isopropanol. The tube was incubated at -20 ºC for 1m min to facilitate DNA precipitation and then centrifuged (8000g, 15 min) to pellet the DNA. Pelleted DNA was finally washed with 1 mL of 70% ethanol, air dried and dissolved in Tris-EDTA (TE) buffer. The primers were designed targeting 18S ribosomal and COX2 genes and were used to calculate the ratio of mtDNA to genomic DNA. Primers used were as follow: mouse 18S, 5`-TGTGTTAGGGGACTGGTGGACA-3` (Forward) and 5`-CATCACCCACTTACCCCCAAAA-3` (Reverse), mouse COX2, 5`- ATAACCGAGTCGTTCTGCCAAT-3` and 5`-TTTCAGAGCATTGGCCATAGAA -3` (reverse).

5.3.13. Electron Microscopy

Twenty-two-month-old mice were fasted overnight and anaesthetized with isoflurane. Intracardial perfusion was performed with 0.01M PBS and then an electron microscopy fixative (consisting of 3% glutaraldehyde, 2.5% paraformaldehyde, 2 mM calcium chloride, 2% sucrose in 0.1 M cacodylate buffer), with tissue processed as previously reported (Le Couteur *et al.*, 2001). Two blocks from different parts of the gastrocnemius were used and from each section 10 images were taken at 5000X on a Jeol 1210 transmission microscope and photographed using a Gatan US 4000MP digital camera. Mitochondrial network, size, and number were quantified blindly using FUJI ImageJ software.

5.3.14. DNA methylation.

Tissue samples were collected and immediately preserved in DNA/RNA Shield™ (Zymo Research; Cat. No. R1100-50) and genomic DNA was purified using Quick-DNA Plus Kit (Zymo Research; Cat. No. D4068), according to the manufacturer's instructions. Sample library preparation and data analysis for mouse DNAge^{Ò} (Epigenetics Aging Clock) were performed by a service provider (Zymo Research). 200 ng of genomic DNA was bisulfite converted using the EZ DNA Methylation-Lightning™ Kit (Zymo Research; Cat. No. D5030). Bisulfite-converted DNA libraries for targeted bisulfite sequencing platform, called SWARM^{Ò} (Simplified Whole-panel Amplification Reaction Method), were prepared according to the manufacturer's instructions and were sequenced on a HiSeq 1500 sequencer for

>1,000X coverage. Sequence reads were identified using Illumina base calling software and aligned to the reference genome using Bismark (http://www.bioinformatics.babraham.ac.uk/projects/bismark/), an aligner optimized for bisulfite sequence data and methylation. The methylation level of each sampled cytosine was estimated as the number of reads reporting a C, divided by the total number of reads reporting a C or T (write these out). DNA methylation levels of >500 age-related CpG loci were used for age prediction using Zymo Research's proprietary mouse DNAge^{Ò} algorithms:

A penalized regression model's coefficients $b_0, b_1, ..., b_n$ relate to transformed age as follows:

$$F(\text{chronological age}) = b_0 + b_1CpG_1 + \cdots + b_nCpG_n + \text{error}$$

DNAge^{Ò} is estimated as follow:

$$DNAge^{TM} = inverse.F(b_0 + b_1CpG_1 + \cdots + b_nCpG_n)$$

5.3.15. Muscle RNA sequencing analysis

Paired-end reads from gastrocnemius muscle RNA-Seq were mapped to the UCSC mm10 genome build using HISAT2 version 2.1.0 (Kim *et al*., 2015). The featureCounts function from the Rsubread package (Rsubread 1.32.2) was used to collect read counts for genes. DESeq2 (DESeq2 1.22.2) was applied for differential expression analysis to all genes with rowSums >= 10.

To compare gene expression in gastrocnemius muscles of ICE, Cre, and WT, a table of normalized read counts was exported from a combined DESeq dataset with all replicates and conditions. The 200 genes with the smallest adjusted p-value for differential expression between Cre and ICE were selected and ordered by the log2-fold-change difference between Cre and Ice. The heatmap.2 (gplots 3.0.1) R function was used to produce a plot of Z-score values for each gene.

5.3.16. Statistical Analysis

Data were analyzed by a one- and two-way ANOVA with multiple comparisons when appropriated. Statistical tests were performed with GraphPad Prism (San Diego, CA, USA). Data are presented as means ± SEM.

5.4. Results

5.4.1. Transient, nonmutagenic DNA damage in mice using the ICE system

To test the hypothesis that epigenetic noise, due to DNA break repair, is a cause of aging, we developed a temporally and spatially controlled genetic system over DNA cutting. The goal of this genetic approach was to create double-stranded breaks (DSBs) slightly above background levels in order to initiate the phenomenon that we have named "RCM" (for redistribution of chromatin modifiers), which is a response without generating mutations and allows us to have meticulous interpretations. Using this system, we took advantage of the characteristics of homing endonucleases, which are selfish DNA elements that cut DNA and then transfer their genetic information to the cut site and differ from the CRISP/Cas9 system in that mutations are extremely rare and absent. We have used I-*Ppo*l, a homing 3' endonuclease from the slime mold *Physarum polycephalum*, which have been used to study the kinetics of DSB repair in mammalian cells (Berkovich *et al*., 2007). I-*Ppo*l has a 15 bp DNA recognition sequence, that occurs 19 times within the mouse genome, although the actual number of sequences that are accessible for cutting *in vivo* have been reported to be lower (Berkovich *et al*., 2007).

We engineered a two-component system that allows us to precisely control the localization and expression of I-*Ppo*l (Figure 5.2 A). First, we controlled the localization of the I-*Ppo*l endonuclease with the fusion of I-*Ppo*l to the C-terminal of a mutant estrogen receptor domain that specifically binds to tamoxifen (ERT2), moving the protein into the nucleus. A loxP-STOP-eGFP-loxP cassette is located upstream to block transcription, whereas an IRES-GFP cassette is located downstream providing a visual readout in cells when the STOP cassette is removed. The second component, consisting of a tamoxifen-regulated Cre recombinase (Cre-ER^{T2}) under the control of the human ubiquitin C promoter, ensured whole-body expression (Ruzankina *et al.*, 2007). When tamoxifen was provided *in vivo*, and these two components are combined, Cre-ER^{T2} moves into the nucleus where it excises the STOP cassette, facilitating transcription of the ER^{T2}-HA-I-*Ppo*l-IRES-GFP gene cassette (Berkovich, Monnat and Kastan, 2007; Ruzankina *et al.*, 2007). Upon removal of tamoxifen, ER^{T2}-I-*Ppo*l moves towards the cytoplasm where it degraded. The I-*Ppo*l recognition sequence (CTCTCTTAA▼GGTAGC) is predicted to cleave the mouse genome at 19 different recognition sites (Argast *et al.*, 1998; Berkovich *et al*., 2007), but in practice only 10% are accessible *in vivo* (Berkovich *et al*., 2007) and only one of them is within an open-reading frame (ORF).

C57Bl6/J transgenic mice containing each of these components were bred and the offspring were used either as controls (Cre only) or experimental mice (Het ER^{T2}-I-Ppol). The

resulting mouse was named Inducible Changes in the Epigenome or “ICE” mice (Figure 5.2 B).

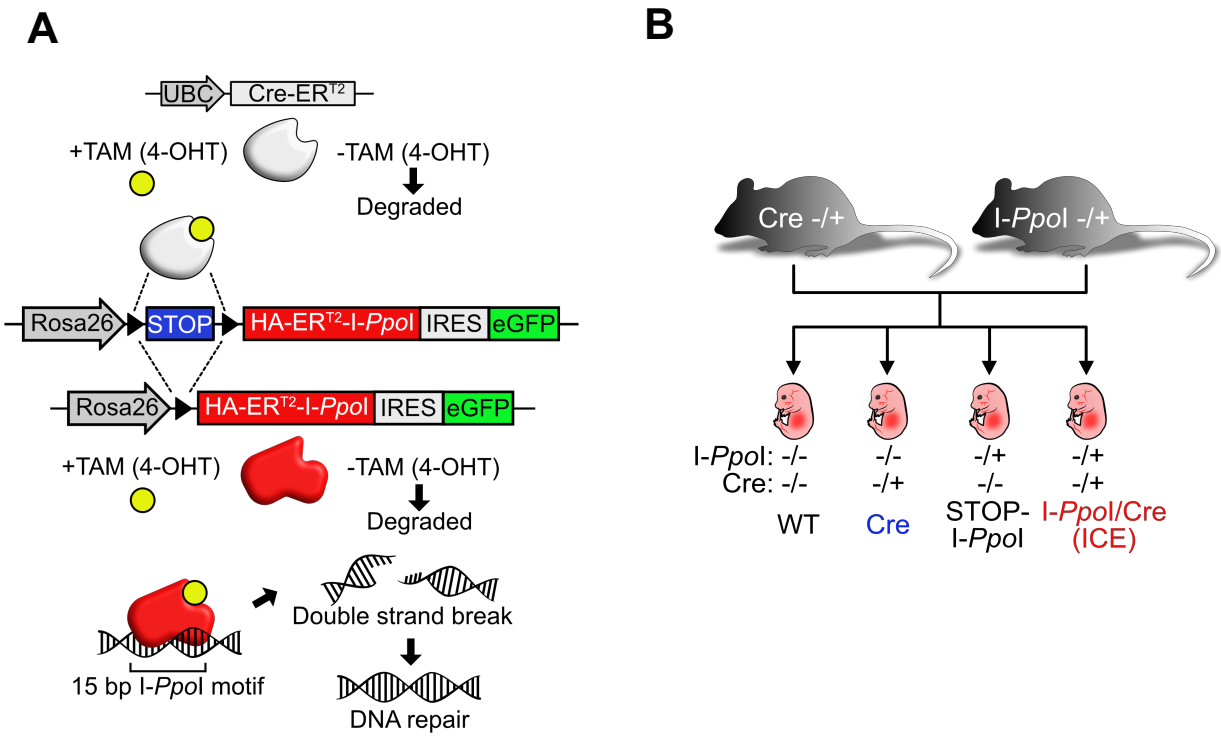

Figure 5.2: The Inducible Changes in the Epigenome “ICE” mouse system. (A) Schematic of the ICE system with a tamoxifen-inducible I-*Ppo*I endonuclease. (B) Breeding scheme to create ICE mice and appropriate controls (WT, Cre and I-*Ppo*I).

We started our experiments by treating ICE mice and littermate Cre controls at 4-5 months of age, using a tamoxifen-containing diet (360 mg/kg) that was provided during three weeks of treatment and then removed. During tamoxifen treatment, the major tissues tested included the heart, kidney, skeletal muscle, and liver, and showed increased levels of HA-I-*Ppo*I as well as markers of DNA damage, gamma-H2AX, confirming that our system was working (Figure 5.3).

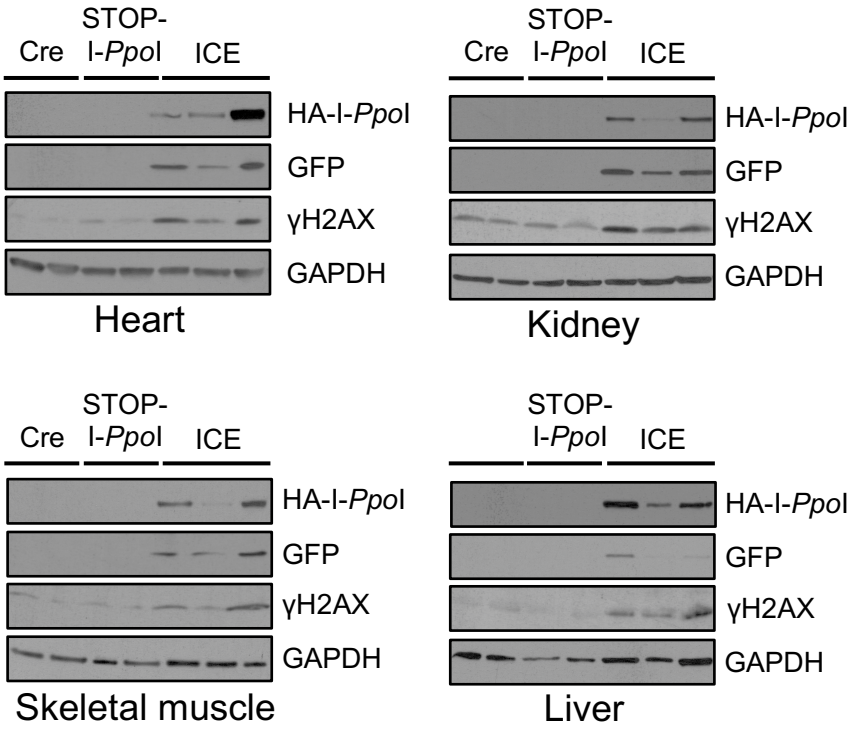

Figure 5.3: Confirmation that the ICE mouse model was successfully generated. Western blot of tissues probed with anti-HA to detect I-*Ppo*I expression and gamma-H2AX.

5.4.2. ICE mice rapidly trigger hallmarks of aging

To provide the first *in vivo* evidence of the epigenetic noise hypothesis, 4-5-month-old ICE mice were treated for three weeks with tamoxifen in order to induce DNA cutting and were then analyzed at the physiological, behavioral, cellular and molecular levels. During the three-week *Ppo*I-induction period, we observed that there were no overt aging-like differences between ICE mice and Cre control littermates. After one-month post-treatment, we started to notice some slight differences in ICE mice, such as loss of hair pigment on the tail, nose, and ears (Figure 5.4 A). However, at ten months post-treatment there was a dramatic difference between ICE mice and Cre controls, both at the visual and physiological levels (Figure 5.4). ICE mice had significantly greater alopecia, loss in fur color and whiskers (Figure 5.4 A) and decreased body weight (Figure 5.4 B). Moreover, frailty index, a noninvasive way to quantify the overall health and quality of life in humans and mice (Whitehead *et al.*, 2014), showed that while 10-12 month post-treatment Cre control mice increased their frailty by 1.5 fold as compared to levels observed 1 month post-treatment, ICE mice showed an increase of 2.6 fold, levels that paralleled those observed in 24 month-old mice (Figure 5.4 C).

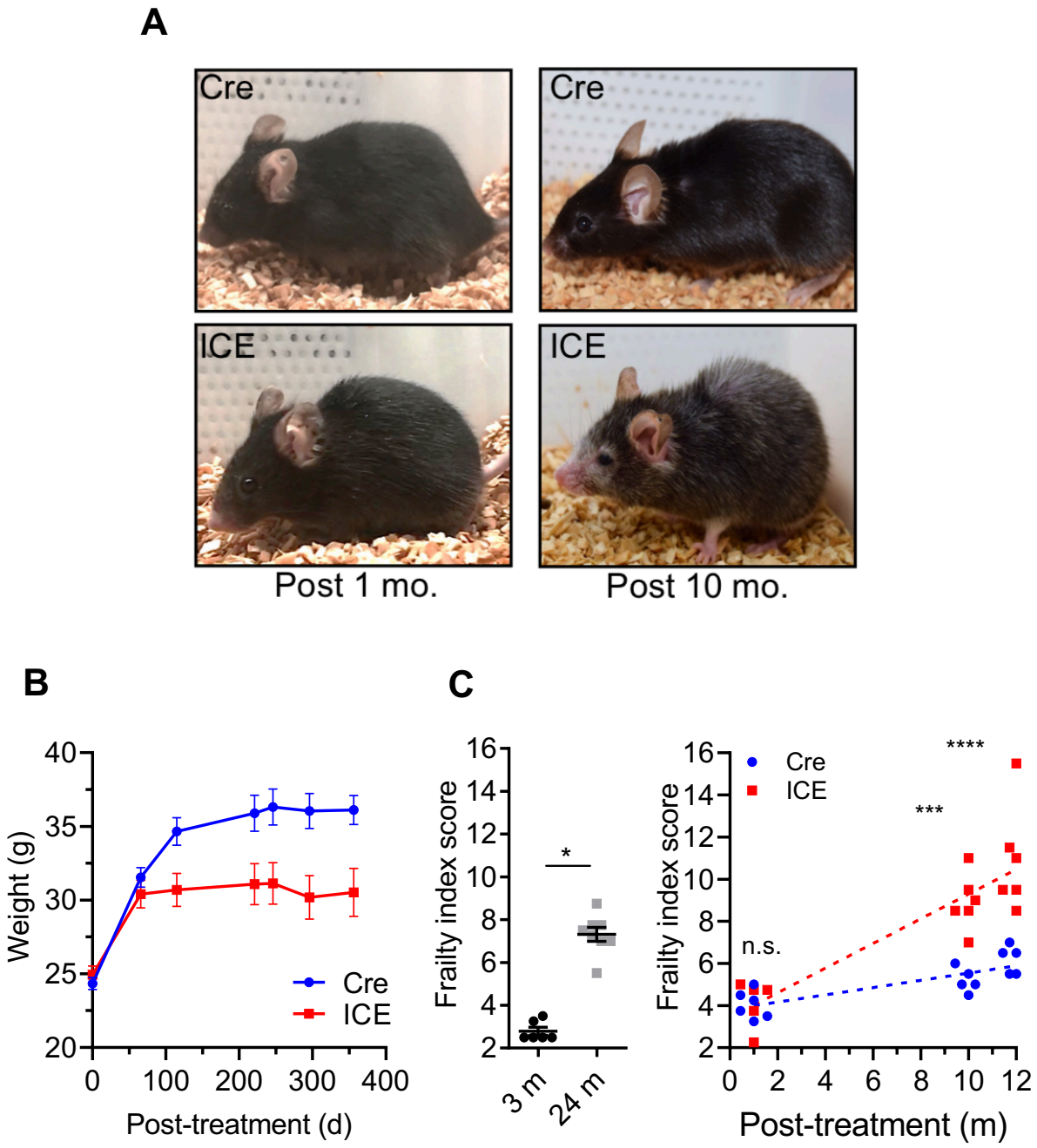

Figure 5.4: Effects of I-*Ppo*l induction on body weight, phenotype, and frailty index. (A) Representative images of Cre and ICE mice. (B) Body weight. (C) Frailty index scores of Cre, ICE, WT 3- and 24-month-old mice. Two-tailed Student's *t*-test (left) and two-way ANOVA-Bonferroni (right). *p < 0.05; ***p < 0.001; ****p < 0.0001. n = 6 mice/group. Data are mean ± SEM.

Kyphosis and osteoporosis, two well-established features of mammalian aging, due to loss of connective tissue in the spine and a decline in cortical bone thickness and density in the trabecular bone in the inner layer, were also analyzed in our ICE model. As shown in figure 5.5 ICE mice exhibited kyphosis and a loss of trabecular bone density as compared with Cre

controls (Figure 5.5 A-B). Moreover, using quantitative MRI, we observed a decrease in total fat mass and an increase in lean mass, as compared with Cre controls (Figure 5.5 C-D). In agreement with the observed difference in body weight, the respiratory exchange ratio was slightly higher in ICE mice, compared with Cre controls (Figure 5.6 A) and motion analysis showed that ICE mice moved less, with a decrease in both vertical (ZTOT) and horizontal (XAMB) movements, mimicking behavior observed in normally aged mice (Figure 5.6 B-C).

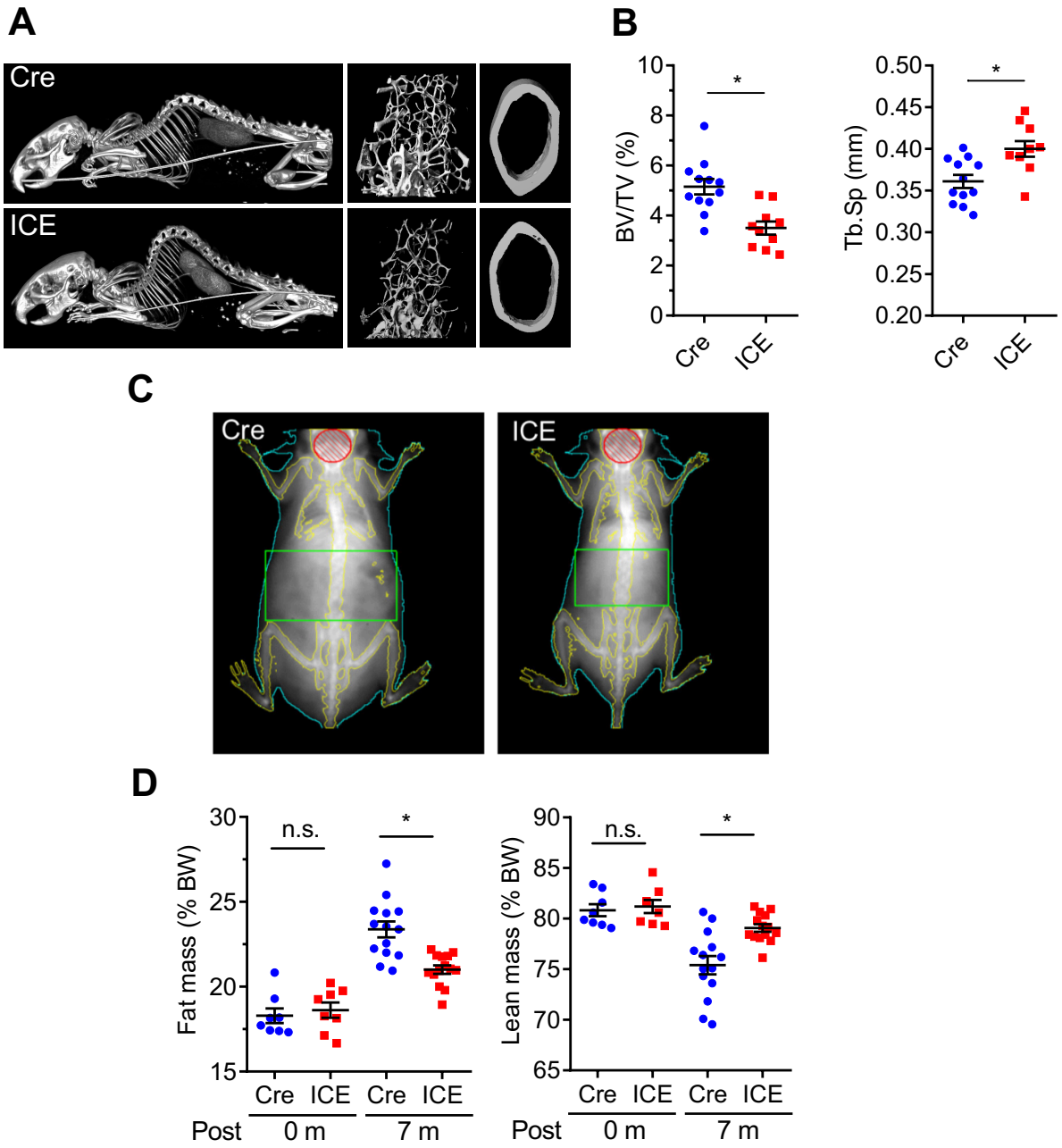

Figure 5.5: ICE mice are an accelerated phenocopy of normal aging. (A, B) CT of whole skeleton and micro-CT of trabecular and cortical bones of Cre and ICE mice. Kyphosis assessment (A), bone/tissue volume (middle) and trabecular separation (right) (B). Two-tailed Student's *t*-test. *p < 0.05. n = 10-12 mice/group. (C) DEXA assessment. (D) Fat mass (left) and lean mass (right). Two-tailed Student's *t*-test. Data are mean ± SEM. *p < 0.05. n = 8-14 mice/group. Data are mean ± SEM.

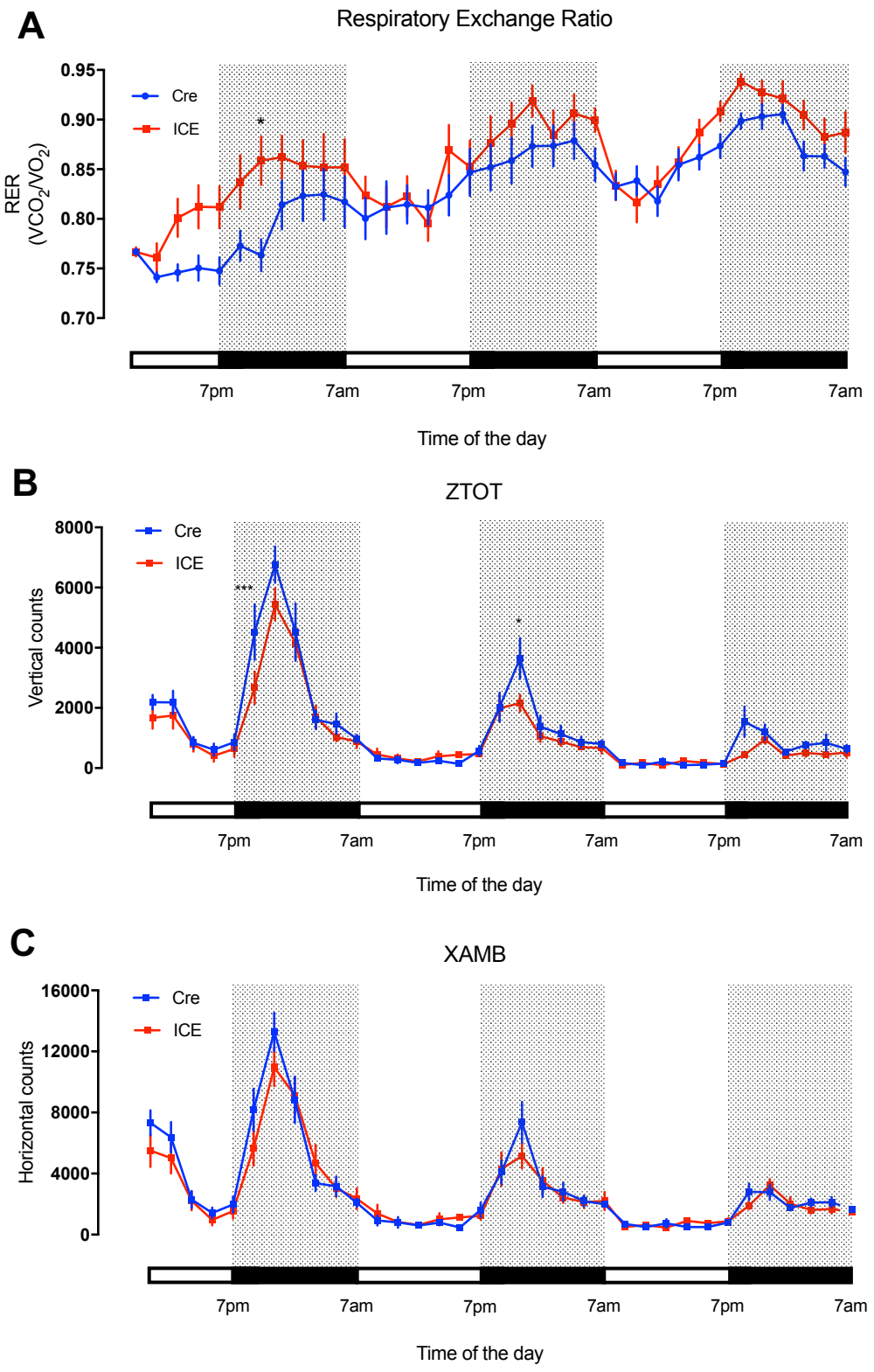

Figure 5.6: ICE mice are an accelerated phenocopy of normal aging. (A) Respiratory exchange ratio (RER) of Cre and ICE mice. Repeated measurements one-way ANOVA. (B) Vertical movement (ZTOT). Two-way ANOVA Tukey's multiple comparisons test. *p < 0.05 (C) Total ambulatory activity (XAMB). Two-way ANOVA Tukey's multiple comparisons test. *p < 0.05. n = 8 mice/group. Data are mean ± SEM.

5.4.3. ICE mice phenocopy age-associated memory loss

We next analyzed the effect of induction of I-*Ppo*I on central nervous system (CNS)-mediated behavioral changes to determine if I-*Ppo*I induction could affect cognitive behavior, a well-studied field in the context of mammalian aging. We first measured spatial learning and memory using the Barnes maze test. During four days of training, there was no notable difference in learning speed or working memory in young versus old mice or in ICE versus Cre mice. However, when we measure long-term memory 7 days after of the first test day, performed in the 5th day of experiment, both old and ICE mice had significant reduction in long-term memory (Figure 5.7 A). Moreover, in anxiety-related test, ICE mice spent more time in open arms on the elevated plus maze test (Figure 5.6 B). However, no differences were observed between Cre and ICE in cognition, as evaluated by Y-maze test (Figure 5.7 C).

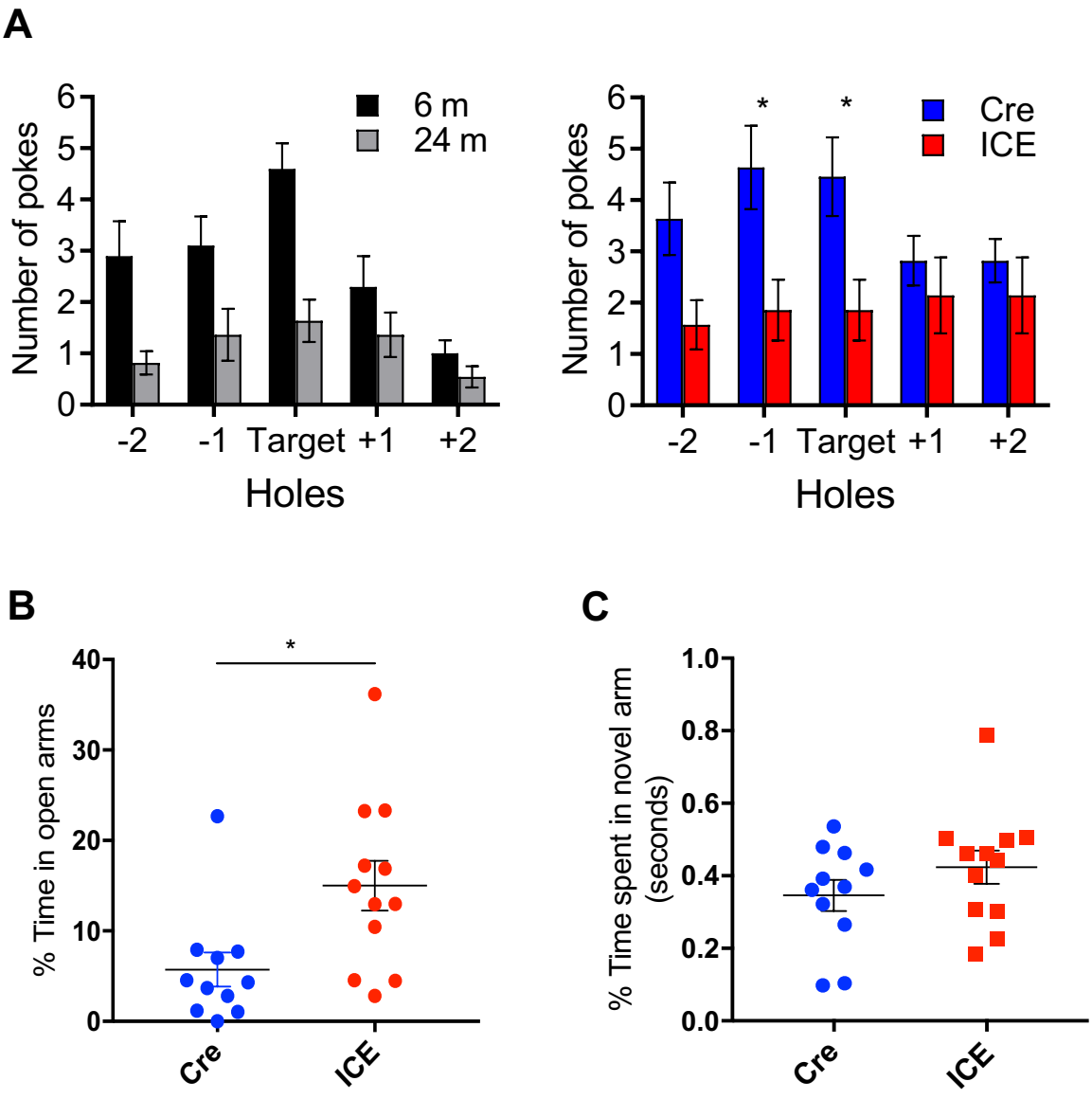

(Legend next page)

Figure 5.7: ICE mouse showed accelerated cognition deuteration. (A) Representative images of Barnes maze tests and mean number of pokes at each hole. Two-way ANOVA-Bonferroni. *p < 0.05. (B) Elevated plus maze test represented by the time spent in open arms. Two-tailed Student's *t*-test. *p < 0.05. n = 11-12 mice/group. (C) Y-maze spontaneous test with time spent in novel arm. Two-tailed Student's *t*-test. n = 11-12 mice/group. Data are mean ± SEM.

5.4.4. ICE mice mimic age-associated muscle dysfunction

Aging is associated with muscle mass loss, described as sarcopenia, as well as decrease in muscle function, mainly caused by loss of muscle homeostasis and decrease metabolism through mitochondria. To determine the effects of I-*Ppo*l muscle metabolism and function, we first addressed exercise and muscle capacities in ICE and Cre mice by using a treadmill tolerance test. The running distance in 10-month post-treated ICE mice decreased significantly relative to Cre mice, which was consistent with normal aging when we compared the running distance between 6- and 24-month-old WT mice (Figure 5.8 A). Analysis of lactate content in the blood post-exercise, which correlates to oxidative capacity of the muscles, showed that ICE mice had increased lactate levels after running, mimicking levels observed in old mice (Figure 5.8 B). Moreover, using limb grip strength we observed a decrease in muscle strength in both old and ICE mice (Figure 5.8 C).

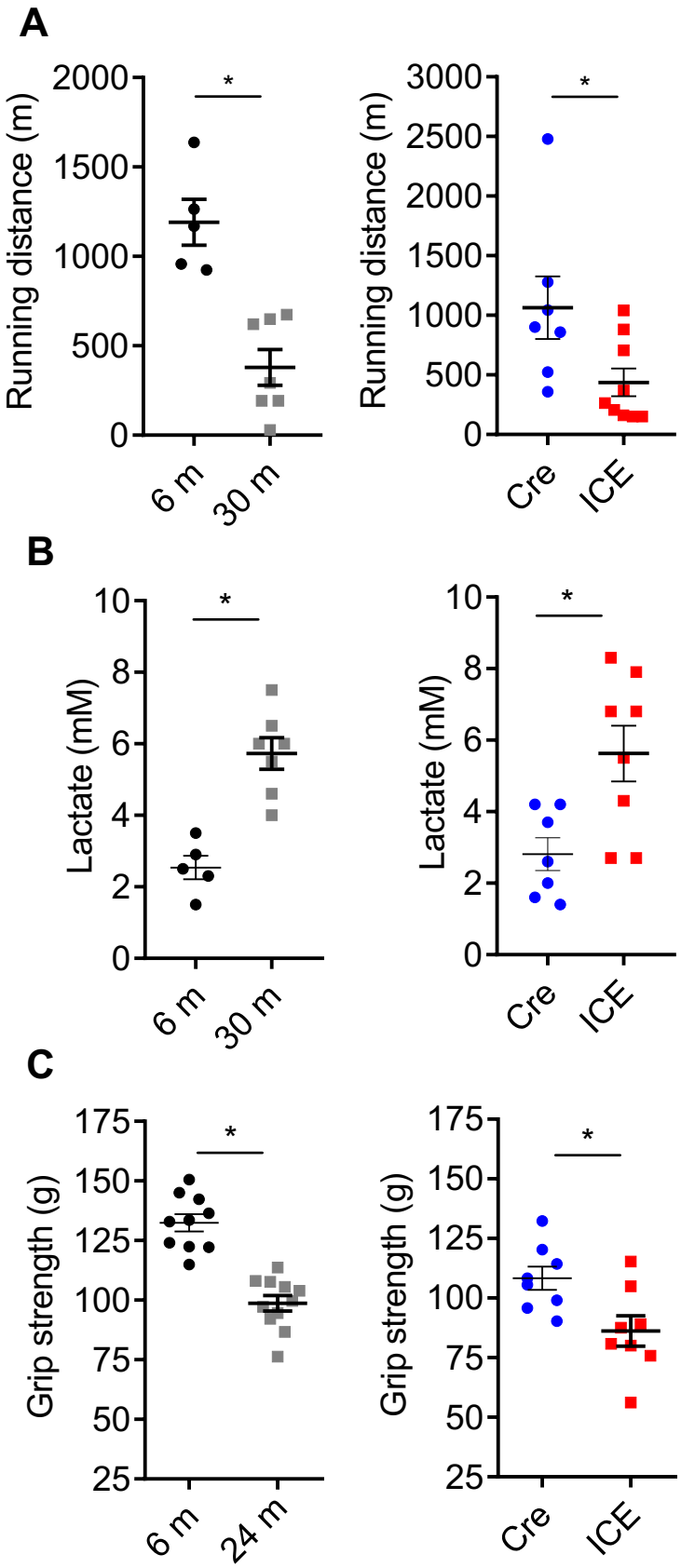

Figure 5.8: ICE mouse muscle showed progeroid features. (A) Treadmill endurance. Two-tailed Student's *t*-test. (B) Blood lactate build-up after exercise in WT 6- 24-month-old, Cre and ICE mice. Two-tailed Student's *t*-test. (C) Grip strength measured as maximal "peak force". Two-tailed Student's *t*-test. *p < 0.05. n = 5-12 mice/group. Data are mean ± SEM.

5.4.4.1. ICE mice phenocopy age-associated muscle dysfunction through decreased mitochondrial metabolism

Muscle oxidative capacity is largely determined by the mitochondrial content and is dependent on mitochondrial biogenesis and mitochondrial oxidative capacity, which relies on oxidative enzyme content and activity. In order to evaluate mitochondrial function, we first analyzed mtDNA copy number, which is intimately related to mitochondrial function. We observed that mtDNA copy number decreased in both aged and ICE mice, as compared with respective controls (Figure 5.9).

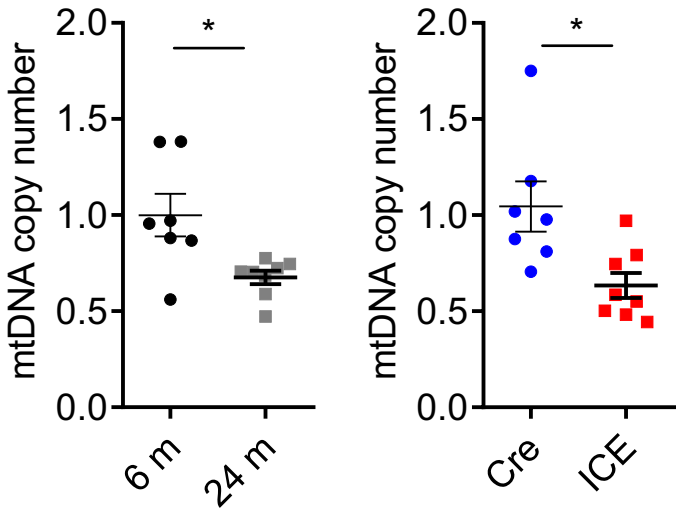

Figure 5.9: ICE mouse muscle showed progeroid features. Mitochondrial DNA copy number. Two-tailed Student's *t*-test. *p < 0.05. n = 5-8 mice/group. Data are mean ± SEM.

We next asked if the observed changes in mtDNA copy number would be associated with changes in mitochondrial number and network. Our analyses of longitudinal section of gastrocnemius muscle using electron microscopy images showed that the distribution of area and perimeter of mitochondria were shifted to the right (Figure 5.10), indicating fewer round mitochondria and a greater proportion of more complex, enlarged shapes. Interestingly, the mitochondrial number didn't change (Figure 5.10 B).

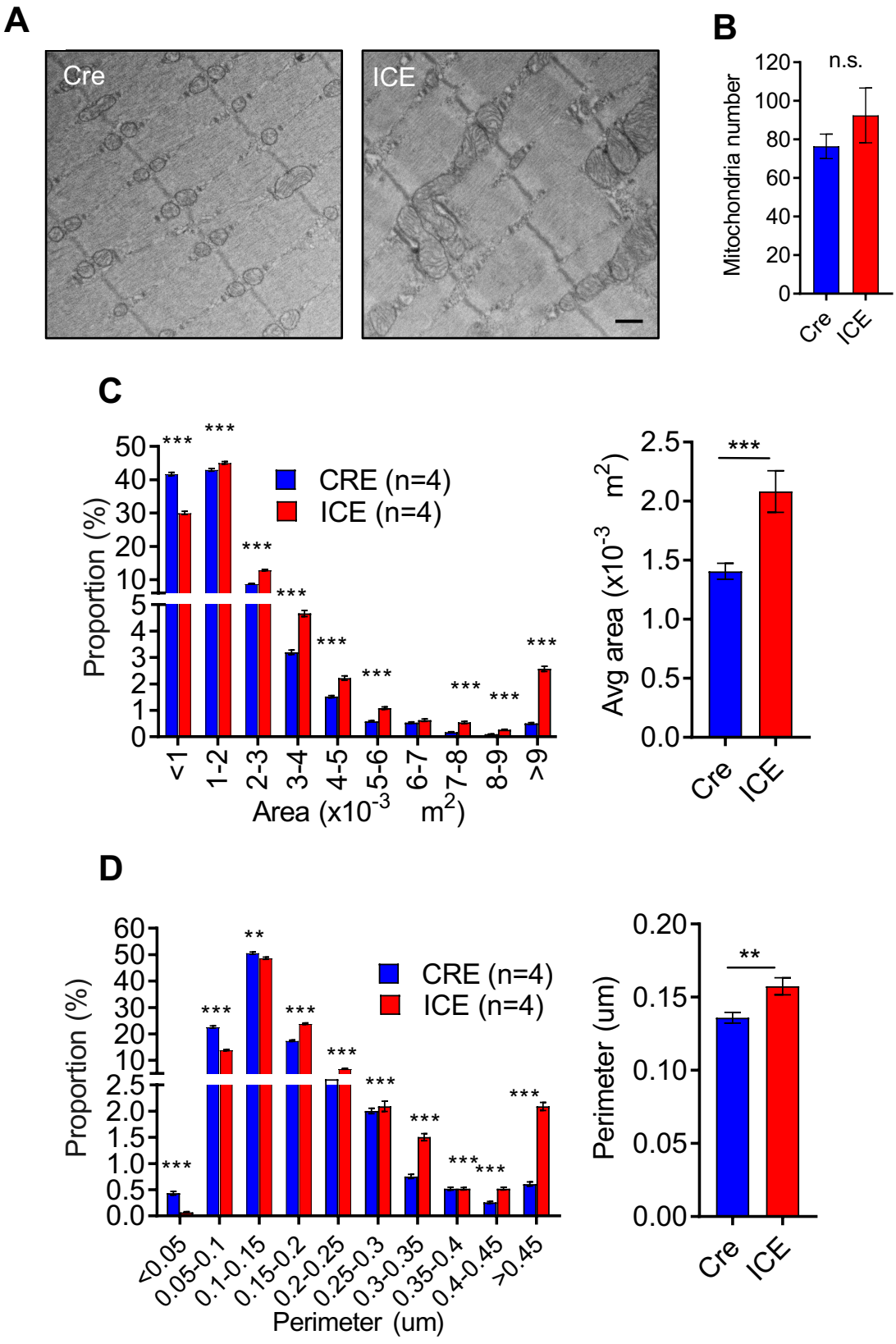

Figure 5.10: ICE mouse muscle showed progeroid features. (A) Representative electron microscopy images of mitochondrial network in cryosectioned section of gastrocnemius. Scale bar, 500 nm. (B) Mitochondrial number. Two-tailed Student's *t*-test. (C) Mitochondrial area. Two-tailed Student's *t*-test. (D) Mitochondrial perimeter. Two-tailed Student's *t*-test. n.s.: $p > 0.05$; *$p < 0.05$; ***$p < 0.001$. n = 4 mice/group. Data are mean ± SEM.

5.4.4.2. Gene expression in ICE muscle mimics normal aging

After our phenotypical observations in ICE mice, we next aimed to determine to what extent I-*Ppo*I induction of DSBs had shifted the physiology of a normal middle-aged mouse towards the physiology of an old mouse. We preformed whole transcriptomic sequencing and pathway analysis in gastrocnemius from ICE and CRE mice, as compared to young and old WT mice. In skeletal muscle, analyses of the top 200 most significantly altered genes between Cre and ICE muscle show that genes that were significantly dysregulated in ICE mice were positively correlated with changes in wild type 24-month-old mice compared to 12-month-old mice (Figure 5.11).

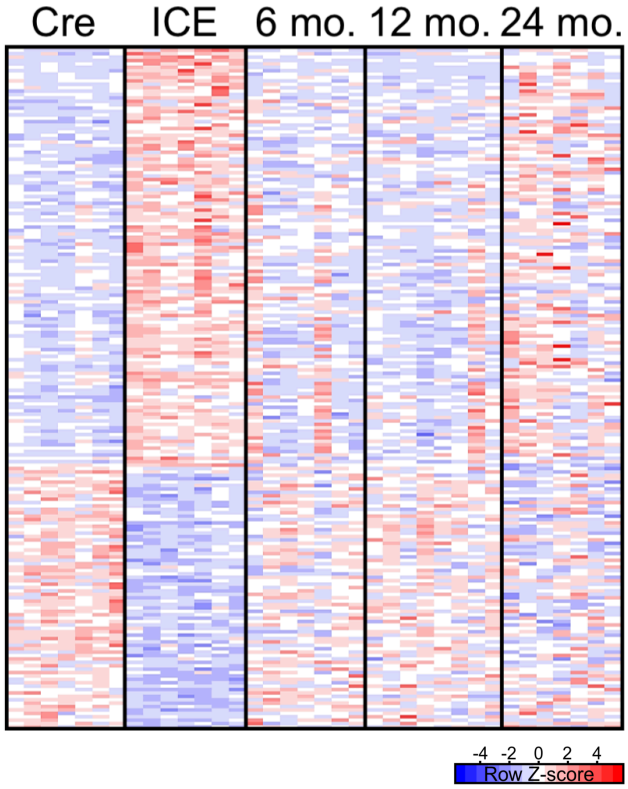

Figure 5.11: Aging is associated with changes in gene expression in the skeletal muscle. Heatmaps of the top 200 most significantly altered genes between Cre and ICE muscle.

Since the epigenome is dynamic by nature, we next asked if environmental or behavioral factors due to I-*Ppo*I induction could cause epigenetic outcomes via changes in DNA methylation, which is currently one of the most promising molecular tests for monitoring aging and predicting life expectancy. To ensure the validity of our muscle epigenetic clock, we started by doing a training set using 2048 CpG sites that are known to change their methylation status over aging to define the age predictor (Figure 5.12 A). After our training set was finalized (R^2=0.9952), we tested our samples using 2048 CpG sites, with a longitudinal set using 18 wild-type mice samples with different ages and produced our muscle epigenetic clock with an

R^2=0.9149 (Figure 5.12 B). To assess the global changes in the DNA methylome in ICE mice, we subjected gastrocnemius muscle samples to our new muscle epigenetic clock. Results were expressed as delta age and represent the difference between epigenetic and chronological age. Despite the fact that at one-month post-treatment there was a slight decrease, we observed an age-dependent increase in both 10- and 14-months post-treatment ICE mice, suggesting an increase in epigenetic aging in muscle mimicking normally aged WT muscle (Figure 5.12 C-D).

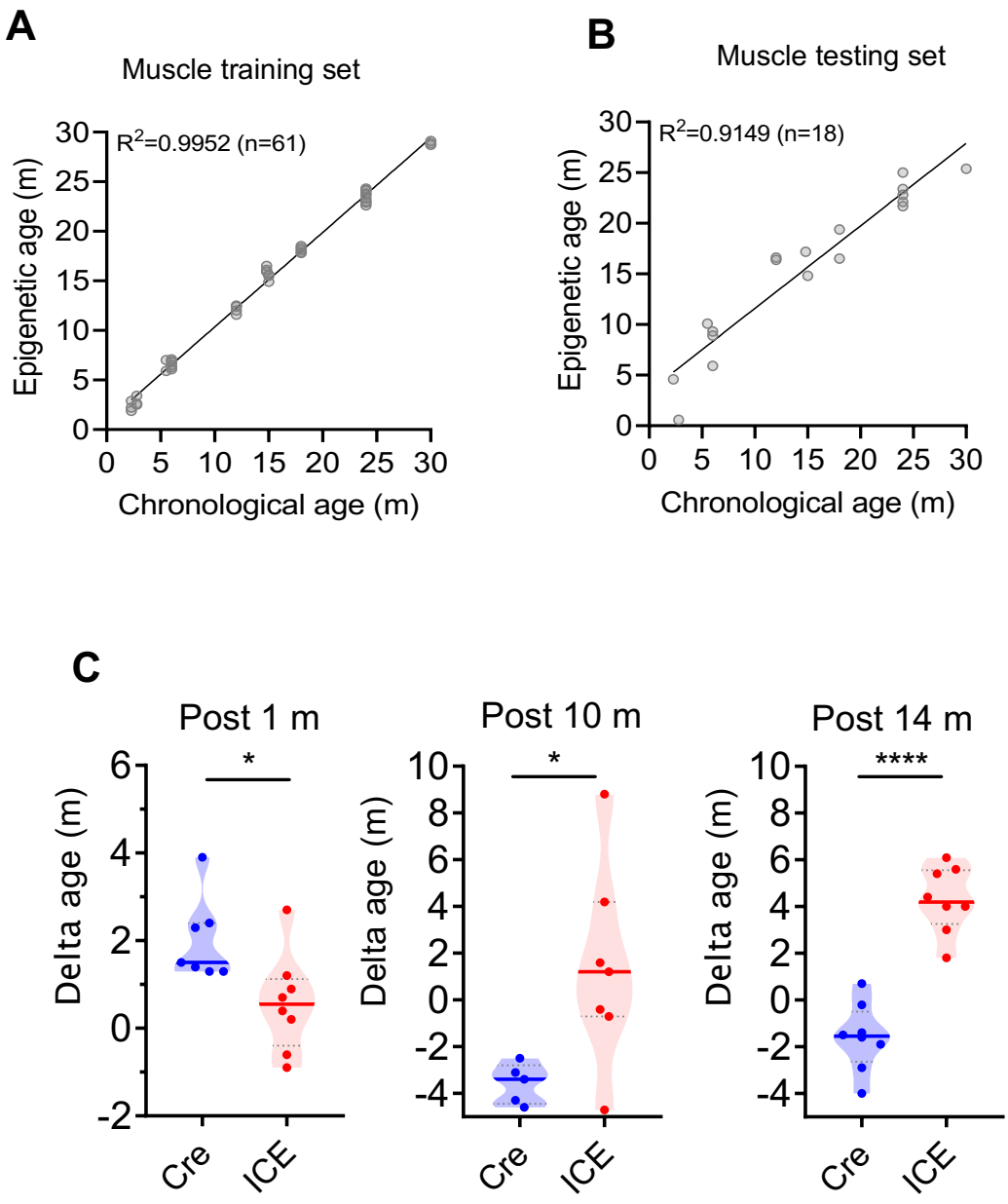

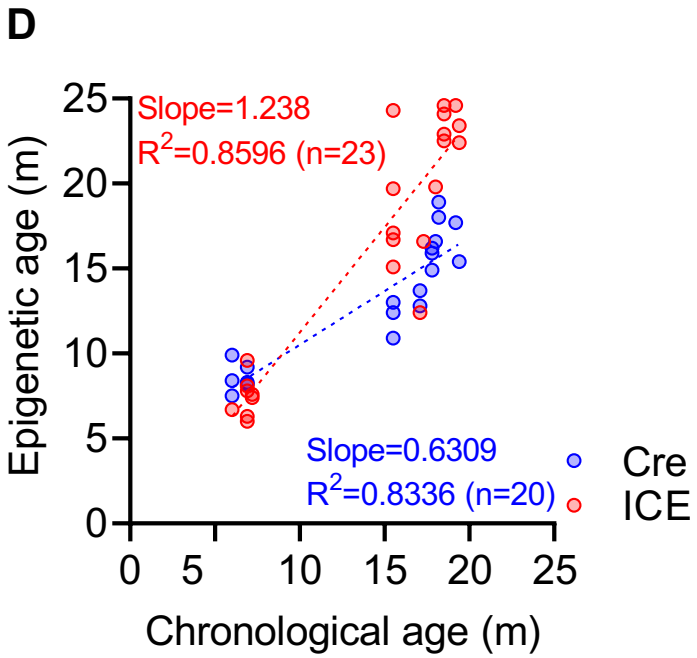

Figure 5.12: ICE mice experience an acceleration of the epigenetic clock. (A) Epigenetic age muscle training set of the clock CpG sites in C57BL/6J mice. (B) Epigenetic age muscle testing set of the clock CpG sites in C57BL/6J mice. (C) Epigenetic delta age (Δ age = epigenetic age – chronological age) of gastrocnemius of Cre and ICE mite at 10- and 14-months post-treatment. (D) Epigenetic age of gastrocnemius of Cre and ICE mice 1-, 10-, and 14-month post-treatment. Linear regression analysis and Spearman correlations. Two-tailed Student's *t*-test. *p<0.05; ***p < 0.0001. n = 5-10 mice/group. Data are mean ± SEM.

5.5. Discussion

Research in lower organisms, such as yeast and invertebrates, will continue to be very important in the aging field for identification of genes of interest as well as for testing genes important for human diseases. However, research in these models has not been performed without its own set of problems. One of the foremost problems is the fact that we know little about the details of normal aging at the cellular and physiological levels in short-lived fly and worms. For instance, it is not known if they die of definable diseases similar to lab rodents. Moreover, normal aging adult flies and worms fail to exhibit at least two key features of human aging: first they do not exhibit alterations in proliferative homeostasis that characterize many common late-in-life human disorders (*e.g.* osteoarthritis, atherosclerosis, prostatic hyperplasia, and malignant neoplasia), and second, while there are chemical communications between invertebrates that allow them to change behavior, the unique multigenerational social interactions in humans are far more complex than those found in flies and worms. For example, identical twins with lower socioeconomic status present shorter leucocyte telomeres (Cherkas *et al.*, 2006) as well as in mothers of children with disabilities (Epel *et al.*, 2004).

Studies on the contribution of epigenetic changes to eukaryotic aging started with research on *S. cerevisiae*, where it was shown that relocalization of chromatin factors and the resulting epigenetic changes were the primary cause of aging in these species (Sinclair and Guarente, 1997). Until now, there was no way to directly test the impact of physiologically-relevant changes in the epigenome in a living mammal. Moreover, as previously described, the best way to induce physiologically-relevant changes in the epigenome is to slightly increase the background levels of DSBs (Oberdoerffer *et al.*, 2008). Originally, the RCM hypothesis was tested in yeast by engineering cells with a galactose-inducible HO endonuclease to cut DNA (Mills *et al*., 1999). A single DSB passing into S-phase was shown to be sufficient to release the yeast sirtuin Sir2 from the silent loci and induce sterility, a hallmark of yeast aging.

In this study, we sought to develop a mouse model to test the role of epigenetic changes on aging where we could tweak the epigenome in a way that mimics normal aging physiology. This innovative system has given us the power to control not only the time and duration of epigenetic change, but also the localization in specific tissues to test non cell-autonomous effects. One of the major advantages in our system as compared to with current methods to generate DNA breaks in mice, such as chemotherapeutic drugs or ionizing radiation, is that we do not induce numerous DNA breaks or mutations, which would confound the study. DNA editing enzymes, such as the homing endonucleases, TALENs, and CRISPR/Cas9, are suitable to use because they cut at specific sites with the homing endonucleases from slime molds presenting the attributes we needed (Mueller *et al.*, 1993; Belfort and Roberts, 1997). These endonucleases cut very rarely, at specific target sites, and can be easily repaired.

Despite the fact that they have never been tested in a living mammal or in the context of aging, we chose the endonuclease I-*Ppo*I because it has been used to study DSB repair in cultured human cells, including the role of SIRT1 and SIRT6 (Berkovich *et al*., 2007; McCord *et al.*, 2009).

Ten months after the three-week tamoxifen treatment, we observed that ICE mice recapitulated a premature aging phenotype at the molecular and physiological levels better than any other currently available mouse model (Vijg and Hasty, 2006), which has allowed us to test whether epigenetic changes are not a simple effect, but rather a cause of aging and aging-related diseases. All of the ICE mice, but none of the Cre controls, gradually developed an aged phenotype over the next 10 months, about 2 times the rate of normal aging. Interestingly, after about 1-month post-treatment, ICE mice stared to experience progressive hair graying, particularly towards the rear, hair loss on limbs and around the nose, and kyphosis (Figure 5.4 A), which are progressive changes typical of wild type C57BL/6 that are 8-12 months older. Importantly, these effects dramatically increased 10 months after treatment (Figure 5.4 A) as shown by the 2.6-fold increase in frailty index, paralleling 24-month-old mice (Figure 5.4 C).

Age-related memory deficits (Guan *et al.*, 2009) and risk for development of neurodegenerative disease (Mastroeni *et al.*, 2009, 2010), such as Alzheimer's disease, increase with age and epigenetic noise has been highly associated with such diseases. Several reports have shown that one of the most dramatic molecular changes observed in aging brain are alterations in epigenetic mechanism that control gene expression. Activity-dependent transcription, synaptic plasticity (Borrelli *et al.*, 2008; Day and Sweatt, 2010), and learning and memory (Guan *et al.*, 2009; Gräff and Tsai, 2013; Sweatt, 2013; Zovkic, Guzman-Karlsson and Sweatt, 2013; Lopez-Atalaya and Barco, 2014) were all shown to be regulated by epigenetic mechanisms. Our performed physiological and behavioral tests indicate that 10 months post-treatment ICE mice showed cognitive impairments, resembling 24-month-old C57 mice. Regarding spatial memory, we observed that ICE mice under-performed in Barnes maze experiments, when compared with age-matched Cre controls, closely resembling deficits observed in aged C57 animals (Figure 5.7 A). Moreover, elevated plus maze showed that ICE mice spent more time in and actively sought out the open arms (Figure 5.7 B), suggesting decreased thigmotaxis and anxiety. Remarkably, no differences were observed in spatial working memory using Y-maze (Figure 5.7 C). Overall, these results showed that DNA damage due I-*Ppo*I induction was able to elicit chromatin remodeling and neuronal functional changes, as observed by impaired cognition in ICE mice as compared to age-matched Cre controls.

An age-related decrease in muscle function implicates quantitative and qualitative changes in skeletal muscle structure and function. Even though it is a slow process with high

variability among individuals, it is observed in all humans independent of physical activity or healthy state (Korhonen *et al.*, 2006; Cheng *et al.*, 2016). Analysis on muscle capacity showed that ICE mice 10 months post-treatment had a significant decrease in ability to run until exhaustion that was accompanied by a decrease in muscle strength (Figure 5.8 C), paralleling 24-month-old mice. Furthermore, loss of muscle homeostasis and decreased metabolism during aging has been associated with decreased mitochondrial oxidative capacity (Kwong and Sohal, 2000; Drew *et al.*, 2003). Indeed, blood lactate content post-exercise (Figure 5.8 B), as well as decreased mtDNA copy number (Figure 5.9) strongly correlated with decreased oxidative capacity of the muscles from ICE mice. Since there is evidence to suggest a link between mitochondrial function and morphology (Shin *et al.*, 2009), we wondered if changes in mitochondrial oxidative capacity and copy number play an important role in the well-documented alterations of mitochondrial morphology in sarcopenic aged muscle (Picard *et al.*, 2013). Electron microscopy analyses of intermyofibrillar mitochondria showed that ICE mice 10 months post-treatment, but not age matched Cre controls, have a deregulated mitochondrial network paralleling sarcopenic aged muscle (Leduc-Gaudet *et al.*, 2015). Additionally, our gene expression analyses clearly showed that epigenetic noise due to I-*Ppo*l induction changed the gene expression of ICE mice 10 months post-treatment, and interestingly, closely paralleled 24-month-old mice (Figure 5.11). Additionally, age matched control Cre mice showed a gene expression pattern that mimics young wild-type mice (Figure 5.11).

Finally, we analyzed muscle epigenetic alterations due to I-*Ppo*l induction based on its DNA methylation status, which has been shown to be serve as a notable predictor of age in several tissues (Leduc-Gaudet *et al.*, 2015). We constructed a vigorous muscle epigenetic clock based on age-dependent behavior of muscle DNA methylomes from C57BL/6J. Based on this clock, we could characterize the changes in biological age of ICE mice 10 months post-treatment, and we clearly found that I-*Ppo*l induction accelerated the epigenetic age in ICE muscle (Figure 5.12), enabling us to conclude that epigenetic alterations are, at least in part, the cause of aging in ICE mice, which provides strong evidence that the ICE mouse could be the first model to accordantly mimic human aging, making this animal model a valuable tool for the medical research community.

CHAPTER 6

Conclusions

Unprecedented advances have been achieved in the aging field over the last few decades, particularly with the discovery that the rate of aging is coordinated, at least in part, by genetic pathways and conserved biochemical processes. Historically, however, researchers have focused their attention on investigating individual pathways in isolated organs as a strategy to unravel the root cause of aging, with the ultimate goal of designing better therapeutic approaches. The discovery that sirtuins have been shown to have extraordinary abilities in disease prevention and may even revert some aspects of aging have led the field to seek for sirtuin activators and study their potential health benefits. Importantly, SIRT1, which is the most studied sirtuin in the family, has been shown to play a key role in the regulation of metabolism, DNA repair, inflammation, chromatin structure, and aging in mammals.

Numerous studies have shown the beneficial effects of STACs on the overall health in rodents in a SIRT1-dependent manner; however, how STACs impart these benefits has been hotly debated, with some researchers proposing that direct activation is an artefact of the assays used *in vitro*. Additionally, resveratrol is a nonspecific compound, meaning that it interacts with numerous proteins within the cell (Howitz and Sinclair, 2008). Taking advantage of a novel model (SIRT1-E222K mice), we have been able to clarify which beneficial effects are mediated by direct activation of SIRT1.

In Chapter 3, we elucidated that the capacity of resveratrol to improve metabolism and protect against obesity and insulin resistance in mice fed with HFD was due to direct activation of SIRT1 and dependent on the E222K residue. Moreover, the beneficial effects of resveratrol in endurance performance were found to be due to direct activation of SIRT1. Since it was reported that SIRT1 was required to increase physical activity in response to CR (Chen *et al.*, 2005), our findings have further clarified that the resveratrol-mediated increase in physical activity was due to direct activation of SIRT1. Importantly, our lab has previously showed for the first time that resveratrol shifts the physiology of middle-aged mice on HFD towards that of mice on standard diet and significantly increases their survival (Baur *et al.*, 2006). Using SIRT1-E222K mice, we have now showed that lifespan extension of mice on HFD is SIRT1-E222K-dependent. On the other hand, we observed that the capacity of resveratrol to alleviate secondary phenotypes typically associated with diabetes, such as diabetic nephropathy and tissue inflammation, were independent of the E222K residue. We found that the reduction of the inflammatory cytokine TNF-α by resveratrol was independent on the E222K residue since the levels were reduced in both WT and SIRT1-E222K mice fed HFD. Moreover, the beneficial effects of resveratrol in reducing cholesterol levels seemed to be independent of the E222K residue as well.

In addition to the beneficial effects of direct activation of SIRTs through STACs, it has been known for several years that up-regulation of the NAD salvage pathway, which recycles NAD^+ from NAM, is able to extend lifespan and mimic CR in yeast (Anderson *et al.*, 2002; Anderson

et al., 2003). NAD^+-boosting molecules represent a newer class of STACs, which are currently receiving much attention in the field, as a way to restore NAD^+ levels in elderly individuals and potentially activate all seven sirtuins with only one compound. In Chapter 4 of this thesis, I present a synergistic strategy to accelerate the ability to test multiple genetic interventions as a suitable approach to study aging and age-related diseases. Combining AAV vectors to overexpress all seven sirtuins together with NAD^+-boosting via NMN in the drinking water, we observed a protection of age-related weight loss as well as numerical extension in median and maximum lifespan. Additional experiments using different cohorts of mice showed an improvement in multiple parameters of walking gait. We also observed an increase in skeletal muscle mass relative to controls. Surprisingly, we did not notice any interaction between both interventions in any of the phenotypes we measured. To our surprise, we did not observe a larger effect from SIRTs AAV delivery. A possible explanation is that while the serotype we utilized, AAV9, is known to have a wider tissue distribution than other serotypes, it predominantly affects liver and heart (Zincarelli *et al.*, 2008).

One of the biggest needs in the aging field is to better understand what the best approach and model might be (Justice and Dhillon, 2016). Rodents and other short-lived mammals have been criticized as poor models of human age-related diseases due to the common practice of using young mice to understand age-related diseases. Even when old mice are used, they do not fully recapitulate human aging because mice only live 2-3 years. Evidence that mammalian gene expression changes with age in the late 1980's was important in helping the field start to uncover the fundamental cause of aging in eukaryotes. Moreover, studies of aging in the budding yeast *S. cerevisiae* provided the first evidence that gene expression changes may not simply be a characteristic of aging but may be an underlying cause (Kennedy *et al.*, 1995, 1997; Imai and Kitano, 1998). Moreover, evidence has been accumulating that a similar epigenetically-driven aging process called "RCM" (relocalization of chromatin factors) might be a cause of aging in mammals (Vijg and Hasty, 2006).

In Chapter 5, we tested an unique mouse model developed in our lab, and we have evidence to suggest that it is the first model to comprehensively and accurately mimic human aging. Understanding basic biological questions and improving medical research will be now possible due to the ability to accelerate epigenetic aging in a mouse model in a temporal and spatial manner. With this model, it will be possible to understand the contributions of specific tissues on the aging of other tissues, and whether healthy tissues can prevent aging in others. Using the ICE mouse model, I presented data which may solve both problems of using short-lived species to model human age-related diseases, by reducing the time it takes to age mice and by pushing epigenetic change in the mice beyond a few years. (rewrite this sentence. We indeed have observed that some of the phenotypes in ICE mice more closely resemble aging in humans than mice, such as memory loss and loss of physical strength.

Continual efforts have been made to find a novel drug to extend lifespan and healthspan in the elderly, and thereby decreasing the length and severity of late-life morbidity, which is a major aim of our times. Pharmaceutical companies are continuing to develop sirtuin activators to improve their therapeutic proprieties; however, the beneficial metabolic effects stimulated by these activators must be investigated with careful attention since side effects due to exaggerated activation of sirtuins may cause serious damage in human patients. In this work, we provide insights into the fundamental mechanisms of the allosteric activation of SIRT1 and clarified some of the health benefits that STACs might mediate via direct SIRT1 activation *in vivo*, a question that has dogged the field for over a decade. Using these results, we can now determine which diseases STACs might be able to treat in humans and how they can be improved to increase their potency. Moreover, the demonstration that DSBs accelerate both the epigenetic clock and the physiology of aging suggests that these two processes are intimately linked. The question now is to know if we will be able to reverse these changes and recover epigenetic information that was lost, as a way to rejuvenate the organism. Given this information, the direction that the field may be heading is to reset the epigenetic clock by reprogramming somatic cells to iPSCs. However, whether or not it is possible to do so and if we can safely reprogram elderly mammals is not yet known. If we succeed in doing so, then our ability to not only understand but also control the aging process may be just around the corner.

REFERENCES

Aksoy, P. *et al.* (2006) 'Regulation of SIRT 1 mediated NAD dependent deacetylation: A novel role for the multifunctional enzyme CD38', *Biochem Biophys Res Commun*, **349**(1), pp. 353–359.

Amir, R. E. *et al.* (1999) 'Rett syndrome is caused by mutations in X-linked MECP2, encoding methyl-CpG-binding protein 2', *Nat Genet*, **23**(2), pp. 185–188.

Anderson, R. M. *et al.* (2002) 'Manipulation of a nuclear NAD + salvage pathway delays aging without altering steady-state NAD + levels', *J Biol Chem*, **277**(21), pp. 18881–18890.

Anderson, R. M., Bitterman, K. J. and Wood, J. G. (2003) 'Nicotinamide and Pnc1 govern lifespan extension by calorie restriction and stress.', *Nature*, **423**(1998), pp. 181–185.

Anderson, R. M. and Weindruch, R. (2012) 'The caloric restriction paradigm: Implications for healthy human aging', *Am J Hum Biol*, **24**(2), pp. 101–106.

Andrade, J. M. O. *et al.* (2014) 'Resveratrol attenuates hepatic steatosis in high-fat fed mice by decreasing lipogenesis and inflammation', *Nutrition*, **30**(7–8), pp. 915–919.

Ansari, H. R. and Raghava, G. P. S. (2010) 'Identification of NAD interacting residues in proteins', *BMC Bioinformatics*, **11**.

Argast, G. M. *et al.* (1998) 'I-PpoI and I-CreI homing site sequence degeneracy determined by random mutagenesis and sequential in vitro enrichment', *J Mol Biol*, **280**(3), pp. 345–353.

Armour, S. M. *et al.* (2009) 'Inhibition of mammalian S6 kinase by resveratrol suppresses autophagy.', *Aging (Albaby, NY)*, **1**(6), pp. 515–528.

Asensi, M. *et al.* (2002) 'Inhibition of cancer growth by resveratrol is related to its low bioavailability', *Free Radic. Biol. Med.*, **33**(3), pp. 387–398.

Aubin, M. *et al.* (2008) 'Female rats fed a high-fat diet were associated with vascular dysfunction and cardiac fibrosis in the absence of overt obesity and hyperlipidemia: therapeutic potential of resveratrol', *J. Pharmacol. Exp. Ther.*, **325**(3), pp. 961–968.

Bai, P. *et al.* (2011) 'PARP-1 inhibition increases mitochondrial metabolism through SIRT1 activation', *Cell Metab*, **13**(4), pp. 461–468.

Baksi, A. *et al.* (2014) 'A phase II, randomized, placebo-controlled, double-blind, multi-dose study of SRT2104, a SIRT1 activator, in subjects with type 2 diabetes', *Br. J. Clin. Pharmacol.*, **78**, pp. 69–77.

Balan, V. *et al.* (2008) 'Life span extension and neuronal cell protection by Drosophila nicotinamidase', *J Biol Chem*, **283**(41), pp. 27810–27819.

Banks, A. S. *et al.* (2008) 'SirT1 Gain of Function Increases Energy Efficiency and Prevents Diabetes in Mice', *Cell Metab.*, **8**(4), pp. 333–41.

Barbosa, M. T. P. *et al.* (2007) 'The enzyme CD38 (a NAD glycohydrolase, EC 3.2.2.5) is necessary for the development of diet-induced obesity', *FASEB J*, **21**(13), pp. 3629–3639.

Bauer, J. H. *et al.* (2004) 'An accelerated assay for the identification of lifespan-extending interventions in Drosophila melanogaster', *Proc. Natl. Acad. Sci.*, **101**(35), pp. 12980–12985.

Bauer, J. H. *et al.* (2009) 'dSir2 and Dmp53 interact to mediate aspects of CR-dependent lifespan extension in D. melanogaster', *Aging (Albaby, NY)*, **1**(1), pp. 38–48.

Baur, J. A. *et al.* (2006) 'Resveratrol improves health and survival of mice on a high-calorie diet', *Nature*, **444**(7117), pp. 337–342.

Baur, J. A. and Sinclair, D. A. (2006) 'Therapeutic potential of resveratrol: the in vivo evidence', *Nat. Rev. Drug. Discov.*, **5**(6), pp. 493–506.

Beirowski, B. *et al.* (2011) 'Sir-two-homolog 2 (Sirt2) modulates peripheral myelination through polarity protein Par-3/atypical protein kinase C (aPKC) signaling', *Proc. Natl. Acad. Sci.*, **108**, pp. E952–E961.

Belfort, M. and Roberts, R. (1997) 'Homing endonucleases: keeping the house in order', *Nucleic Acids Res.*, **25**(17), pp. 3379–3388.

Benton, C. R., Wright, D. C. and Bonen, A. (2008) 'PGC-1α-mediated regulation of gene expression and metabolism: implications for nutrition and exercise prescriptions', *Appl Physiol Nutr Metab.*, **33**(5), pp. 843–862.

Berkovich, E., Monnat, R. J. and Kastan, M. B. (2007) 'Roles of ATM and NBS1 in chromatin structure modulation and DNA double-strand break repair', *Nat Cell Biol*, **9**(6), pp. 683–690.

Berkovich, E., Monnat, R. and Kastan, M. (2008) 'Assessment of protein dynamics and DNA repair following generation of DNA double-strand breaks at defined genomic sites', *Nat Protoc*, **3**(5), pp. 915–922.

Bitterman, K. J. *et al.* (2002) 'Inhibition of silencing and accelerated aging by nicotinamide, a putative negative regulator of yeast Sir2 and human SIRT1', *J Biol Chem*, **277**(47), pp. 45099–45107.

Blander, G. and Guarente, L. (2004) 'The Sir2 family of protein deacetylases', *Annu Rev Biochem*, **73**, pp. 417–435.

Bobrowska, A. *et al.* (2012) 'SIRT2 ablation has no effect on tubulin acetylation in brain, cholesterol biosynthesis or the progression of Huntington's disease phenotypes in vivo', *PLoS ONE 7*, **7**(4), p. e34805.

Boe, O. *et al.* (2006) 'Inflammation and insulin resistence', *J. Clin. Invest.*, **116**(7), pp. 1793–801.

Bogan, K. L. and Brenner, C. (2008) 'Nicotinic Acid, Nicotinamide, and Nicotinamide Riboside: A Molecular Evaluation of NAD + Precursor Vitamins in Human Nutrition', *Annu Rev Nutr*, **28**(1), pp. 115–130.

Boily, G. *et al.* (2008) 'SirT1 regulates energy metabolism and response to caloric restriction in mice', *PLoS ONE 3*, **3**(3), p. e1759.

Boily, G. *et al.* (2009) 'SirT1-null mice develop tumors at normal rates but are poorly protected by resveratrol', *Oncogene*, **28**(32), pp. 2882–2893.

Bonkowski, M. S. and Sinclair, D. A. (2016) 'Slowing ageing by design: the rise of NAD+ and sirtuin-activating compounds', *Nat Rev Mol Cell Biol*. Nature Publishing Group, **230**(2001), pp. 2–3.

Bordone, L. *et al.* (2006) 'Sirt1 regulates insulin secretion by repressing UCP2 in pancreatic beta cells', *PLoS Biol.*, **4**(2), p. e31.

Bordone, L. *et al.* (2007) 'SIRT1 transgenic mice show phenotypes resembling calorie restriction', *Aging Cell*, **6**(6), pp. 759–67.

Bordone, L. and Guarente, L. (2005) 'Calorie restriction, SIRT1 and metabolism: Understanding longevity', *Nat Rev Mol Cell Biol*, **6**(4), pp. 298–305.

Borra, M. T. *et al.* (2004) 'Substrate Specificity and Kinetic Mechanism of the Sir2 Family of Deacetylases', *Biochemistry*, **43**, pp. 9877–87.

Borrelli, E. *et al.* (2008) 'Decoding the Epigenetic Language of Neuronal Plasticity', *Neuron*. Elsevier Inc., **60**(6), pp. 961–974.

Boutant, M. and Cantó, C. (2014) 'SIRT1 metabolic actions: Integrating recent advances from mouse models', *Mol. Metab.*, **3**(1), pp. 5–18.

Brandt, A. and Vilcinskas, A. (2015) 'Synthetic The Fruit Fly Drosophila melanogaster as a Model for Aging Research in Molecular Imprinting', *Adv Biochem Eng Biotechnol.*, **123**(July 2015), pp. 127–141.

Brasnyó, P. *et al.* (2011) 'Resveratrol improves insulin sensitivity, reduces oxidative stress and activates the Akt pathway in type 2 diabetic patients', *Br. J. Nutr.*, **106**(03), pp. 383–389.

Brown, V. A. *et al.* (2010) 'Repeat dose study of the cancer chemopreventive agent resveratrol in healthy volunteers: Safety, pharmacokinetics, and effect on the insulin-like growth factor axis', *Cancer Res.*, **70**(22), pp. 9003–9011.

Brunet, A. and Berger, S. L. (2014) 'Epigenetics of aging and aging-related disease', *J Gerontol A Biol Sci Med Sci*, **69**(1), pp. 17–20.

Bryk, M. *et al.* (2007) 'Transcriptional silencing of Ty1 elements in the RDN1 locus of yeast.', *Genes Dev.*, **11**(2), pp. 255–269.

Buhroo, Z. I. *et al.* (2018) 'Molecular basis of growth and aging in model organisms with special reference to the silkworm Bombyx mori: A review', *Journal of Entomology and Zoology Studies*, **6**(4), pp. 740–751.

Burger, O., Baudisch, A. and Vaupel, J. W. (2012) 'Human mortality improvement in evolutionary context', *Proc Natl Acad Sci*, **109**(44), pp. 18210–18214.

Burkewitz, K., Weir, H. and Mair, W. (2016) 'AMP-activated protein kinase', *Exp Suppl*, **107**, pp. 227–256.

Burnett, C. *et al.* (2011) 'Absence of effects of Sir2 overexpression on lifespan in C. elegans and Drosophila', *Nature*, **477**(7365), pp. 482–485.

Çakir, I. *et al.* (2009) 'Hypothalamic Sirt1 regulates food intake in a rodent model system', *PLoS ONE*, **4**, p. e8322.

Camacho-Pereira, J. *et al.* (2016) 'CD38 Dictates Age-Related NAD Decline and Mitochondrial Dysfunction through an SIRT3-Dependent Mechanism', *Cell Metabolism*, **23**(6), pp. 1127–1139.

Cambronne XA *et al.* (2016) 'Biosensor reveals multiple sources for mitochondrial NAD^+.', *Science*, **352**(6292), pp. 1471–1474.

Cameron, W. D. *et al.* (2016) 'Apollo-NADP+: A spectrally tunable family of genetically encoded sensors for NADP+', *Nat Methods*, **13**(4), pp. 352–358.

Canto, C. *et al.* (2009) 'AMPK regulates energy expenditure by modulating NAD+ metabolism and SIRT1 activity', *Nature,* **458**, pp. 1056–1060.

Cantó, C. *et al.* (2010) 'Interdependence of AMPK and SIRT1 for metabolic adaptation to fasting and exercise in skeletal muscle', *Cell Metab.* Elsevier Ltd, **11**(3), pp. 213–219.

Cantó, C. *et al.* (2012) 'The NAD(+) precursor nicotinamide riboside enhances oxidative metabolism and protects against high-fat diet-induced obesity', *Cell Metab.*, **15**, pp. 838–847.

Chalkiadaki, A. and Guarente, L. (2012) 'High-fat diet triggers inflammation-induced cleavage of SIRT1 in adipose tissue to promote metabolic dysfunction', *Cell Metab.* Elsevier Inc., **16**(2), pp. 180–188.

Chambon, P., Weill, J. D. and Mandel, P. (1963) 'Nicotinamide mononucleotide activation of a new DNA-dependent polyadenylic acid synthesizing nuclear enzyme', *Biochem Biophys Res Commun*, **11**(1), pp. 39–43.

Check-Hayden, E. (2015) 'Anti-ageing pill pushed as bona fide drug', *Nature*, **522**, pp. 265–266.

Chen, D. *et al.* (2005) 'Increase in activity during calorie restriction requires Sirt1', *Science*, **310**(December), pp. 2005–2005.

Chen, D. *et al.* (2008) 'Tissue-specific regulation of SIRT1 by calorie restriction service Tissue-specific regulation of SIRT1 by calorie restriction', *Genes Dev.*, **22**, pp. 1753–1757.

Chen, S. *et al.* (2013) 'Repression of RNA Polymerase I upon Stress Is Caused by Inhibition of RNA-Dependent Deacetylation of PAF53 by SIRT7', *Mol. Cell*. Elsevier Inc., **52**(3), pp. 303–313.

Chen, Y. *et al.* (2012) 'Quantitative Acetylome Analysis Reveals the Roles of SIRT1 in Regulating Diverse Substrates and Cellular Pathways', *Mol. Cell Proteomics*, **11**(10), pp. 1048–1062.

Cheng, S. *et al.* (2016) 'What makes a 97-year-old man cycle 5,000 km a year?', *Gerontology*, **62**(5), pp. 508–512.

Cherkas, L. F. *et al.* (2006) 'The effects of social status on biological aging as measured by white-blood-cell telomere length', *Aging Cell*, **5**(5), pp. 361–365.

Chow, H. M. and Herrup, K. (2015) 'Genomic integrity and the ageing brain', *Nat Rev Neurosci.* Nature Publishing Group, **16**(11), pp. 672–684.

Christensen, K. *et al.* (2013) 'Physical and cognitive functioning of people older than 90 years: A comparison of two Danish cohorts born 10 years apart', *Lancet*. Elsevier Ltd, **382**(9903), pp. 1507–1513.

Clark, S. J. *et al.* (2012) 'Association of sirtuin 1 (SIRT1) gene SNPs and transcript expression levels with severe obesity.', *Obesity*. Nature Publishing Group, **20**(1), pp. 178–185.

Cohen, H. Y. *et al.* (2004) 'Calorie Restriction Promotes Mammalian Cell Survival by Inducing the SIRT1 Deacetylase', *Science*, **305**, pp. 390–392.

Conze, D. B., Crespo-Barreto, J. and Kruger, C. L. (2016) 'Safety assessment of nicotinamide riboside, a form of Vitamin B 3', *Hum Exp Toxicol*, **35**(11), pp. 1149–1160.

Cooper, R. *et al.* (2014) 'Physical capability in mid-life and survival over 13 years of follow-up: British birth cohort study', *BMJ*, **348**.

Costa, C. D. S. *et al.* (2010) 'SIRT1 transcription is decreased in visceral adipose tissue of morbidly obese patients with severe hepatic steatosis', *Obesity Surg.*, **20**(5), pp. 633–639.

Cournil, A. and Kirkwood, T. B. L. (2001) 'If you would live long, choose your parents well', *Trends Genet*, **17**(5), pp. 1–3.

Le Couteur, D. G. *et al.* (2001) 'Pseudocapillarization and associated energy limitation in the aged rat liver', *Hepatology*, **33**(3), pp. 537–543.

Crimmins, E. M. (2015) 'Lifespan and healthspan: Past, present, and promise', *Gerontologist*, **55**(6), pp. 901–911

Crowell, J. A. *et al.* (2004) 'Resveratrol-associated renal toxicity', *Toxicol. Sci.*, **82**(2), pp. 614–619.

Cruickshanks, H. A. *et al.* (2013) 'Senescent Cells Harbour Features of the Cancer Epigenome', *Nat Cell Biol.* Nature Publishing Group, **15**(12), pp. 1495–1506.

Crujeiras, A. B. *et al.* (2008) 'Sirtuin gene expression in human mononuclear cells is modulated by caloric restriction', *Eur. J. Clin. Invest.*, **38**(9), pp. 672–678.

Cuperus, G., Shafaatian, R. and Shore, D. (2002) 'Locus specificity determinants in the multifunctional yeast silencing protein Sir2', *EMBO J.*, **19**(11), pp. 2641–2651.

Dai, H. *et al.* (2010) 'SIRT1 activation by small molecules: Kinetic and biophysical evidence for direct interaction of enzyme and activator', *J. Biol. Chem.*, **285**(43), pp. 32695–32703.

Dai, H. *et al.* (2015) 'Crystallographic structure of a small molecule SIRT1 activator-enzyme complex', *Nat. Commun.*, **6**(May), pp. 1–10.

Das, A. *et al.* (2018) 'Impairment of an Endothelial NAD+-H2S Signaling Network Is a Reversible Cause of Vascular Aging', *Cell*, **173**(1), pp. 74-89.e20.

Day, J. J. and Sweatt, J. D. (2010) 'DNA methylation and memory formation', *Nat Neurosci*, **13**(11), pp. 1319–1323.

Ding, S. *et al.* (2018) 'Resveratrol reduces the inflammatory response in adipose tissue and improves adipose insulin signaling in high-fat diet-fed mice', *PeerJ*, **6**, p. e5173.

Dölle, C. *et al.* (2010) 'Visualization of subcellular NAD pools and intra-organellar protein localization by poly-ADP-ribose formation', *Cell Mol Life Sci.*, **67**(3), pp. 433–443.\

Dong, Y. *et al.* (2011) 'SIRT1 is associated with a decrease in acute insulin secretion and a sex specific increase in risk for type 2 diabetes in Pima Indians', *Mol. Genet. Metab.* Elsevier B.V., **104**(4), pp. 661–665.

Drew, B. *et al.* (2003) 'Effects of aging and caloric restriction on mitochondrial energy production in gastrocnemius muscle and heart', *Am J Physiol Regul Integr Comp Physiol.*, **284**(2), pp. R474–R480.

Du, J. *et al.* (2011) 'Sirt5 Is a NAD-Dependent Protein Lysine Demalonylase and Desuccinylase', *Science*, **334**(6057), pp. 806–809.

Epel, E. *et al.* (2004) 'Accelerated telomere shortening in response to life stress', *Proc. Natl. Acad. Sci.*, **101**(49), pp. 17312–17315.

Escande, C. *et al.* (2013) 'Flavonoid apigenin is an inhibitor of the NAD+ase CD38: Implications for cellular NAD+ metabolism, protein acetylation, and treatment of metabolic syndrome', *Diabetes*, **62**(4), pp. 1084–1093.

Essuman, K. *et al.* (2017) 'The SARM1 Toll/Interleukin-1 Receptor Domain Possesses Intrinsic NAD+ Cleavage Activity that Promotes Pathological Axonal Degeneration.', *Neuron*. Elsevier Inc., **93**(6), pp. 1334-1343.e5.

Fabrizio, P. *et al.* (2001) 'Regulation of longevity and stress resistance by Sch9 in yeast', *Science*, **292**(5515), pp. 288–290.

Feige, J. N. *et al.* (2008) 'Specific SIRT1 Activation Mimics Low Energy Levels and Protects against Diet-Induced Metabolic Disorders by Enhancing Fat Oxidation', *Cell Metab.*, **8**(5), pp. 347–358.

Feldman, J. L. *et al.* (2015) 'Kinetic and structural basis for Acyl-group selectivity and NAD^+ dependence in sirtuin-catalyzed deacylation', *Biochemistry*, **54**(19), pp. 3037–3050.

Feser, J. and Tyler, J. (2011) 'Chromatin structure as a mediator of aging', *FEBS Letters*, **585**(13), pp. 2041–2048.

Fiori, J. L. *et al.* (2013) 'Resveratrol prevents β-cell dedifferentiation in nonhuman primates given a high-fat/high-sugar diet', *Diabetes*, **62**(10), pp. 3500–3513.

Fischer-Posovszky, P. *et al.* (2010) 'Resveratrol regulates human adipocyte number and function in a Sirt1-dependent manner', *Am. J. Clin. Nutr.*, **92**(1), pp. 5–15.

Flanagan, J., Chan, D. and Leder, P. (1991) 'Transmembrane form of the kit ligand growth factor is determined by alternative splicing and is missing in the SId mutant', *Cell*, **64**(5), pp. 1025–1035.

De Flora, A. *et al.* (2005) 'Age at onset: An essential variable for the definition of genetic risk factors for sporadic Alzheimer's disease', *Ann N Y Acad Sci*, **1057**, pp. 260–278.

Fogel, R. W. and Costa, D. L. (1997) 'A Theory of Technophysio Evolution, With Some Implications for Forecasting Population, Health Care Costs, and Pension Costs', *Demography*, **34**(1), p. 49.

Fontana, L., Partridge, L. and Longo, V. (2010) 'Extending healthy life span--from yeast to humans', *Science*, **328**, pp. 321–6.

Fraga, M. *et al.* (2005) 'Epigenetic Differences Arise During the Lifetime of Monozygotic Twins', *Proc. Natl. Acad. Sci.*, **31**(3), p. 204.

Frankel, E., Waterhouse, A. and Kinsella, J. (1993) 'Inhibition of human LDL oxidation by resveratrol', *Lancet*, **341**, pp. 1103–4.

Frederick, D. W. *et al.* (2015) 'Increasing NAD synthesis in muscle via nicotinamide phosphoribosyltransferase is not sufficient to promote oxidative metabolism', *J Biol Chem*, **290**(3), pp. 1546–1558.

Friedman, D. B. and Johnson, T. E. (1988a) 'A mutation in the age-1 gene in Caenorhabditis elegans lengthens life and reduces hermaphrodite fertility', *Genetics*, **118**, pp. 75–86.

Friedman, D. B. and Johnson, T. E. (1988b) 'Three mutants that extend both mean and maximum life span of the nematode, Caenorhabditis elegans, define the age-1 gene', *J. Gerontol.*, **43**, pp. B102–B109.

Fröjdö, S. *et al.* (2007) 'Resveratrol is a class IA phosphoinositide 3-kinase inhibitor', *Biochem. J.*, **406**(3), pp. 511–518.

Frye, R. A. (1999) 'Characterization of five human cDNAs with homology to the yeast SIR2 gene: Sir2-like proteins (Sirtuins) metabolize NAD and may have protein ADP-ribosyltransferase activity', *Biochem Biophys Res Commun.*, **260**(1), pp. 273–279.

Frye, R. A. (2000) 'A polymorphism in the growth hormone (GH)-releasing hormone (GHRH) receptor gene is associated with elevated response to GHRH by human pituitary somatotrophinomas in vitro.', *Biochem. Biophys. Res. Commun.*, **273**(1), pp. 793–798.

Fulco, M. *et al.* (2008) 'Glucose Restriction Inhibits Skeletal Myoblast Differentiation by Activating SIRT1 through AMPK-Mediated Regulation of Nampt', *Dev. Cell*, **14**(5), pp. 661–673.

Fulco, M. and Sartorelli, V. (2008) 'Comparing and contrasting the roles of AMPK and SIRT1 in metabolic tissues', *Cell Cycle*, **7**(23), pp. 3669–3679.

Gerhart-Hines, Z. *et al.* (2011) 'The cAMP/PKA Pathway Rapidly Activates SIRT1 to Promote Fatty Acid Oxidation Independently of Changes in NAD+', *Mol. Cell*, **44**(6), pp. 851–863.

Ghisays, F. *et al.* (2015) 'The N-Terminal Domain of SIRT1 Is a Positive Regulator of Endogenous SIRT1-Dependent Deacetylation and Transcriptional Outputs', *Cell Rep.* The Authors, **10**(10), pp. 1665–1673.

Gillum, M. P. *et al.* (2011) 'SirT1 regulates adipose tissue inflammation', *Diabetes*, **60**(12), pp. 3235–3245.

Gledhill, J. R. *et al.* (2007) 'Mechanism of inhibition of bovine F1-ATPase by resveratrol and related polyphenols', *Proc. Natl. Acad. Sci.*, **104**(34), pp. 13632–13637.

Gnoni, G. V. and Paglialonga, G. (2009) 'Resveratrol inhibits fatty acid and triacylglycerol synthesis in rat hepatocytes', *Eur. J. Clin. Invest.*, **39**(3), pp. 211–218.

Goldberg, A. D., Allis, C. D. and Bernstein, E. (2007) 'Epigenetics: A Landscape Takes Shape', *Cell*, **128**(4), pp. 635–638.

Goldman, R. D. *et al.* (2004) 'Accumulation of mutant lamin A causes progressive changes in nuclear architecture in Hutchinson–Gilford progeria syndrome', *Proc. Natl. Acad. Sci.*, **101**(24), pp. 8963–8968.

Gomes, A. *et al.* (2013) 'Declining NAD(+) induces a pseudohypoxic state disrupting nuclear-mitochondrial communication during aging', *Cell*, **155**, pp. 1624–1638.

Gong, B. *et al.* (2013) 'Nicotinamide riboside restores cognition through an upregulation of proliferator-activated receptor-γ coactivator 1α regulated β-secretase 1 degradation and mitochondrial gene expression in Alzheimer's mouse models', *Neurobiol Aging.* Elsevier Ltd, **34**(6), pp. 1581–1588.

Gräff, J. and Tsai, L. H. (2013) 'Histone acetylation: Molecular mnemonics on the chromatin', *Nat Rev Neurosci*. Nature Publishing Group, **14**(2), pp. 97–111.

Greer, E. L., Dowlatshahi, D., *et al.* (2007) 'An AMPK-FOXO Pathway Mediates Longevity Induced by a Novel Method of Dietary Restriction in C. elegans', *Curr Biol*, **17**(19), pp. 1646–1656.

Greer, E. L., Oskoui, P. R., *et al.* (2007) 'The energy sensor AMP-activated protein kinase directly regulates the mammalian FOXO3 transcription factor', *J Biol Chem*, **282**(41), pp. 30107–30119.

Grieger, J. C., Choi, V. W. and Samulski, R. J. (2006) 'Production and characterization of adeno-associated viral vectors', *Nat Protoc.*, **1**(3), pp. 1412–1428.

Guan, J. S. *et al.* (2009) 'HDAC2 negatively regulates memory formation and synaptic plasticity', *Nature*. Nature Publishing Group, **459**(7243), pp. 55–60.

Guarente, L. (2011) 'Franklin H. Epstein Lecture: Sirtuins, Aging, and Medicine', *N. Engl. J. Med.*, **364**, pp. 2235–2244.

Guarente, L. (2013) 'Calorie restriction and sirtuins revisited', *Genes Dev*, **27**(19), pp. 2072–2085.

Haffner, C. D. *et al.* (2015) 'Discovery, synthesis, and biological evaluation of thiazoloquin(az)olin(on)es as potent CD38 inhibitors', *J Med Chem*, **58**(8), pp. 3548–3571.

Haigis, M. C. *et al.* (2006) 'SIRT4 Inhibits Glutamate Dehydrogenase and Opposes the Effects of Calorie Restriction in Pancreatic ?? Cells', *Cell*, **126**(5), pp. 941–954.

Haigis, M. C. and Guatente, L. P. (2006) 'Mammalian sirtuins-energing role in physiology, aging, and calorie restriction', *Genes Dev.*, **20**, pp. 2913–2921.

Haigis, M. C. and Sinclair, D. A. (2010) 'Mammalian sirtuins: biological insights and disease relevance', *Annu. Rev. Pathol.,* **5**, pp. 253–295.

Haithcock, E. *et al.* (2005) 'Age-related changes of nuclear architecture in Caenorhabditis elegans', *Proc. Natl. Acad. Sci.*, **102**(46), pp. 16690–16695.

Hannum, G. *et al.* (2013) 'Genome-wide Methylation Profiles Reveal Quantitative Views of Human Aging Rates', *Mol Cell*. Elsevier Inc., **49**(2), pp. 359–367.

Harden, A. and Young, W. J. (1906) 'The Alcoholic Ferment of Yeast-Juice', *Proc. R. Soc. Lond. B Biol. Sci*, **78**, pp. 369–375.

Harel, I. *et al.* (2015) 'A platform for rapid exploration of aging and diseases in a naturally short-lived vertebrate', *Cell*, **160**(5), pp. 1013–1026.

Harrison, D. E. *et al.* (2009) 'Rapamycin fed late in life extends lifespan in genetically heterogeneous mice', *Nature*. Nature Publishing Group, **460**(7253), pp. 392–395.

Herranz, D. *et al.* (2010) 'Sirt1 improves healthy ageing and protects from metabolic syndrome-associated cancer.', *Nat. Commun.*, **1**, p. 3.

Herskind, A. M. *et al.* (1996) 'The heritability of human longevity: A population-based study of 2872 Danish twin pairs born 1870-1900', *Hum Genet.*, **97**(3), pp. 319–323.

Hirschey, M. D. *et al.* (2011) 'SIRT3 deficiency and mitochondrial protein hyperacetylation accelerate the development of the metabolic syndrome', *Mol. Cell*, **44**(2), pp. 177–190.

Horvath, S. (2013) 'DNA methylation age of human tissues and cell types', *Genome Biol*, **14**(R115), pp. 1–4.

Horvath, S. (2015) 'Erratum to DNA methylation age of human tissues and cell types', *Genome Biol.*, **16**(1), pp. 1–5.

Hotamisligil, G. S. (2006) 'Inflammation and metabolic disorders', *Nature*, **444**, pp. 860–867.

Hou, X. *et al.* (2008) 'SIRT1 regulates hepatocyte lipid metabolism through activating AMP-activated protein kinase', *J. Biol. Chem.*, **283**(29), pp. 20015–20026.

Houtkooper, R. H. *et al.* (2010) 'The secret life of NAD+: An old metabolite controlling new metabolic signaling pathways', *Endocr Rev*, **31**(2), pp. 194–223.

Houtkooper, R. H. *et al.* (2013) 'Mitonuclear protein imbalance as a conserved longevity mechanism', *Nature*. Nature Publishing Group, **497**(7450), pp. 451–457.

Howitz, K. *et al.* (2003) 'Small molecule activators of sirtuins extend Saccharomyces cerevisiae lifespan', *Nature*, **425**, pp. 191–196.

Howitz, K. T. and Sinclair, D. A. (2008) 'Xenohormesis: Sensing the Chemical Cues of Other Species', *Cell*, **133**(3), pp. 387–391.

Hsu, H. C. *et al.* (2013) 'Structural basis for allosteric stimulation of Sir2 activity by sir4 binding', *Genes Dev.*, **27**(1), pp. 64–73.

Hubbard, B. P. *et al.* (2013) 'Evidence for a common mechanism of SIRT1 regulation by allosteric activators.', *Science*, **339**(6124), pp. 1216–1219.

Hubbard, B. P. and Sinclair, D. A. (2014) 'Small molecule SIRT1 activators for the treatment of aging and age-related diseases', *Trends Pharmacol. Sci.* Elsevier Ltd, **35**(3), pp. 146–154.

Huber, J. L. *et al.* (2010) 'SIRT1-independent mechanisms of the putative sirtuin enzyme activators SRT1720 and SRT2183', *Future Med. Chem.*, **2**, pp. 1751–1759.

Imai, S. *et al.* (2000) 'Transcriptional silencing and longevity protein Sir2 is an NAD-dependent histone deacetylase', *Nature*, **403**(6771), pp. 795–800.

Imai, S. *et al.* (no date) 'Sir2: An NAD-dependent histone deacetylase that connects chromatin silencing, metabolism, and aging', *Cold Spring Harb Symp Quant Biol.*, **65**, pp. 297–302.

Imai, S. I. and Guarente, L. (2016) 'It takes two to tango: Nad+ and sirtuins in aging/longevity control', *NPJ Aging Mech Dis*. The Author(s), **2**(1), pp. 1–6.

Imai, S. ichiro and Guarente, L. (2014) 'NAD+ and sirtuins in aging and disease', *Trends Cell Biol*. Elsevier Ltd, **24**(8), pp. 464–471.

Ivanov, V. N. *et al.* (2008) 'Resveratrol sensitizes melanomas to TRAIL through modulation of antiapoptotic gene expression', *Exp. Cell Res.*, **314**(5), pp. 1163–1176.

Iwabu, M. *et al.* (2010) 'Adiponectin and AdipoR1 regulate PGC-1alpha and mitochondria by Ca(2+) and AMPK/SIRT1.', *Nature*. Nature Publishing Group, **464**(7293), pp. 1313–1319.

Jagger, C. *et al.* (2008) 'Inequalities in healthy life years in the 25 countries of the European Union in 2005: a cross-national meta-regression analysis', *Lancet*. Elsevier Ltd, **372**, pp. 2124–2131.

Jarolim, S. *et al.* (2004) 'A novel assay for replicative lifespan in', *FEMS Yeast Res.*, **5**(2), pp. 169–177.

Jeon, B. T. *et al.* (2012) 'Resveratrol attenuates obesity-associated peripheral and central inflammation and improves memory deficit in mice fed a high-fat diet', *Diabetes*, **61**(6), pp. 1444–1454.

Jiang, B. *et al.* (2013) 'Resveratrol attenuates early diabetic nephropathy by down-regulating glutathione S-transferases mu in diabetic rats', *J. Med. Food*, **16**(6), pp. 481–486.

Jiang, H. *et al.* (2013) 'SIRT6 regulates TNF-α secretion through hydrolysis of long-chain fatty acyl lysine', *Nature*. Nature Publishing Group, **496**(7443), pp. 110–113.

Jimenez-Gomez, Y. *et al.* (2013) 'Resveratrol improves adipose insulin signaling and reducestheinflammatoryresponsein adiposetissue of rhesus monkeys on high-fat, high-sugar diet', *Cell Metab.* Elsevier Inc., **18**(4), pp. 533–545.

Jing, E., Gesta, S. and Kahn, C. R. (2007) 'SIRT2 Regulates Adipocyte Differentiation through FoxO1 Acetylation/Deacetylation', *Cell Metabolism*, **6**(2), pp. 105–114.

Johnson, S. C., Rabinovitch, P. S. and Kaeberlein, M. (2013) 'mTOR is a key modulator of ageing and age-related disease', *Nature*, **493**(7432), pp. 338–345.

Juan, M., Vinardell, M. and Planas, J. (2002) 'The daily oral administration of high doses of trans-resveratrol to rats for 28 days is not harmful', *J. Nutr.*, **132**, pp. 257–260.

Jung, M. and Pfeifer, G. P. (2015) 'Aging and DNA methylation', *BMC Biol*, **13**(1), pp. 1–8.

Justice, M. J. and Dhillon, P. (2016) 'Using the mouse to model human disease: increasing validity and reproducibility', *Dis Model Mech*, **9**(2), pp. 101–103.

Kaeberlein, M. *et al.* (2005) 'Substrate-specific activation of sirtuins by resveratrol', *J. Biol. Chem.*, **280**(17), pp. 17038–17045.

Kaeberlein, M., Burtner, C. and Kennedy, B. (2007) 'Recent developments in yeast aging', *PLoS Genet*, **3**(5), pp. 655–660.

Kaeberlein, M., Mcvey, M. and Guarente, L. (1999) 'The SIR2/3/4 complex and SIR2 alone promote longevity in Saccharomyces cerevisiae by two different mechanisms', *Genes Dev.*, **13**(19), pp. 2570–2580.

Kanfi, Y. *et al.* (2012a) 'The sirtuin SIRT6 regulates lifespan in male mice', *Nature*. Nature Publishing Group, **483**(7388), pp. 218–221.

Kanfi, Y. *et al.* (2012b) 'The sirtuin SIRT6 regulates lifespan in male mice', *Nature*. Nature Publishing Group, **483**(7388), pp. 218–221.

Kapahi, P. *et al.* (2004) 'Regulation of Lifespan in Drosophila by Modulation of Genes in the TOR Signaling Pathway', *Curr Biol*, **14**, pp. 885–90.

Kauppinen, A. *et al.* (2013) 'Antagonistic crosstalk between NF-kB and SIRT1 in the regulation of inflammation and metabolic disorders', *Cellular Signal*. Elsevier B.V., **25**(10), pp. 1939–1948.

Kennedy, B. K. *et al.* (1995) 'Mutation in the silencing gene S/R4 can delay aging in S. cerevisiae', *Cell*, **80**(3), pp. 485–496.

Kennedy, B. K. *et al.* (1997) 'Redistribution of silencing proteins from telomeres to the nucleolus is associated with extension of life span in S. cerevisiae', *Cell*, **89**(3), pp. 381–391.

Kenyon, C. *et al.* (1993) 'A C. elegans mutant that lives twice as long as wild type', *Nature*, **363**, pp. 210–211.

Kenyon, C. (2011) 'The first long-lived mutants: Discovery of the insulin/IGF-1 pathway for ageing', *Philos Trans R Soc Lond B Biol Sci*, **366**(1561), pp. 9–16.

Kenyon, C. J. (2010) 'The genetics of ageing', *Nature*, **464**, pp. 504–512.

Kim, D., Langmead, B. and Salzberg, S. L. (2015) 'HISAT: A fast spliced aligner with low memory requirements', *Nat Methods.* Nature Publishing Group, **12**(4), pp. 357–360.

Kim, E. J. *et al.* (2007) 'Active Regulator of SIRT1 Cooperates with SIRT1 and Facilitates Suppression of p53 Activity', *Mol. Cell*, **28**(2), pp. 277–290.

Klar, A. J. S., Fogel, S. and Macleod, K. (1979) 'MAR1-A Regulator of the HMa and HMalpha Loci in Saccharromyces cerevisiae.', *Genetics*, **93**, pp. 37–50.

Knight, C. M. *et al.* (2011) 'Mediobasal hypothalamic SIRT1 is essential for Resveratrol's effects on insulin action in rats', *Diabetes*, **60**(11), pp. 2691–2700.

Kontis, V. *et al.* (2017) 'Future life expectancy in 35 industrialised countries: projections with a Bayesian model ensemble', *Lancet*. The Author(s). Published by Elsevier Ltd. This is an Open Access article under the CC BY license, **389**, pp. 1323–1335.

Korhonen, M. T. *et al.* (2006) 'Aging, muscle fiber type, and contractile function in sprint-trained athletes', *J Appl Physiol (1985)*, **101**(3), pp. 906–917.

Koutnikova, H. *et al.* (2009) 'Identification of the UBP1 locus as a critical blood pressure determinant using a combination of mouse and human genetics', *PLoS Genetics*, **5**(8).

Kowald, A. and Kirkwood, T. B. L. (1996) 'A network theory of ageing: The interactions of defective mitochondria, aberrant proteins, free radicals and scavengers in the ageing process', *Mutat Res*, **316**(5–6), pp. 209–236.

Kreutzenberg, S. V. De *et al.* (2010) 'Downregulation of the Longevity-Associated Protein Potential Biochemical Mechanisms', *Diabetes*, **59**(April), pp. 1006–1015.

Krueger, J. G. *et al.* (2015) 'A Randomized, placebo-controlled study of SRT2104, a SIRT1 activator, in patients with moderate to severe psoriasis', *PLoS ONE*, **10**(11), pp. 1–14.

Kwong, L. K. and Sohal, R. S. (2000) 'Age-related changes in activities of mitochondrial electron transport complexes in various tissues of the mouse', *Arch Biochem Biophys*, **373**(1), pp. 16–22.

Lagouge, M. *et al.* (2006) 'Resveratrol improves mitochondrial function and protects against metabolic disease by activating SIRT1 and PGC-1alpha', *Cell*, **127**, pp. 1109–1122.

Lakshminarasimhan, M. *et al.* (2013) 'Sirt1 activation by resveratrol is substrate sequence-selective', *Aging (Albaby, NY)*, **5**(3), pp. 151–154.

Lan, F., Cacicedo, Jose M., *et al.* (2008) 'SIRT1 modulation of the acetylation status, cytosolic localization, and activity of LKB1: Possible role in AMP-activated protein kinase activation', *J Biol Chem*, **283**(41), pp. 27628–27635.

Lan, F., Cacicedo, Jose M, *et al.* (2008) 'SIRT1 modulation of the acetylation status, cytosolic localization, and activity of LKB1. Possible role in AMP-activated protein kinase activation', *J. Biol. Chem.,* **283**(41), pp. 27628–27635.

Landry, J. *et al.* (2000) 'The silencing protein SIR2 and its homologs are NAD-dependent protein deacetylases', *Proc Natl Acad Sci*, **97**(11), pp. 5807–5811.

Landry, J., Slama, J. T. and Sternglanz, R. (2000) 'Role of NAD+ in the deacetylase activity of the SIR2-like proteins', *Biochem Biophys Res Commun*, **278**(3), pp. 685–690.

Larson, K. *et al.* (2012) 'Heterochromatin formation promotes longevity and represses ribosomal RNA synthesis', *PLoS Genet*, **8**(1).

Larsson, N. *et al.* (1998) 'Mitochondrial transcription factor A is necessary for mtDNA maintenance and embryogenesis in mice', *Nat Genet*, **18**(3).

Laurent, G. *et al.* (2013) 'SIRT4 coordinates the balance between lipid synthesis and catabolism by repressing malonyl CoA decarboxylase', *Mol. Cell*, **50**(5), pp. 686–698.

Leduc-Gaudet, J.-P. *et al.* (2015) 'Mitochondrial morphology is altered in atrophied skeletal muscle of aged mice', *Oncotarget*, **6**(20).

Levy, J. C., Matthews, D. R. and Hermans, M. P. (1998) 'Correct homeostasis model assessment (HOMA) evaluation uses the computer program', *Diabetes Care*, **21**(12), pp. 2191–2192.

Li, J. *et al.* (2017) 'A conserved NAD+ binding pocket that regulatesprotein-protein interactions during aging', *Science*, **355**(March), pp. 1312–1317.

Li, P. *et al.* (2012) 'Interferon gamma (IFN-γ) disrupts energy expenditure and metabolic homeostasis by suppressing SIRT1 transcription', *Nucleic Acids Res.*, **40**(4), pp. 1609–1620.

Li, Y. *et al.* (2008) 'SirT1 Inhibition Reduces IGF-I/IRS-2/Ras/ERK1/2 Signaling and Protects Neurons', *Cell Metab.*, **8**(1), pp. 38–48.

Liang, F., Kume, S. and Koya, D. (2009) 'SIRT1 and insulin resistance', *Nat Rev Endocrinol*. Nature Publishing Group, **5**(7), pp. 367–373.

Libri, V. *et al.* (2012) 'A pilot randomized, placebo controlled, double blind phase I trial of the novel SIRT1 activator SRT2104 in elderly volunteers', *PLoS One*, **7**(12), p. e51395.

Lin, S. *et al.* (2002) 'Calorie restriction extends Saccharomyces cerevisiae lifespan by increasing respiration', *Nature*, **418**(6895), pp. 336–340.

Lin, S. J., Defossez, P. A. and Guarente, L. (2000) 'Requirement of NAD and SIR2 for life-span extension by calorie restriction in saccharomyces cerevisiae', *Science*, **289**(5487), pp. 2126–2128.

Liszt, G. *et al.* (2005) 'Mouse Sir2 homolog SIRT6 is a nuclear ADP-ribosyltransferase', *J. Biol. Chem.*, **280**(22), pp. 21313–21320.

Liu, B. *et al.* (2012) 'Resveratrol rescues SIRT1-dependent adult stem cell decline and alleviates progeroid features in laminopathy-based progeria', *Cell Metab.* Elsevier Inc., **16**(6), pp. 738–750.

Liu, M. *et al.* (2010) 'Resveratrol inhibits mTOR signaling by targeting DEPTOR', *J. Biol. Chem.*, **285**(4), pp. 36387–36394.

Long, A. N. *et al.* (2015) 'Effect of nicotinamide mononucleotide on brain mitochondrial respiratory deficits in an Alzheimer's disease-relevant murine model', *BMC Neurol*, **15**(1), pp. 1–14.

Longo, V. D. (2009) 'Linking sirtuins, IGF-I signaling, and starvation', *Exp. Gerontol*. Elsevier Inc., **44**(1–2), pp. 70–74.

Longo, V. and Kennedy, B. (2006) 'Sirtuins in aging and age-related diseases', *Cell*, **126**, pp. 257–268.

Lopez-Atalaya, J. P. and Barco, A. (2014) 'Can changes in histone acetylation contribute to memory formation?', *Trends Genet*. Elsevier Ltd, **30**(12), pp. 529–539.

López-Otín, C. *et al.* (2013) 'The hallmarks of aging.', *Cell*, **153**(6), pp. 1194–1217.

MacDonald, M. E. *et al.* (1993) 'A novel gene containing a trinucleotide repeat that is expanded and unstable on Huntington's disease chromosomes', *Cell*, **72**(6), pp. 971–983.

Magni, G. *et al.* (1999) 'Enzymology of NAD+ synthesis', *Adv Enzymol Relat Areas Mol Biol.*, **73**, pp. 135–182.

Mair, W. and Dillin, A. (2008) 'Aging and Survival: The Genetics of Life Span Extension by Dietary Restriction', *Annu Rev Biochem*, **77**(1), pp. 727–754.

Mangerich, A. *et al.* (2010) 'Inflammatory and age-related pathologies in mice with ectopic expression of human PARP-1', *Mech Ageing Dev*, **131**(6), pp. 389–404.

Marier, J.-F. *et al.* (2002) 'Metabolism and disposition of resveratrol in rats: extent of absorption, glucuronidation, and enterohepatic recirculation evidenced by a linked-rat model.', *J. Pharmacol. Exp. Ther.*, **302**(1), pp. 369–373.

Martin-Montalvo, A. *et al.* (2013) 'Metformin improves healthspan and lifespan in mice', *Nat Commun*, **4**, p. 2192.

Masoro, E. (2002) *Caloric Restriction: A Key to Understanding and Modulating Aging*, *Elsevier, Amsterdam*.

Mastroeni, D. *et al.* (2009) 'Epigenetic differences in cortical neurons from a pair of monozygotic twins discordant for Alzheimer's disease', *PLoS ONE*, **4**(8), pp. 1–6.

Mastroeni, D. *et al.* (2010) 'Epigenetic changes in Alzheimer's disease: Decrements in DNA methylation', *Neurobiol Aging*. Elsevier Inc., **31**(12), pp. 2025–2037.

Mathias, R. A. *et al.* (2014) 'Sirtuin 4 is a lipoamidase regulating pyruvate dehydrogenase complex activity', *Cell*. Elsevier Inc., **159**(7), pp. 1615–1625.

Matsuzaki, H. *et al.* (2003) 'Insulin-induced phosphorylation of FKHR (Foxo1) targets to proteasomal degradation', *Proc Natl Acad Sci*, **100**(20), pp. 11285–11290.

McCay, C., Crowell, M. and Maynard, L. (1935) 'The effect of retarded growth upon the length of life span and upon the ultimate body size', *Nutrition*, **5**, pp. 155–171.

McCord, R. A. *et al.* (2009) 'SIRT6 stabilizes DNA-dependent protein kinase at chromatin for DNA double-strand break repair.', *Aging*, **1**(1), pp. 109–121.

McMurray, M. A. and Gottschling, D. E. (2003) 'An age-induced switch to a hyper-recombinational state', *Science*, **301**(5641), pp. 1908–1911.

Menzies, K. J. *et al.* (2013) 'Sirtuin 1-mediated effects of exercise and resveratrol on mitochondrial biogenesis', *J. Biol. Chem.*, **288**(10), pp. 6968–6979.

Mercken, E. M. *et al.* (2012) 'Of mice and men: The benefits of caloric restriction, exercise, and mimetics', *Ageing Res Rev*. Elsevier B.V., **11**, pp. 390–398.

Mercken, E. M. *et al.* (2014) 'SRT2104 extends survival of male mice on a standard diet and preserves bone and muscle mass', *Aging Cell*, **13**, pp. 787–796.

Michan, S. and Sinclair, D. (2007) 'Sirtuins in mammals: insights into their biological function.', *Biochem. J.*, **404**(1), pp. 1–13.

Michishita, E. *et al.* (2005) 'Evolutionarily Conserved and Nonconserved Cellular Localizations and Functions of Human SIRT Proteins', *Mol. Biol. Cell.*, **16**, pp. 4623–4635.

Migliaccio, E. *et al.* (1999) 'The p66(shc) adaptor protein controls oxidative stress response and life span in mammals', *Nature*, **402**(6759), pp. 309–313.

Miller, R. A. *et al.* (2014) 'Rapamycin-mediated lifespan increase in mice is dose and sex dependent and metabolically distinct from dietary restriction', *Aging Cell*, **13**, pp. 468–477.

Mills, K. D., Sinclair, D. A. and Guarente, L. (1999) 'MEC1-dependent redistribution of the Sir3 silencing protein from telomeres to DNA double-strand breaks', *Cell*, **97**(5), pp. 609–620.

Mills, K. F. *et al.* (2016) 'Long-Term Administration of Nicotinamide Mononucleotide Mitigates Age-Associated Physiological Decline in Mice', *Cell Metab*. Elsevier Inc., **24**(6), pp. 795–806.

Milne, J. C. *et al.* (2007) 'Small molecule activators of SIRT1 as therapeutics for the treatment of type 2 diabetes.', *Nature*, **450**(7170), pp. 712–716.

Minor, R. K. *et al.* (2011) 'SRT1720 improves survival and healthspan of obese mice.', *Sci. Rep.*, **1**, p. 70.

Mitchell, S. J. *et al.* (2014) 'The SIRT1 activator SRT1720 extends lifespan and improves health of mice fed a standard diet', *Cell Rep.* Elsevier, **6**(5), pp. 836–843.

Montero-Pau, J. and Africa Gómez, and J. M. (2008) 'Application of an inexpensive and high-throughput genomic DNA extraction method for the molecular ecology of zooplanktonic diapausing eggs', *Limnol. Oceanogr.: Methods*, **6**, pp. 218–222.

Mootha, V. *et al.* (2004) 'Erralpha and Gabpa/b specify PGC-1alpha-dependent oxidative phosphorylation gene expression that is altered in diabetic muscle', *Proc. Natl. Acad. Sci.*, **101**(17).

Morselli, E. *et al.* (2009) 'Autophagy mediates pharmacological lifespan extension by spermidine and resveratrol.', *Aging (Albaby, NY)*, **1**(12), pp. 961–970.

Moschen, A. R. *et al.* (2013) 'Adipose tissue and liver expression of SIRT1, 3, and 6 increase after extensive weight loss in morbid obesity', *J. Hepatol.* European Association for the Study of the Liver, **59**(6), pp. 1315–1322.

Mostoslavsky, R. *et al.* (2006) 'Genomic instability and aging-like phenotype in the absence of mammalian SIRT6', *Cell*, **124**(2), pp. 315–329.

Mouchiroud, L., Houtkooper, R. H., Moullan, N., Katsyuba, E., Ryu, D., Cantó, C., *et al.* (2013) 'The NAD+/sirtuin pathway modulates longevity through activation of mitochondrial UPR and FOXO signaling', *Cell*, **154**(2).

Mouchiroud, L., Houtkooper, R. H., Moullan, N., Katsyuba, E., Ryu, D., Cantó, C., *et al.* (2013) 'The NAD+/sirtuin pathway modulates longevity through activation of mitochondrial UPR and FOXO signaling', *Cell*, **154**(2).

Mouchiroud, L., Houtkooper, R. H. and Auwerx, J. (2013) 'NAD + metabolism , a therapeutic target for age-related metabolic disease', *Crit Rev Biochem Mol Biol*, **48**(4).

Moynihan, K. A. *et al.* (2005) 'Increased dosage of mammalian Sir2 in pancreatic β cells enhances glucose-stimulated insulin secretion in mice', *Cell Metab.*, **2**(2), pp. 105–117.

Mueller, J. *et al.* (1993) 'Homing endonucleases', in *In Nucleases, S.M. Linn, R.S. Lloyd, and R.J. Roberts, eds. (Cold Spring Harbor, NY: Cold Spring Harbor Laboratory Press)*, pp. 111–143.

Muñoz-Najar, U. and Sedivy, J. M. (2011) 'Epigenetic Control of Aging', *Antioxid Redox Signal*, **14**(2), pp. 241–259.

Nakamura, Y. *et al.* (2008) 'Localization of mouse mitochondrial SIRT proteins: Shift of SIRT3 to nucleus by co-expression with SIRT5', *Biochem. Biophys. Res. Commun.*, **366**(1), pp. 174–179.

Niccoli, T. and Partridge, L. (2012) 'Ageing as a risk factor for disease', *Curr Biol*. Elsevier Ltd, **22**, pp. R741–R752.

North, B. J. *et al.* (2003) 'The Human Sir2 Ortholog, SIRT2, Is an NAD+ -Dependent Tubulin Deacetylas', *Mol. Cell*, **11**, pp. 437–444.

North, B. J. and Verdin, E. (2004) 'Sirtuins: Sir2-related NAD-dependent protein deacetylases', *Genome Biol*, **5**(5), pp. 1–12.

North, B. J. and Verdin, E. (2007) 'Interphase nucleo-cytoplasmic shuttling and localization of SIRT2 during mitosis', *PLoS ONE*, **2**(8), p. e784.

O'Sullivan, R. J. and Karlseder, J. (2012) 'The great unravelling: Chromatin as a modulator of the aging process', *Trends Biochem Sci*. Elsevier Ltd, **37**(11), pp. 466–476.

Oberdoerffer, P. *et al.* (2008) 'SIRT1 Redistribution on Chromatin Promotes Genomic Stability but Alters Gene Expression during Aging', *Cell*. Elsevier Inc., **135**(5), pp. 907–918.

Oberdoerffer, P. and Sinclair, D. A. (2007) 'The role of nuclear architecture in genomic instability and ageing', *Nat Rev Mol Cell Biol.*, **8**(9), pp. 692–702.

Oeppen, J. and Vaupel, J. W. (2002) 'Broken Limits to Life Expectancy', *Science*, **296**(5570), pp. 1029–1031.

Onyango, P. *et al.* (2002) 'SIRT3, a human SIR2 homologue, is an NAD- dependent deacetylase localized to mitochondria Patrick', *Proc. Natl. Acad. Sci.*, **99**, pp. 13653–13658.

Pacholec, M. *et al.* (2010) 'SRT1720, SRT2183, SRT1460, and resveratrol are not direct activators of SIRT1', *J. Biol. Chem.*, **285**(11), pp. 8340–8351.

Pal, S. and Tyler, J. K. (2016) 'Epigenetics and aging', *Sci. Adv*, **2**(e1600584), pp. 1–19.

Pang, W. *et al.* (2013) 'Sirt1 Inhibits Akt2-Mediated Porcine Adipogenesis Potentially by Direct Protein-Protein Interaction', *PLoS ONE*, **8**, p. e71576.

Park, S. J. *et al.* (2012) 'Resveratrol ameliorates aging-related metabolic phenotypes by inhibiting cAMP phosphodiesterases', *Cell*. Elsevier Inc., **148**(3), pp. 421–433.

Partridge, L., Deelen, J. and Slagboom, P. E. (2018) 'Facing up to the global challenges of ageing', *Nature*. Springer US, **561**(7721), pp. 45–56.

Patti, M. E. *et al.* (2003) 'Coordinated reduction of genes of oxidative metabolism in humans with insulin resistance and diabetes: Potential role of PGC1 and NRF1.', *Proc. Natl. Acad. Sci.*, **100**(14), pp. 8466–8471.

Pawlikowska, L. *et al.* (2009) 'Association of common genetic variation in the insulin/IGF1 signaling pathway with human longevity', *Aging Cell*, **8**(4), pp. 460–472.

Pearson, K. J. *et al.* (2008) 'Resveratrol delays age-related deterioration and mimics transcriptional aspects of dietary restriction without extending life span', *Cell Metab.* Elsevier Inc., **8**(2), pp. 157–168.

Pedersen, S. B. *et al.* (2008) 'Low Sirt1 expression, which is upregulated by fasting, in human adipose tissue from obese women.', *Int. J. Obes.*, **32**(8), pp. 1250–1255.

Peeters, A. V. *et al.* (2008) 'Association of SIRT1 gene variation with visceral obesity', *Hum. Genet.*, **124**(4), pp. 431–436.

Peters, T., Ausmeier, K. and Rüther, U. (1999) 'Cloning of Fatso (Fto), a novel gene deleted by the fused toes (Ft) mouse mutation', *Mamm Genome*, **10**(10), pp. 983–986.

Pfluger, P. T. *et al.* (2008) 'Sirt1 protects against high-fat diet-induced metabolic damage', *Proc. Natl. Acad. Sci.*, **105**(28), pp. 9793–98.

Picard, F. *et al.* (2004) 'Sirt1 promotes fat mobilization in white adipocytes by repressing PPAR-gamma.', *Nature*, **429**(6993), pp. 771–776.

Picard, M. *et al.* (2013) 'Acute exercise remodels mitochondrial membrane interactions in mouse skeletal muscle', *J. Appl. Physiol.*, **115**(10), pp. 1562–1571.

Pirinen, E. *et al.* (2014) 'Pharmacological inhibition of poly(ADP-ribose) polymerases improves fitness and mitochondrial function in skeletal muscle', *Cell Metab*, **19**(6), pp. 1034–1041.

Poulain, M., Herm, A. and Pes, G. (2013) 'The Blue Zones: areas of exceptional longevity around the world', *Vienna Yearb Popul Res*, **11**, pp. 87–108.

Poulet, B. *et al.* (2014) 'Modifications of gait as predictors of natural osteoarthritis progression in Str/Ort mice', *Arthritis Rheumatol.*, **66**(7), pp. 1832–1842.

Poulsen, P. *et al.* (2007) 'The epigenetic basis of twin discordance in age-related diseases', *Pediatr Res.*, **61**, pp. 38–42.

Price, N. L. *et al.* (2012) 'SIRT1 is required for AMPK activation and the beneficial effects of resveratrol on mitochondrial function', *Cell Metab.,* **15**(5), pp. 675–690.

Purushotham, A., Xu, Q. and Li, X. (2012) 'Systemic SIRT1 insufficiency results in disruption of energy homeostasis and steroid hormone metabolism upon high-fat-diet feeding.', *FASEB J.*, **26**(2), pp. 656–667.

Qiao, L. and Shao, J. (2006) 'SIRT1 regulates adiponectin gene expression through Foxo1-C/enhancer- binding protein transcriptional complex', *J. Biol. Chem.*, **281**(52), pp. 39915–39924.

Quarrie, J. K. and Riabowol, K. T. (2004) 'Murine models of life span extension.', *Science of aging knowledge environment : SAGE KE*, **2004**(31).

Rajman, L., Chwalek, K. and Sinclair, D. A. (2018) 'Therapeutic Potential of NAD-Boosting Molecules: The In Vivo Evidence', *Cell Metab*. Elsevier Inc., **27**(3), pp. 529–547.

Ramadori, G. *et al.* (2008) 'Brain SIRT1: anatomical distribution and regulation by energy availability.', *J. Neurosci.*, **28**(40), pp. 9989–9996.

Ramadori, G. *et al.* (2009) 'Central administration of resveratrol improves diet-induced diabetes', *Endocrinology*, **150**, pp. 5326–33.

Ramsey, K. M. *et al.* (2008) 'Age-associated loss of Sirt1-mediated enhancement of glucose-stimulated insulin secretion in beta cell-specific Sirt1-overexpressing (BESTO) mice', *Aging Cell*, **7**(1), pp. 78–88.

Rascón, B. *et al.* (2012) 'The lifespan extension effects of resveratrol are conserved in the honey bee and may be driven by a mechanism related to caloric restriction', *Aging (Albaby, NY)*, **4**(7), pp. 499–508.

Ratajczak, J. *et al.* (2016) 'NRK1 controls nicotinamide mononucleotide and nicotinamide riboside metabolism in mammalian cells', *Nat Commun*, **7**, pp. 1–12.

Renaud, S. and de Lorgeril, M. (1992) 'Wine, alcohol, platelets, and the French paradox for coronary heart disease', *Lancet*, **339**, pp. 1523–6.

Revollo, J. R., Grimm, A. A. and Imai, S. I. (2004) 'The NAD biosynthesis pathway mediated by nicotinamide phosphoribosyltransferase regulates Sir2 activity in mammalian cells', *J Biol Chem.*, **279**(49), pp. 50754–50763.

Richard, J. (1987) '[Coronary risk factors. The French paradox]', *Arch. Mal. Coeur. Vaiss.*, **80**, p. Spec No:17-21.

Riordan, J. R. *et al.* (1989) 'Identification of the cystic fibrosis gene: cloning and characterization of complementary DNA', *Science*, **245**(4922), pp. 1066–1073.

Rivera, L. *et al.* (2009) 'Long-term resveratrol administration reduces metabolic disturbances and lowers blood pressure in obese Zucker rats', *Biochem. Pharmacol.*, **77**(6), pp. 1053–1063.

Rocha, K. K. R. *et al.* (2009) 'Resveratrol toxicity: effects on risk factors for atherosclerosis and hepatic oxidative stress in standard and high-fat diets', *Food Chem. Toxicol.* Elsevier Ltd, **47**(6), pp. 1362–1367.

Rodgers, J. T. *et al.* (2005) 'Nutrient control of glucose homeostasis through a complex of PGC-1alpha and SIRT1', *Nature*, **434**, pp. 113–8.

Rogina, B. and Helfand, S. L. (2004) 'Sir2 mediates longevity in the fly through a pathway related to calorie restriction', *Proc. Natl. Acad. Sci.*, **101**(45), pp. 15998–16003.

Ruggiero, C. *et al.* (2008) 'High basal metabolic rate is a risk factor for mortality: The Baltimore Longitudinal Study of Aging', *J Gerontol A Biol Sci Med Sci*, **63**(7), pp. 698–706.

Rutanen, J., Yaluri, N. and Modi, S. (2010) 'SIRT1 mRNA expression may be associated with energy expenditure and insulin sensitivity', *Diabetes*, **59**(April), pp. 829–835.

Ruzankina, Y. *et al.* (2007) 'Deletion of the Developmentally Essential Gene ATR in Adult Mice Leads to Age-Related Phenotypes and Stem Cell Loss', *Cell Stem Cell*, **1**(1), pp. 113–126.

Ryu, D. *et al.* (2014) 'A SIRT7-dependent acetylation switch of GABPβ1 controls mitochondrial function', *Cell Metab.* Elsevier Inc., **20**(5), pp. 856–869.

Sajish, M. and Schimmel, P. (2015) 'A human tRNA synthetase is a potent PARP1-activating effector target for resveratrol', *Nature*. Nature Publishing Group, **519**(7543), pp. 370–373.

Sargent, M. (2010) 'Why twins age differently', *Nature*, **464**(7292), pp. 1130–1131.

Satoh, A. *et al.* (2013) 'Sirt1 extends life span and delays aging in mice through the regulation of Nk2 Homeobox 1 in the DMH and LH', *Cell Metab*. Elsevier Inc., **18**(3), pp. 416–430.

Sauve, A. A. *et al.* (2001) 'Chemistry of Gene Silencing: The Mechanism of NAD + -Dependent Deacetylation Reactions', *Biochemistry*, **40**(51), pp. 15456–15463.

Scaffidi, P. and Misteli, T. (2006) 'Lamin A-dependent nuclear defects in human aging', *Science*, **312**, pp. 1059–1063.

Scher, M. B., Vaquero, A. and Reinberg, D. (2007) 'SirT3 is a nuclear NAD+ -dependent histone deacetylase that translocates to the mitochondria upon cellular stress Michael', *Genes Dev.*, **21**, pp. 920–928.

Schmidt, M. T. *et al.* (2004) 'Coenzyme specificity of Sir2 protein deacetylases. Implications for physiological regulation', *J. Biol. Chem.*, **279**(38), pp. 40122–40129.

Schwer, B. *et al.* (2002) 'The human silent information regulator (Sir)2 homologue hSIRT3 is a mitochondrial nicotinamide adenine dinucleotide-dependent deacetylase', *J. Cell Biol.*, **158**(4), pp. 647–657.

Sen, P. *et al.* (2016) 'Epigenetic Mechanisms of Longevity and Aging', *Cell*. Elsevier Inc., **166**(4), pp. 822–839.

Shang, J. *et al.* (2008) 'Resveratrol improves non-alcoholic fatty liver disease by activating AMP-activated protein kinase', *Acta Pharmacol. Sin.*, **29**(6), pp. 698–706.

Shin, S. *et al.* (2009) 'Role of Nrf2 in prevention of high-fat diet-induced obesity by synthetic triterpenoid CDDO-imidazolide.', *Eur. J. Pharmacol.,*. Elsevier B.V., **620**(1–3), pp. 138–144.

Shumaker, D. K. *et al.* (2006) 'Mutant nuclear lamin A leads to progressive alterations of epigenetic control in premature aging', *Proc. Natl. Acad. Sci.*, **103**(23), pp. 8703–8708.

Siebler, J. and Galle (2016) 'Treatment of Non-Alcoholic Fatty Liver Disease', *World J Gastroenterol*, **12**.

Silva, J. P. and Wahlestedt, C. (2010) 'Role of Sirtuin 1 in metabolic regulation', *Drug Discov. Today*. Elsevier Ltd, **15**(17–18), pp. 781–791.

Sinclair, D. A. (2005) 'Toward a unified theory of caloric restriction and longevity regulation', *Mech. Ageing Dev.*, **126**(9 SPEC. ISS.), pp. 987–1002.

Sinclair, D. A. and Guarente, L. (1997) 'Extrachromosomal rDNA circles - A cause of aging in yeast', *Cell*, **91**(7), pp. 1033–1042.

Sinclair, D. a and Guarente, L. (2014) 'Small-molecule allosteric activators of sirtuins.', *Annu Rev Pharmacol Toxicol*, **54**, pp. 363–380.

Sirtris Pharma (2007) 'Methods and related compositions for treating or preventing obesity, insulin resistance disorders, and mitochondrial-associated disorders'.

Smeal, T. *et al.* (1996) 'Loss of transcriptional silencing causes sterility in old mother cells of S. cerevisiae', *Cell*, **84**(4), pp. 633–642.

Smith, J. J. *et al.* (2009) 'Small molecule activators of SIRT1 replicate signaling pathways triggered by calorie restriction in vivo', *BMC Syst. Biol.*, **3**:31.

Smith, J. S. *et al.* (2000) 'A phylogenetically conserved NAD+-dependent protein deacetylase activity in the Sir2 protein family', *Proc Natl Acad Sci*, **97**(12), pp. 6658–6663.

Smith, J. S. and Boeke, J. D. (1997) 'An unusual form of transcriptional silencing in yeast ribosomal DNA', *Genes Dev.*, **11**(2), pp. 241–254.

Smoliga, J. M., Baur, J. A. and Hausenblas, H. A. (2011) 'Resveratrol and health – A comprehensive review of human clinical trials', *Mol. Nutr. Food Res.*, **55**, pp. 1129–1141.

Song, Y. S. *et al.* (2013) 'Association between low SIRT1 expression in visceral and subcutaneous adipose tissues and metabolic abnormalities in women with obesity and type 2 diabetes', *Diabetes Res. Clin. Pract.* Elsevier Ireland Ltd, **101**(3), pp. 341–348.

Spindler, S. R. (2010) ‘Caloric restriction: From soup to nuts’, *Ageing Res Rev*. Elsevier B.V., **9**, pp. 324–353.

Stein, L. R. and Imai, S. I. (2014) ‘Specific ablation of Nampt in adult neural stem cells recapitulates their functional defects during aging’, *EMBO J*, **33**(12), pp. 1321–1340.

Stenholm, S. *et al.* (2017) ‘Body mass index as a predictor of healthy and disease-free life expectancy between ages 50 and 75: A multicohort study’, *Int J Obes (Lond)*, **41**(5), pp. 769–775.

Stünkel, W. and Campbell, R. M. (2011) ‘Sirtuin 1 (SIRT1): the misunderstood HDAC’, *J. Biomol. Screen.*, **16**(10), pp. 1153–1169.

Subramanian, L. *et al.* (2010) ‘Resveratrol: Challenges in translation to the clinic - A critical discussion’, *Clin. Cancer Res.*, **16**(24), pp. 5942–5948.

Suh, Y. *et al.* (2008) ‘Functionally significant insulin-like growth factor I receptor mutations in centenarians’, *Proc Natl Acad Sci*, **105**(9), pp. 3438–3442.

Sun, C. *et al.* (2007) ‘SIRT1 improves insulin sensitivity under insulin-resistant conditions by repressing PTP1B’, *Cell Metab.*, **6**(4), pp. 307–319.

Sweatt, J. D. (2013) ‘The emerging field of neuroepigenetics’, *Neuron*. Elsevier Inc., **80**(3), pp. 624–632.

Tan, M. *et al.* (2014) ‘Lysine glutarylation is a protein posttranslational modification regulated by SIRT5’, *Cell Metab.*, **19**(4), pp. 605–617.

Tanno, M. *et al.* (2007) ‘Nucleocytoplasmic shuttling of the NAD+-dependent histone deacetylase SIRT1’, *J. Biol. Chem.*, **282**(9), pp. 6823–6832.

Tanny, J. C. *et al.* (1999) ‘An enzymatic activity in the yeast Sir2 protein that is essential for gene silencing’, *Cell*, **99**(7), pp. 735–745.

Tanny, J. C. *et al.* (2004) ‘Budding Yeast Silencing Complexes and Regulation of Sir2 Activity by Protein-Protein Interactions’, *Mol. Cell. Biol.*, **24**(16), pp. 6931–6946.

Timmers, S. *et al.* (2011) ‘Calorie restriction-like effects of 30 days of resveratrol supplementation on energy metabolism and metabolic profile in obese humans’, *Cell Metab.* Elsevier Inc., **14**(5), pp. 612–622.

Tissenbaum, H. A. (2012) ‘Genetics, life span, health span, and the aging process in caenorhabditis elegans’, *J Gerontol A Biol Sci Med Sci.*, **67** A(5), pp. 503–510.

Tissenbaum, H. A. and Guarente, L. (2001) ‘Increased dosage of a sir-2 gene extends lifespan in Caenorhabditis elegans’, *Nature*, **410**(6825), pp. 227–230.

Trammell, S. A. *et al.* (2016) 'Nicotinamide Riboside Is a Major NAD+ Precursor Vitamin in Cow Milk', *J Nutr*, **146**(5), pp. 957–963.

Trammell, S. A. J., Schmidt, M. S., *et al.* (2016) 'Nicotinamide riboside is uniquely and orally bioavailable in mice and humans', *Nat Commun*. Nature Publishing Group, **7**, pp. 1–14.

Trammell, S. A. J., Weidemann, B. J., *et al.* (2016) 'Nicotinamide riboside opposes type 2 diabetes and neuropathy in mice', *Sci Rep*. Nature Publishing Group, **6**(May), pp. 1–7.

Trzebiatowski, J. R. and Escalante-semerena, J. C. (1997) 'Purification and characterization of CobT, the nicotinate-mononucleotide 5,6-dimethylbenzimidazole phosphoribosyltransferase enzyme from Salmonella typhimurium LT2', *J Biol Chem*, **272**(28), pp. 17662–17667.

Tsang, A. W. and Escalante-Semerenat, J. C. (1999) 'CobB, a new member of the SIR2 family of eucaryotic regulatory proteins, is required to compensate for the lack of nicotinate mononucleotide:5,6- dimethylbenzimidazole phosphoribosyltransferase activity in cobT mutants during cobalamin biosynthesis in Sal', *J Biol Chem*, **273**(48), pp. 31788–31794.

Tsurumi, A. and Li, W. X. (2012) 'Global heterochromatin loss: A unifying theory of aging?', *Epigenetics*, **7**(7), pp. 680–688.

Tullet, J. M. A. *et al.* (2014) 'DAF-16/FoxO Directly Regulates an Atypical AMP-Activated Protein Kinase Gamma Isoform to Mediate the Effects of Insulin/IGF-1 Signaling on Aging in Caenorhabditis elegans', *PLoS Genet*, **10**(2).

Um, J. *et al.* (2010) 'AMP-activated protein kinase-deficient mice are resistant to the metabolic effects of resveratrol', *Diabetes*, **59**(3).

Ummarino, S. *et al.* (2017) 'Simultaneous quantitation of nicotinamide riboside, nicotinamide mononucleotide and nicotinamide adenine dinucleotide in milk by a novel enzyme-coupled assay', *Food Chem.*, **221**, pp. 161–168.

Vakhrusheva, O. *et al.* (2008) 'Sirt7 increases stress resistance of cardiomyocytes and prevents apoptosis and inflammatory cardiomyopathy in mice', *Circ. Res.*, **102**(6), pp. 703–710.

Vaupel, J. *et al.* (1998) 'Biodemographic trajectories of longevity.', *Science*, **280**, pp. 855–860.

Vaziri, H. *et al.* (2001) 'hSIR2SIRT1 functions as an NAD-dependent p53 deacetylase', *Cell*, **107**(2), pp. 149–159.

Vellai, T. *et al.* (2003) 'Genetics: influence of TOR kinase on lifespan in C. elegans', *Nature*, **426**, p. 620.

Venkatasubramanian, S. *et al.* (2013) 'Cardiovascular effects of a novel SIRT1 activator, SRT2104, in otherwise healthy cigarette smokers', *J. Am. Heart Assoc.*, **2**, p. e000042.

Vijg, J. and Hasty, P. (2006) 'Mouse Models of Accelerated Aging', in *Handbook of Models for Human Aging*, pp. 601–618.

Villeponteau, B. (1997) 'The heterochromatin loss model of aging', *Exp Gerontol.*, **32**(4–5), pp. 383–394.

Viswanathan, M. *et al.* (2005) 'A role for SIR-2.1 regulation of ER stress response genes in determining C. elegans life span', *Dev. Cell*, **9**(5), pp. 605–615.

Wachter, K. W. and Finch, C. E. (1997) 'Between Zeus and the Salmon', in *Washington (DC): National Academies Press (US)*.

Waddington, C. (1942) 'Endeavour', **1**, pp. 18–20.

Waddington, C. (1957) 'The strategy of the genes. A discussion of some aspects of theoretical biology', (London: Allen & Unwin).

Waite, L. J. (2004) *Aging, Health, and Public Policy: Demographic and Economic Perspectives (Population Council, 2004).*

Walle, T. *et al.* (2004) 'High absortion but very low bioavaibility of oral resveratrol in humans', *Drug Metab. Dispos.*, **32**(12), pp. 1377–1382.

Wang, R. *et al.* (2011) 'Hepatic Sirt1 deficiency in mice impairs mTorc2/Akt signaling and results in hyperglycemia, oxidative damage, and insulin resistance', *J. Clin. Invest.*, **121**(11), pp. 4477–4490.

Wang, T. *et al.* (2006) 'Structure of Nampt/PBEF/visfatin, a mammalian NAD+ biosynthetic enzyme', *Nat Struct Mol Biol*, **13**(7), pp. 661–662.

Wang, X. *et al.* (2016) 'Nicotinamide mononucleotide protects against β-amyloid oligomer-induced cognitive impairment and neuronal death', *Brain Res.* Elsevier, **1643**, pp. 1–9.

Wang, Y., Liang, Y. and Vanhoutte, P. M. (2011) 'SIRT1 and AMPK in regulating mammalian senescence: A critical review and a working model', *FEBS Lett.* Federation of European Biochemical Societies, **585**(7), pp. 986–994.

Wang, Y. and Tissenbaum, H. A. (2006) 'Overlapping and distinct functions for a Caenorhabditis elegans SIR2 and DAF-16/FOXO', *Mech. Ageing Dev.*, **127**(1), pp. 48–56.

Warburg, O. and Christian, W. (1936) 'Pyridin, the hydrogen-transferring component of the fermentation enzymes (pyridine nucleotide)', *Biochem Z*, **287**, p. 291.

Westendorp, R. G. J. and Kirkwood, T. B. L. (1998) 'Human longevity at the cost of reproductive success', *Nature*, **396**(6713), pp. 743–746.

Weyrich, P. *et al.* (2008) 'SIRT1 genetic variants associate with the metabolic response of Caucasians to a controlled lifestyle intervention - The TULIP Study', *BMC Med. Genet.*, **9**, pp. 1–7.

Whitehead, J. C. *et al.* (2014) 'A clinical frailty index in aging mice: Comparisons with frailty index data in humans', *J Gerontol A Biol Sci Med Sci.*, **69**(6), pp. 621–632.

WHO (2015) *World Report on Ageing and Health. http://who.int/ageing/events/world-report-2015-launch/en/*.

Wood, J. *et al.* (2004) 'Sirtuin activators mimic caloric restriction and delay ageing in metazoans', **430**, pp. 2–6.

Xu, F. *et al.* (2010) 'Lack of SIRT1 (mammalian sirtuin 1) activity leads to liver steatosis in the SIRT1+/- mice: A role of lipid mobilization and inflammation', *Endocrinology*, **151**(6), pp. 2504–2514.

Yamazaki, Y. *et al.* (2009) 'Treatment with SRT1720, a SIRT1 activator, ameliorates fatty liver with reduced expression of lipogenic enzymes in MSG mice', *Am. J. Physiol. Endocrinol. Metab.*, **297**, pp. E1179-E1186.

Yang, H., Baur, J. A., *et al.* (2007) 'Design and synthesis of compounds that extend yeast replicative lifespan', *Aging Cell*, **6**(1), pp. 35–43.

Yang, H., Yang, T., *et al.* (2007) 'Nutrient-Sensitive Mitochondrial NAD+ Levels Dictate Cell Survival', *Cell*, **130**(6), pp. 1095–1107.

Yao, Z. *et al.* (2017) 'Nicotinamide mononucleotide inhibits JNK activation to reverse Alzheimer disease', *Neurosci Lett.* Elsevier Ireland Ltd, **647**, pp. 133–140.

Yeung, F. *et al.* (2004) 'Modulation of NF-kappaB-dependent transcription and cell survival by the SIRT1 deacetylase.', *EMBO J.*, **23**(12), pp. 2369–2380.

Yoshino, J., Mills, Kathryn F, *et al.* (2011) 'Nicotinamide mononucleotide, a key NAD(+) intermediate, treats the pathophysiology of diet- and age-induced diabetes in mice', *Cell Metab.* Elsevier Inc., **14**(4), pp. 528–536.

Yoshino, J., Mills, Kathryn F., *et al.* (2011) 'Nicotinamide mononucleotide, a key NAD + intermediate, treats the pathophysiology of diet- and age-induced diabetes in mice', *Cell Metab*. Elsevier Inc., **14**(4), pp. 528–536.

Yoshino, J. *et al.* (2012) 'Resveratrol supplementation does not improve metabolic function in nonobese women with normal glucose tolerance', *Cell Metab.* Elsevier Inc., **16**(5), pp. 658–664.

Yoshino, J., Baur, J. A. and Imai, S. ichiro (2017) 'NAD + Intermediates: The Biology and Therapeutic Potential of NMN and NR', *Cell Metab*. Elsevier Inc., **27**(3), pp. 513–528.

Yoshizaki, T. *et al.* (2009) 'Sirt1 exerts anti-inflammatory effect and improves insulin sensitivity in adipocytes', *Mol. Cell. Biol.*, **29**(5), pp. 1363–1374.

Yoshizaki, T. *et al.* (2010) 'SIRT1 inhibits inflammatory pathways in macrophages and modulates insulin sensitivity.', *Am. J. Physiol. Endocrinol. Metab.*, **298**(3), pp. E419–E428.

Yu, J. *et al.* (2013) 'Metabolic characterization of a Sirt5 deficient mouse model', *Sci. Rep.*, 3(2806), pp. 1–7.

Zane, L., Sharma, V. and Misteli, T. (2014) 'Common features of chromatin in aging and cancer: Cause or coincidence?', *Trends Cell Biol*. Elsevier Ltd, **24**(11), pp. 686–694.

Zarse, K. *et al.* (2010) 'Differential effects of resveratrol and SRT1720 on lifespan of adult Caenorhabditis elegans', *Horm Metab. Res.*, **42**, pp. 837–839.

Zeng, Y. *et al.* (2017) 'Survival, disabilities in activities of daily living, and physical and cognitive functioning among the oldest-old in China: a cohort study', *Lancet*. Elsevier Ltd, **389**(10079), pp. 1619–1629.

Zhang, H. *et al.* (2016) 'NAD+ repletion improves mitochondrial and stem cell function and enhances life span in mice', *Science*, **2693**(April), p. aaf2693.
Zhang, J. (2006) 'Resveratrol inhibits insulin responses in a SirT1-independent pathway.', *Biochem. J.*, **397**(3), pp. 519–527.

Zhang, T. *et al.* (2012) 'Regulation of Poly(ADP-ribose) Polymerase-1-dependent Gene Expression through Promoter-directed Recruitment of a Nuclear NAD + Synthase', *J Biol Chem*, **287**(15), pp. 12405–12416.

Zhang, W. *et al.* (2015) 'Aging stem cells. A Werner syndrome stem cell model unveils heterochromatin alterations as a driver of human aging.', *Science*, **348**(6239), pp. 1160–1163.

Zhang, Y. *et al.* (1994) 'Positional cloning of the mouse obese gene and its human homologue', *Nature*, **372**, pp. 425–432.

Zhong, L. *et al.* (2010) 'The Histone Deacetylase Sirt6 Regulates Glucose Homeostasis via Hif1alpha', *Cell*. Elsevier Ltd, **140**(2), pp. 280–293.

Zillikens, M. C. *et al.* (2009) 'SIRT1 genetic variation is related to body mass index and risk of obesity', *Diabetes*, **58**(12), pp. 2828–2834.

Zincarelli, C. *et al.* (2008) 'Analysis of AAV serotypes 1-9 mediated gene expression and tropism in mice after systemic injection', *Mol Ther*. The American Society of Gene Therapy, **16**(6), pp. 1073–1080.

Zini, R. *et al.* (1999) 'Effects of resveratrol on the rat brain respiratory chain', *Drugs Exp. Clin. Res.*, **25.**

Zorn, J. A. and Wells, J. A. (2010) ‘Turning enzymes on with small molecules’, *Nat. Chem. Biol.* Nature Publishing Group, **6**(3), pp. 179–188.

Zovkic, I. B., Guzman-Karlsson, M. C. and Sweatt, J. D. (2013) ‘Epigenetic regulation of memory formation and maintenance’, *Learn Mem.*, **20**(2), pp. 61–74.

SUPPLEMENTARY TABLES

Appendix 1: Mouse Frailty Score Card

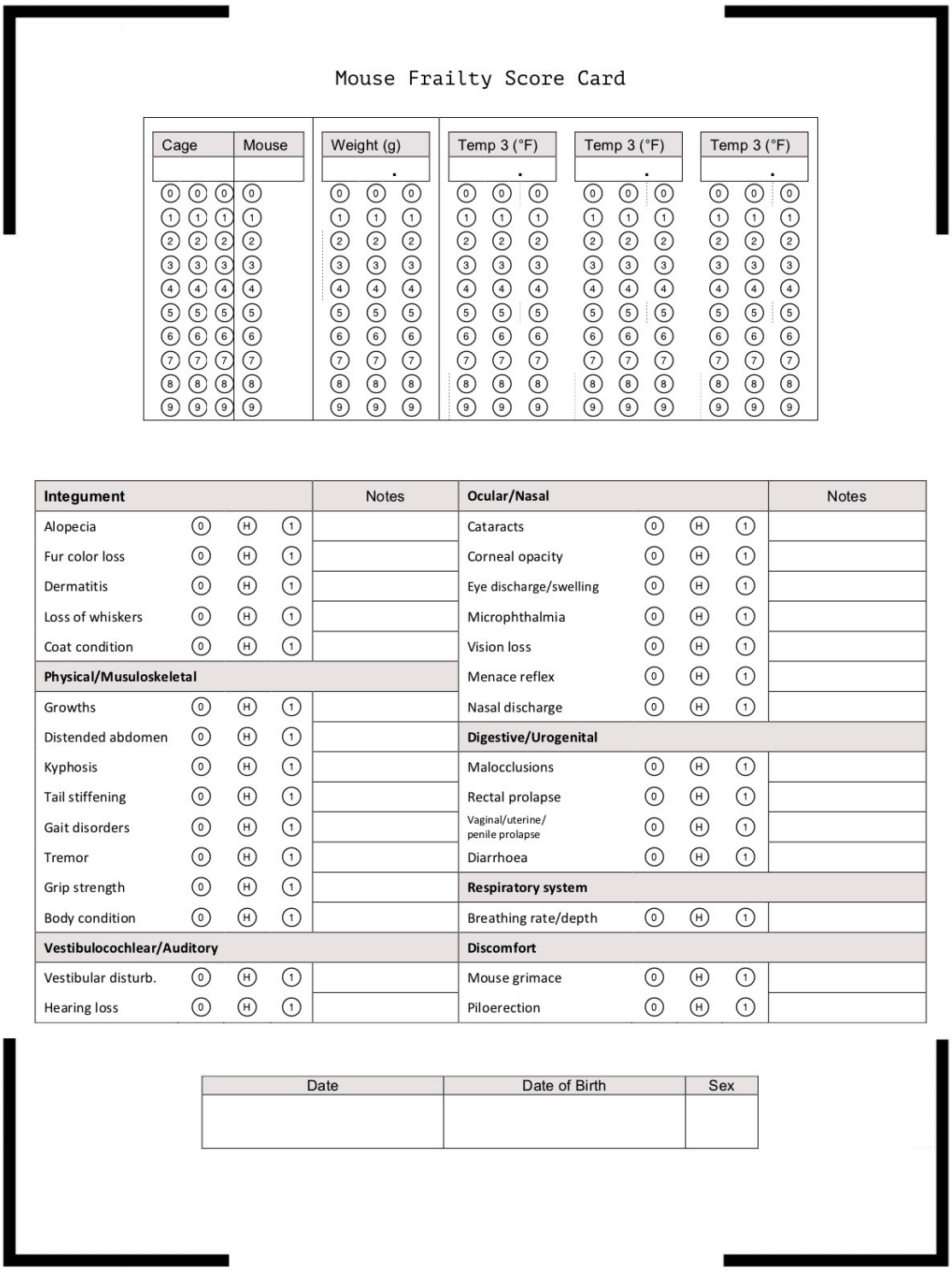

Mouse Frailty Score Card

Cage	Mouse	Weight (g)	Temp 3 (°F)	Temp 3 (°F)	Temp 3 (°F)
		.	.	.	.

Integument		Notes	Ocular/Nasal		Notes
Alopecia	0 H 1		Cataracts	0 H 1	
Fur color loss	0 H 1		Corneal opacity	0 H 1	
Dermatitis	0 H 1		Eye discharge/swelling	0 H 1	
Loss of whiskers	0 H 1		Microphthalmia	0 H 1	
Coat condition	0 H 1		Vision loss	0 H 1	
Physical/Musuloskeletal			Menace reflex	0 H 1	
Growths	0 H 1		Nasal discharge	0 H 1	
Distended abdomen	0 H 1		**Digestive/Urogenital**		
Kyphosis	0 H 1		Malocclusions	0 H 1	
Tail stiffening	0 H 1		Rectal prolapse	0 H 1	
Gait disorders	0 H 1		Vaginal/uterine/ penile prolapse	0 H 1	
Tremor	0 H 1		Diarrhoea	0 H 1	
Grip strength	0 H 1		**Respiratory system**		
Body condition	0 H 1		Breathing rate/depth	0 H 1	
Vestibulocochlear/Auditory			**Discomfort**		
Vestibular disturb.	0 H 1		Mouse grimace	0 H 1	
Hearing loss	0 H 1		Piloerection	0 H 1	

Date	Date of Birth	Sex

Table 1: Primers List

Gene	Forward Primer	Reverse Primer
PGC-1α	GGGTCAGAGGAAGAGATAAAGTTG	CACCAAACCCACAGAAAACAG
TFAm	ATATGTAACGGTCATCAGTG	CTTTGAGCCTTGACAGAAG
NRF-1	ATGGACCTGCTGGACTTG	TGTTGTGAATAATGCTGCTATG
COX2	ATAACCGAGTCGTTCTGCCAAT	TTTCAGAGCATTGGCCATAGAA
RSP18	TGTGTTAGGGGACTGGTGGACA	CATCACCCACTTACCCCCAAAA

Table 2: Antibodies List

Antibody	Supplier
Tubulin	Millipore Sigma
Sirt1	Sigma-Aldrich
Sirt2	Cell Signaling
Sirt3	Cell Signaling
Sirt4	Kindly provided by Dra. Marcia Haigis (Harvard Medical School, MA, USA)
Sirt5	Cell Signaling
Sirt6	Cell Signaling
Sirt7	Cell Signaling
γH2AX	Cell Signaling
GAPDH	Millipore Sigma
GFP	Abcam
HA antibody HRP conjugated	Sigma-Aldrich
I-PpoI	Promega